AAMRL-TR-88-005

MEASUREMENT OF HYBRID III DUMMY PROPERTIES AND ANALYTICAL SIMULATION DATA BASE DEVELOPMENT

Ints Kaleps, PhD
Biodynamics & Bioengineering Division
Harry G. Armstrong Aerospace Medical Research Laboratory

Richard P. White, Jr.
Systems Research Laboratories, Inc.
2800 Indian Ripple Road
Dayton, OH 45440

Robert M. Beecher, PhD
Beecher Research Company
323 Greenmount Boulevard
Dayton, OH 45419

Jennifer Whitestone
Systems Research Laboratories, Inc.
2800 Indian Ripple Road
Dayton, OH 45440

Louise A. Obergefell
Biodynamics & Bioengineering Division
Harry G. Armstrong Aerospace Medical Research Laboratory

FEBRUARY 1988

SUMMARY REPORT FOR AUGUST 1985 TO DECEMBER 1987

HARRY G. ARMSTRONG AEROSPACE MEDICAL RESEARCH LABORATORY
HUMAN SYSTEMS DIVISION
AIR FORCE SYSTEMS COMMAND
WRIGHT-PATTERSON AIR FORCE BASE, OHIO 45433-6573

NOTICES

When US Government drawings, specifications, or other data are used for any purpose other than a definitely related Government procurement operation, the Government thereby incurs no responsibility nor any obligation whatsoever, and the fact that the Government may have formulated, furnished, or in any way supplied the said drawings, specifications, or other data, is not to be regarded by implication or otherwise, as in any manner licensing the holder or any other person or corporation, or conveying any rights or permission to manufacture, use, or sell any patented invention that may in any way be related thereto.

Please do not request copies of this report from the Armstrong Aerospace Medical Research Laboratory. Additional copies may be purchased from:

National Technical Information Service
5285 Port Royal Road
Springfield, Virginia 22161

Federal Government agencies and their contractors registered with Defense Technical Information Center should direct requests for copies of this report to:

Defense Technical Information Center
Cameron Station
Alexandria, Virginia 22314

TECHNICAL REVIEW AND APPROVAL

AAMRL-TR-88-005

This report has been reviewed by the Office of Public Affairs (PA) and is releasable to the National Technical Information Service (NTIS). At NTIS, it will be available to the general public, including foreign nations.

This technical report has been reviewed and is approved for publication.

FOR THE COMMANDER

JAMES W. BRINKLEY
Director
Biodynamics & Bioengineering Division
Harry G. Armstrong Aerospace Medical Research Laboratory

REPORT DOCUMENTATION PAGE

Form Approved
OMB No. 0704-0188

1a. REPORT SECURITY CLASSIFICATION Unclassified	1b. RESTRICTIVE MARKINGS
2a. SECURITY CLASSIFICATION AUTHORITY	3. DISTRIBUTION/AVAILABILITY OF REPORT Approved for public release; distribution is unlimited.
2b. DECLASSIFICATION/DOWNGRADING SCHEDULE	
4. PERFORMING ORGANIZATION REPORT NUMBER(S) AAMRL-TR-88-005	5. MONITORING ORGANIZATION REPORT NUMBER(S)
6a. NAME OF PERFORMING ORGANIZATION Harry G. Armstrong Aerospace Medical Research Laboratory 6b. OFFICE SYMBOL (If applicable) AAMRL/BBM	7a. NAME OF MONITORING ORGANIZATION
6c. ADDRESS (City, State, and ZIP Code) Wright-Patterson AFB OH 45433-6573	7b. ADDRESS (City, State, and ZIP Code)
8a. NAME OF FUNDING/SPONSORING ORGANIZATION 8b. OFFICE SYMBOL (If applicable)	9. PROCUREMENT INSTRUMENT IDENTIFICATION NUMBER
8c. ADDRESS (City, State, and ZIP Code)	10. SOURCE OF FUNDING NUMBERS PROGRAM ELEMENT NO. 62202F; PROJECT NO. 7231; TASK NO. 20; WORK UNIT ACCESSION NO. 13

11. TITLE (Include Security Classification)
Measurement of Hybrid III Dummy Properties and Analytical Simulation Data Base Development

12. PERSONAL AUTHOR(S)
Ints Kaleps, Richard P. White, Jr., Robert M. Beecher, Jennifer Whitestone, Louise A. Obergefell

13a. TYPE OF REPORT	13b. TIME COVERED	14. DATE OF REPORT (Year, Month, Day)	15. PAGE COUNT
Summary	FROM Aug 85 TO Dec 87	February 1988	223

16. SUPPLEMENTARY NOTATION
Effort partially funded by the National Highway Traffic Safety Administration.

17. COSATI CODES			18. SUBJECT TERMS (Continue on reverse if necessary and identify by block number)
FIELD	GROUP	SUB-GROUP	
20	11		Biodynamics, Modeling, Dummies, Simulation
12	05		

19. ABSTRACT (Continue on reverse if necessary and identify by block number)

The dimensional, inertial, surface compliance and joint range-of-motion and resistive properties of a standard and a pedestrian or standing Hybrid III dummy were measured. The data were averaged, between the two dummies and their right and left sides, to form one representative data set for all body segments except the abdomen (lumbar spine), pelvis and upper legs. These segments were distinctly different for the two dummies and two separate data sets were prepared for them. The data were further reduced to the specific input format requirements for the Crash Victim Simulation (CVS) and Articulated Total Body (ATB) model programs. A simulation of an automobile crash event was performed to demonstrate the correctness of the data format and physical consistency of the input data. The report describes the measuring methodology, presents the raw measured data, discusses the methods and assumptions used in the data reduction and reformatting to the CVS/ATB model input data requirements, presents reduced data as well as the final simulation input

20. DISTRIBUTION/AVAILABILITY OF ABSTRACT ☒ UNCLASSIFIED/UNLIMITED ☐ SAME AS RPT. ☐ DTIC USERS	21. ABSTRACT SECURITY CLASSIFICATION Unclassified
22a. NAME OF RESPONSIBLE INDIVIDUAL Ints Kaleps	22b. TELEPHONE (Include Area Code) (513) 255-3665 22c. OFFICE SYMBOL AAMRL/BBM

DD Form 1473, JUN 86 — Previous editions are obsolete.

19. ABSTRACT (Continued)

formatted data and shows graphical results from the demonstration simulations in which responses of the standard Hybrid III, the standing Hybrid III and a Part 572 dummy, exposed to identical impact conditions, are compared.

PREFACE

The work described herein was performed at the Harry G. Armstrong Aerospace Medical Research Laboratory (AAMRL) and was supported by both Air Force and National Highway Traffic Safety Administration Funding (Interagency Agreement No. DTNH22-86-X-07477). The various tasks necessary for the total program were performed in part by AAMRL, Systems Research Laboratory, Inc. and University of Dayton Research Institute personnel. Of the two Hybrid III dummies tested in this program the standing dummy belonged to AAMRL and the seated dummy was provided by General Motors.

(Revised 5/6/87)

TABLE OF CONTENTS

LIST OF FIGURES

LIST OF TABLES

1.0 INTRODUCTION

The use of analytical computer based models for the prediction of human response to mechanical forces for both safety evaluation of various systems and the design of new systems is becoming a standard practice. This is particularly true in the area of automobile crash and subsequent occupant response investigations and in studies of crewmember responses during ejection from aircraft. In these applications, as well as others, the use of models is a complementary process to physical system testing and provides considerable benefits in an overall program seeking to identify and quantify potential system hazards and subsequently provide direction for system improvement. Specifically, models can be beneficial in reducing the number of required tests and thus reducing program cost; they provide insight into various physical mechanisms that may be occurring but which may not be obvious or readily observed in actual testing; they allow for a convenient means of investigating the effects of parameter changes; they can be used in test design to define the optimum configuration and conditions; they can be used independently of an actual test to investigate the general feasibility of concepts; and ultimately, with sufficient validation and a soundly developed data base, they may be used directly as an injury assessment tool. While these benefits are substantial their realization requires not only a sound analytic methodology but also an appropriate and sound data base that properly characterizes the system being modeled.

This program has sought to develop such a data base for the Hybrid III dummy. The Hybrid III dummy is extensively used in automotive crash testing, is generally considered to be the most advanced of automotive testing dummies currently available and is in the process of being adopted by the National Highway Traffic Safety Administration as a standard for automotive safety compliance testing. While the ultimate objective of this program was to develop a data base for the Crash Victim Simulator (CVS) and Articulated Total Body (ATB) computer models by reducing the data to the exact input formats required for these programs, the directly measured data is also presented to provide an explanation of the methodology used in measuring the dummy properties and also to provide data that users of other models could reduce according to their model input formatting requirements.

The measurement objectives in this program, though not necessarily the methods, are the same as in the study on the Part 572 dummy conducted by Fleck, et al [1]. The Part 572 dummy is a derivative of the General Motors Hybrid II dummy which, in many respects, is similar to the presently investigated Hybrid III dummy. While a direct comparison of the data sets is not made in this report, simulations with identical dynamic exposure conditions were performed using the Part 572 and Hybrid III dummy data sets and the results are reported.

Two Hybrid III dummies were measured in this study. An illustration of the two types of manikins, standing and seated, is shown in Figure 1. One dummy had freely articulating hips, is commonly referred to as a pedestrian testing dummy, and in this study is denoted as the standing dummy. The other dummy was the standard Hybrid III with a pelvis section molded in a sitting position. This dummy is denoted as the seated dummy. The intent of this program was to develop one standard data set for the Hybrid III and in effect, this was done with the seated dummy data base. However, the pelvic and upper leg structure of the standing dummy was substantially different and thus a different data set was developed for this portion of the body. The result was that all body data properties for the two dummies and their left and right sides were averaged to produce one common data set for the total body, except for the pelvis (including lumbar spine) and upper legs. Two data sets were prepared for the pelvis and upper legs and each combined with the common, averaged data set to form the seated and standing Hybrid III data sets.

This report describes the measurement methodology, the results of the measurements, the data reduction methods, the assumptions and methods for reformatting to the CVS/ATB model format and a demonstration simulation comparing the Part 572 and Hybrid III dummy responses under identical conditions.

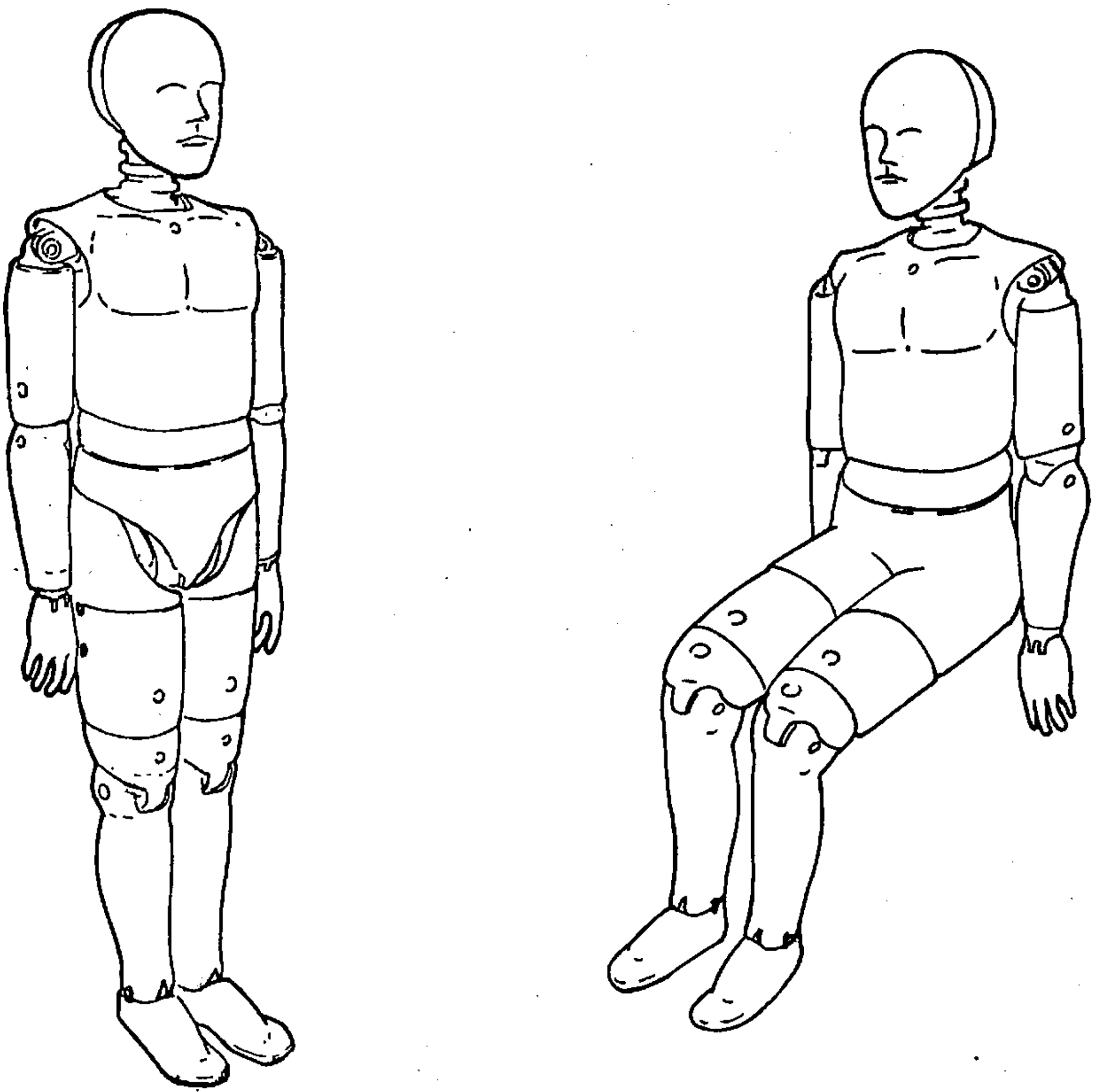

Figure 1. Hybrid III Standing and Seated Manikins

2.0 TECHNICAL DISCUSSION

2.1 Physical Measurement of Manikin Properties

In this section the various physical measurements that were made on both manikins are presented and discussed. In general, each subsection presents and discusses the procedure developed, the equipment used and includes both a presentation and discussion of the results obtained. Each pertinent data set, i.e. mass properties, external dimensions, joint characteristics, etc, has been separated into the various subsections for clarity and for easy reference.

2.1.1 Measurement of Manikin External Dimensions

2.1.1.1 Description of Measurement Procedure

One of the requirements of this study was to obtain a series of external measurements on the Hybrid III following the measurement descriptions presented in USG 2485, "Hybrid III Exterior Dimensions". These measurements are shown in Figures 2 and 3 and the dimensions in Table 1. The table and figures were prepared by General Motors and provided to DOT (Backaitis, Personal Communication) [2]. The objective of these tests was to make the same set of measurements of the standing and seated Hybrid III manikins being investigated in this study. The manikins were assembled and positioned as in Figures 2 and 3. Each one was seated on a box which was placed against a vertical wall, and the manikins were placed upright so that the back of the pelvis and thorax touched the wall. The instruments used to conduct the measurements were a GPM Gneupel anthropometer and a Keuffel & Esser steel tape measure. Both instruments had a reading resolution of one millimeter.

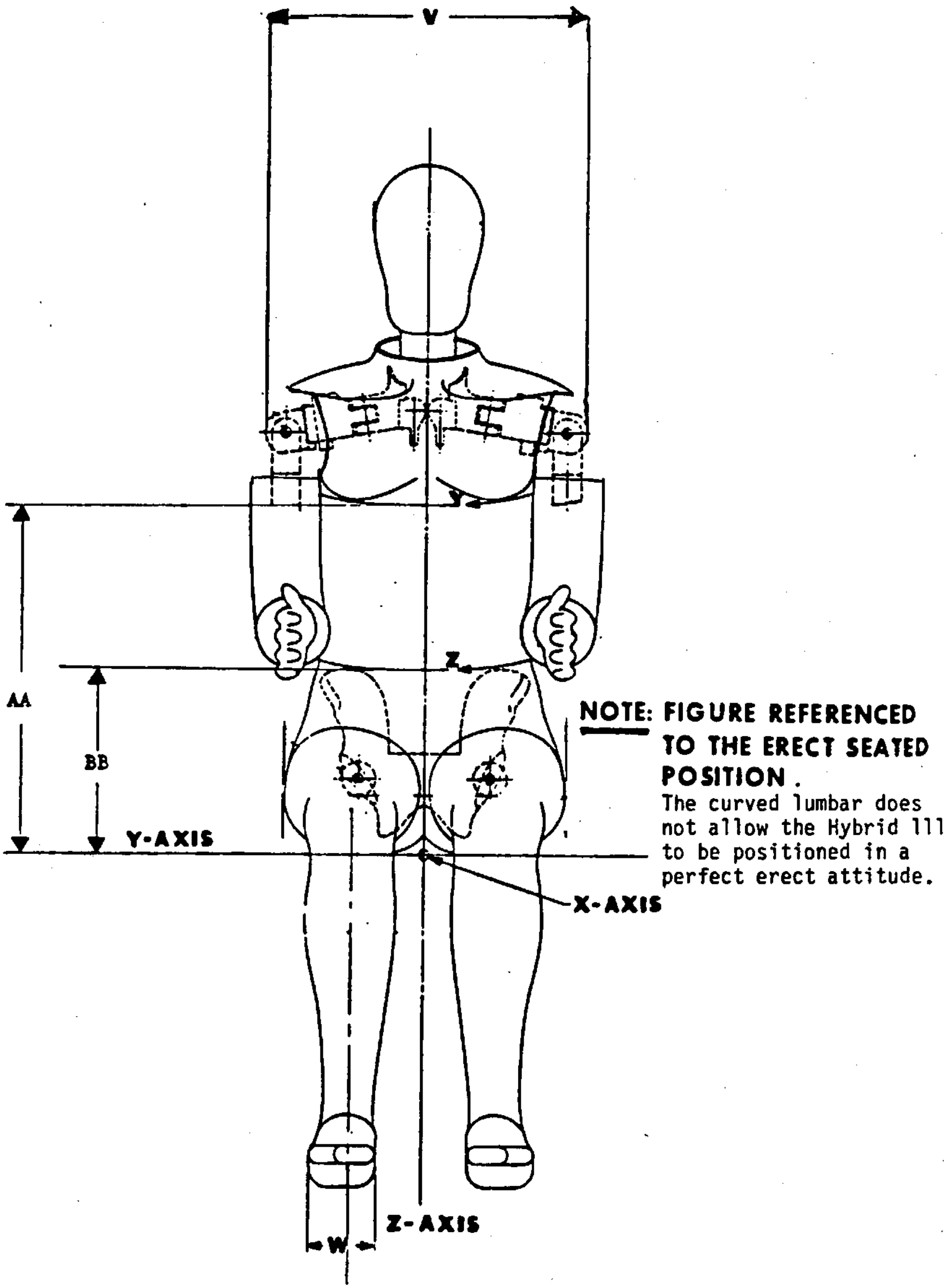

Figure 2. Hybrid III Exterior Body Dimensions - Front View

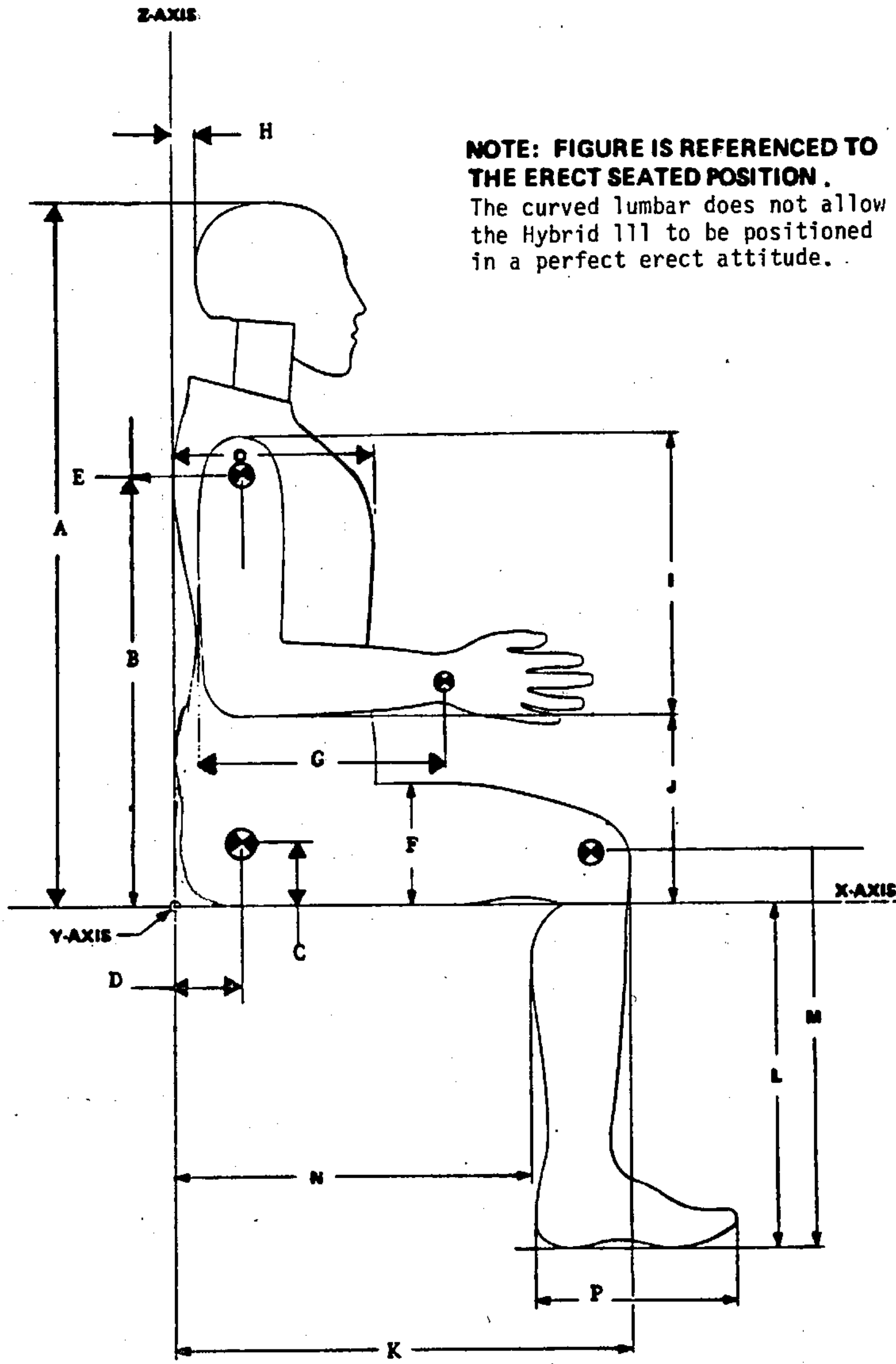

Figure 3. Hybrid III Exterior Body Dimensions - Side View

TABLE 1
HYBRID III EXTERIOR DIMENSIONS

Dimensional Symbol	Description	Assembly Dimension (inches)
A (U)	Sitting Height (Erect)	34.8±.2
B	Shoulder Pivot Height	20.2±.3
C	"H" Point Height	3.4ref±.1
D	"H" Point Location from Back Line	5.4ref±.1
E	Shoulder Pivot Location from Back Line	3.5±.2
F (Q)	Thigh Clearance	5.8±.3
G	Back of Elbow to Wrist Pivot	11.7±.3
H	Occiput to Z-Axis	1.7±.1
I (I)	Shoulder - Elbow Length	13.3±.3
J (J)	Elbow Rest Height	7.9±.4
K (P)	Buttock-Knee Length	23.3±.5
L (L)	Popliteal Height	17.4±.5
M (M)	Knee Pivot Height	19.4±.3
N (N)	Buttock-Popliteal Length	18.3±.5
O (O)	Chest Depth	8.7±.3
P (S)	Foot Length	10.2±.3
V (V)	Shoulder Breadth	16.9±.3
W (W)	Foot Breadth	3.9±.3
Y (Y)	Chest Circumference (with chest jacket)	38.8±.6
Z (Z)	Waist Circumference	33.5±.6
AA	Location for Measurement of Chest Circumference	17.0±.1
BB	Location for Measurement of Waist Circumference	9.0±.1

( ) SAE J963 Measurement

Note: The "H" point is located 1.83 inches forward and 2.57 inches down from the center of the pelvis angle reference hole.

2.1.1.2 Discussion of Results

The results of the measurements made on both manikins are presented and compared with those listed in USG 2485 in Table 2. During the conduct of the measurements, a few problems were encountered. One of which was the inability to locate the "H" point as per the instructions presented in USG 2485. The "H" point, as described in USG 2485, is "located 1.83 inches forward and 2.57 inches down from the center of the pelvic reference hole." There are three holes on each side of the seated pelvis and none on the standing pelvis. It was, therefore, unclear which was the pelvic reference hole. Proceeding from each hole as described in USG 2485, did not result in the location of any structural feature, such as the hip pivot, which might be interpreted as the "H" point. Therefore, no measurements using the "H" point were obtained.

A second problem was that the head did not touch the wall when each manikin was positioned in its upright, seated position. The neck/thorax attachment fixture of the Hybrid III neck permits the angle of the neck, relative to the thorax, to be varied. For the subject tests, the neck was set at 0 degrees. This is as specified by General Motors in the inspection and check out procedure [3]. The reported value for sitting height is the maximum that could be obtained by pushing the head back (which is the case in measuring this dimension on human subjects). Measuring sitting height with the manikin head in its usual position results in a value of 0.3 inches less than that listed in USG 2485.

Other discrepancies between the dimensions listed in USG 2485 and the current measurements are in the chest depth and the locations (height above the seat pan) for measurement of the chest and waist circumferences. From the drawings describing these dimensions, chest depth was interpreted as the maximum depth measured on the two manikins. No ready explanation can be offered for the differences in

TABLE 2

EXTERNAL DIMENSIONS

Hybrid III Exterior Dimensions (inches) as Listed in Table 2.1.

DIMENSION SYMBOL	DESCRIPTION	USG 2485 ASSEMBLY DIMENSIONS	HYBRID III STANDING	HYBRID III SEATED
A	Sitting Height (erect)	34.8±.2	33.9	34.6
B	Shoulder Pivot Height	20.2±.3	20.4	19.9
C	"H" Point Height	3.4ref±.1	--	--
D	"H" Point Location from Back Line	5.4ref±.1	--	--
E	Shoulder Pivot Location from Back Line	3.5±.2	3.7	4.4
F	Thigh Clearance	5.8±.3	6.0	5.9
G	Back of Elbow to Wrist Pivot	11.7±.1	11.6	11.5
H	Occiput to Z-Axis	1.7±.1	2.4	4.3
I	Shoulder-Elbow Length	13.3±.3	13.4	13.6
J	Elbow Rest Height	7.9±.4	7.6	7.4
K	Buttock-Knee Length	23.3±.5	23.4	23.3
L	Popliteal Height	17.4±.5	18.0	17.9
M	Knee Pivot Height	19.4±.3	19.3	19.1
N	Buttock-Popliteal Length	18.3±.5	18.7	18.9
O	Chest Depth	8.7±.3	10.6	10.5
P	Foot Length	10.2±.3	10.1	10.2
V	Shoulder Breadth	16.9±.3	16.7	16.8
W	Foot Breadth	3.9±.3	3.7	3.8
Y	Chest Circumference (with chest jacket)	38.8±.6	38.8	37.6
Z	Waist Circumference	33.5±.6	33.5	33.7
AA	Location for Measurement of Chest Circumference	17.0±.1	16.5	16.1
BB	Location for Measurement of Waist Circumference	9.0±.1	10.4	10.0

Note - The "H" point is described as being located 1.83 inches forward and 2.57 inches down from the center of the pelvic angle reference hole.

dimension values. The locations for chest and waist circumferences were interpreted from the USG 2485 drawings as being just below the breast and at the lower edge of the thorax jacket, respectively.

2.1.2 Measurement of Manikin Segment Geometry and Axis System Descriptions

The geometry of each segment is specified with respect to a coordinate system embedded in the segment. This was done by measuring the three-dimensional coordinates of a number of landmark points on the segment in a laboratory reference system, using prescribed combinations of these points to establish a segment coordinate system and then transforming all the landmark coordinate points from the laboratory system to the local segment coordinate system. The following sections describe this process in detail.

2.1.2.1 Description of Basic Measurement Techniques

The dummy segment geometrical measurements were performed while the segment was mounted in a segment reference box which was used in the inertial property measurement tests. Three dimensional points were measured on the segment and on the box using a jointed, electromechanical device with axis-mounted potentiometers called a Perceptor, manufactured by Micro Control Systems, Inc. The measuring system, with an arm segment in a box, is shown in Figure 4. The Perceptor was interfaced through a control terminal to a Perkin-Elmer 3240 minicomputer, where recorded points were stored for analysis. Interactive FORTRAN programs were written to control the recording, labelling, and analysis of points.

Recording began with the manikin segment immobilized in the three-sided test box used in mass properties testing. Points were recorded by first entering a label through the console, then positioning the end of the Perceptor stylus at the appropriate location and triggering the recording with a foot pedal. Some points on the segment could not be reached because of box obstruction. To remedy this problem, the segment

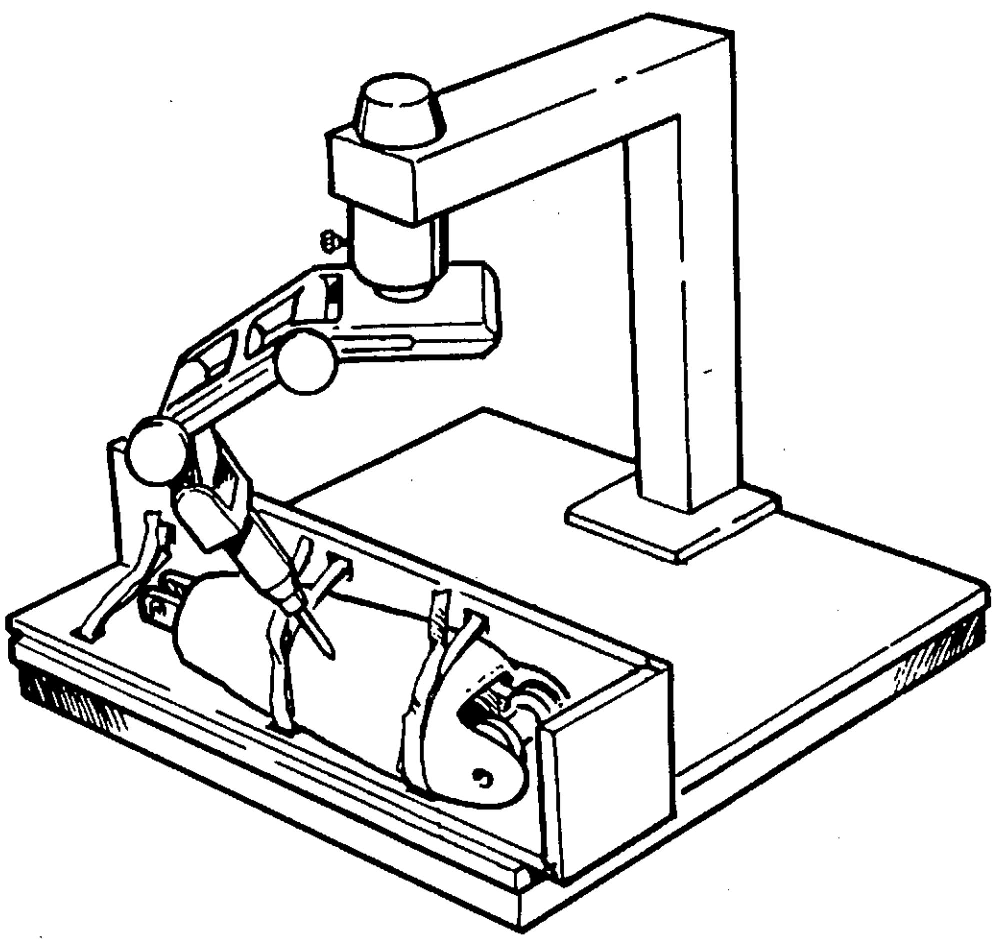

Figure 4. The Perceptor Shown with Manikin Forearm in Test Box

was removed from the box after recording at least three non-colinear reference points on both the box and segment, then repeating the recording of segment reference points along with the other desired points. This procedure permitted the calculation of transformation matrices which defined the three-dimensional displacements of the different sets of points into a common axis system.

2.1.2.2 Definition and Location of Landmarks and Axis Systems

In order to compare the data measured for the Hybrid III with three dimensional human data, a series of landmarks were recorded which were analogous to the anthropometric landmarks used to define the axes on stereophotogrammetrically recorded data of adult men and women [4] & [5]. Points for defining joint and joint axes locations were also recorded and were used as the basis for defining local mechanical coordinate systems which were directly related to the mechanical structure of the manikin. The criteria for locating "anatomical" landmarks on the manikin were their spatial relationship with relevant structural features (i.e., joints), the similarity of the manikin external geometry to humans, and the desirability of having axes defined by landmarks on the segment itself. This procedure was hindered by structural and geometric features which were dissimilar to humans or not present, and by the fact that a landmark may not, even in humans, be located on the relevant segment. For example, the upper arm anatomical axes are defined by three anatomical landmarks which would not be considered to be present on the Hybrid III upper arm (see Table 9, Right Upper Arm). Acromiale, the lateral-most point on the acromion process of the shoulder (part of the Hybrid III torso), was located for the upper arm as the superior edge of the lateral side of the soft covering. The lateral and medial humeral epicondyles in humans are located on the upper arm, but also define the elbow axis. In the Hybrid III, the surface covering the elbow is part of the forearm (see Table 11, Right Forearm). Thus, for the purpose of defining the upper arm axes, the epicondyles on the upper arm were located at the medial and lateral inferior edges of the soft covering. While none of the three axis-defining landmarks for this segment are in the ideal locations, the planes are analogous to the human system and permit a reasonable comparison between human and manikin properties.

Section 2.1.6 presents the definitions of each of the landmarks used to define axes for each of the Hybrid III axis systems. Most landmarks were located at positions that were reasonable analogues of those of humans, or, as in the upper arm, in positions which would define anatomical axes as similar as possible to those defined for humans in the stereophotometric studies.

The anatomical axes are generally defined by two vectors, $\vec{a}$ and $\vec{b}$, formed by three non-linear landmarks on the segment surface. The vectors $\vec{a}$ and $\vec{b}$ define a plane, with $\vec{a} \times \vec{b} = \vec{c}$ defining a vector normal to the plane which is orthoganal to both $\vec{a}$ and $\vec{b}$. The directions of $\vec{a}$ and $\vec{b}$ are chosen so that the directions of the axes follow the general convention of x forward, y to the left, and z upward. In order to assure the proper orientation of these axes and the desired location of the origin, sometimes more than three points are used to specify the axis vectors and origin. The individual axis systems are defined, segment by segment, in section 2.1.6.

2.1.2.3 Transformation of Data Between Axis Systems

Three-dimensional coordinates of points are initially measured on the segments and the box by the Perceptor and recorded in a laboratory reference system designated by R. Three points on the box are used to define a coordinate system designated by B, and all the points are transformed to this box coordinate system. This system is used in the measurement and calculation process of segment inertial properties.

From the points measured on the segments and the inertial property measurements, three segment based coordinate systems are calculated. An anatomical system designated by A and defined by equivalent anatomical surface landmarks; a local mechanical reference system designated by L and defined by segment mechanical features, for example joint centers and rotation axes; and a principal axes system designated by P and obtained by segment inertia tensor diagonalization are established and transformations between them calculated.

These transformations are in the form of 3X3 cosine matrices, and their operation on vectors is given by

$$\vec{r}_A = A_{AP}\vec{r}_P$$
$$\vec{r}_L = A_{LA}\vec{r}_A$$
$$\vec{r}_P = A_{PL}\vec{r}_L$$

where $\vec{r}_A$, $\vec{r}_L$, $\vec{r}_P$ are the same vectors but with components in the anatomical, local and principal coordinate systems respectively.

The cosine matrices, [A], are orthogonal and have the convenient property if two are know the third can be calculated by the matrix product

$$A_{IK} = A_{IM}A_{MK}.$$

It was decided to present the results of the testing of the two Hybrid III manikins in the form of a mean representative data set. As described below, the method for arriving at the representative geometry is in part an averaging of the two manikins, and in part an effort to account for the symmetry designed into the manikins. Each of the limb segments, four data sets, right and left from both manikins, were combined (exceptions were the upper leg, pelvis, and spine which differed in the manikins and were treated separately). For the axial segments - head, neck, thorax, and pelvis - mirrored data sets were created so that a symmetrical representation would result.

The y component of the vector from the local reference origin (center of mass) to a joint center was reflected from the right side to the left side by changing the signs. The mirror images of axial segments (head, neck, thorax, and pelvis) were created by averaging the values of right and left side landmarks.

The mean value of the CG vector was calculated for each body segment. This vector was noted to have a random lateral variation about the segment long axis, so an adjustment for consistency was made by setting the Y coordinate value to 0.0.

The results are presented for each segment in section 2.1.6 where the representative values of the landmark coordinates in local reference and anatomical axes are presented along with the matrix (A_{AL}) for transforming points from local to anatomical systems.

2.1.3 Measurement and Determination of the Mass Properties of the Manikin Segments

2.1.3.1 Discussion of Measurement Techniques and Equipment Utilized

2.1.3.1.1 Segment Mass

The equipment used to measure the mass of the manikin segments was an electronic weighing scale and a segment holder, a three sided rectangular balsa wood box. The mass properties of the balsa boxes were measured beforehand and stored in data files on a supporting Hewlett Packard 85-B microcomputer. The segment was extracted from adjoining segments and tested with the joint hardware as listed in Table 3. The segment was weighed in the box and the box weight was subtracted to obtain the segment weight. These boxes provided a means to easily and securely house the manikin segment in a fixed position while its mass properties were being determined. A representative box is shown in Figure 5. A velcro strap was used, along with masking tape when necessary, to rigidly fasten the segment within the box so that no relative motion was possible.

TABLE 3

Hybrid III Segments and Corresponding Joint Hardware and Instrumentation

Segment	Joint Hardware	Instrumentation	Part Numbers
Head	occipital condyle pin	head-neck load cell three accelerometers	78051-61
Neck	upper neck bracket	n/a	78051-90 78051-307
Thorax	shoulders	n/a	78051-89
Pelvis (w/spine)	n/a	lumbar load cell	78051-70 78051-60 78051-13 78051-25
Pelvis (w/out spine)	n/a	lumbar load cell	78051-60 78051-13 78051-25
Upper Arm (right side)	n/a	n/a	78051-174 78051-126 78051-191
Forearm (right side)	elbow	n/a	78051-194 78051-204 78051-199 78051-200 78051-201 78051-202 78051-203 78051-128
Hand (right side)	wrist	n/a	78051-209 78051-214
Upper Leg (right side)	hip	n/a	78051-51 78051-47 78051-27 78051-6 78051-72 78051-96 78051-276
Lower Leg (right side)	knee	n/a	78051-74 78051-278 78051-139 78051-272 78051-203 78051-129 78051-337 78051-271
Foot (right side)	ankle	n/a	78051-285 78051-96

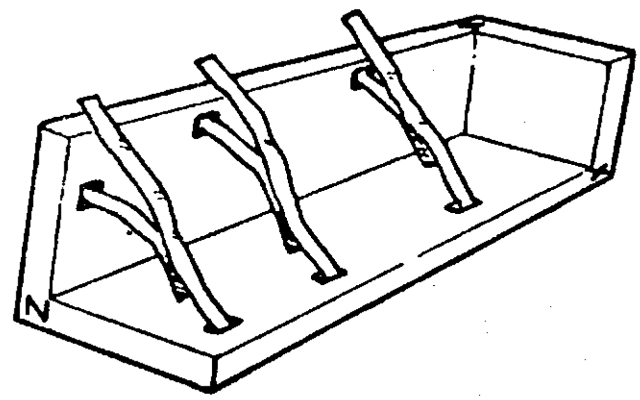

Figure 5. Balsa Segment Holding Box

These boxes were similar, although not identical to those used by Lephart [6] in his studies. The boxes were carefully constructed of multiple layers of laminated, light-weight, cross-grained balsa wood, with particular attention being paid to the three outer edges so that they were orthogonal. These mutually perpendicular edges defined a box axis system, the origin of which was at the point where the three outer box edges intersected, and with respect to which the subsequent inertial property measurements were made.

2.1.3.1.2 Segment Center of Gravity Location

The test equipment used to locate the manikin segments' center of gravity (cg) positions included an electronic weighing scale, an aluminum knife-edge, an adjustable stand, and the Perceptor, an electronic position coordinate digitizer. The knife-edge/electronic scale assembly configured for measurement is shown in Figure 6. The methodology employed to locate the cg is very straightforward being based on a balance of moments about one edge of the plate.

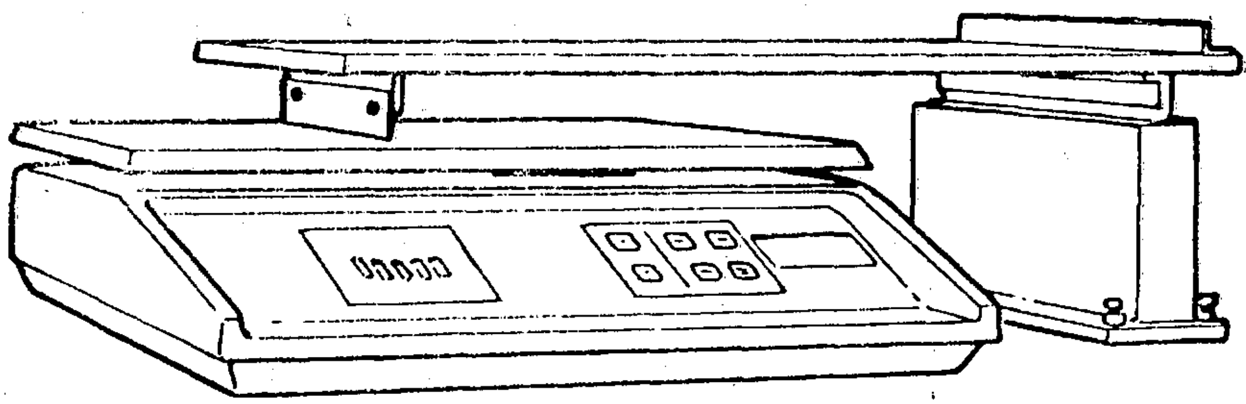

Figure 6. Test Equipment Used For Determining Segment Center of Gravity

The knife-edge-plate was carefully constructed such that the two knife blades were parallel and the right knife blade and the chock, on the upper surface of the plate, were longitudinally coincident. As shown in Figure 6, this plate was mounted horizontally onto the adjustable stand and scale surface. After the plate was positioned level on the scale and stand, the scale was tared to zero prior to a measurement. Figure 7 shows the components configured for measuring the 'X' component of the cg location of the forearm segment. The "loaded" box was placed on the plate so that one of the box edges was positioned firmly against the chock. The restoring moment due to the scale reaction force was calculated from the scale reading, measured in this position, and the known blade separation distance. The restoring moment is simply the scale reading multiplied by its moment arm, the blade separation distance. The cg position of the box + segment with respect to the box edge in contact with the chock can then be calculated, using the weight of the box + segment, by a balance of moments as shown at the bottom of Figure 7. Performing three such measurements, each with a different box axis perpendicular to the chock, established the three dimensional

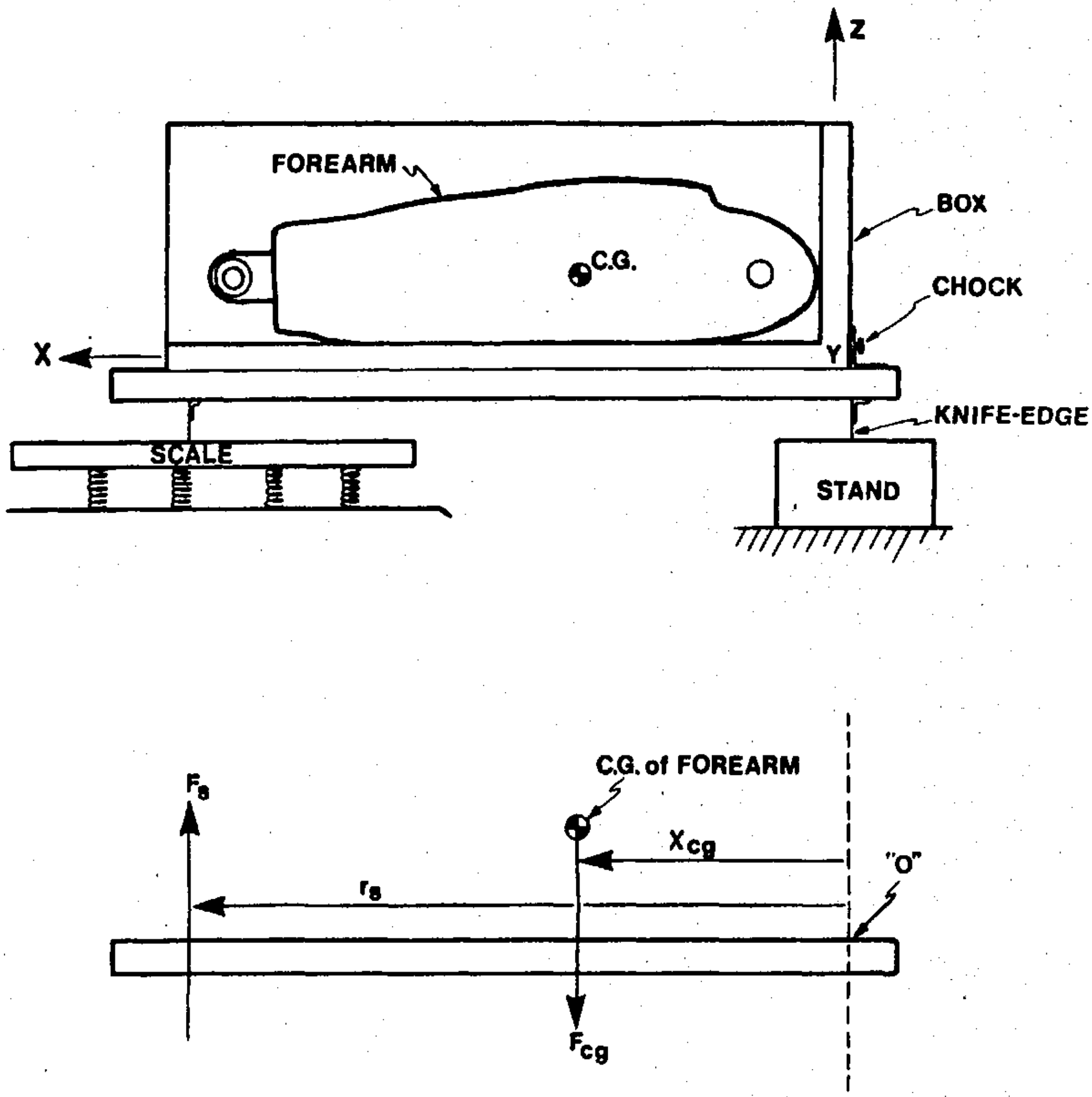

F_s = Scale reading of box+forearm on knife edge plate

F_{cg} = Weight of box+test object

r_s = Known blade seperation distance

X_{cg} = C.G. co-ordinate of box+forearm with respect to boxedge in contact with the chock

$$\Sigma M_O = \emptyset: \qquad F_s r_s - F_{cg} X_{cg} = 0$$

$$\therefore \quad X_{cg} = \frac{F_s r_s}{F_{cg}}$$

Figure 7. Test Setup and Procedure for Determining Segment Center of Gravity

location of the box + segment cg with respect to the box origin. Since an identical procedure had already been performed on the box alone, the segment center of gravity location was calculated by subtraction of the box moment components.

To preserve the identity of the segment center of gravity position when the segment was removed from the box required the identification of test object landmark geometric interrelationships with respect to the box axis system. Landmarks for each segment were chosen that had either "anatomical" or "mechanical" significance. That is, these landmarks helped define segment based anatomical or local mechanical axis systems as described in section 2.1.2. Identifying the coordinates of at least three non-collinear segment landmarks, while the segment was still housed within the box, provided not only locations from which to reference the cg position, but also sufficient geometric information to calculate transformation matrices that were later used to manipulate the segment's inertial property data. Shown in Figure 8, along with the forearm segment, is the Micro Control System's Perceptor, a potentiometer based three-dimensional position coordinate recorder, which was used to digitize the segment landmarks.

2.1.3.1.3 Segment Inertia

The equipment used to measure the segment's inertia tensor consisted of a Space Electronics Inc. Mass Properties Instrument (MPI), a compressed air or nitrogen source, a gas dryer/filter, a Hewlett Packard HP 85-B microcomputer, and a balsa wood jig. The controlling hardware of the MPI, the gas dryer/filter, and the HP 85-B are shown in Figure 9, and the structure housing the torsional pendulum itself is shown in Figure 10.

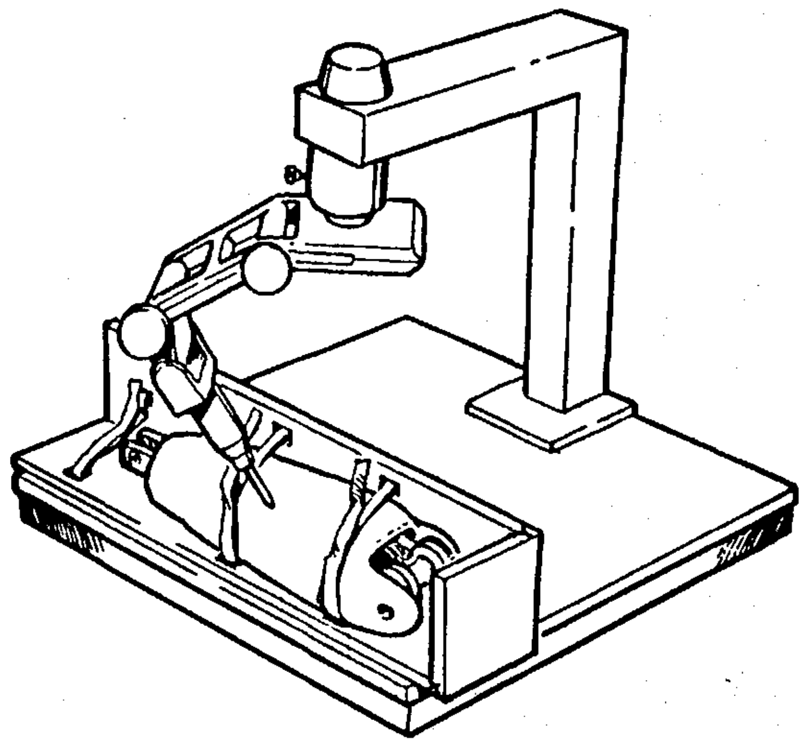

Figure 8. Perceptor Measurement System

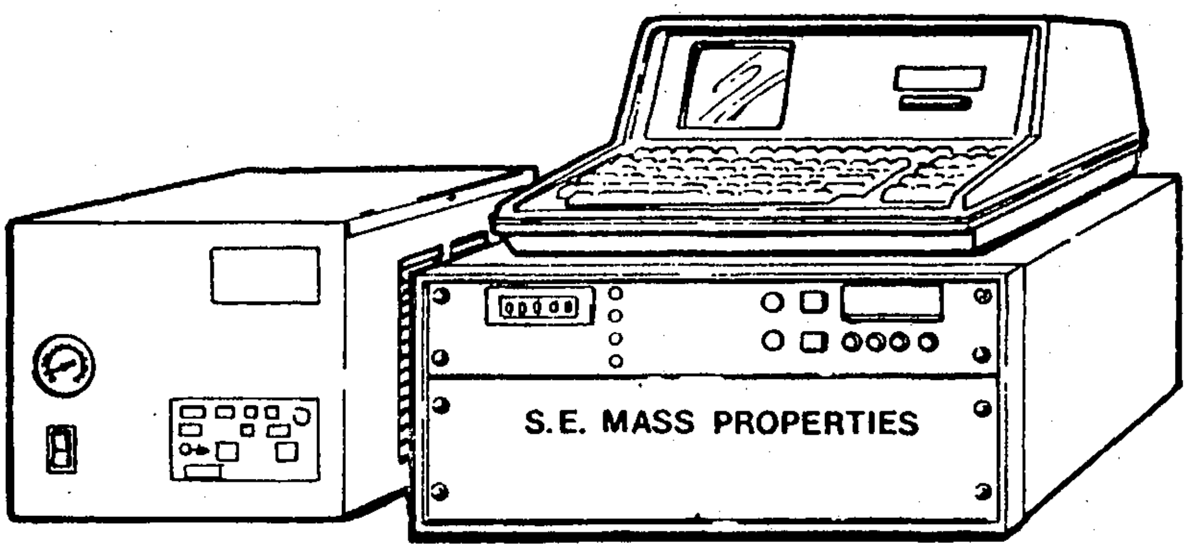

Figure 9. Gas Dryer and MPI Instrumentation

The main component of the MPI is an inverted torsional pendulum. This pendulum is coupled to a platter and grid plate assembly that rides on a spherical gas bearing perfused with either clean, dry compressed air or nitrogen. In essence the MPI is a precision timing instrument. The moment of inertia of a manikin segment is calculated from the time period of the pendulum's torsional oscillations. The MPI produces an initial, repeatable torsional perturbation and, subsequently through a photocell device, measures the resulting period of the pendulum's torsional oscillations. The MPI is most accurate when the cg of the segment and/or box being tested is placed directly on the axis of the torsional pendulum. Software on the HP 85-B provided the coordinates where the box was to be mounted on the grid plate, such that the cg of the test object was placed within 0.35 inches of the pendulum axis. The box was firmly secured to the grid plate via double sided tape and masking tape "anchors" when necessary. Figure 11 illustrates the forearm mounted on the grid plate for a moment of inertia measurement.

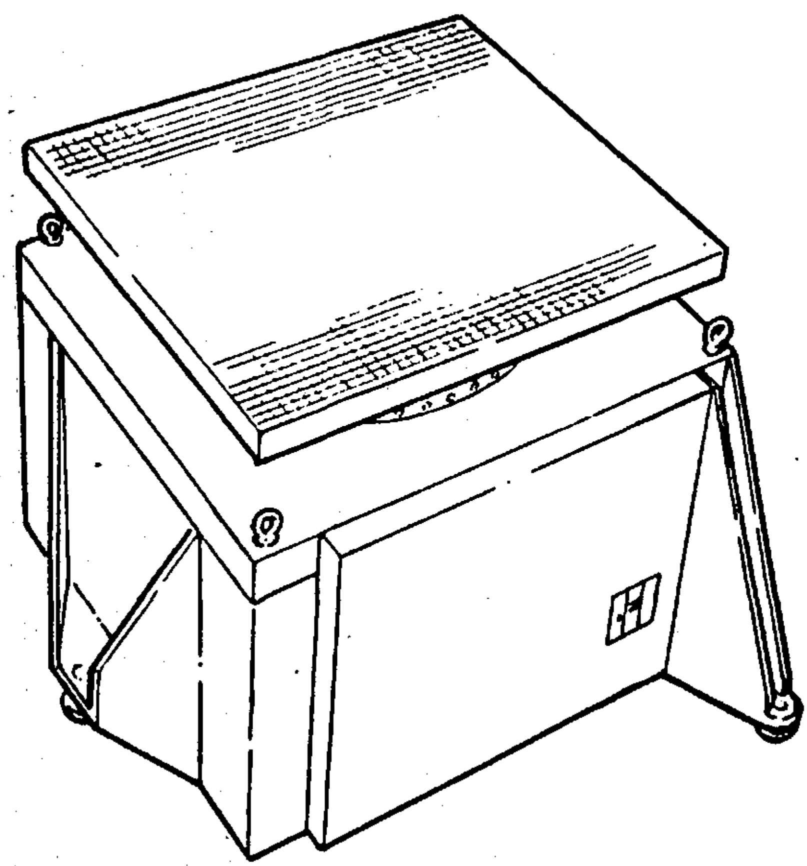

Figure 10. Inertial Measurement Equipment

Six quantities must be measured to completely identify the inertia tensor of the manikin segment. The moments of inertia were measured

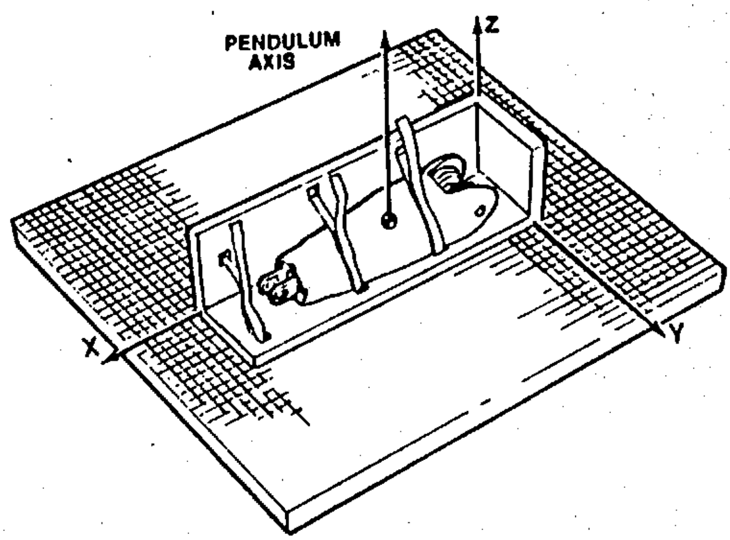

Figure 11. Forearm Mounted on MPI Platform to Determine Moment of Inertia

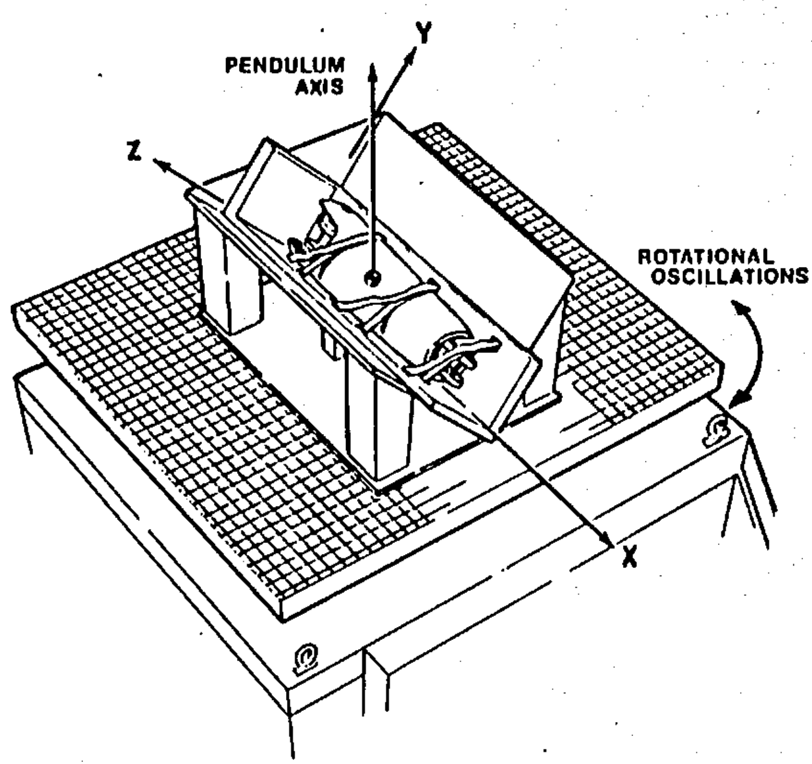

Figure 12. Forearm Mounted in Jig on MPI Platform to Determine Moment of Inertia about an Oblique Angle

about each of the three box axes, in turn, mounted perpendicular to the surface of the grid plate, as in Figure 11 and about three oblique angles as shown, for example, in Figure 12. Note that the composite box + segment + jig cg is positioned over the pendulum axis. The following expression was used to determine the products of inertia, Pxy, with A being the angle of inclination of the x and y axes from the grid plate:

$$Pxy = \frac{Ixx + Iyy * Tan^2 A - (1 + Tan^2 A) * Ixy}{2 * Tan A} .$$

Simplification of the method involved incorporating a jig which held the segments at 45 degrees to the grid plate yielding the following equation that was ultimately used to compute the products of inertia:

$$Pxy = \frac{Ixx + Iyy - 2 * Ixy}{2}$$

For a detailed theoretical development of these mathematical expressions the reader is directed to Chandler, et. al. [7].

In order to isolate the inertial properties of the manikin segments alone, the inertial contributions of the box and jig had to be accounted for in the procedure. Identical moment of inertia measurements were performed on the boxes used with the segments. The box properties, defined with respect to their centers of gravity, were stored in data files on the HP 85-B. Data processing software used the parallel-axis-theorem (PAT) to subtract out the box properties. The PAT is stated as follows:

$$I_A = I_0 + M * D_{A0}^2 .$$

where I_A is the moment of inertia about an arbitrary axis "A", I_0 is the moment of inertia about the axis "0" through center of mass, M is the mass of the object, and D_{A0}^2 is the squared distance between the two parallel axes "A" and "0". The exact placement of the box origin on the grid plate is recorded for each step in the measurement process. Since the net cg location of the box and the segment are known with respect to the box origin, this origin was placed on the table platform so as to align the net box and segment cg with the pendulum axis. Thus the PAT was employed as follows in a three step sequence:

1) $$I_{BP} = I_{BO} + M_B D_{PO}^2$$

Where

I_{BP} = moment of the box about the pendulum axis

I_{BO} = moment of the box about an axis parallel to the pendulum axis but centered at the box cg

M_B = mass of the box

D_{PO}^2 = the squared distance from the pendulum axis to the box cg

2) $$I_{SP} = I_{(S+B)P} - I_{BP}$$

Where

I_{SP} = moment of the segment (alone) about the pendulum axis

$I_{(S+B)P}$ = moment (as measured) of the segment + box about the pendulum axis

I_{BP} = as above

3) $$I_{SO} = I_{SP} - M_S D_{OP}^2$$

Where

I_{SO} = moment of segment about its cg

I_{SP} = as above

M_S = mass of segment

D_{OP}^2 = the squared distance from the pendulum axis to the segment cg

Step 1) above provides the moment of inertia of the empty box defined at the exact position that it was placed on the grid plate during the box plus segment measurement. Step 2), in turn, subtracts the box contribution from the composite box plus segment moment of inertia that was actually measured in the test, yielding the moment of inertia of the segment alone about the pendulum axis. Step 3) provides the moment of inertia of the segment alone about an axis which passes through its own cg, i.e. an element of its inertia tensor. The moments of inertia used to calculate the products of inertia are transformed in an identical fashion. Note the jig contribution is accounted for implicitly since it was considered as part of the box properties.

After the six unique elements of the segment inertia tensor were identified, this inertia tensor was diagonalized using software on the HP 85-B. The diagonalization produced three principal moments of inertia and a 3X3 matrix of direction cosines which defined the orientation of the three principal directions. Since the segments were measured in a box, the principal directions were oriented with respect to the specific box axis system. Further transformations, as described in section 2.1.2.3, redefined the principal directions with respect to either anatomical or local mechanical axes.

The moments of inertia and the principal axes directions with respect to the local segment axes for each of the manikin segments are presented in the data tables of Section 2.1.6.

2.1.3.2 Accuracy of Measurement Techniques

Geometric test objects, whose inertial properties could be precisely analytically calculated, were used to evaluate the accuracy of the mass properties procedure. Geometric weights, in the range of 0.15 lbs to 19.6 lbs, were used to determine the percent error versus magnitude of moment of inertia and the error associated with locating the center of gravity. In addition, the measured orientations of the principal axes were compared to the known orientations to determine the accuracy of this procedure.

The resulting percent error of the measured moment of inertia was found to increase with decreasing magnitudes of moment or, the smaller the moment, the larger the error. The maximum percent error for the smallest moment found with parts representing components of the Hybrid

III manikin was less than 3%. Given an average moment of 100 to 150 $lb\text{-}in^2$ for the segments, the associated error is about 0.5%. The maximum principal axis direction orientation error was determined to be ± 6 degrees and the maximum percent error of locating the center of gravity was ± 0.3 cm in each of the coordinate directions.

2.1.3.3 Presentation and Discussion of Results

The segment weights, cg locations and principal moments for the seated and standing manikins are presented in Tables 4, 5 and 6, respectively. Values for right and left limbs are averaged individually for the seated and standing manikin. Values for each segment for both manikins were averaged and are presented in the far right columns in all three tables. Note that for several manikin segments, properties are unique because of the different designs for the seated versus standing manikins. For these segments (the pelvis, lumbar spine and upper legs) the properties were not averaged. The cg locations are given in Table 5 with respect to the anatomical coordinate system which is defined for each segment in Section 2.1.6.

TABLE 4

SEGMENT WEIGHTS

Segment	Manikin	Manikin Wt. (lbs)	Ave. Wt. (lbs)
Head	Seated	9.92	9.92
	Standing	9.92	
Neck	Seated	2.67	2.67
	Standing	2.67	
Thorax	Seated	38.85	39.22
	Standing	39.58	
Pelvis	Seated	49.35	49.35
(w/spine)	Standing	24.57	24.57
Pelvis	Seated	44.46	44.46
(w/o spine)	Standing	21.91	21.91
Lumbar	Seated*	4.89	4.89
Spine	Standing*	2.66	2.66
Upper	Seated	13.71	13.71
Leg	Standing	19.98	19.98
Lower	Seated	7.27	7.24
Leg	Standing	7.21	
Foot	Seated	2.76	2.76
	Standing	2.76	
Upper	Seated	4.59	4.60
Arm	Standing	4.61	
Forearm	Seated	3.89	3.80
	Standing	3.70	
Hand	Seated	1.29	1.29
	Standing	1.29	

* 1 lb subtracted due to steel plate attachment.

TABLE 5

SEGMENT CENTER OF GRAVITY LOCATIONS IN THE ANATOMICAL COORDINATE SYSTEM

Segment	Manikin	CG Coordinates (in)		Average CG Coordinates (in)
Head	Seated	X:	-0.12	-0.12
		Y:	0.00	0.00
		Z:	0.67	0.67
	Standing	X:	-0.12	
		Y:	0.00	
		Z:	0.67	
Neck	Seated	X:	3.74	3.74
		Y:	0.00	0.00
		Z:	3.05	3.05
	Standing	X:	3.74	
		Y:	0.00	
		Z:	3.05	
Thorax	Seated	X:	3.82	3.63
		Y:	0.00	0.00
		Z:	5.64	5.83
	Standing	X:	3.43	
		Y:	0.00	
		Z:	6.01	
Pelvis (w/spine)	Seated	X:	-3.32	-3.32
		Y:	0.00	0.00
		Z:	0.77	0.77
	Standing	X:	-4.02	-4.02
		Y:	0.00	0.00
		Z:	0.45	0.45
Pelvis (w/o spine)	Seated	X:	-3.34	-3.34
		Y:	0.00	0.00
		Z:	0.30	0.30
	Standing	X:	-4.22	-4.22
		Y:	0.00	0.00
		Z:	0.09	0.09
Lumbar Spine	Seated	X:	0.35	0.35
		Y:	0.00	0.00
		Z:	-2.56	-2.56
	Standing	X:	0.00	0.00
		Y:	0.00	0.00
		Z:	-2.56	-2.56

TABLE 5 (CONTINUED)

Segment	Manikin	CG Coordinates (in)	Average CG Coordinates (in)
Upper Leg	Seated	X: 0.00	0.00
		Y: 2.78 (-) Left	2.78 (-) Left
		Z: -9.76	-9.76
	Standing	X: 0.39	0.39
		Y: 3.15 (-) Left	3.15 (-) Left
		Z: -6.10	-6.10
Lower Leg	Seated	X: 0.18	
		Y: -2.18	
		Z: -5.27	0.00
			-2.01 (+) Left
	Standing	X: -0.12	-5.12
		Y: -1.84	
		Z: -4.96	
Foot	Seated	X: -4.15	
		Y: 0.00	
		Z: 0.54	-3.99
			0.00
	Standing	X: -3.82	0.50
		Y: 0.00	
		Z: 0.45	
Upper Arm	Seated	X: -0.05	
		Y: 1.64	
		Z: -4.97	0.00
			1.69 (-) Left
	Standing	X: 0.01	-4.88
		Y: 1.73	
		Z: -4.78	
Forearm	Seated	X: 0.84	
		Y: 0.59	
		Z: -3.05	0.92
			0.37 (-) Left
	Standing	X: -1.00	-3.03
		Y: 0.15	
		Z: -3.00	
Hand	Seated	X: -0.82	
		Y: -0.49	
		Z: 0.48	0.84
			0.53 (-) Left
	Standing	X: -0.85	0.50
		Y: -0.56	
		Z: 0.52	

TABLE 6

SEGMENT PRINCIPAL MOMENTS OF INERTIA

Segment	Manikin	Principal Moments of Inertia (lbs sec^2 in)		Averaged Principal Moments of Inertia (lbs sec^2 in)
Head	Seated	X:	0.1408	
		Y:	0.2128	
		Z:	0.1956	0.1408
				0.2128
	Standing	X:	0.1408	0.1956
		Y:	0.2128	
		Z:	0.1956	
Neck	Seated	X:	0.0254	
		Y:	0.0257	
		Z:	0.0084	0.0254
				0.0257
	Standing	X:	0.0254	0.0084
		Y:	0.0257	
		Z:	0.0084	
Thorax	Seated	X:	2.5506	
		Y:	2.0184	
		Z:	1.6836	2.6203
				2.0517
	Standing	X:	2.6899	1.7336
		Y:	2.0849	
		Z:	1.7835	
Pelvis (w/spine)	Seated	X:	2.5109	2.5109
		Y:	1.6110	1.6110
		Z:	1.4925	1.4925
	Standing	X:	0.8879	0.8879
		Y:	0.7293	0.7293
		Z:	0.5659	0.5659
Pelvis (w/o spine)	Seated	X:	2.4575	2.4575
		Y:	1.2969	1.2969
		Z:	1.2080	1.2080
	Standing	X:	0.8019	0.8019
		Y:	0.6182	0.6182
		Z:	0.4678	0.4678
Lumbar Spine	Seated	X:	0.0612	0.0612
		Y:	0.0593	0.0593
		Z:	0.0205	0.0205
	Standing	X:	0.0196	0.0196
		Y:	0.0196	0.0196
		Z:	0.0083	0.0083

TABLE 6 (CONTINUED)

Segment	Manikin	Principal Moments of Inertia (lbs sec^2 in)		Averaged Principal Moments of Inertia (lbs sec^2 in)
Upper Leg	Seated	X:	0.6092	0.6092
		Y:	0.5934	0.5934
		Z:	0.1068	0.1068
	Standing	X:	1.4494	1.4494
		Y:	1.4968	1.4968
		Z:	0.1989	0.1989
Lower Leg	Seated	X:	0.6726	
		Y:	0.6744	
		Z:	0.0313	0.6708
				0.6745
	Standing	X:	0.6689	0.0397
		Y:	0.6745	
		Z:	0.0480	
Foot	Seated	X:	0.0069	
		Y:	0.0512	
		Z:	0.0491	0.0067
				0.0524
	Standing	X:	0.0065	0.0491
		Y:	0.0536	
		Z:	0.0490	
Upper Arm	Seated	X:	0.1035	
		Y:	0.1018	
		Z:	0.0102	0.1025
				0.0997
	Standing	X:	0.1014	0.0110
		Y:	0.0976	
		Z:	0.0117	
Forearm	Seated	X:	0.1203	
		Y:	0.1152	
		Z:	0.0060	0.1191
				0.1128
	Standing	X:	0.1179	0.0069
		Y:	0.1103	
		Z:	0.0077	
Hand	Seated	X:	0.0114	
		Y:	0.0093	
		Z:	0.0033	0.0115
				0.0093
	Standing	X:	0.0115	0.0036
		Y:	0.0093	
		Z:	0.0038	

2.1.4 Measurement of Manikin Joint Physical Characteristics

In order to properly reflect natural limitations in human joint freedom of motion, the Hybrid III dummies have built-in joint stops. While these stops are structurally well defined, their effective position can be somewhat modified by some local structural deformation and by the interaction of the soft flesh coverings. Joint resistive properties can also be modified by applying resistive torque through friction devices in the manikin joints. This frictional force is user adjustable and is mainly used for maintaining constant manikin position prior to the main impact exposure. In the tests described herein, the net effect of all the parameters which contribute to joint resistive torque were measured except that of the joint friction mechanism.

2.1.4.1 Measurement of Joint Resistance Torque as a Function of Joint Rotational Angle

The ATB/CVS model joint modeling capability requires the representation of joint torque resistance as a function of angular rotation. The joint characteristic testing in this study was designed to provide this data. In general, the testing approach involved the rigid clamping of one of two articulated segments, the forcing of the free segment through a planar arc using a load cell and measuring the force required and the angle of rotation. Using this process, both for loading and unloading, resulted in joint load deflection characteristics.

2.1.4.1.1 Description of Joints and Test Set-Up

With the exception of the hip, which has a ball and socket joint, the articulations of the shoulder, elbow, wrist, knee, and ankle are pin jointed clevices. For a pin joint, the two clevices of the adjoining segments are hinged together by a bolt and washer combination that provides a planar range of motion with the hardware, stops, or soft covering determining the particular range of motion. While the joints can be tightened to provide variable joint resistance, all joints within this study were loosely torqued to allow free range of motion within the limits of the soft and hard stops.

For a joint under investigation, only the two adjoining segments were used to conduct the test. One segment was clamped solidly to a holding frame in a manner that would hold the weight of the test object without interfering with the range of motion. In addition, the stationary segment was positioned so that the joint axis was parallel to the gravity vector to eliminate the effect of the torque about the joint due to the weight of the rotating segment.

2.1.4.1.2 Instrumentation Utilized

A Waters 5K potentiometer and a Strainsert 250 lb single-axis load cell were used to measure the angle of rotation and the applied force, respectively. The output of these transducers were fed to a Hewlett-Packard X - Y recorder. Calibrations of the potentiometer, used to record joint rotation, indicated that the potentiometer had a 0.1 degree of accuracy and good linearity. The load cell was wired through a bridge balance and amplifier to the y-axis of the x-y recorder and was periodically calibrated. The load cell had a 0.75 lb accuracy.

For the loosely torqued joints, the bolt holding the two clevices rotated through the full range of motion with the movement of the rotating segment. This rotating bolt was attached directly to the axis of the potentiometer through an interface fixture which was designed to fit the head of the hex bolt. The load cell was positioned perpendicular to the limb axis and parallel with the plane of rotational motion. See, for example, Figure 13. Using the load cell as the force application device, the free segment was manually rotated through the entire range of motion. The resulting force versus angle curve was recorded on the x-y plotter. The desired torque versus angle characteristics were then determined by measuring the length of the mobile segment lever arm and multiplying this length by the measured force.

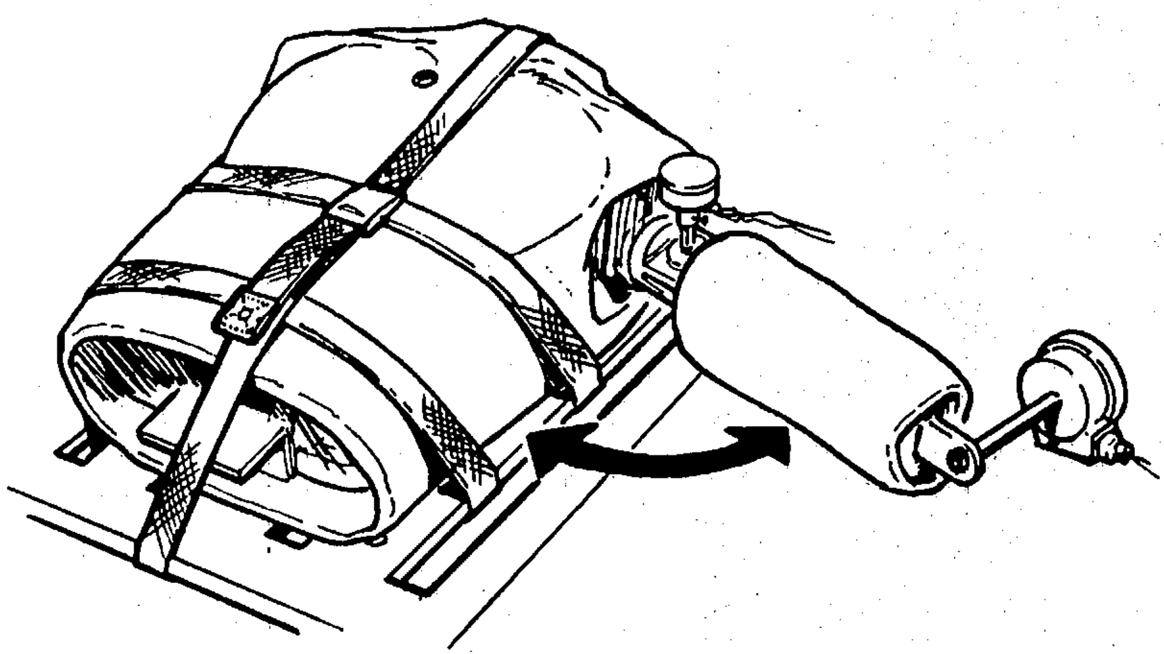

Figure 13. Shoulder Abduction-Adduction Test Setup

Generally, the curve displayed a flat region of joint torque with angle of rotation within the free range of motion, that range which experiences little or no resistance. A summary table of the free range of motion of each joint is found in Table 7. The interference of soft covering or soft stops generally increased the resistance in a nonlinear manner. This nonlinearity further increased as the joint hard stop was reached. The direction of motion was reversed to measure the unloading characteristic and the loading characteristic in the opposite direction. While the polarity of the curves may vary depending on the polarity of the instrumentation for a particular test, the curves could be compared by identifying the maximum ranges of motion and the corresponding applied torques. To define the curves, arrows depict the direction of loading and unloading of the joint and the extreme ends of the curve are labeled with extension, flexion, abduction, or adduction. The start positions are also noted.

2.1.4.1.3 Tests

2.1.4.1.3.1 Shoulder

Flexion-extension and abduction-adduction movement of the shoulder is provided by two pin joints. Assuming the upper arm in the anatomical position, (hanging vertically down with the long bone axis parallel to the mid-sagittal plane), flexion-extension motion is obtained by rotating the arm forward and backward while remaining parallel to the mid-saggital plane. Again assuming the anatomical position, abduction-adduction motion is obtained by rotating the upper arm away from and toward the body while remaining within the frontal plane. Flexion-extension characteristics were tested with initial abduction angles of 0 and 45 degrees. The angles were approximated with the aid of a goniometer and the abduction-adduction pin joint was tightly torqued to hold this position. Abduction-adduction tests were performed with 0 and 90 degrees of flexion.

Abduction-adduction angle of rotation of 0° flexion was measured by first positioning the upper torso horizontally and holding it securely

TABLE 7

Summary of Free Joint Range of Motion

Joint	Range of Motion	Left/Right	Seated/Standing	Free Range of Motion
Shoulder	ab-ad @ 0 flex	right	standing	126 degrees
Shoulder	ab-ad @ 0 flex	left	standing	138 degrees
Shoulder	ab-ad @ 0 flex	right	seated	120 degrees
Shoulder	ab-ad @ 0 flex	left	seated	98 degrees
Shoulder	ab-ad @ 90 flex	right	standing	117 degrees
Shoulder	ab-ad @ 90 flex	left	standing	114 degrees
Shoulder	ab-ad @ 90 flex	right	seated	116 degrees
Shoulder	ab-ad @ 90 flex	left	seated	122 degrees
Shoulder	flex-ext @ 0 abd	right	standing	230 degrees
Shoulder	flex-ext @ 0 abd	left	standing	174 degrees
Shoulder	flex-ext @ 0 abd	right	seated	215 degrees
Shoulder	flex-ext @ 0 abd	left	seated	210 degrees
Shoulder	flex-ext @ 45 abd	right	standing	216 degrees
Shoulder	flex-ext @ 45 abd	left	standing	209 degrees
Shoulder	flex-ext @ 45 abd	right	seated	251 degrees
Shoulder	flex-ext @ 45 abd	left	seated	218 degrees
Elbow	flex-ext @ 0 rot	right	standing	77 degrees
Elbow	flex-ext @ 0 rot	left	standing	77 degrees
Elbow	flex-ext @ 90 rot	right	standing	72 degrees
Elbow	flex-ext @ 90 rot	left	standing	78 degrees
Elbow	flex-ext @ 180 rot	right	standing	81 degrees
Elbow	flex-ext @ 180 rot	left	standing	74 degrees
Elbow	flex-ext @ 270 rot	right	standing	75 degrees
Elbow	flex-ext @ 270 rot	left	standing	74 degrees
Elbow	flex-ext @ 0 rot	right	seated	90 degrees
Elbow	flex-ext @ 0 rot	left	seated	87 degrees
Elbow	flex-ext @ 90 rot	right	seated	86 degrees
Elbow	flex-et @ 90 rot	left	seated	86 degrees
Elbow	flex-ext @ 180 rot	right	seated	84 degrees
Elbow	flex-ext @ 180 rot	left	seated	92 degrees

TABLE 7 (Continued)

Joint	Range of Motion	Left/Right	Seated/Standing	Free Range of Motion
Elbow	flex-ext @ 270 rot	right	seated	no plot
Elbow	fle-ext @ 270 rot	left	seated	84 degrees
Wrist	flex-ext @ 0 rot	right	standing	104 degrees
Wrist	flex-ext @ 0 rot	left	standing	89 degrees
Wrist	flex-ext @ 90 rot	right	standing	105 degrees
Wrist	flex-ext @ 90 rot	left	standing	86 degrees
Wrist	flex-ext @ 180 rot	right	standing	99 degrees
Wrist	flex-ext @ 180 rot	left	standing	104 degrees
Wrist	flex-ext @ 270 rot	right	standing	108 degrees
Wrist	flex-ext @ 270 rot	left	standing	86 degrees
Wrist	flex-ext @ 0 rot	right	seated	123 degrees
Wrist	flex-ext @ 0 rot	left	seated	119 degrees
Wrist	flex-ext @ 90 rot	right	seated	107 degrees
Wrist	flex-ext @ 90 rot	left	seated	107 degrees
Wrist	flex-ext @ 180 rot	right	seated	122 degrees
Wrist	flex-ext @ 180 rot	left	seated	105 degrees
Wrist	flex-ext @ 270 rot	right	seated	116 degrees
Wrist	flex-ext @ 270 rot	left	seated	119 degrees
Knee	flex-ext	left	standing	84 degrees
Knee	flex-ext	right	seated	90 degrees
Knee	flex-ext	left	seated	86 degrees
Ankle	flex-ext	right	standing	54 degrees
Ankle	flex-ext	left	standing	33 degrees
Ankle	flex-ext	right	seated	66 degrees
Ankle	flex-ext	left	seated	68 degrees
Hip	flex-ext	right	standing	78 degrees
Hip	flex-ext	left	standing	27 degrees
Hip	abd-add	right	standing	47 degrees
Hip	abd-add	left	standing	60 degrees
Hip	flex-ext	right	seated	0 degrees
Hip	flex-ext	left	seated	0 degrees
Hip	abd-add	right	seated	0 degrees
Hip	abd-add	left	seated	0 degrees

with straps placed across the thorax. See Figure 13. This position of the thorax was chosen to insure that the abduction-adduction axis of rotation was parallel with the gravity vector. The upper arm was attached to the thorax with the shoulder joint loosely torqued. An interface fixture, designed to fit the head of the hex bolt, held the potentiometer shaft directly in line with the joint axis.

A load cell, whose axis was fixed horizontally and perpendicular to the long bone axis of the upper arm, was used to measure the applied force. An attachment which fit the elbow joint clevice was designed to properly orient the load cell with respect to the long bone. The potentiometer recorded the angle of rotation as the upper arm was manually rotated through the full range of motion.

Figures 14 and 15 show the results of testing the left and right shoulder joint of both manikins. Compared to the seated manikin, the range of motion was about 50 degrees higher for standing manikin. The tests also indicated that due to the soft covering interference, the total range of motion was a function of the force applied to the upper arm for both manikins. The free range of motion, that is the range which experiences no resistance, was larger for the standing manikin, indicating that the differences in the range of motion must be the structural characteristics of the manikins.

Starting from the anatomical position, the joint experiences resistance at about 7° adduction due to the soft covering before mechanical hardware provided a hardstop. At abduction angles of 120 to 135°, interference of the acromion covering became increasingly pronounced with increasing torque. It is believed that, because of the soft covering interference, the hard mechanical stop was not reached in the test.

The test setup for the 90o flexion abduction-adduction joint test is illustrated in Figure 16. At 90° flexion, the abduction-adduction tests were conducted in the same manner as the 0° flexion abduction-adduction tests.

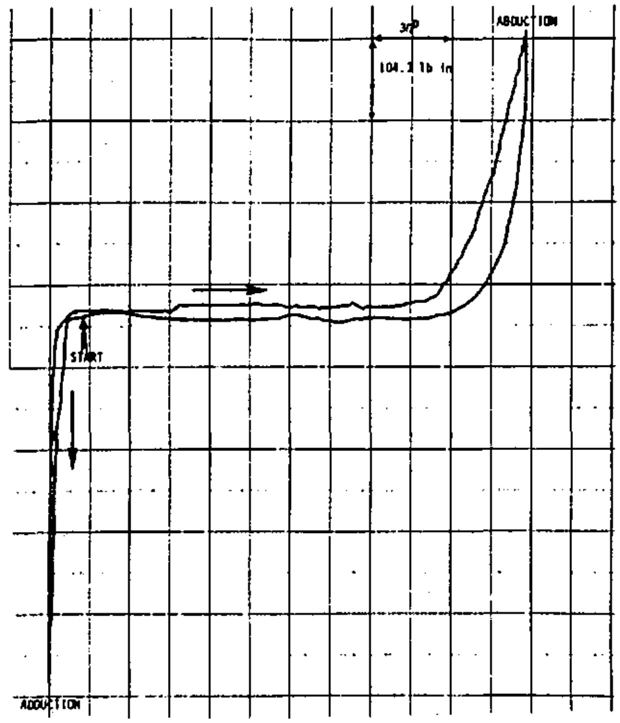

RIGHT SHOULDER

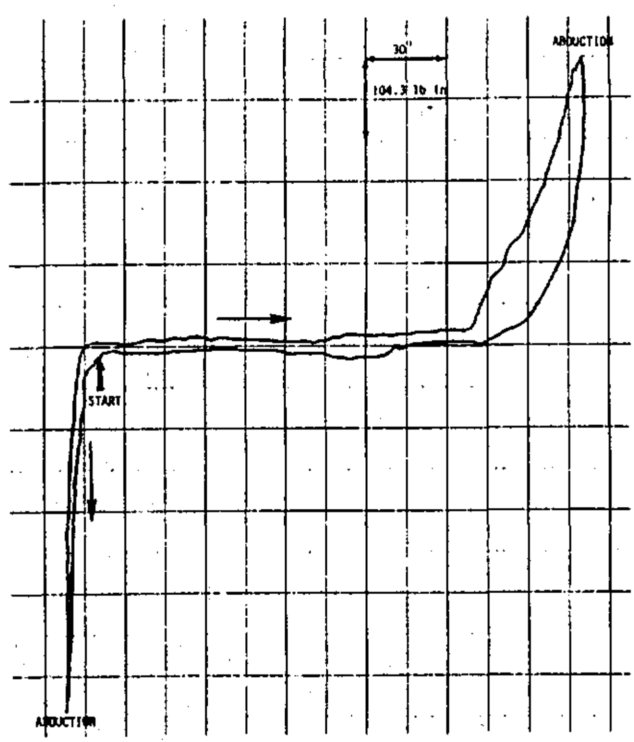

LEFT SHOULDER

FIGURE 14. SHOULDER ABDUCTION-ADDUCTION AT 0° FLEXION FOR STANDING MANIKIN

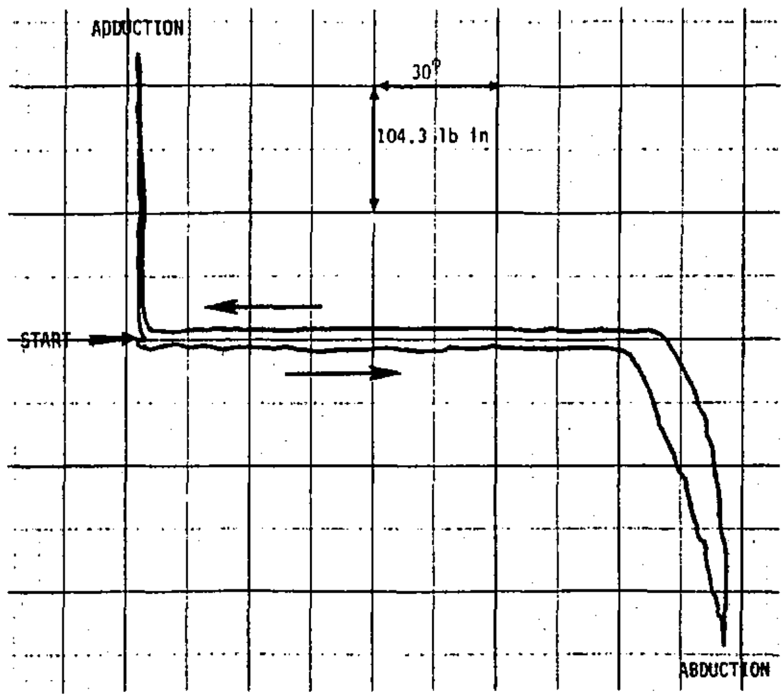

RIGHT SHOULDER

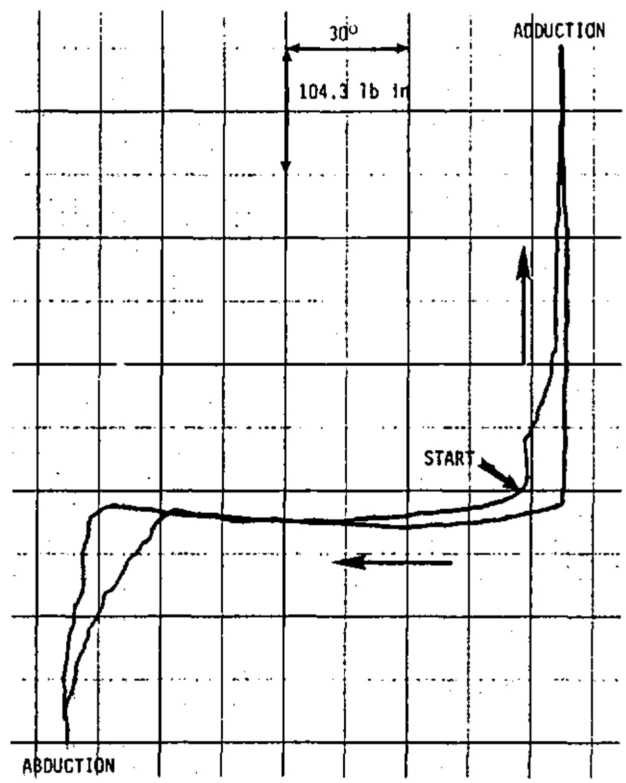

LEFT SHOULDER

FIGURE 15. SHOULDER ABDUCTION-ADDUCTION AT 0° FLEXION FOR SEATED MANIKIN

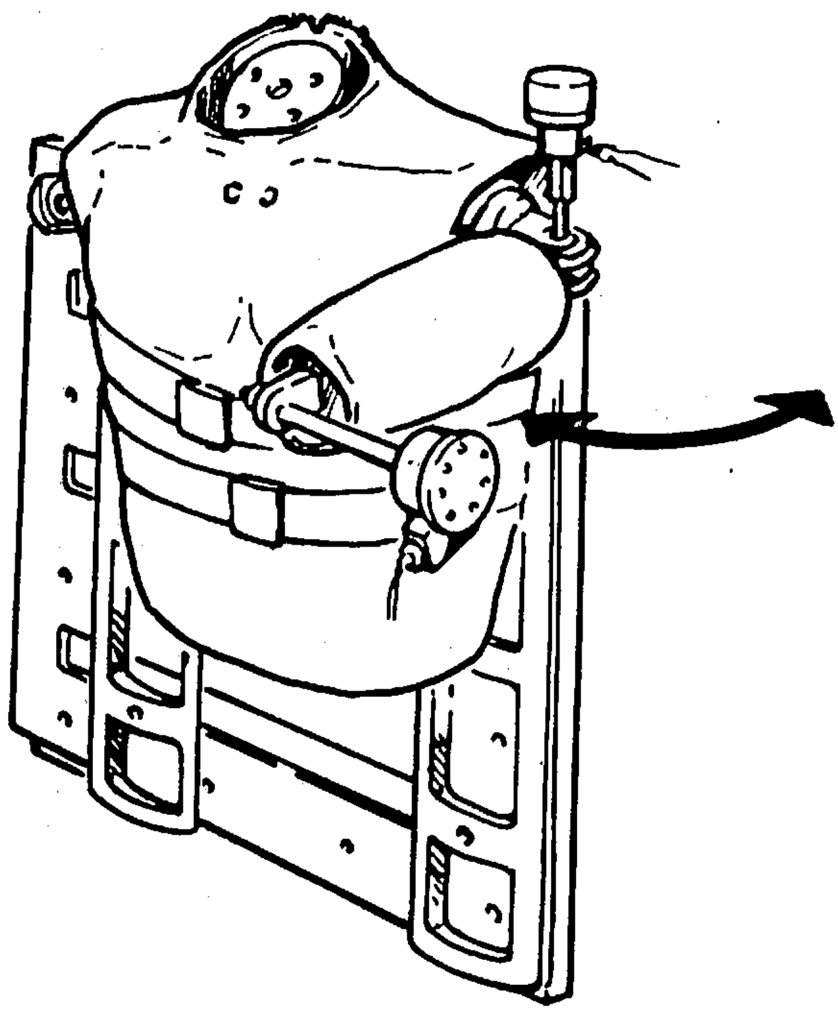

Figure 16. Shoulder Abduction-Adduction at 90° Flexion Test Setup

The resulting curves for the 90° flexion abduction-adduction tests are presented in Figures 17 and 18. Free range of motion were slightly larger for the standing manikin as were the total range of motion values indicating a structural difference between the two manikins. The range of motion for adduction motion revealed soft stops due to skin to skin interaction of the upper arm with the soft covering of the upper thoracic region.

The flexion-extension tests performed at 0 and 45 degrees initial adduction angles required the use of a fixture designed to track the joint rotation of the flexion-extension joint axis. As illustrated in Figure 19, the potentiometer shaft was centered on the joint axis with a V-shaped attachment. The test was performed with the thorax securely strapped and supported while on its side.

Figures 20 through 23 display the resulting joint resistance versus angle of rotation curves for the flexion-extension. Range of motion values were similar for the 0 and 45° position, for right and left joints and for both manikins.

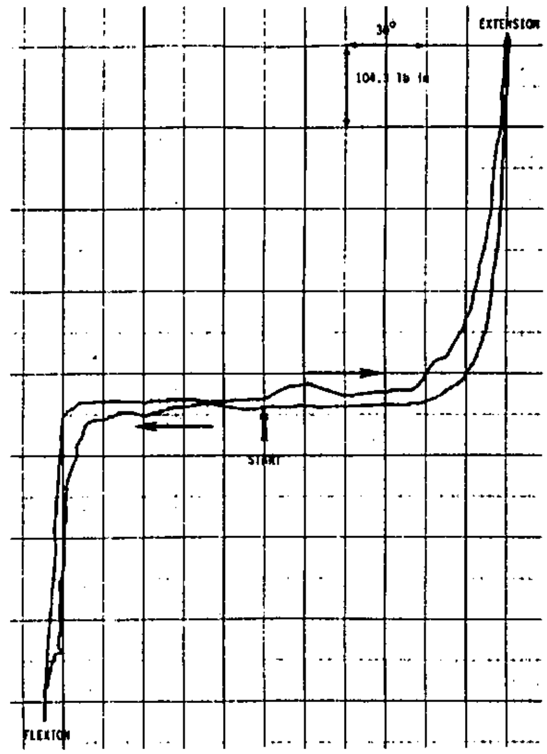

RIGHT SHOULDER

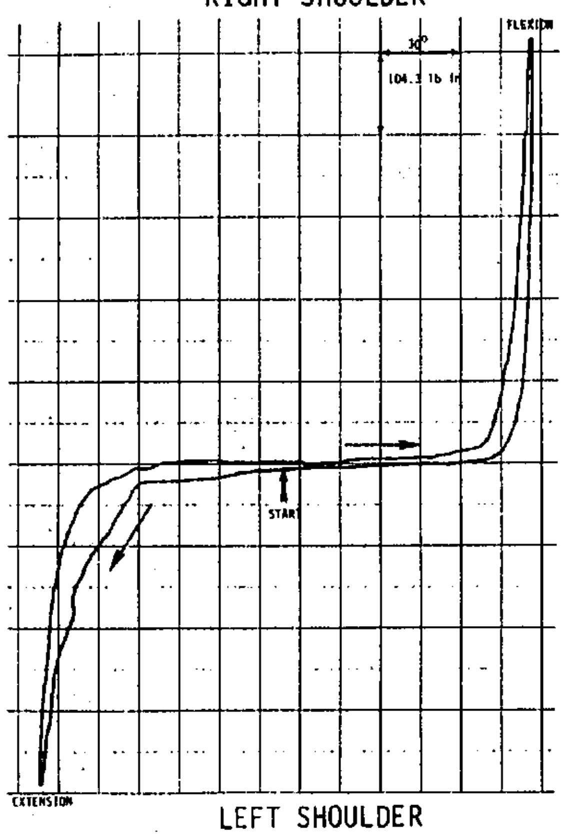

LEFT SHOULDER

FIGURE 17. SHOULDER ABDUCTION-ADDUCTION AT 90° FLEXION FOR STANDING MANIKIN

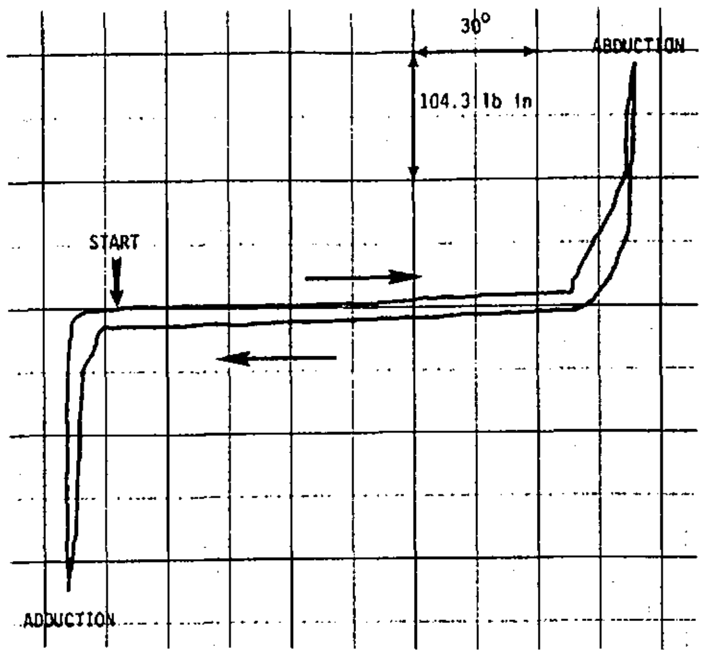

RIGHT SHOULDER

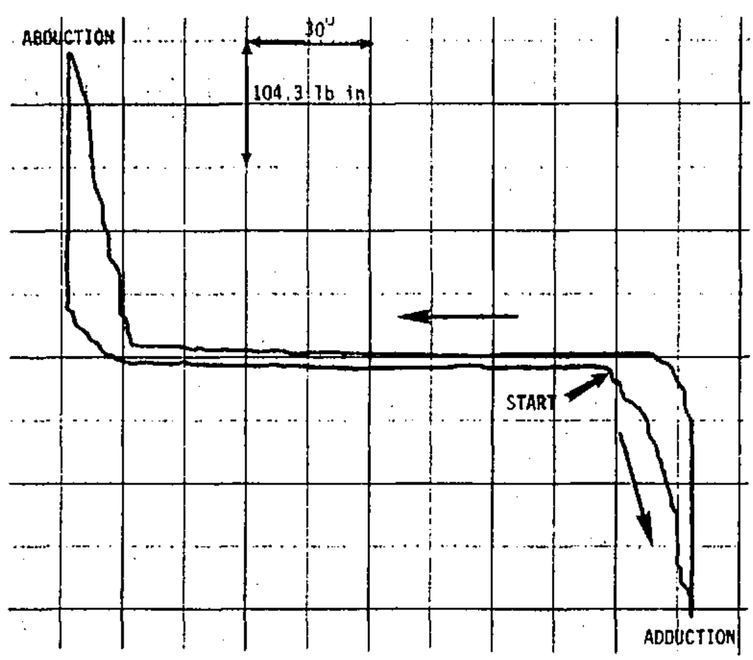

LEFT SHOULDER

FIGURE 18. SHOULDER ABDUCTION-ADDUCTION AT 90° FLEXION FOR SEATED MANIKIN

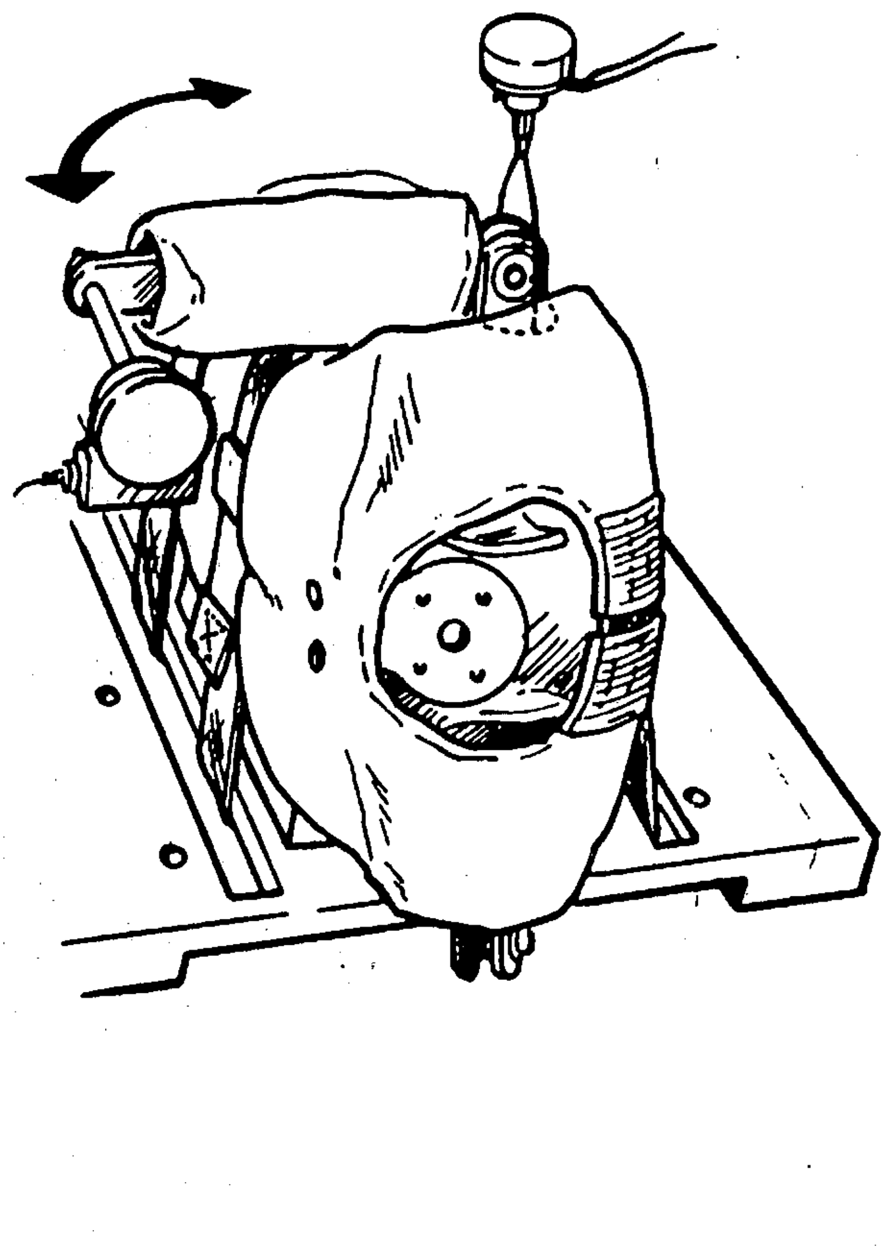

Figure 19. Shoulder Flexion-Extension at 0° Abduction Test Setup

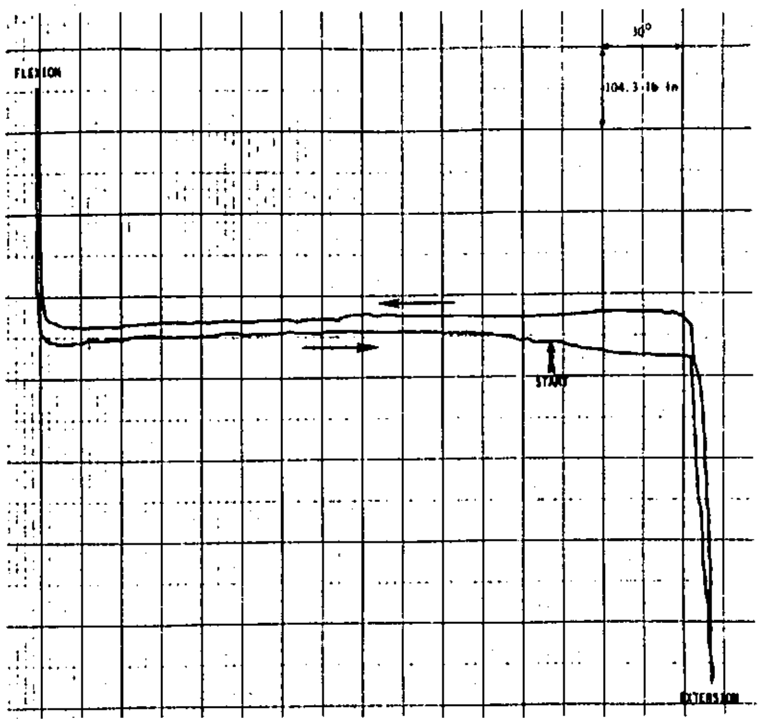

RIGHT SHOULDER

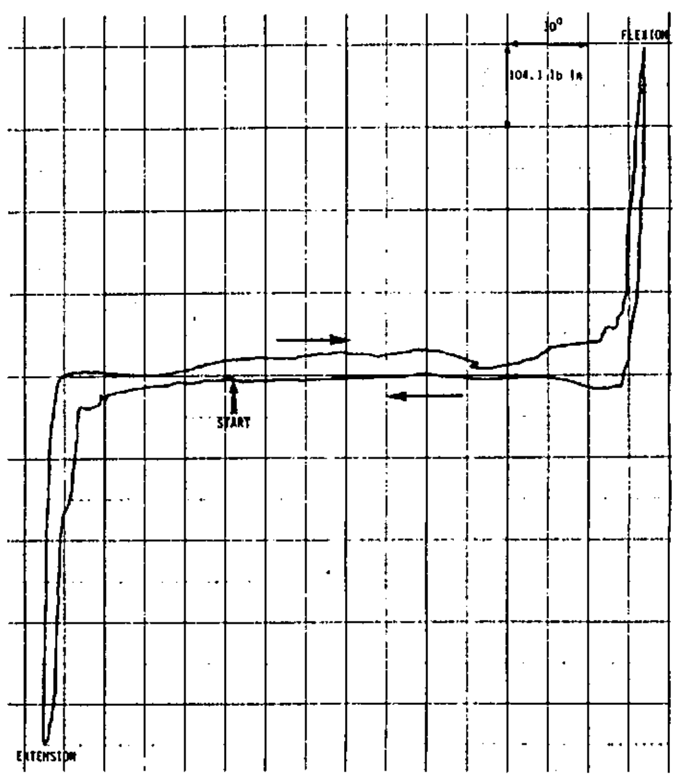

LEFT SHOULDER

FIGURE 20. SHOULDER FLEXION-EXTENSION AT 0° ABDUCTION FOR STANDING MANIKIN

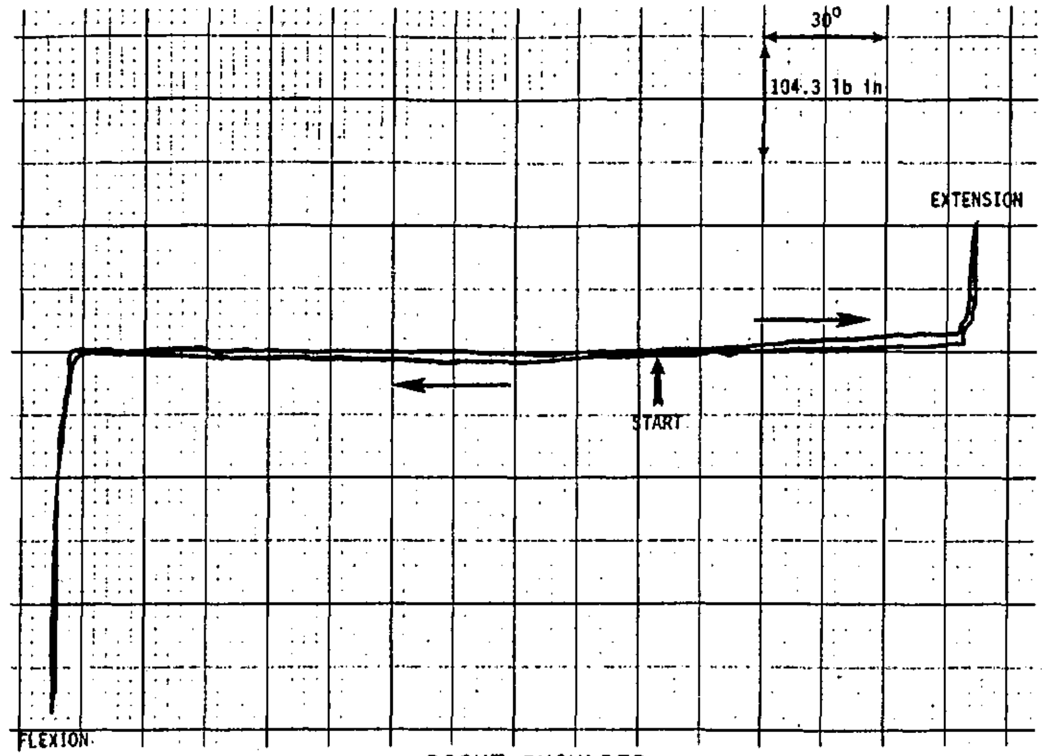

RIGHT SHOULDER

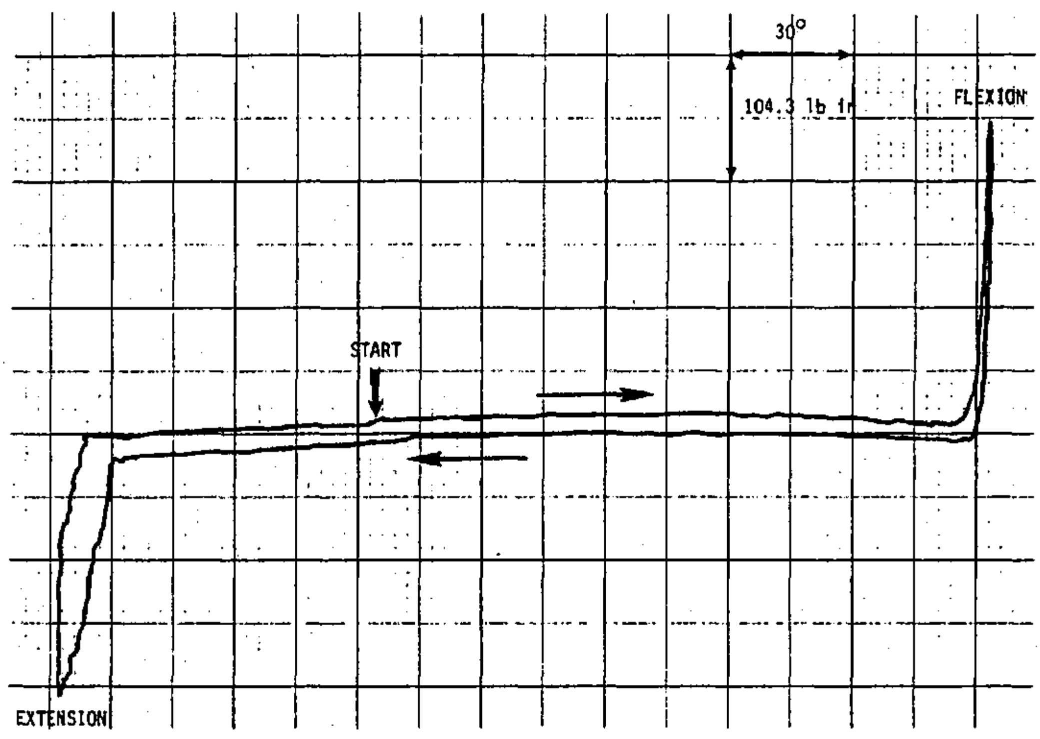

LEFT SHOULDER

FIGURE 21. SHOULDER FLEXION-EXTENSION AT 0° ABDUCTION FOR SEATED MANIKIN

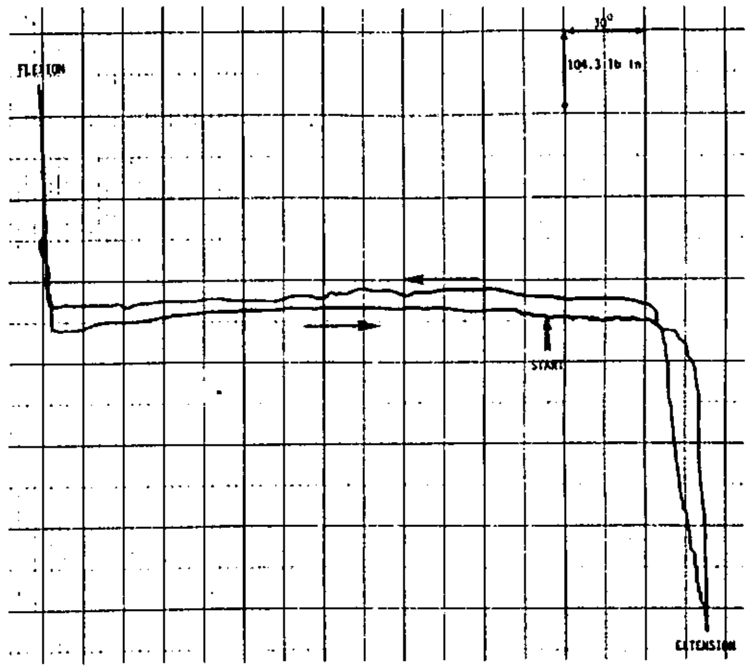

RIGHT SHOULDER

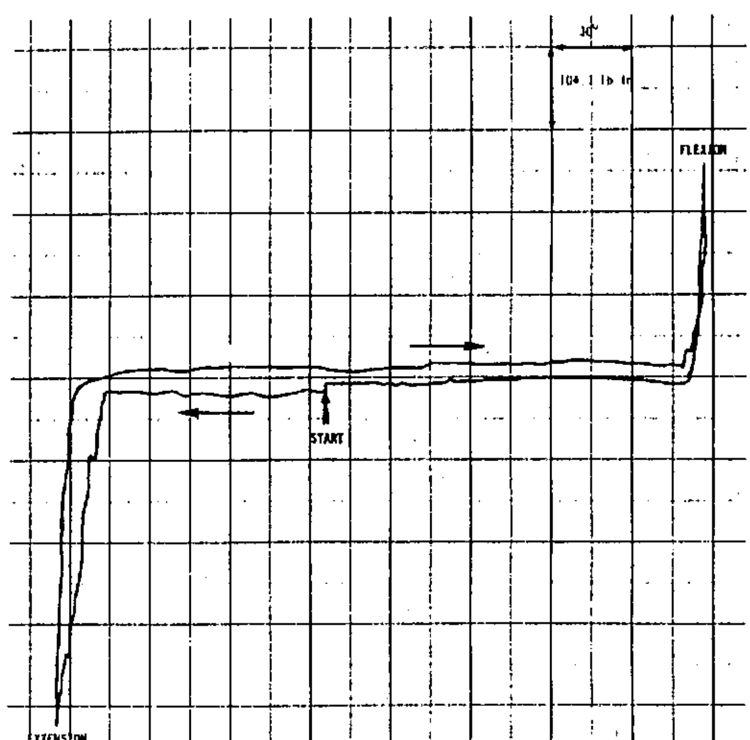

LEFT SHOULDER

FIGURE 22. SHOULDER FLEXION-EXTENSION AT 45° ABDUCTION FOR STANDING MANIKIN

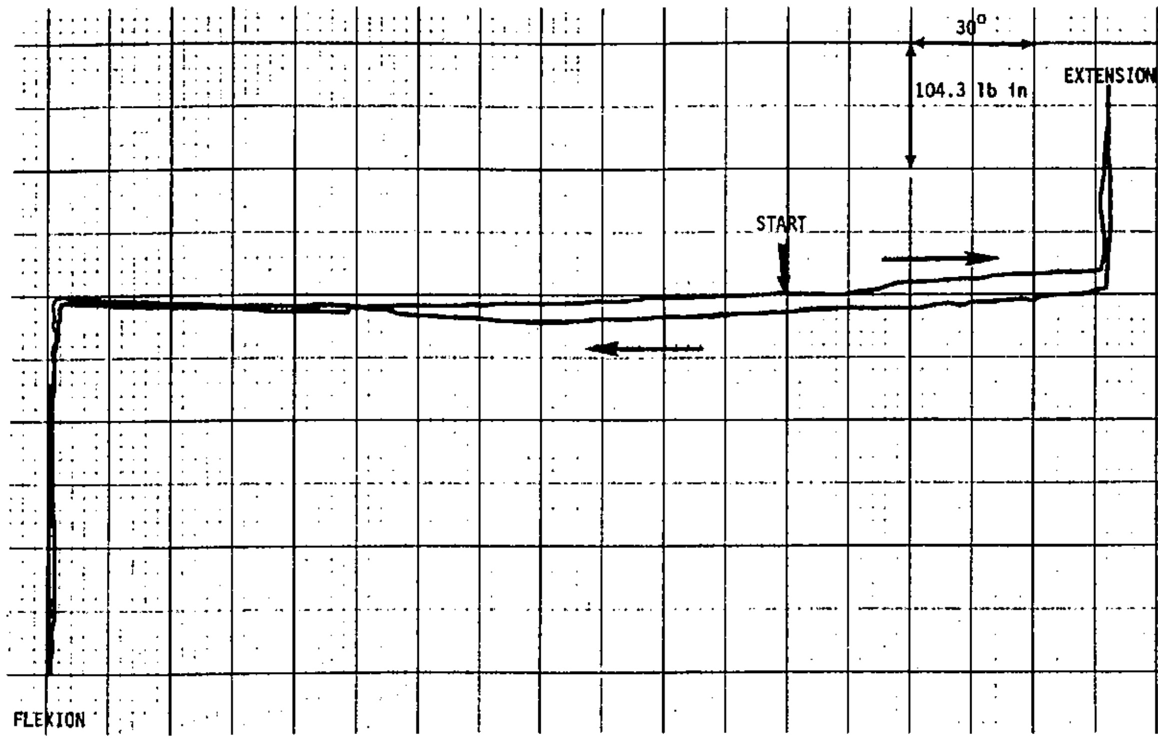

RIGHT SHOULDER

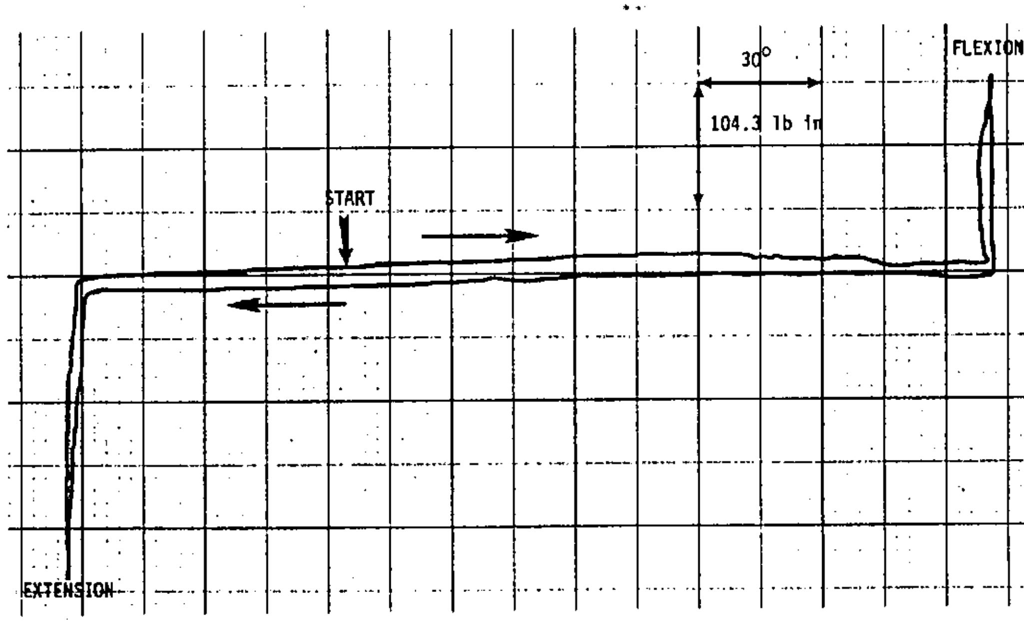

LEFT SHOULDER

FIGURE 23. SHOULDER FLEXION-EXTENSION AT 45° ABDUCTION FOR SEATED MANIKIN

2.1.4.1.3.2 Elbow

The elbow joints allow relative rotational motion of the forearm with respect to the upper arm. Flexion-extension movement is provided by a pin joint while a sleeve joint allows rotation about the long bone axis. The medial angle of rotation is a full 360°for both manikins while flexion-extension motion of the forearm is limited by hard stops and soft covering interference. The flexion-extension joint torque characteristics were tested with initial angles of 0°, 90°, 180°, and 270° of medial rotation (rotation of the forearm toward the body). With the forearm attached, the upper arm was clamped securely to the holding fixture aligning the flexion-extension joint vertically as illustrated in Figure 24. The elbow joint was placed at the edge of the holding fixture where full extension of the forearm would be possible. Using the fixture designed to fit the head of the bolt, the potentiometer shaft was aligned with the joint axis. The load cell was attached to the distal clevice of the forearm, aligning the load cell axis horizontally and perpendicular to the forearm long axis. Using the load cell to apply the load, the forearm was rotated through the full range of motion.

The resulting plots of flexion-extension tests for all four angles of medial rotation are presented in Figures 25 through 32 for the left and right elbow joints for both manikins. Range of motion results were higher for the seated manikin. Generally, for both manikins during the 0 degree rotation flexion-extension tests, extension was limited by hard stops at about 15 degrees. Flexion generally had a free range of motion of about 90 degrees. At this point, increasing resistance to free motion was produced by soft covering interference of the upper arm with the forearm. For the 180° medial rotation flexion-extension tests, the ranges of motion are similar to those found with a 0° rotation angle for both manikins. For this set of tests, the soft skin interactions during flexion provide a nonlinear torque response and interaction with a hard stop is not obvious.

For the 90° and 270° initial medial rotation flexion-extension tests, the ranges of motion were again larger for the seated manikin. Free

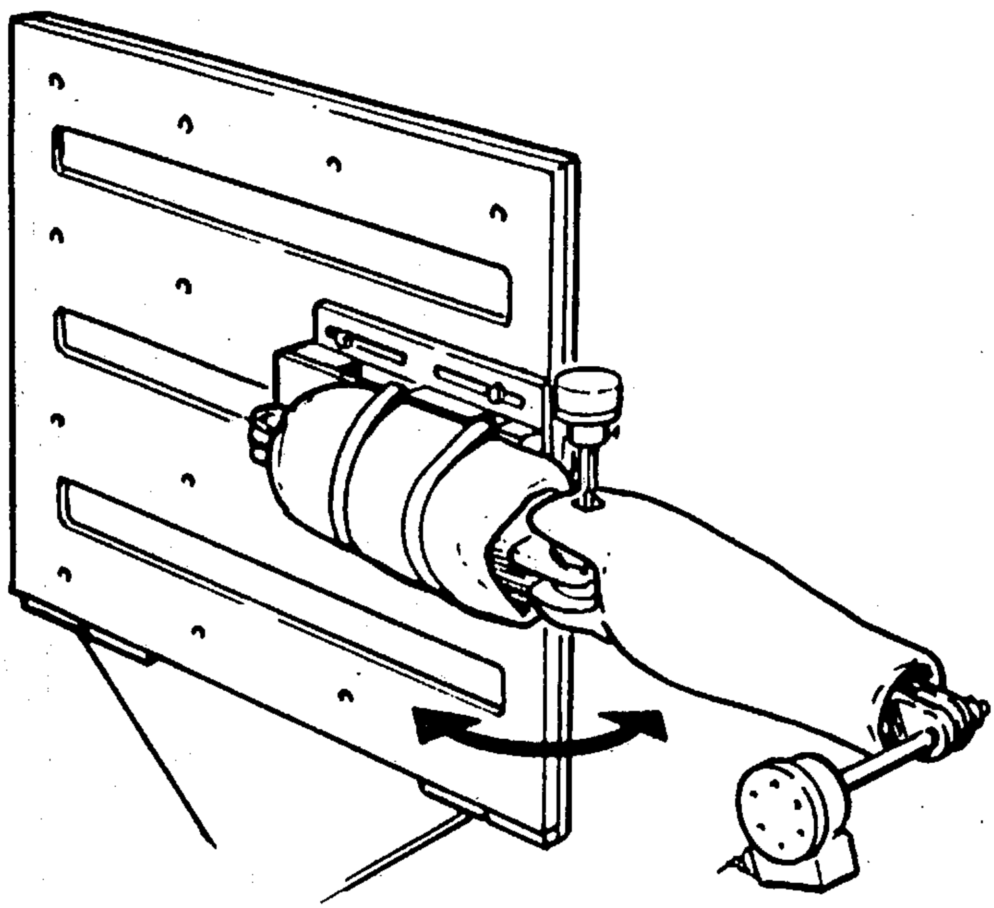

Figure 24. Elbow Flexion-Extension at 90° Medial Rotation Test Setup

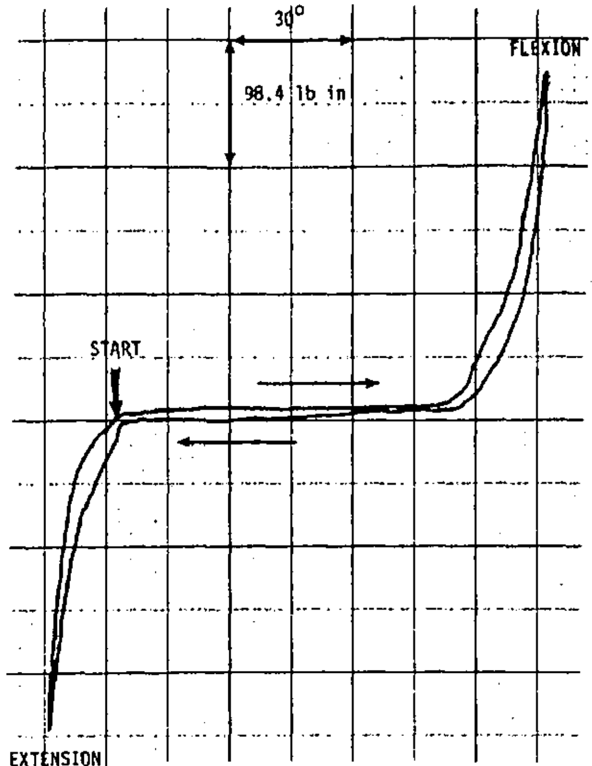

RIGHT ELBOW

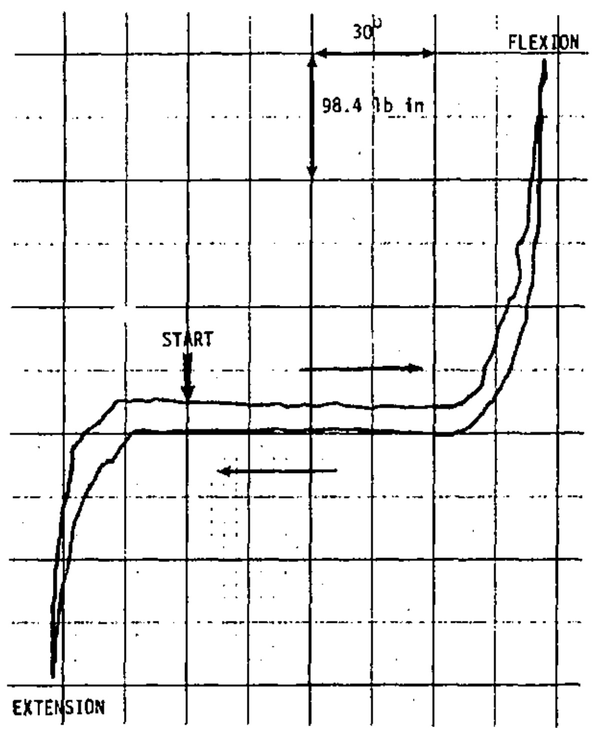

LEFT ELBOW

FIGURE 25. ELBOW FLEXION-EXTENSION AT 0° ROTATION FOR STANDING MANIKIN

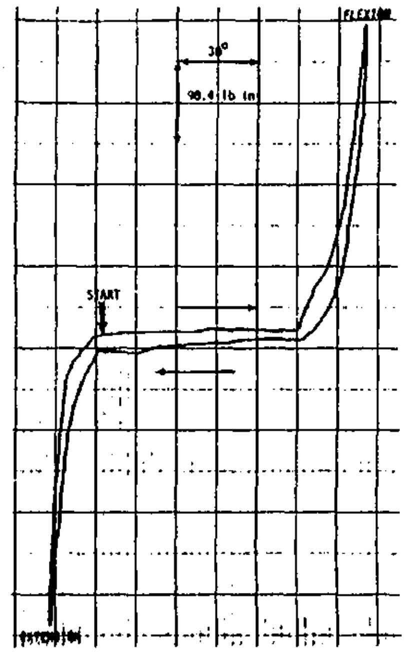

RIGHT ELBOW

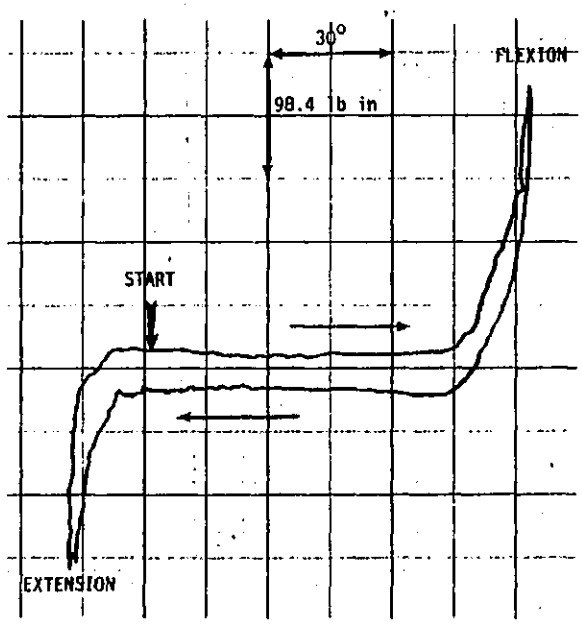

LEFT ELBOW

FIGURE 26. ELBOW FLEXION-EXTENSION AT 90° MEDIAL ROTATION FOR STANDING MANIKIN

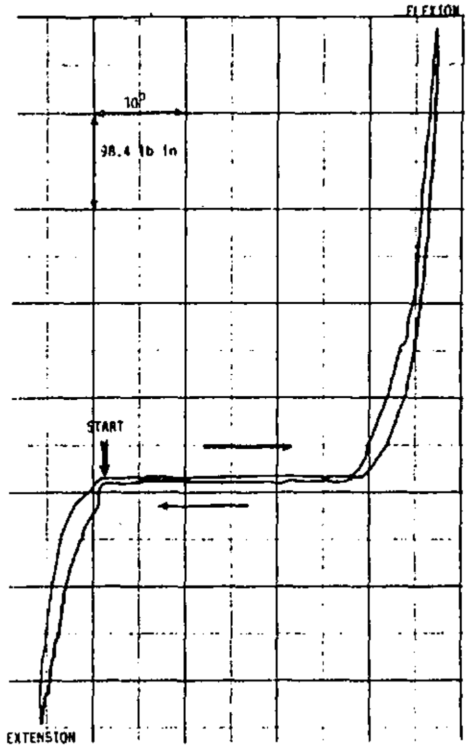

RIGHT ELBOW

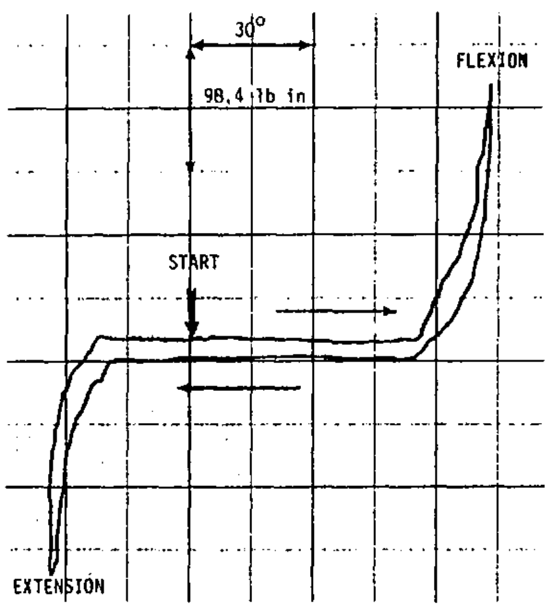

LEFT ELBOW

FIGURE 27. ELBOW FLEXION-EXTENSION AT 180° MEDIAL ROTATION FOR STANDING MANIKIN

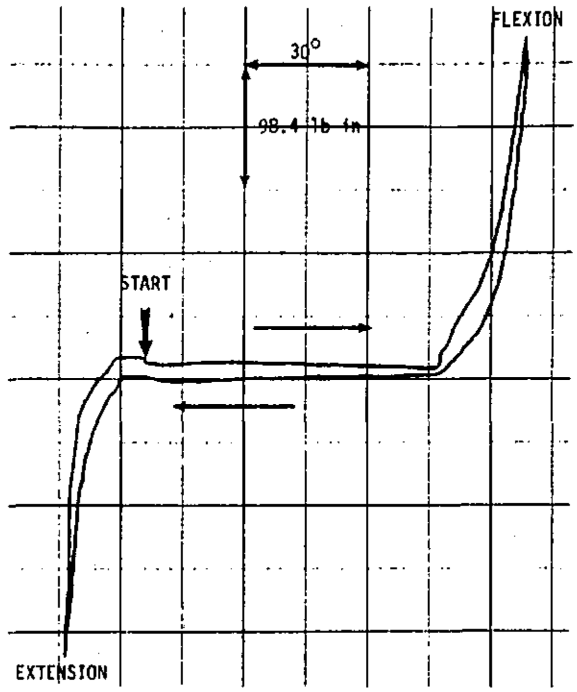

RIGHT ELBOW

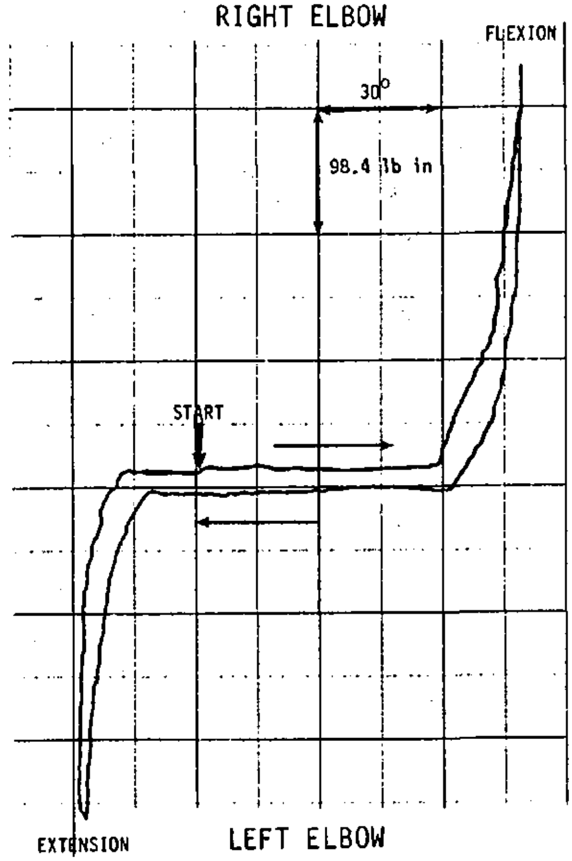

LEFT ELBOW

FIGURE 28. ELBOW FLEXION-EXTENSION AT 270° MEDIAL ROTATION FOR STANDING MANIKIN

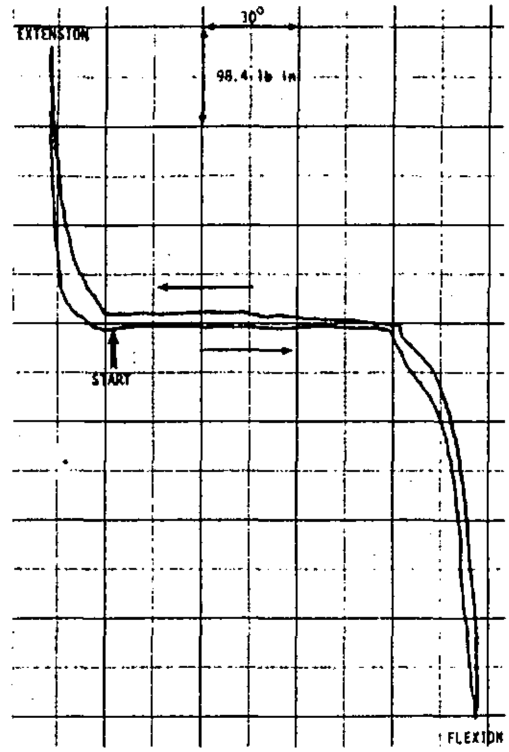

RIGHT ELBOW

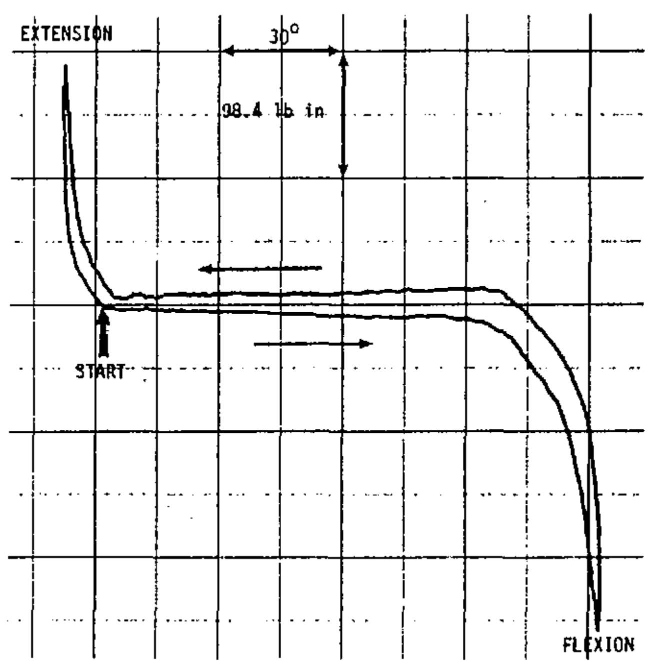

LEFT ELBOW

FIGURE 29. ELBOW FLEXION-EXTENSION AT 0° ROTATION FOR SEATED MANIKIN

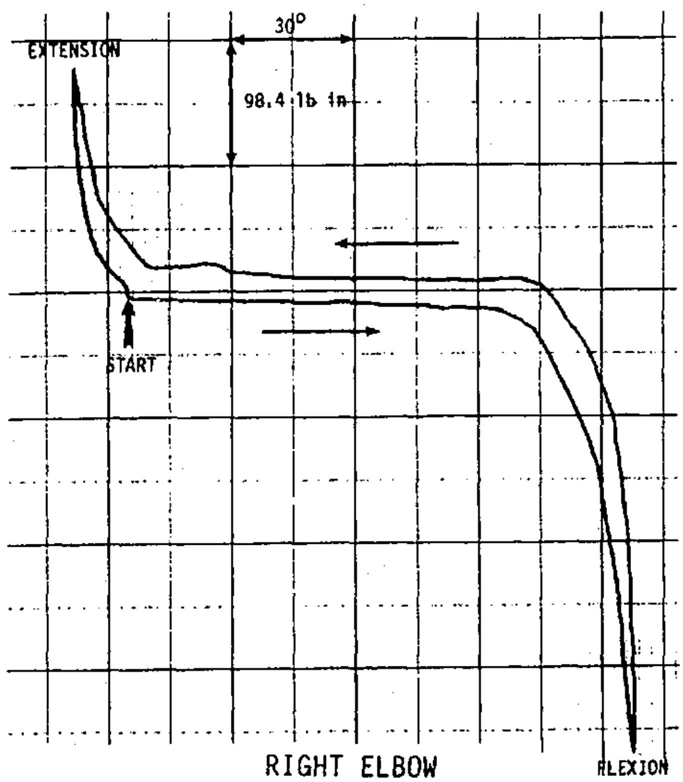

RIGHT ELBOW

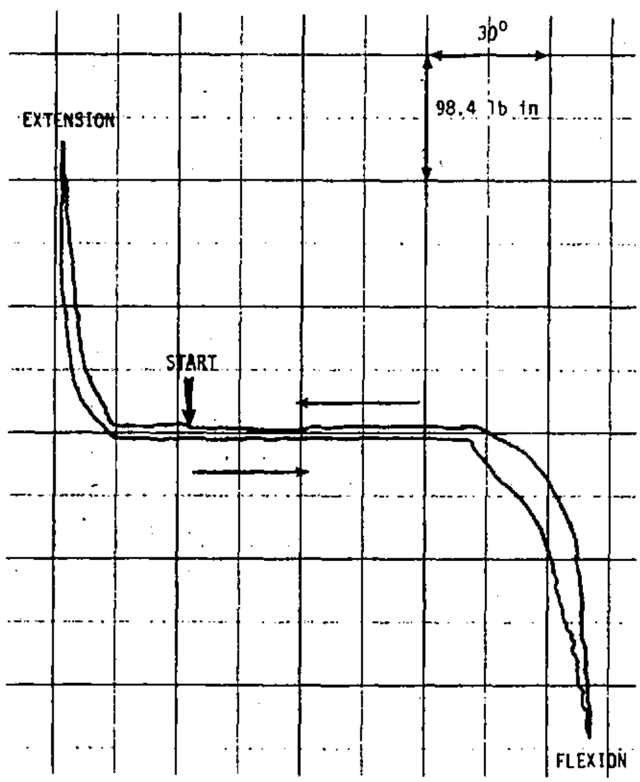

LEFT ELBOW

FIGURE 30. ELBOW FLEXION-EXTENSION AT 90° MEDIAL ROTATION FOR SEATED MANIKIN

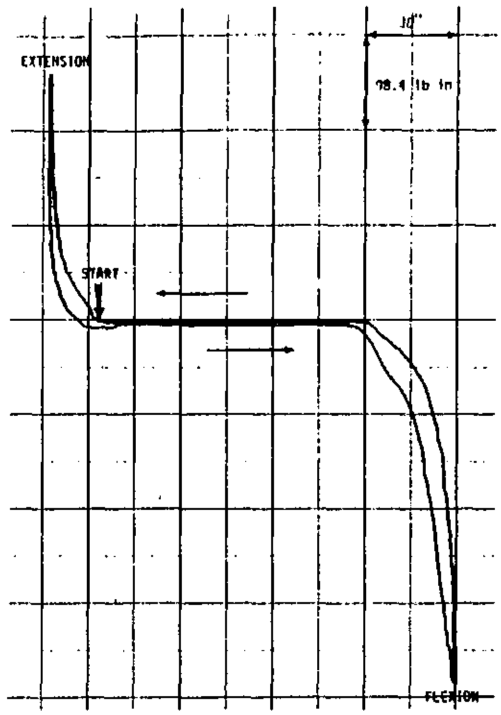

RIGHT ELBOW

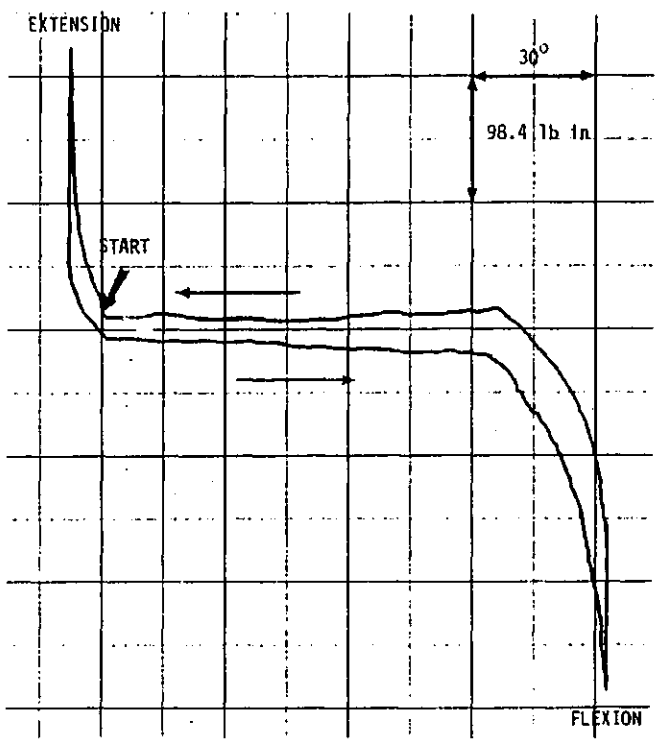

LEFT ELBOW

FIGURE 31. ELBOW FLEXION-EXTENSION AT 180° MEDIAL ROTATION FOR SEATED MANIKIN

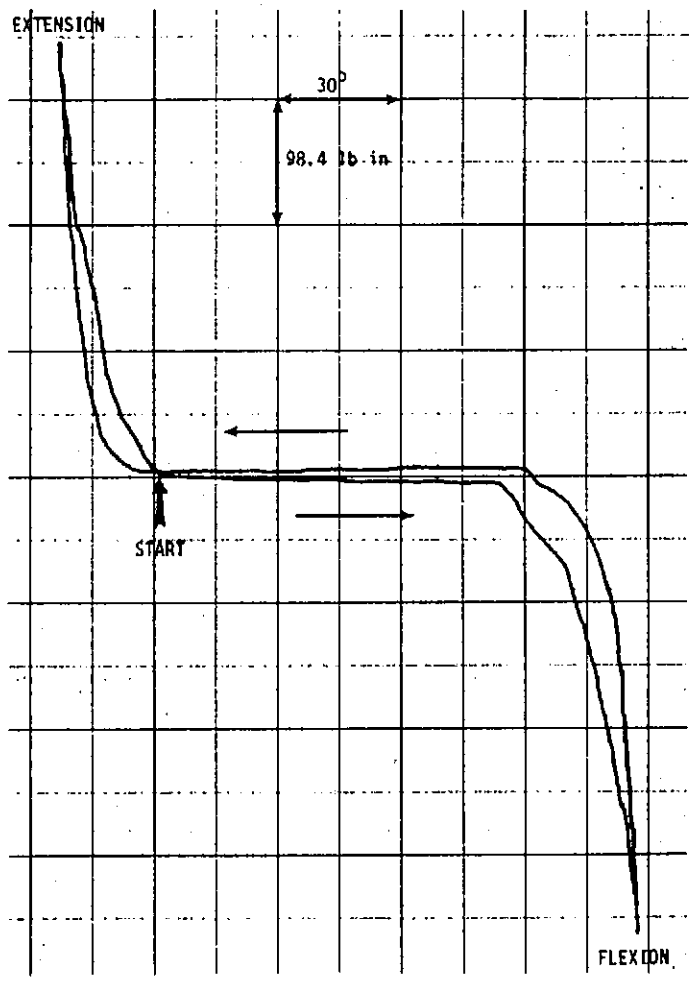

LEFT ELBOW

FIGURE 32. ELBOW FLEXION-EXTENSION AT 270° MEDIAL ROTATION FOR SEATED MANIKIN (NO RIGHT COMPLIMENT)

range of motion values were also greater for the seated manikin indicating a structural difference between the two manikins. The extension hard stops were not as obvious as those found in the 0° and 180° medial rotation flexion-extension tests due to increased soft covering interactions.

2.1.4.1.3.3 Wrist

The wrist pin joint allows flexion-extension motion of the hand with respect to the forearm. An additional sleeve joint allows the hand to rotate about the long axis of the forearm. Flexion-extension motion was tested with 0°, 90°, 180°, and 270° of medial rotation. Illustrated in Figure 33 is a left wrist at 90° medial rotation during a flexion-extension test. The forearm was used as the rotating segment since the elbow clevice is more easily adapted to the load cell. A rubber wedge, which fit the contour of the palm, was used to assist in rigidly securing the hand to the support structure.

The hand was positioned so that the wrist joint axis was oriented vertically to eliminate the effects of gravity on the applied torque. The potentiometer shaft was directly aligned with the axis through a fixture designed to fit the head of the bolt. The load cell was attached to the proximal end of the forearm with a rod designed to fit the clevice.

The resulting plots of the flexion-extension tests for left and right wrist joints of both manikins are found in Figures 34 through 41. Range of motion results indicate significant differences between the two manikins, but relative consistency for a given manikin between left and right joints. The seated manikin generally showed a total range of motion 40 to 50 degrees greater than the standing manikin. For these tests, the larger torque values resulted in larger ranges of motion, indicating that the differences in the ranges of motion are a function of the extent to which soft covering of the forearm was compressed by the palm of the hand. Slopes of the force/rotation curves near the limits of travel for the seated manikin appear to be larger than those

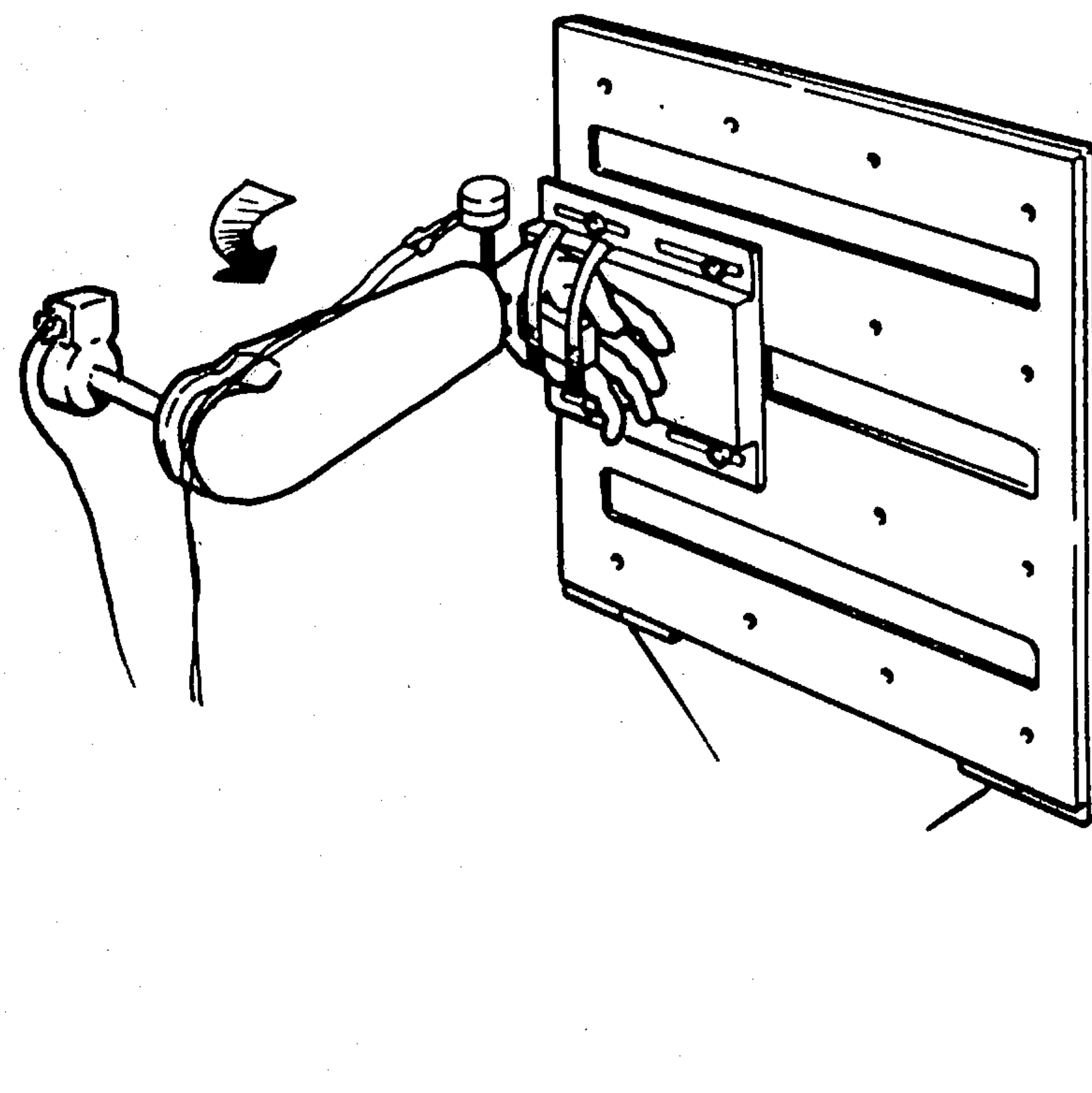

Figure 33. Wrist Flexion-Extension at 90° Medial Rotation Test Setup

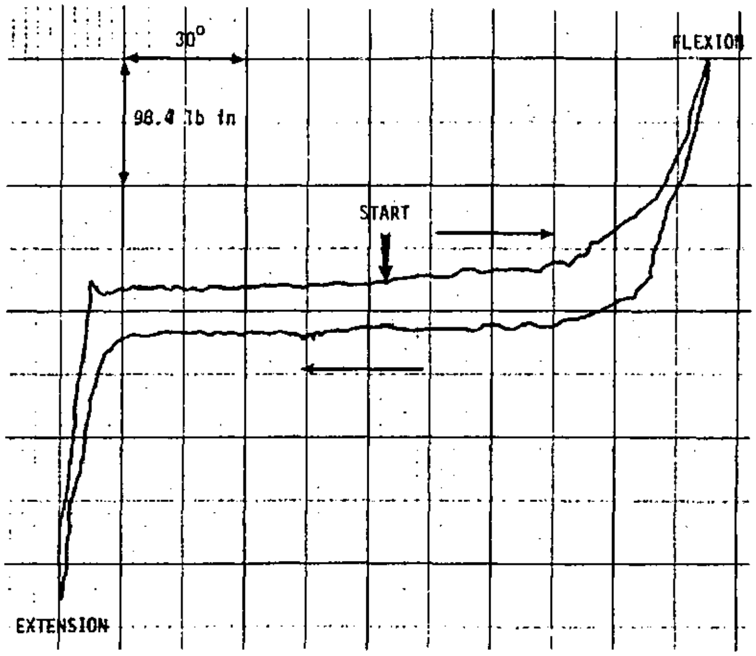

RIGHT WRIST

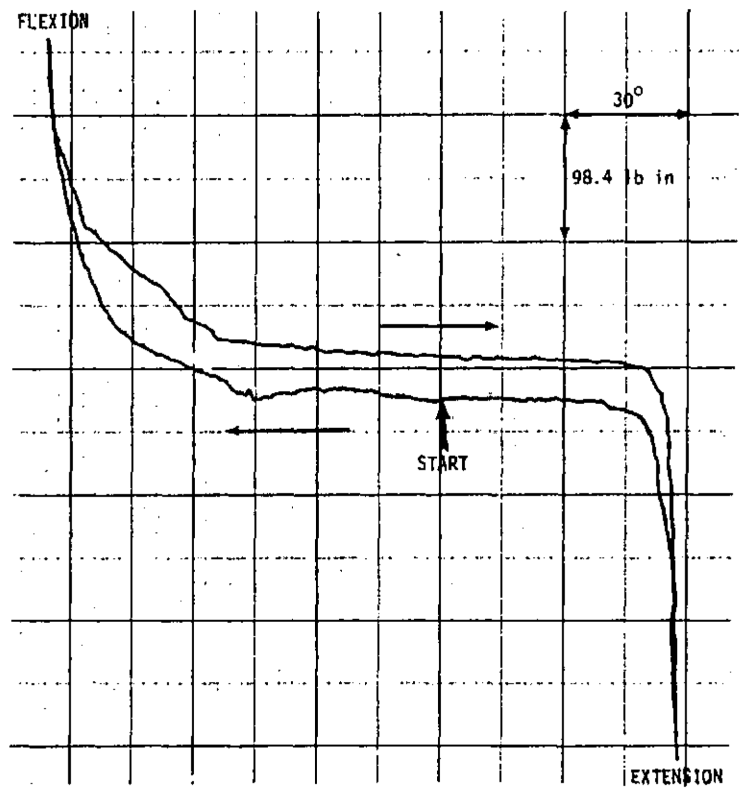

LEFT WRIST

FIGURE 34. WRIST FLEXION-EXTENSION AT 0° ROTATION FOR STANDING MANIKIN

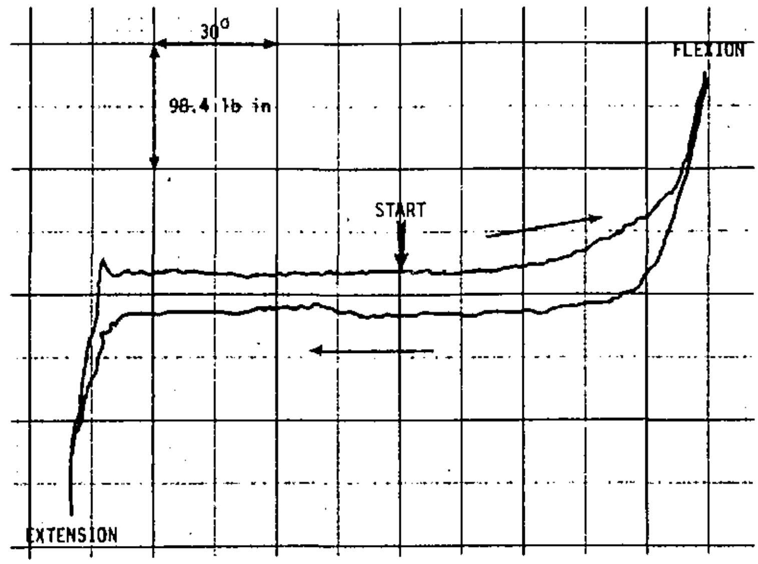

RIGHT WRIST

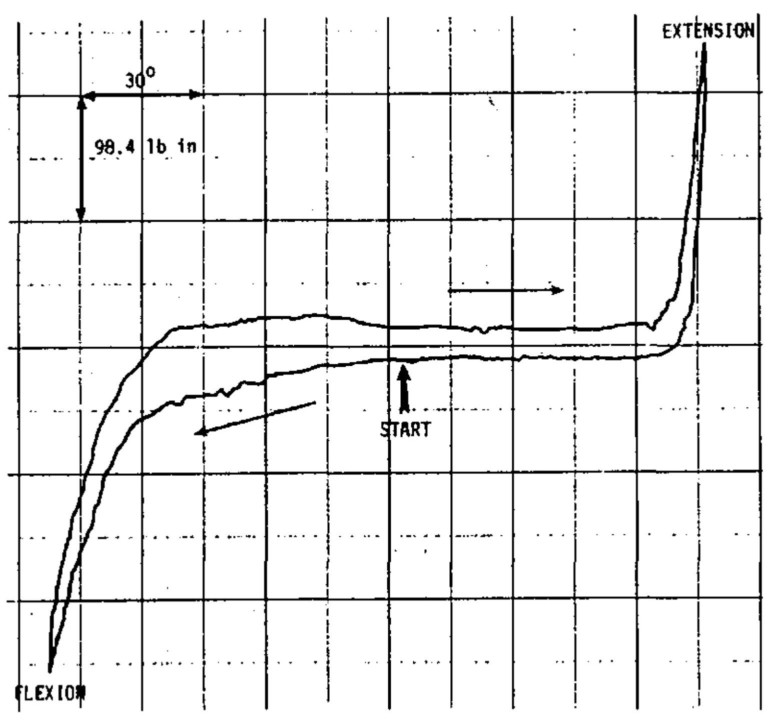

LEFT WRIST

FIGURE 35. WRIST FLEXION-EXTENSION AT 90° MEDIAL ROTATION FOR STANDING MANIKIN

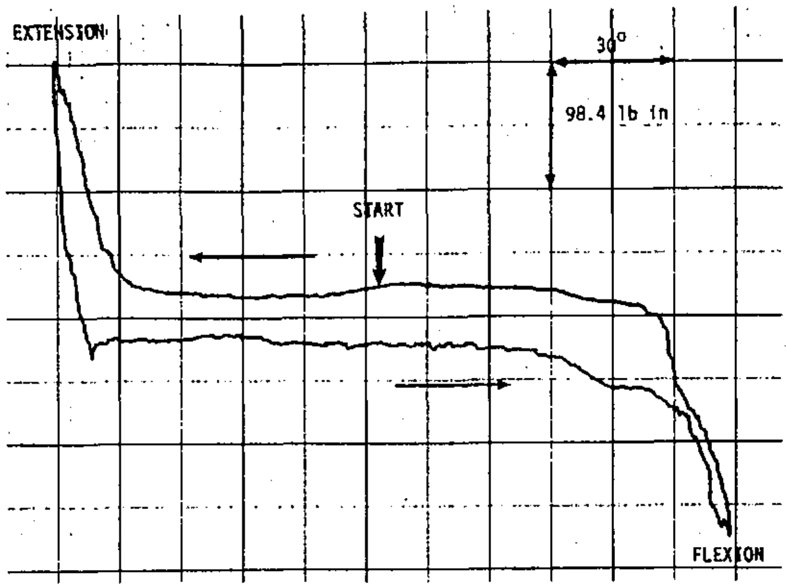

RIGHT WRIST

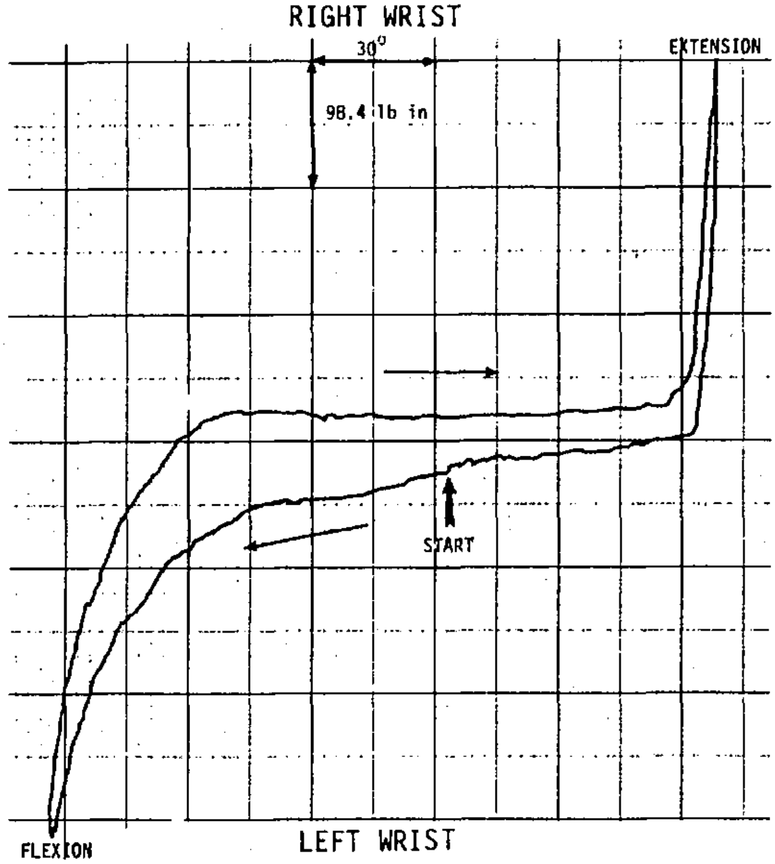

LEFT WRIST

FIGURE 36. WRIST FLEXION-EXTENSION AT 180° MEDIAL ROTATION FOR STANDING MANIKIN

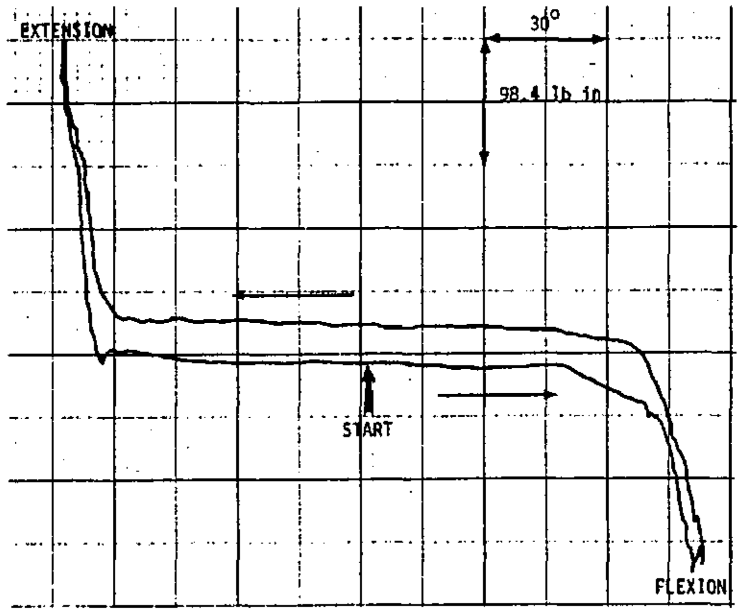

RIGHT WRIST

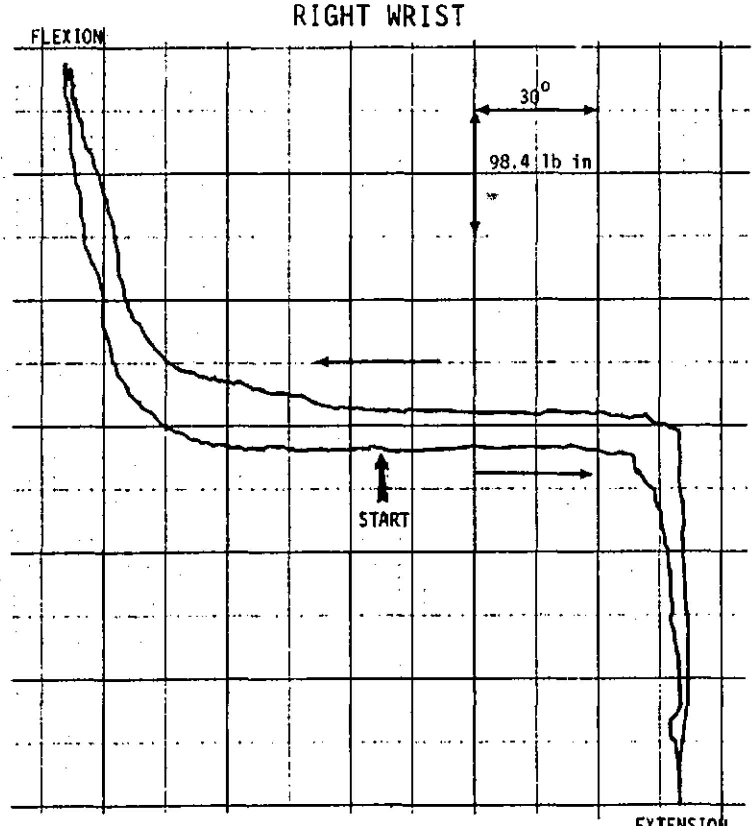

LEFT WRIST

FIGURE 37. WRIST FLEXION-EXTENSION AT 270° MEDIAL ROTATION FOR STANDING MANIKIN

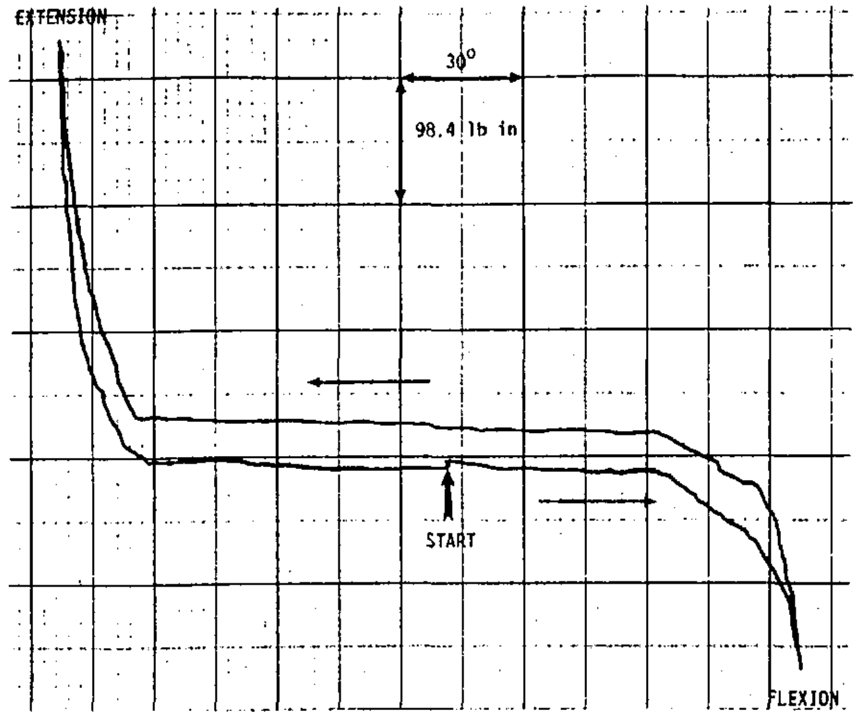

RIGHT WRIST

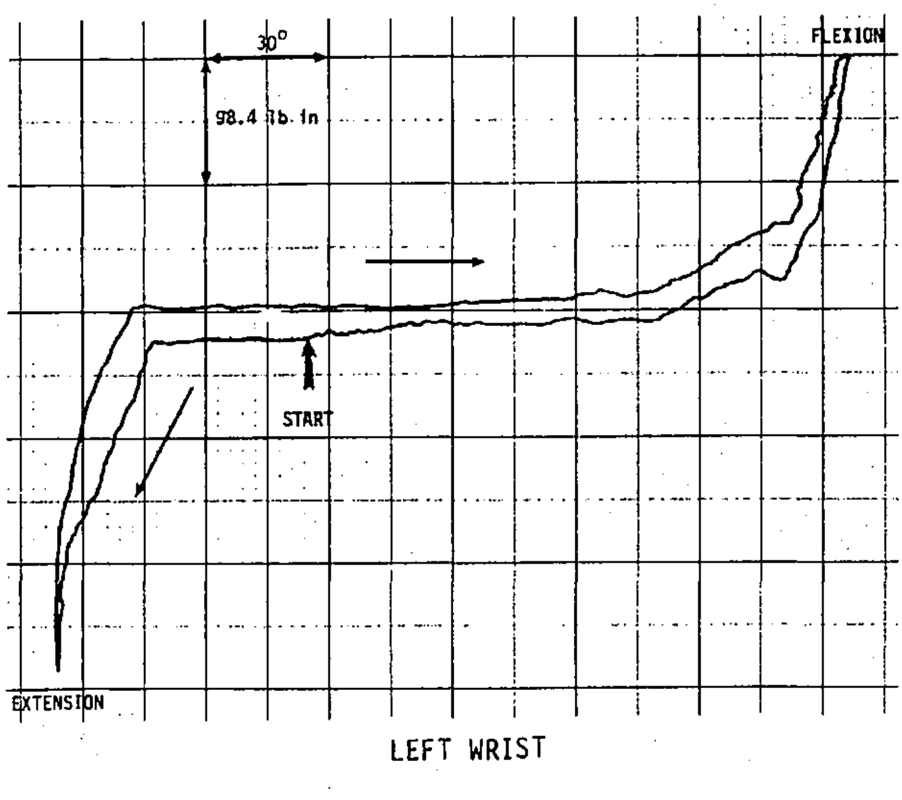

LEFT WRIST

FIGURE 38. WRIST FLEXION-EXTENSION AT 0° ROTATION FOR SEATED MANIKIN

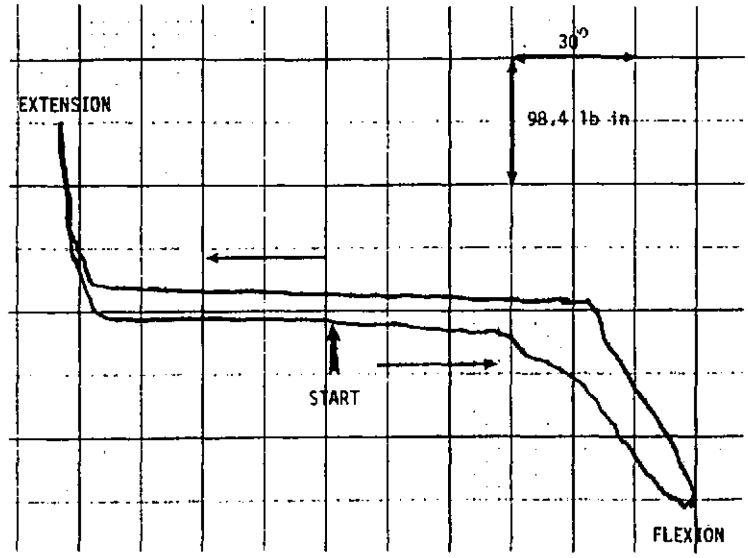

RIGHT WRIST

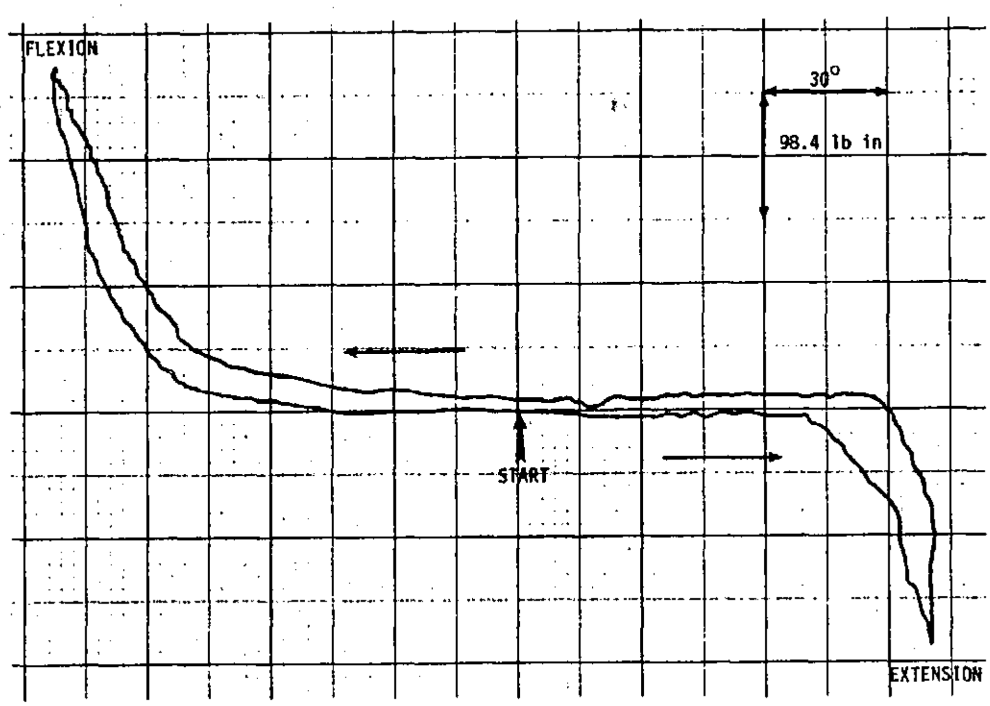

LEFT WRIST

FIGURE 39. WRIST FLEXION-EXTENSION AT 90° MEDIAL ROTATION FOR SEATED MANIKIN

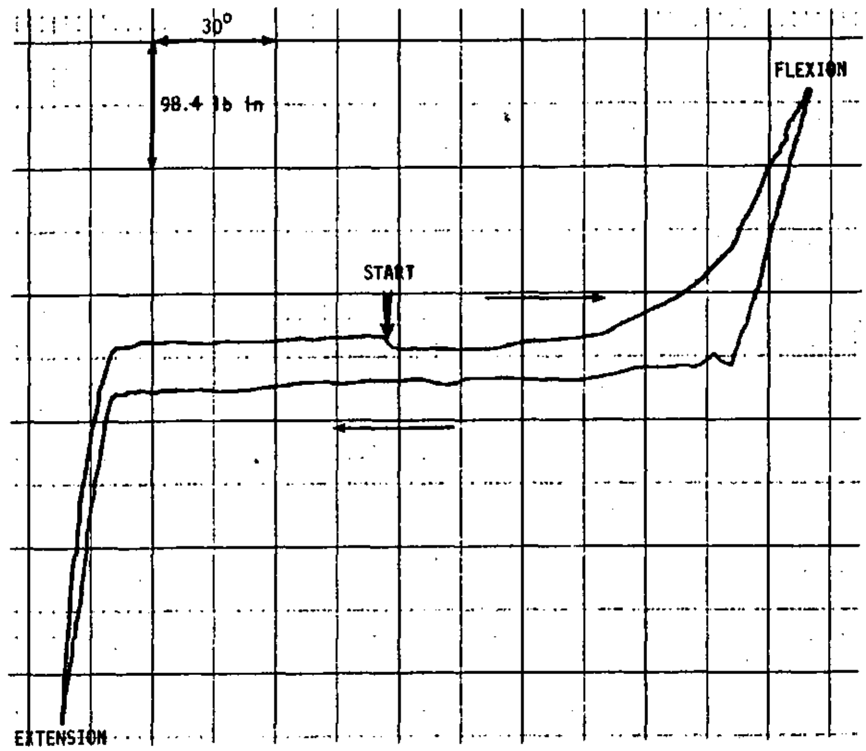

RIGHT WRIST

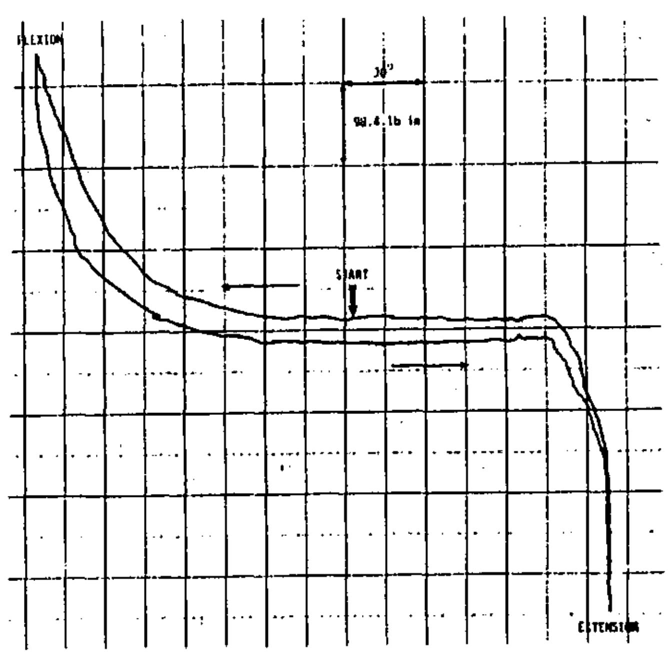

LEFT WRIST

FIGURE 40. WRIST FLEXION-EXTENSION AT 180° MEDIAL ROTATION FOR SEATED MANIKIN

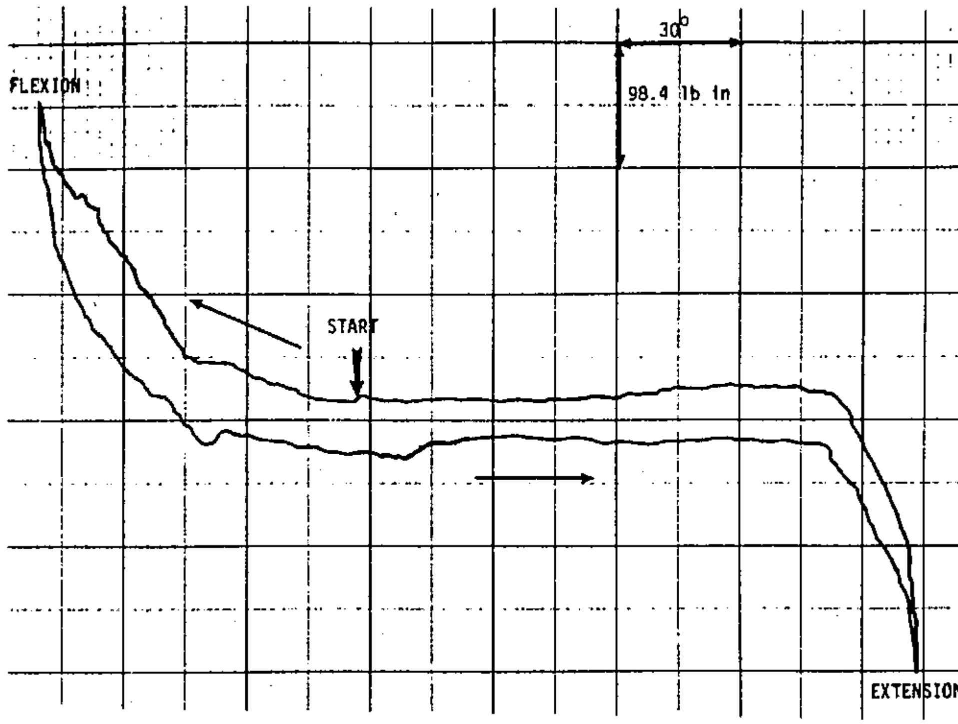

RIGHT WRIST

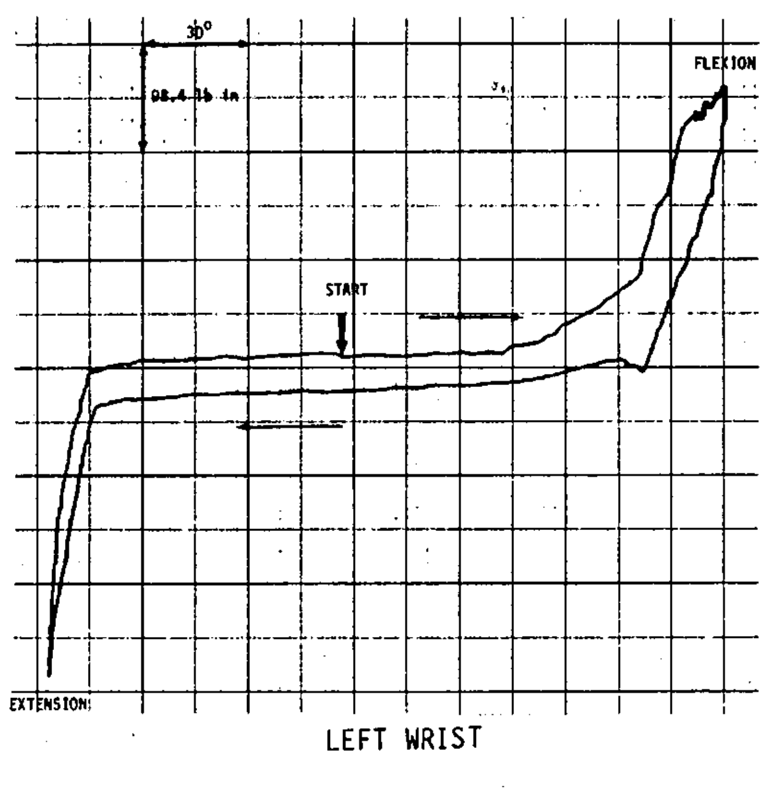

LEFT WRIST

FIGURE 41. WRIST FLEXION-EXTENSION AT 270° MEDIAL ROTATION FOR SEATED MANIKIN

found with the standing manikin which indicates that the wrist was rotated closer to the flexion hard stop.

For the 0° and 180° medial rotation flexion-extension tests, the extension range of motion was governed by an obvious hard stop as is evident in the plotted results. The 90° and, to some extent, the 270° medial rotation flexion-extension plots, however, display a more nonlinear response at the maximum deflection of extension, a result of soft covering interactions.

2.1.4.1.3.4 Knee

The knee joint, a pin joint, allows flexion-extension motion of the lower leg with respect to the upper leg. With the upper leg securely strapped to the holding fixture and the knee joint axis oriented vertically, the lower leg was rotated through its range of motion as illustrated in Figure 42. The knee joint was positioned at the edge of the holding fixture to allow a full unobstructed range of extension motion. The potentiometer was directly aligned with the knee axis and the load cell was attached to the distal end of the lower leg with an attachment fabricated to fit the ankle joint. With the load cell axis positioned horizontally and perpendicular to the axis of the rotating segment, the lower leg was manually rotated through the full range of motion.

The resulting data plots are found in Figures 43 and 44. While the right knee of the standing manikin was not tested, two flexion-extension tests of the left knee were performed on the standing manikin to indicate the degree to which the range of motion is a function of torque applied to the knee joint. The plot displaying the larger range of motion also shows a greater force applied to the load cell. Although the free range of motion and extension angles appear similar, the angle of flexion rotation is increased with increasing load. It is noted that the ranges of motion were similar for both the standing and seated manikin.

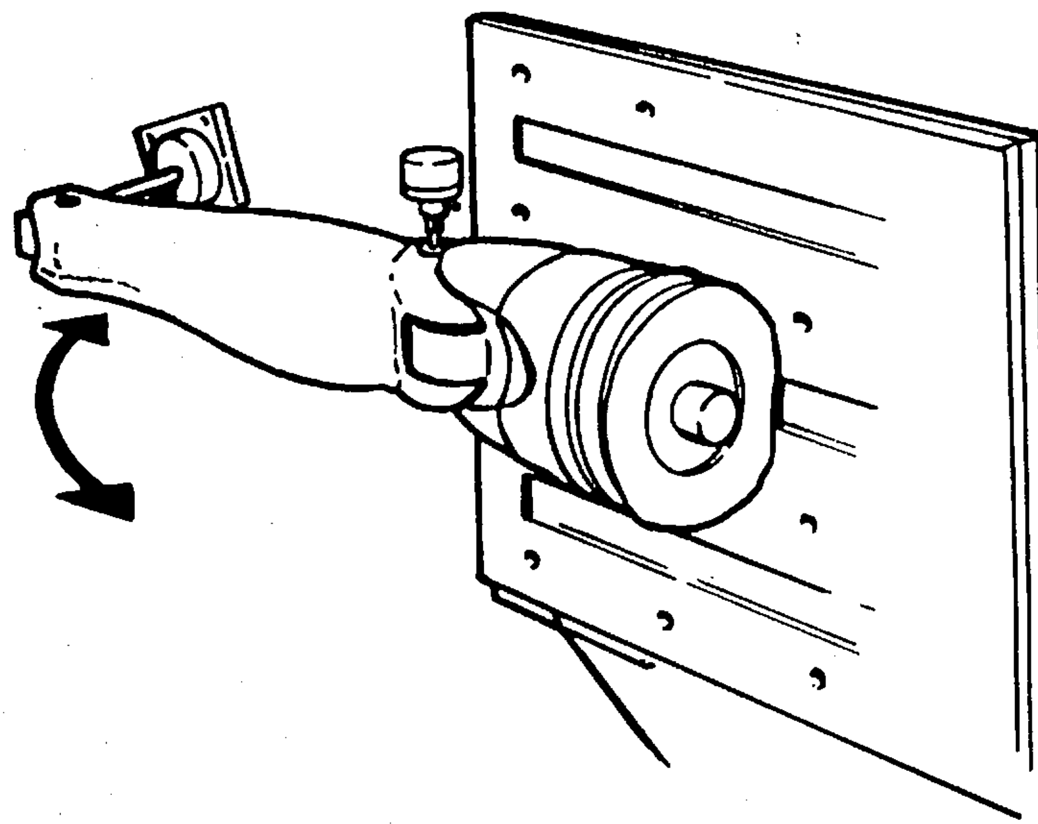

Figure 42. Knee Flexion-Extension Test Setup

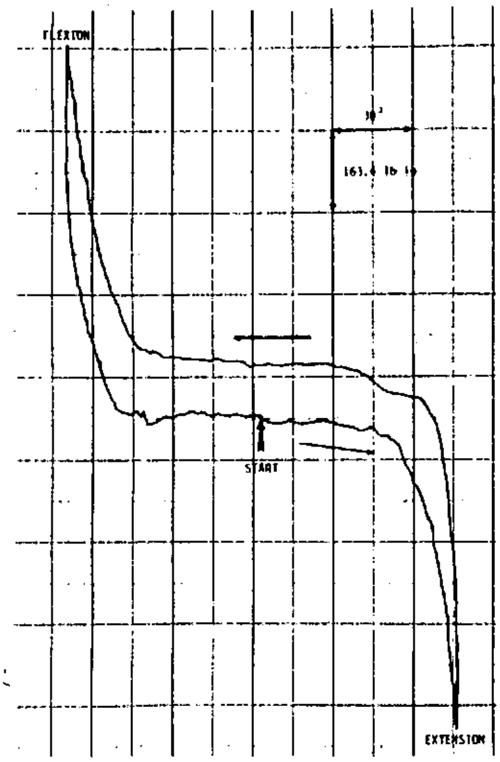

LEFT KNEE

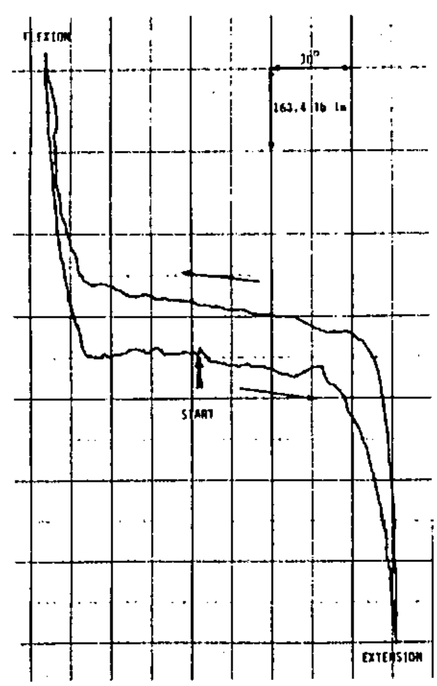

LEFT KNEE

FIGURE 43. KNEE FLEXION-EXTENSION FOR STANDING MANIKIN (NO RIGHT COMPLIMENT)

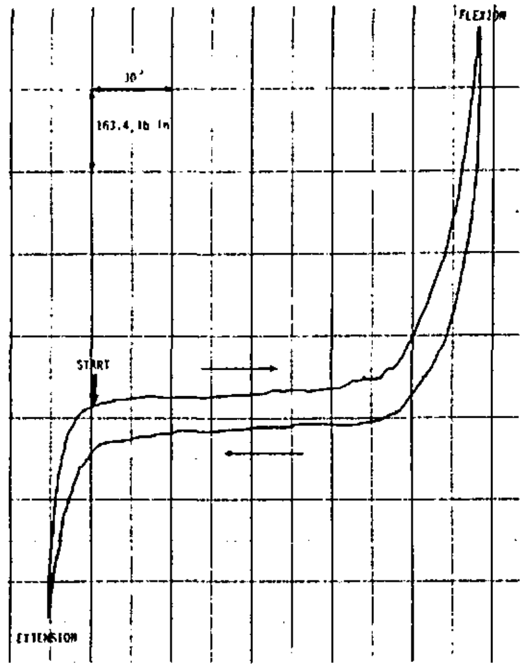

RIGHT KNEE

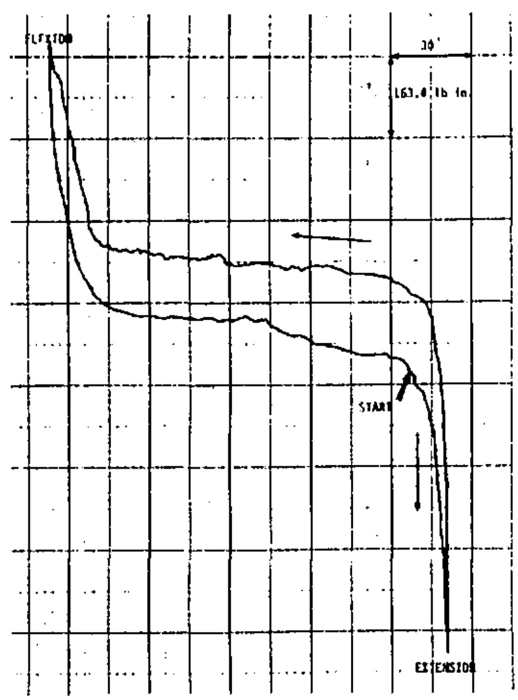

LEFT KNEE

FIGURE 44. KNEE FLEXION-EXTENSION FOR SEATED MANIKIN

2.1.4.1.3.5 Ankle

The ankle pin joint allows plantar flexion and dorsiflexion of the foot with respect to the lower leg. The lower leg was used as the rotating segment and the foot was securely clamped to the holding fixture, orienting the joint axis vertically. See Figure 45. The potentiometer shaft was aligned with the ankle bolt and the load cell was attached to the proximal end of the lower leg, the rotating segment, and was positioned horizontally and perpendicular to the long bone axis. Both left and right ankle joints were tested on each manikin.

The resulting joint resistance versus angle of rotation plots are presented in Figures 46 and 47. Range of motion values indicate consistency between left and right joints on each manikin, but a 15 to 30 degree larger range of motion for the seated manikin. These differences do not appear to be a function of torque, but are due to structural differences between the manikins. For all of the resulting ankle curves, the stops which govern both flexion and extension appear to be due to hard mechanical stops.

2.1.4.1.3.6 Hip

The hip joint, which is a ball and socket joint, allows movement in the flexion-extension, abduction-adduction, and rotational directions. For this joint, the resistance of the ball to move within the ball and socket joint is determined by the tightness of cap screws holding the covering plate. For a joint loosely torqued, however, resistance is primarily provided by skin to skin interactions and hard stops. The seated pelvis is molded such that the upper leg is in a 90 degree flexion orientation. The standing pelvis is molded to allow free rotation in the flexion-extension and abduction-adduction directions. The flexion-extension and abduction-adduction tests were performed at a 90 degree flexion starting position for the seated manikin and in the anatomical standing starting position for the standing manikin.

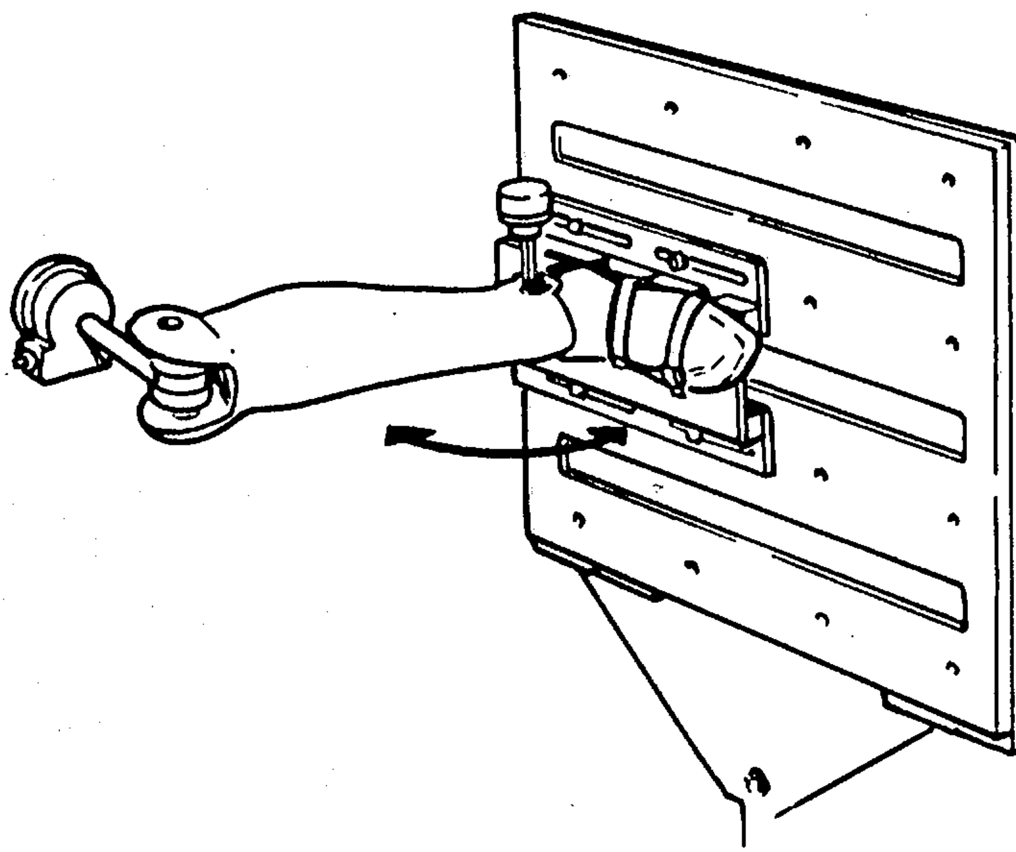

Figure 45. Ankle Flexion-Extension Test Setup

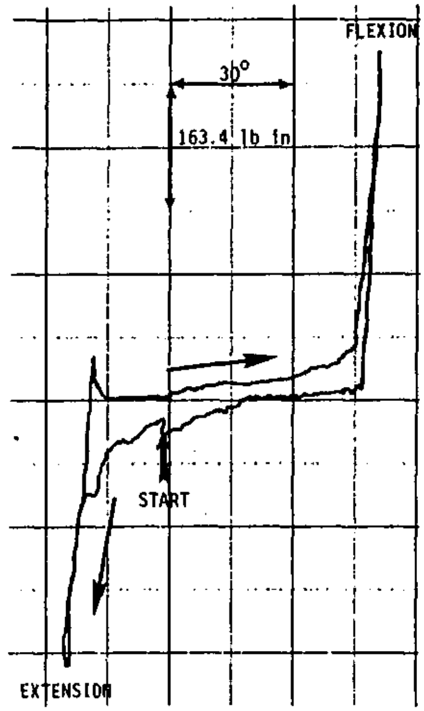

RIGHT ANKLE

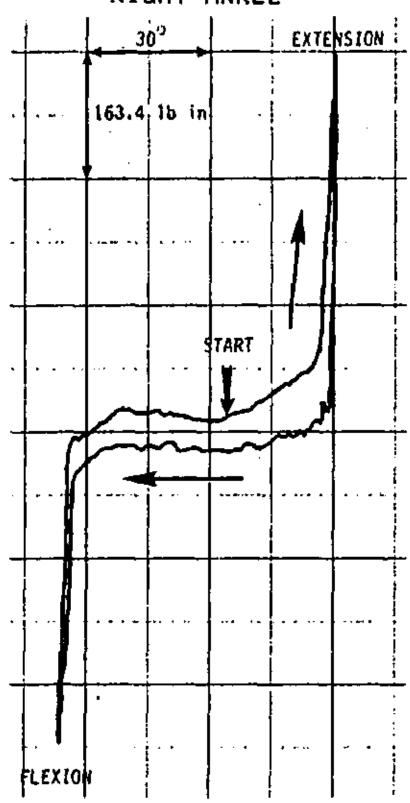

LEFT ANKLE

FIGURE 46. ANKLE FLEXION-EXTENSION FOR STANDING MANIKIN

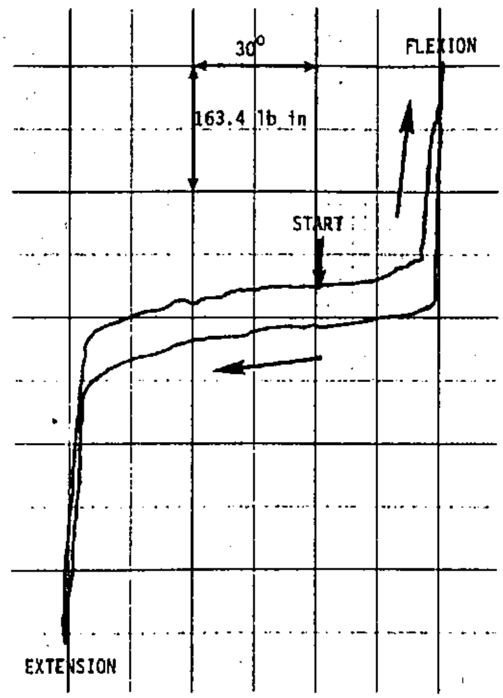

RIGHT ANKLE

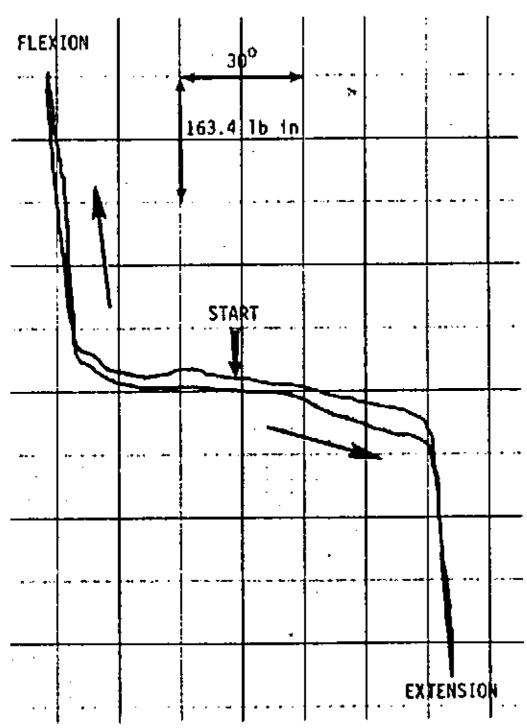

LEFT ANKLE

FIGURE 47. ANKLE FLEXION-EXTENSION FOR SEATED MANIKIN

Since the ball and socket joint is centered within the molded pelvis, the pot used to measure the rotation angle was centered over the joint and was manually rotated to follow the joint rotation. For abduction-adduction tests, the seated and standing pelvis were positioned upright, supported, and secured as shown in Figure 48. The load cell axis was positioned horizontally and perpendicular to the upper leg long bone axis and was used to manually rotate the leg through the range of motion.

For the flexion-extension tests, the pelvis was positioned on its side to orient the joint axis vertically as shown in Figure 49. The potentiometer axis was again held above the joint and positioned coaxially with the axis of rotation. The pot was rotated manually to follow the rotation of the upper leg. The load cell axis was positioned horizontally and perpendicular to the upper leg long axis and the load cell was used to manually rotate the upper leg through the range of motion. Flexion-extension and abduction-adduction tests were conducted on the left and right joints for both manikins.

Joint torque versus angle of rotation results are presented in Figures 50 through 53. Range of motion values from the seated manikin are as much as 126 degrees smaller than the standing manikin. These differences are an obvious result of mechanical structure differences and the skin to skin interaction of the seated pelvis. The seated pelvis has an extended hip flesh which surrounds the uppermost part of the upper leg and, thus, greatly restricts the range of motion for both flexion-extension and abduction-adduction movement. The curves display no free range of motion for the seated manikin. The standing manikin, however, is not restricted and allows a limited amount of free range of motion before reaching soft covering interference.

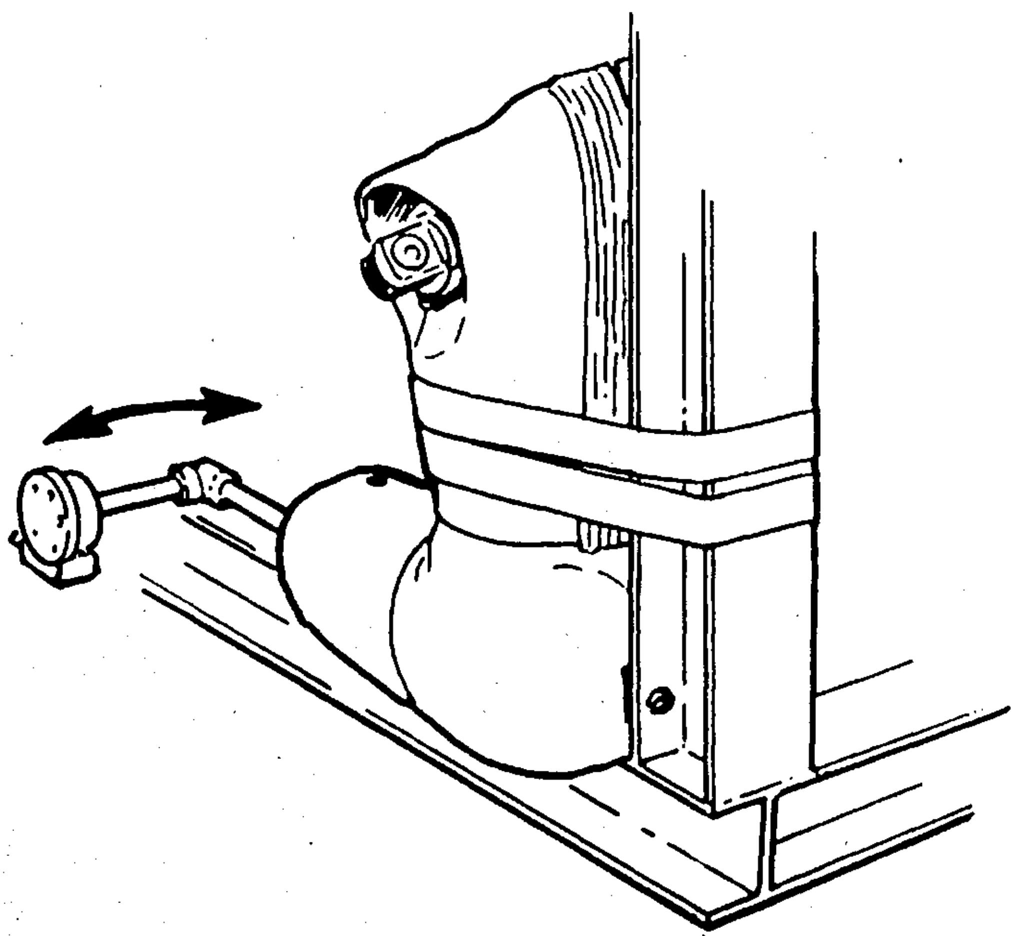

Figure 48. Hip Abduction-Adduction Test Setup

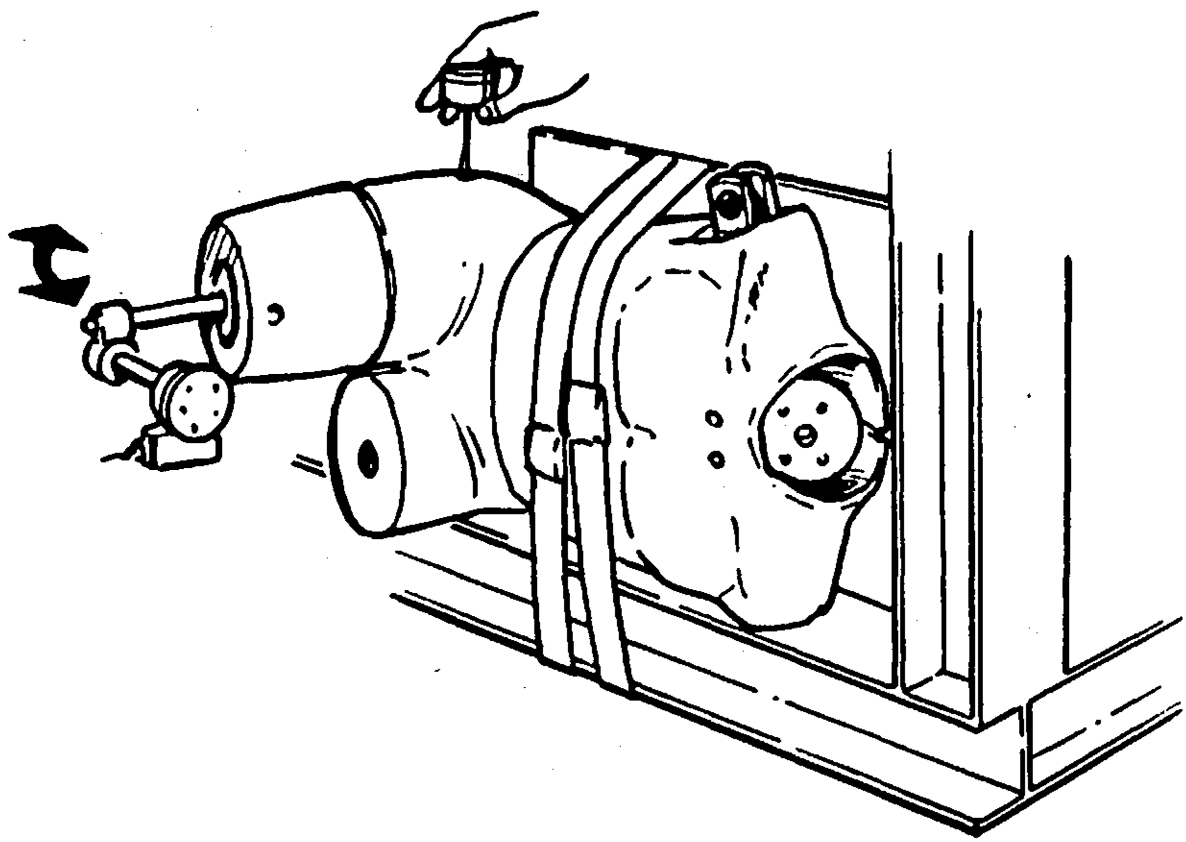

Figure 49. Hip Flexion-Extension Test Setup

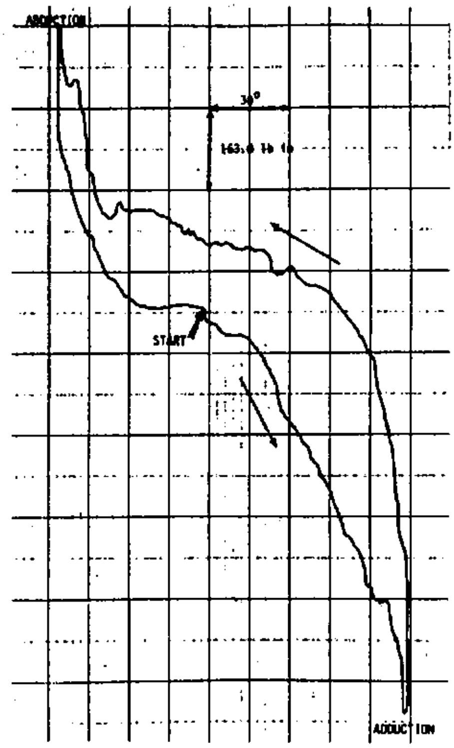

RIGHT HIP

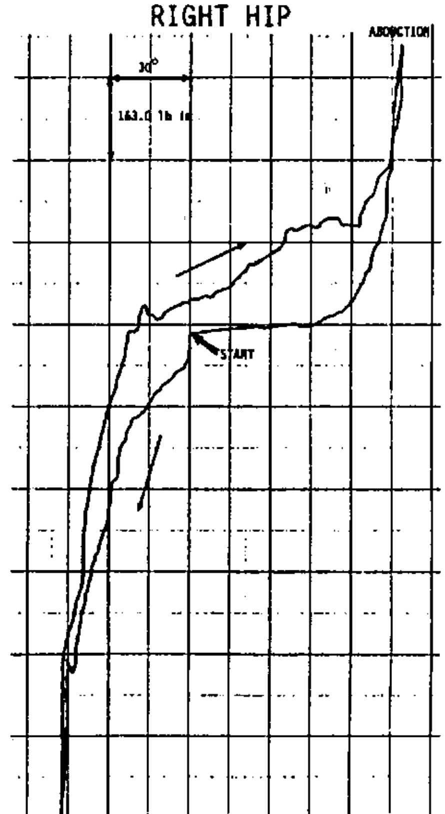

ADDUCTION LEFT HIP

FIGURE 50. HIP ABDUCTION-ADDUCTION FOR STANDING MANIKIN

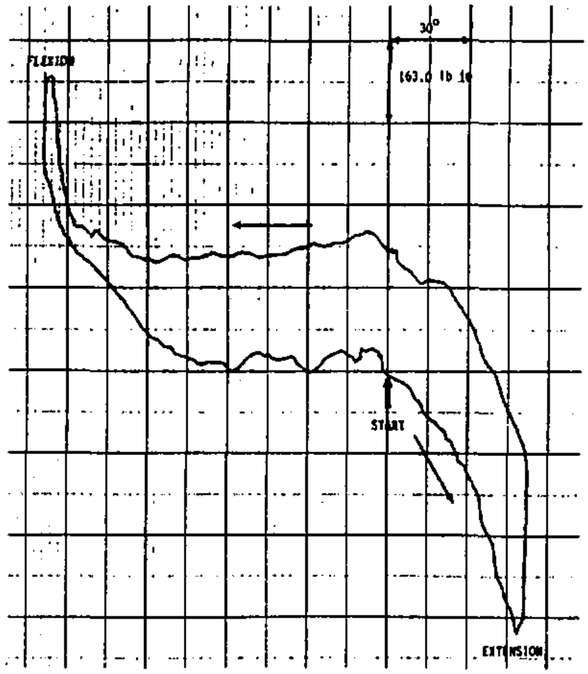

RIGHT HIP

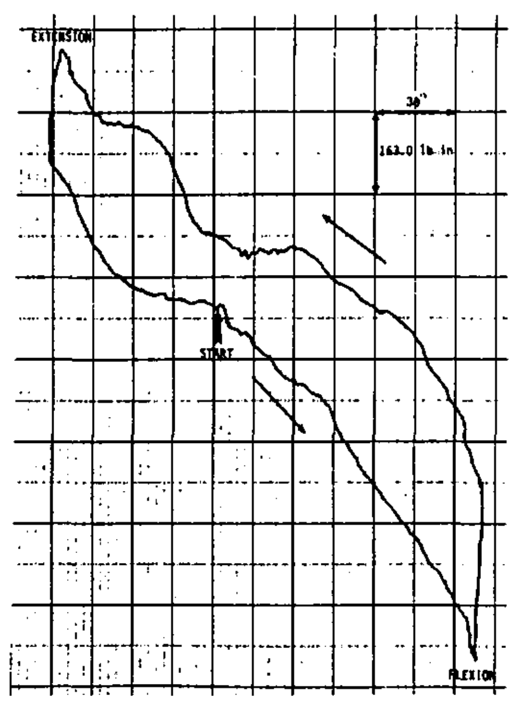

LEFT HIP

FIGURE 51. HIP FLEXION-EXTENSION FOR STANDING MANIKIN

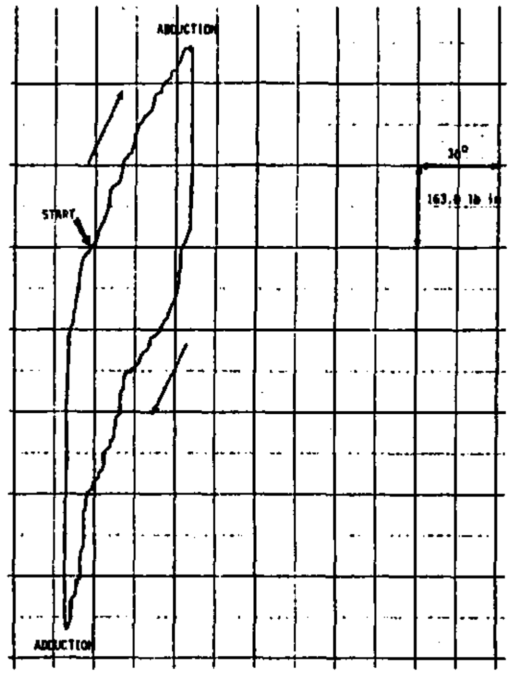

RIGHT HIP

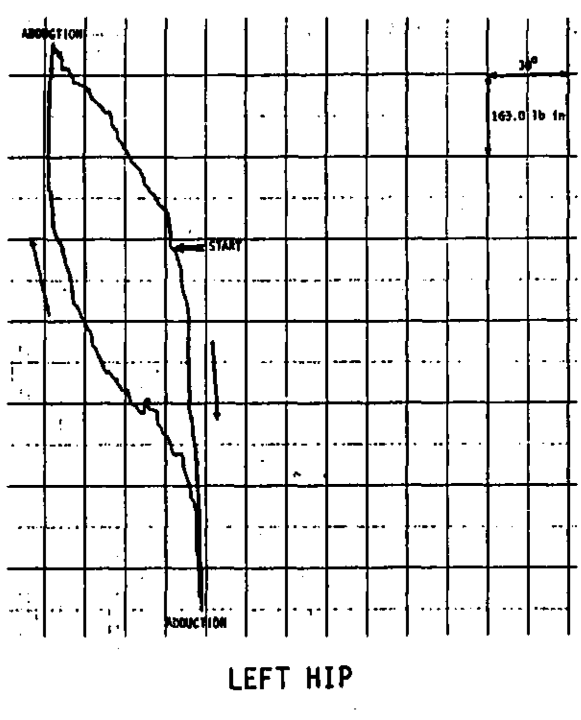

LEFT HIP

FIGURE 52. HIP ABDUCTION-ADDUCTION FOR SEATED MANIKIN

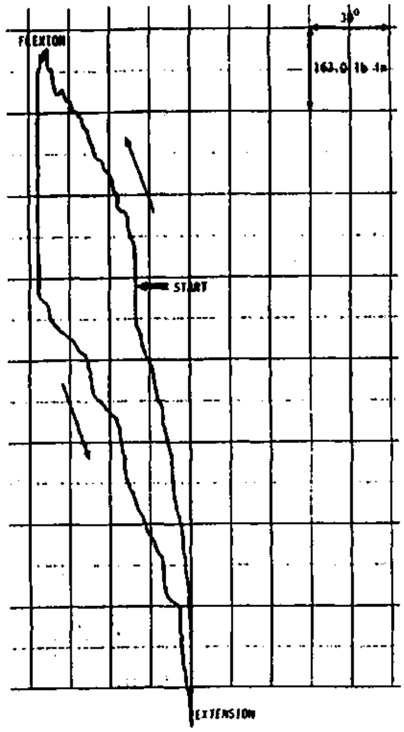

RIGHT HIP

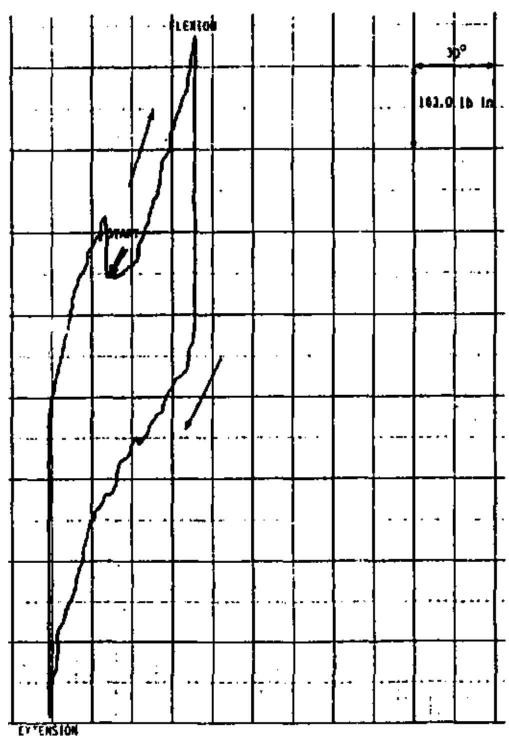

LEFT HIP

FIGURE 53. HIP FLEXION-EXTENSION FOR SEATED MANIKIN

2.1.4.2 Determination of Joint Range of Motion

The range of motion of a joint is determined by hard stops, soft stops, and soft covering interactions. The hard stops provide definite motion limitations of a joint, while the soft stops or soft covering interactions prevent free range of motion and produce resistance as a function of angle of rotation. In the latter case, a well defined range of motion value cannot be determined as this value becomes a function of force applied to the rotating segment. The higher the torque applied, the more the skin or soft stop deforms, and the greater the range of motion. The slope of the force/deflection curve provides some indication of how close to the full range of motion the joint has been moved. As the slope approaches infinity, where no amount of applied torqued increases the angle of rotation, the value of the range of motion at this point is the maximum. For most of the experimental curves developed, however, the maximum range possible was not reached.

The values for the range of motion differed between the left and right joints for a single manikin and also from manikin to manikin. For example, the joint characteristic curves of wrist flexion-extension at 0^{o} medial rotation joint tests for the standing and seated manikin, shown in Figures 34 and 38, show that the free range of motion, that range which experiences little or no resistance, is approximately 30^{o} greater for the right joint than was measured on the left joint of the standing manikin. Additionally, the values for extension beyond the free range of motion are about 10^{o} greater for the seated manikin than the values measured for the standing manikin. The larger values for the seated manikin suggest a structural difference between the two manikins.

2.1.4.3 Determination of the Characteristics of the Lumbar Spine

The molded rubber lumbar spine allows flexion-extension and lateral movement of the thorax with respect to the pelvis. Deflection resistance of the spine is dependent upon the characteristics of the natural rubber, the shape of the spine, and the strength of the steel cable or cables, which are centered axially through the spine. The seated manikin spine is curved to simulate the seated posture while the standing manikin spine is a straight cylinder. Both spines were tested to determine their respective stiffness properties.

2.1.4.3.1 Spine of Standing Manikin

The straight spine of the standing manikin was statically tested in flexion. Since the spine is cylindrically symmetric, the bending stiffnesses in flexion, extension, and lateral directions are the same. Two tests were peformed to evaluate the degree of repeatability in determining the moment versus angle of deflection curve. These tests were conducted about an hour apart to allow a recovery period for the rubber to release its stored energy from the previous test.

In the test setup the spine was positioned horizontally and the base of the spine was securely clamped to a holding frame. The top of the spine was attached to a cable through which the load was applied. This test setup is illustrated in Figure 54. A load cell was attached to the cable and the applied load was measured and plotted against the angular rotation of the tip of the spine, measured by an inclinometer. Section 2.1.4.4.1.2 describes the method used to convert the measured force to the applied moment at the base of the spine.

The results of the tests are presented in Figure 55. Shown are plots of applied moment versus angle of rotation. As can be seen from the plots, the straight spine displayed a linear response with applied moment over the angle of rotation tested which results in a stiffness value of about 48 in-lb/deg for bending in all three directions. To further quantify the spine stiffness, the spine should be deflected beyond 30 degrees.

Although the straight spine had the same bending stiffnesses in all directions, the abdominal insert provides a stiffening effect in the flexion and lateral directions when inserted in the manikin. To determine this stiffening effect, the spine was statically tested with

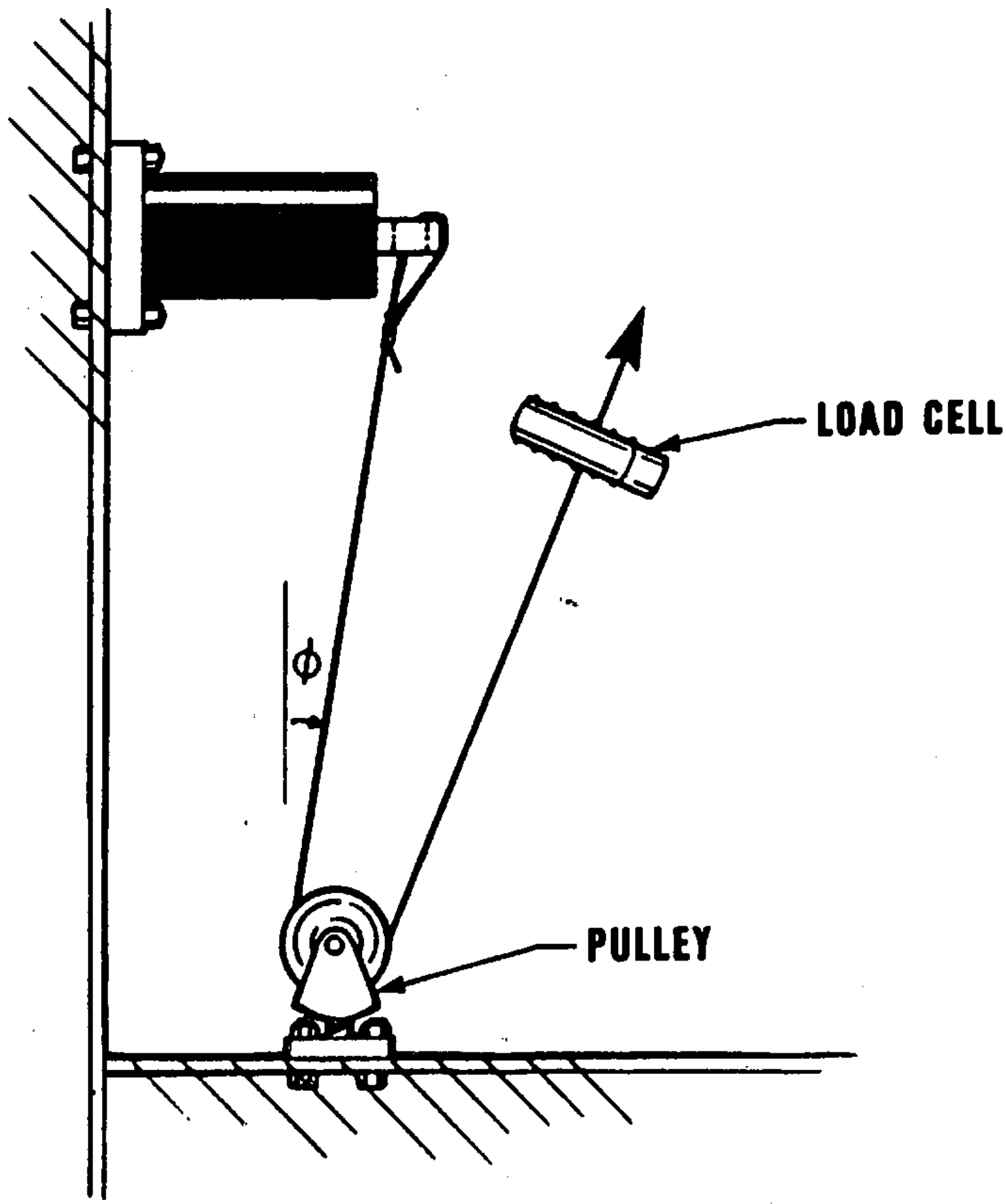

Figure 54. Static Bending Test Setup for the Straight Spine

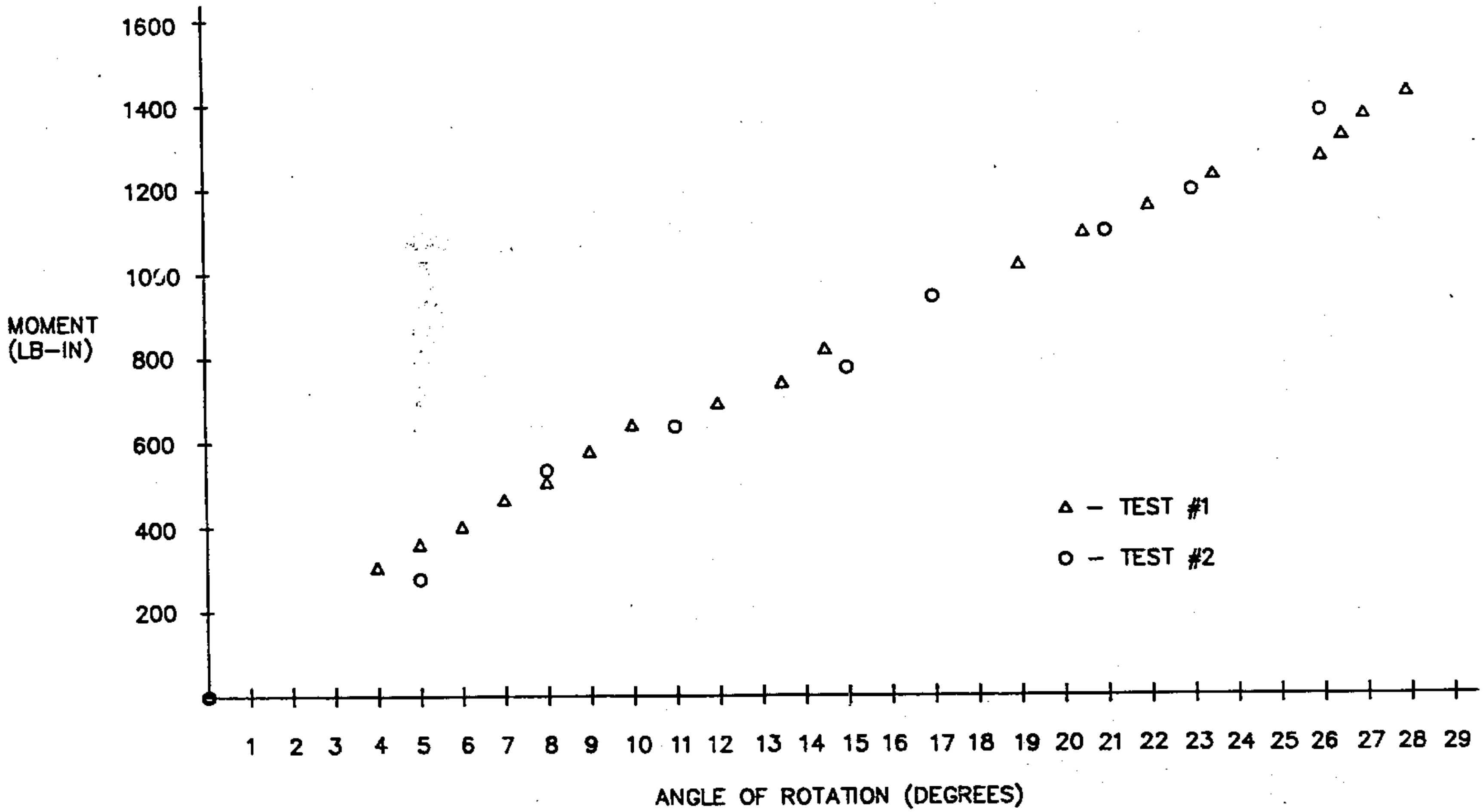

Figure 55. Straight Lumbar Spine Bending Test

and without the abdomen. As illustrated in Figure 56, the lumbar spine was tested while attached to both the pelvis and thorax. An aluminum cavity located on the backside of the pelvis allowed the assembly to be directly bolted to the frame. The nut on the spine's steel cable was torqued to 10 in-lb to comply with GM standards and the tests were spaced about an hour apart to allow the rubber a recovery period. A pneumatic piston was used to incrementally load and then unload the spine through an attached flexible cable. A Strainsert 1000 lb. single-axis load cell was used to monitor the applied load. Recording deflection with an inclinometer, the load cell readings were measured to provide moment versus deflection curves. Only the loading portion of the curve was used to determine stiffness properties. Two tests were performed, both with and without the adominal insert, to determine the repeatability of the test. Presented in Figure 57 are the resulting curves found with and without the abdominal insert. The resulting stiffness is about 23% higher with the abdomen in place.

Applying the percent increase due to the addition of the abdominal insert to the baseline bending stiffness of the straight spine, the resulting stiffness is approximately 60 in-lb/deg. This stiffness coincides with flexion and lateral movement as the abdominal insert interacts with the spine during bending in these two directions. The stiffness of 48 in-lb/deg is used for extension since there is no interaction with the abdominal insert during bending in this direction.

2.1.4.3.2 Spine of the Seated Manikin

The curved spine positions the manikin in a seated posture. This spine, although cylindrically shaped, is curved and so exhibits different stiffness characteristics for bending in the flexion, extension, and lateral directions. All three bending directions were statically tested for their respective stiffnesses.

Figure 58 illustrates the static flexion test setup for the curved spine. The top of the spine was attached to a cable through which the load was applied. A load cell and an inclinometer were used to measure

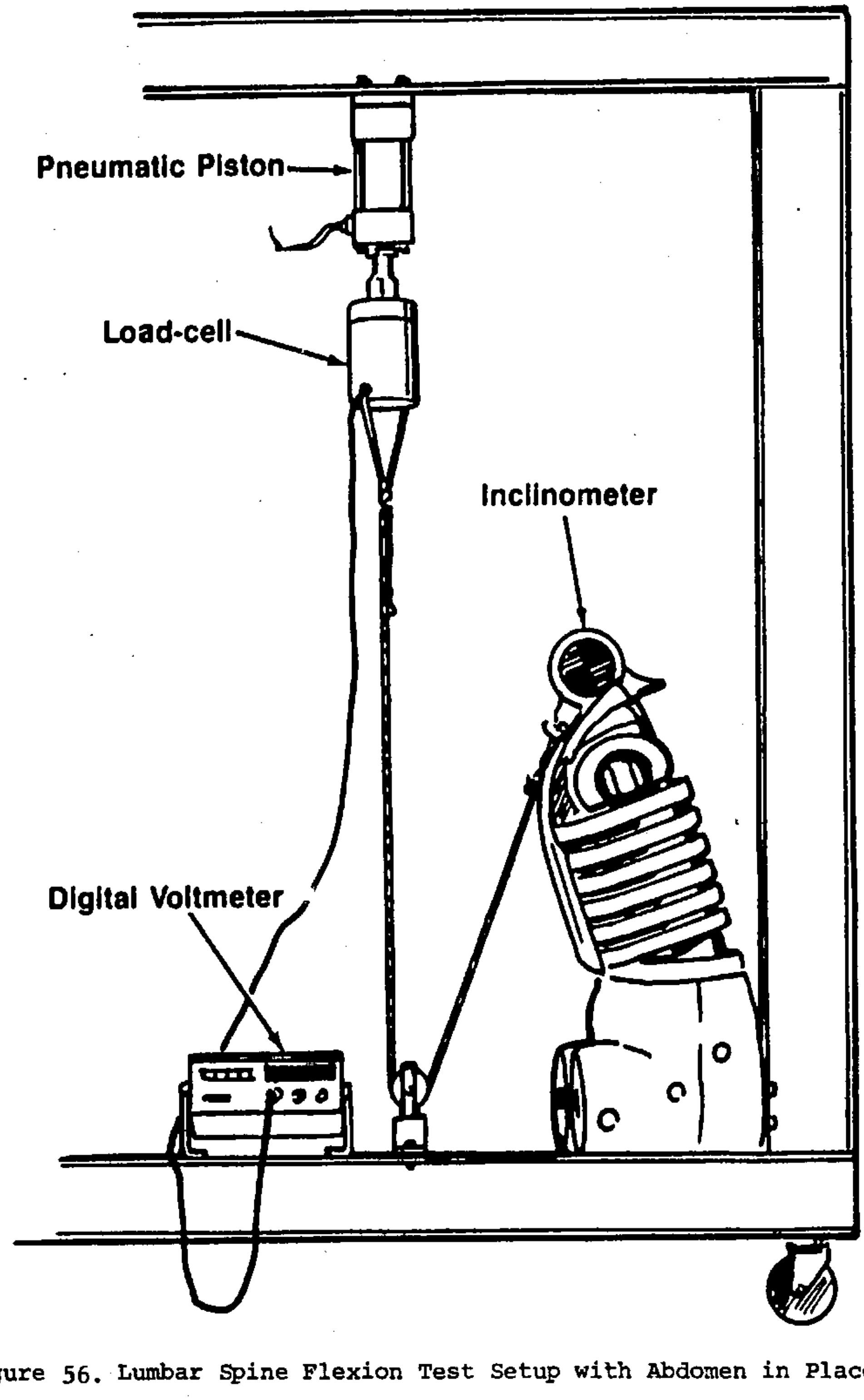

Figure 56. Lumbar Spine Flexion Test Setup with Abdomen in Place

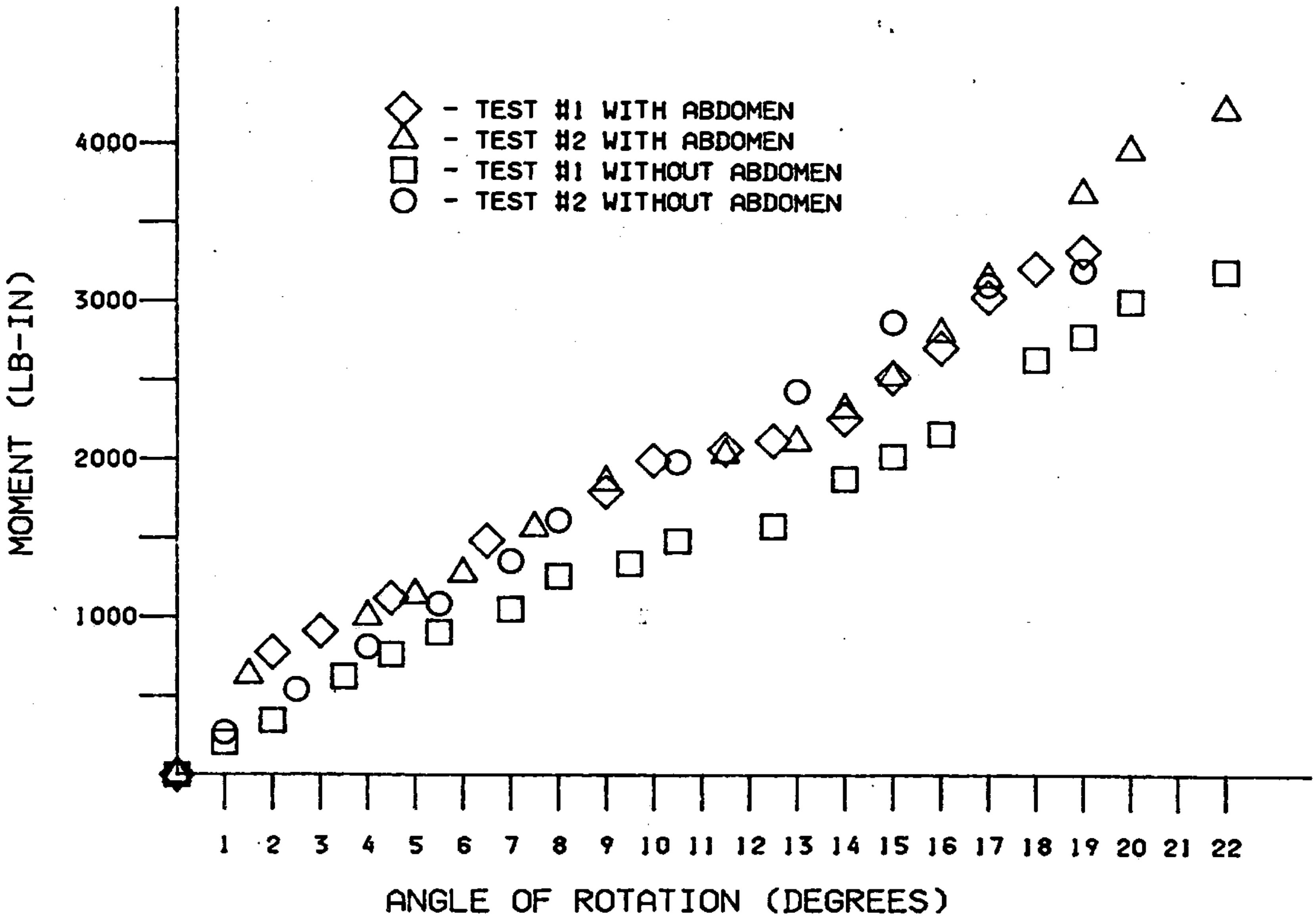

Figure 57. Straight Lumbar Spine Flexion Test with and without Abdomen

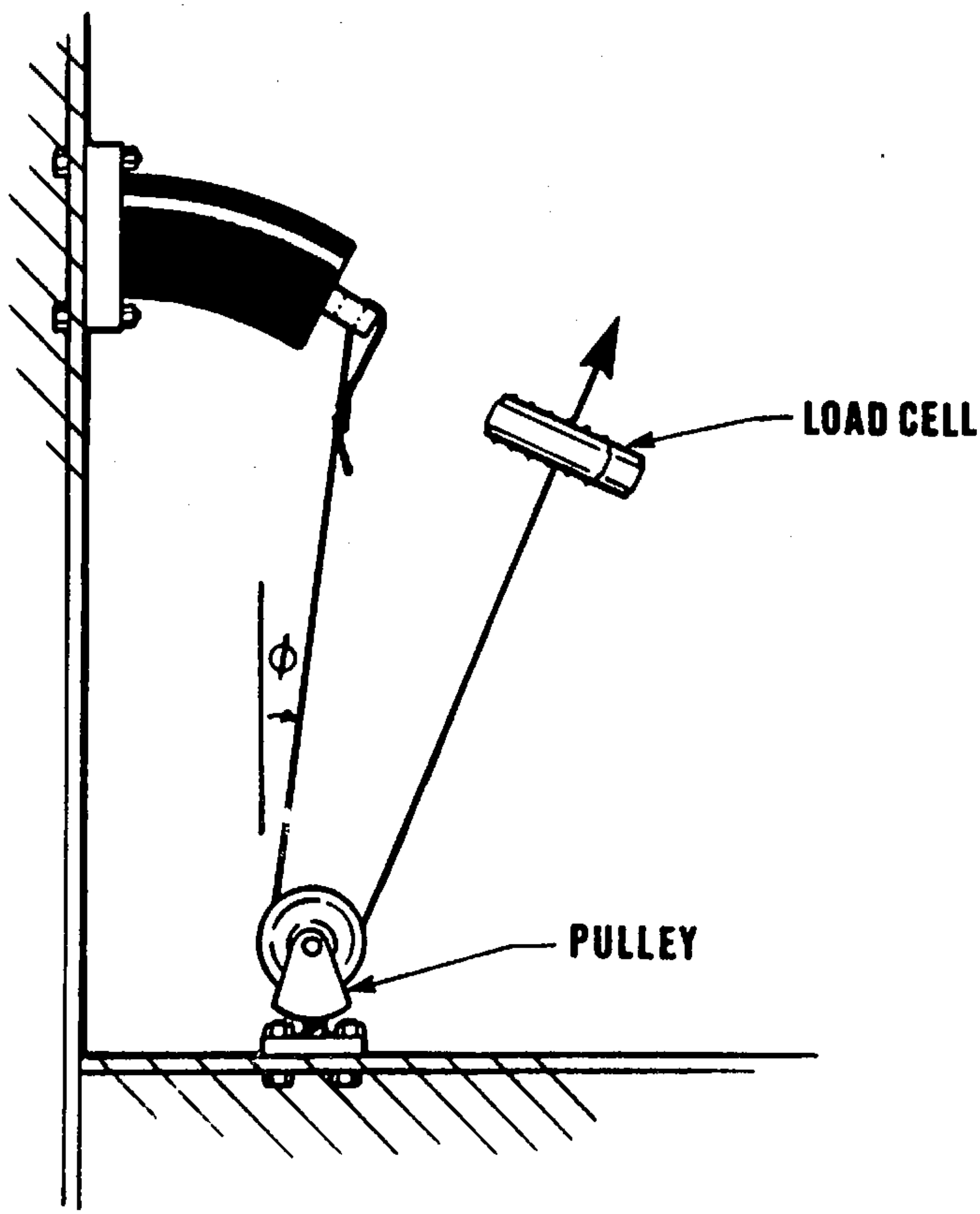

Figure 58. Static Flexion Test Setup for the Curved Spine

the applied load and the angle of rotation of the spine, respectively. These tests were also conducted in a similar manner for extension and lateral directions and were spaced about an hour apart to allow for a recovery period.

The method used to resolve the measured force to the applied load at the base of the spine is described in Section 2.1.4.4.1.2. Plots of the data are presented in Figure 59 through 61.

These curved spine static bending tests were performed over about 6^{o} of inclination. In tests performed with the curved spine attached to the thorax and pelvis it was noted that the force-deflection characteristic softens slightly with increasing angle. Due to this softening, the stiffness for small angles is greater than that for large angles. Since a linear approximation for the stiffness over large angles (20^{o} - 30^{o}) was used, a 16.2% of adjustment was made to the slopes in Figures 59 through 61. This adjustment was obtained from the force-deflection curve without abdominal insert in Figure 62 by comparing the slope for points up to 6^{o} to the average slope over the full curve. Testing the curved spine to deflections of 20-30 degrees would verify these adjustment figures. Testing the curved spine beyond the 30^{o} deflection would further quantify the spine's nonlinear characteristics.

To obtain the stiffening effect of the abdominal insert, the curved spine was also tested while attached to both the pelvis and thorax with and without the abdomen as described in Section 2.1.4.3.1. The resulting moment versus angle of rotation curves are presented in Figure 62. With the addition of the abdomen, the stiffness values appear to increase by 13% over that of the basic spine. Applying this percent increase to the stiffness values of flexion and lateral bending to account for the interaction with the abdominal insert during bending in these directions, stiffness values for flexion and lateral bending are 230 in-lb/deg and 340 in-lb/deg, respectively. The stiffness for extension is 150 in-lb/deg.

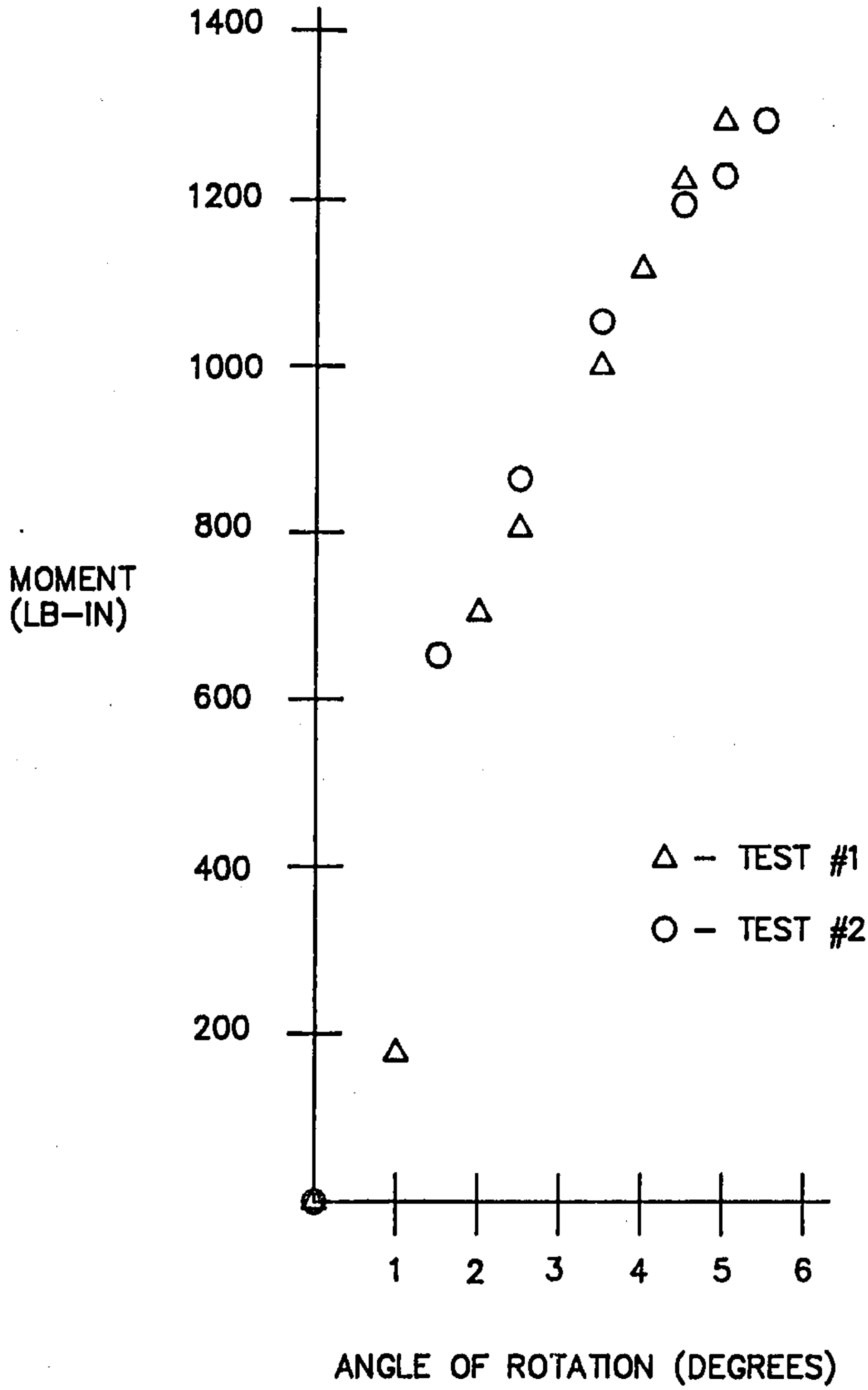

Figure 59. Curved Lumbar Spine Flexion Test

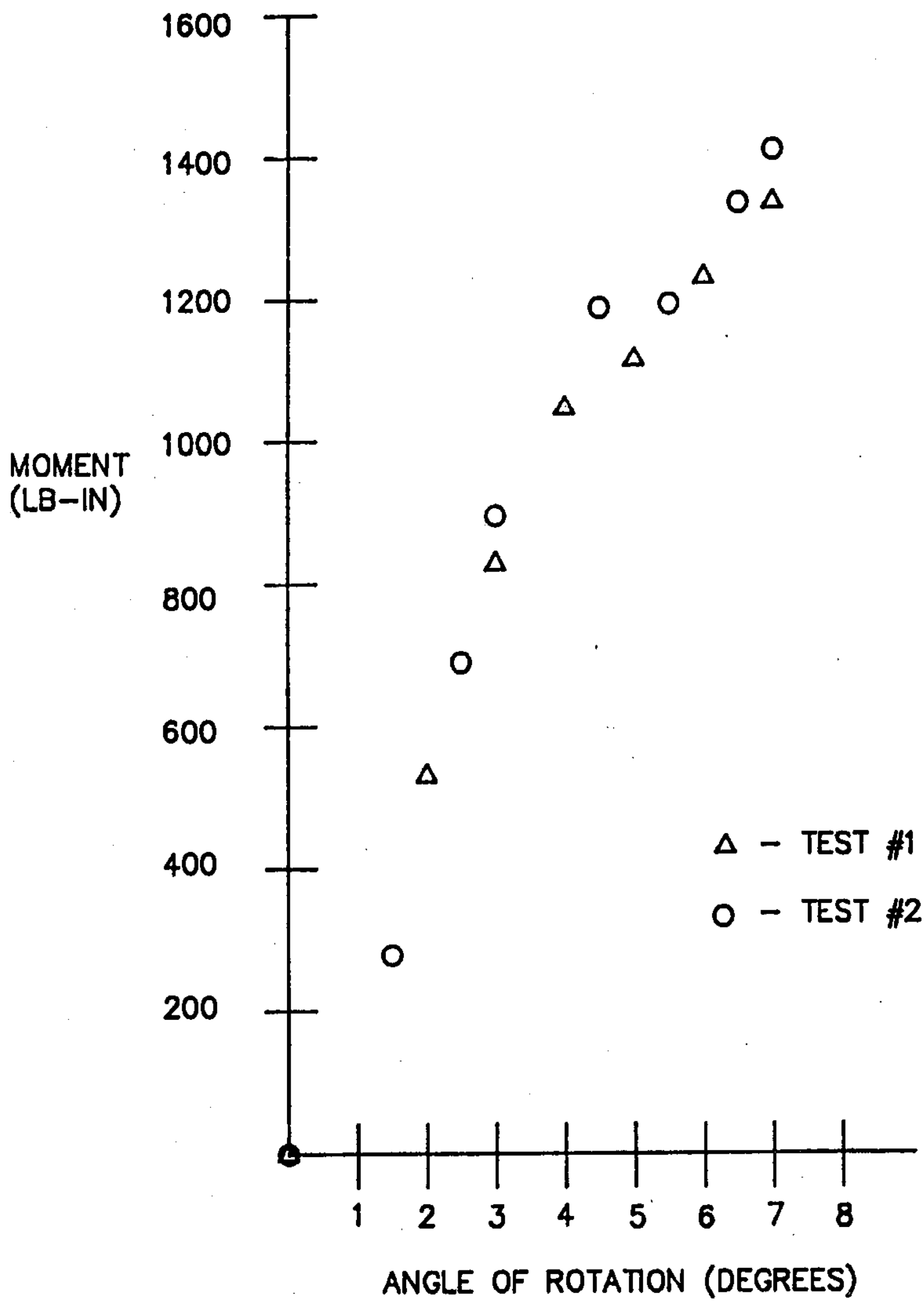

Figure 60. Curved Lumbar Spine Extension Test

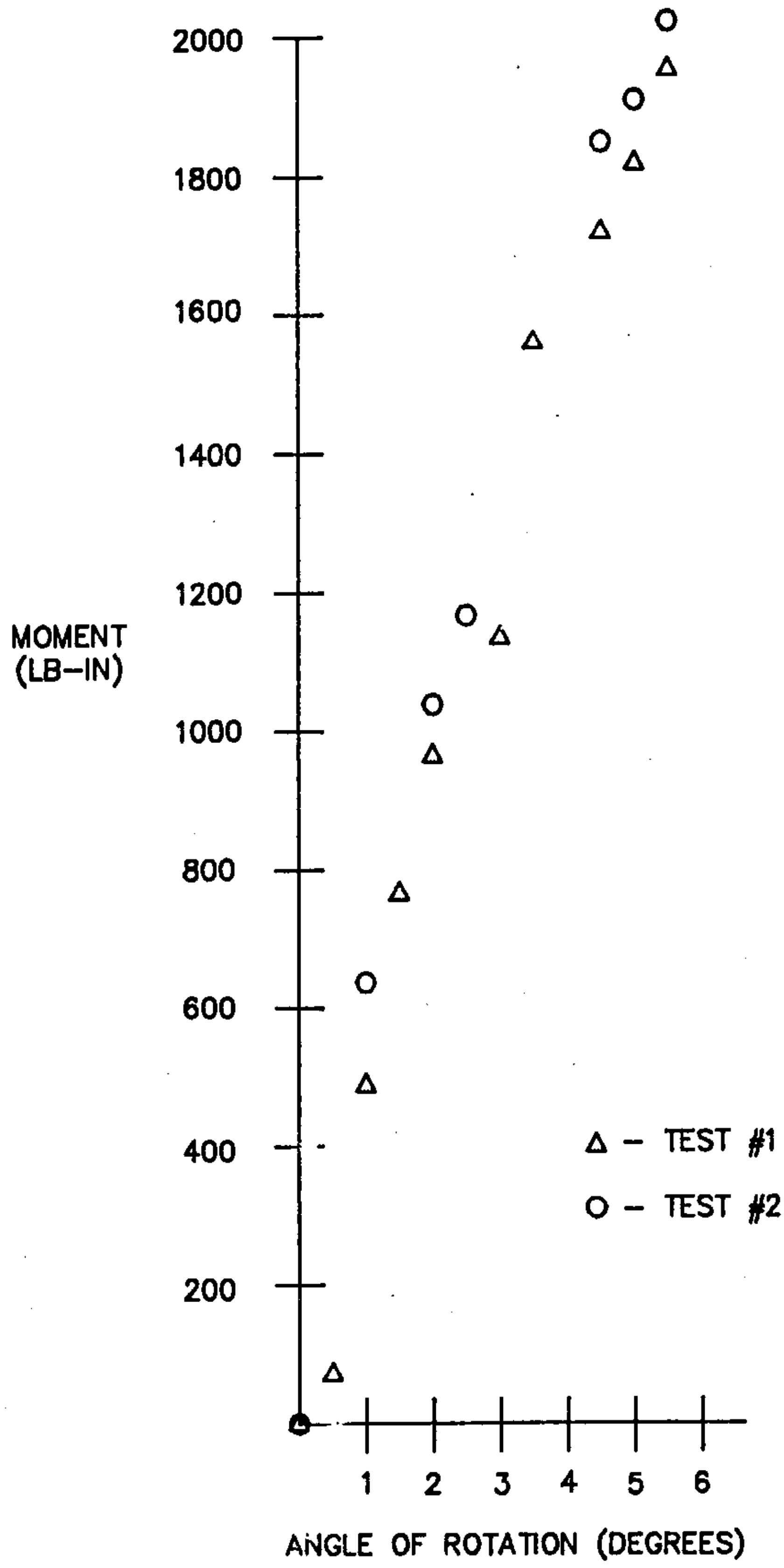

Figure 61. Curved Lumbar Spine Lateral Bending Test

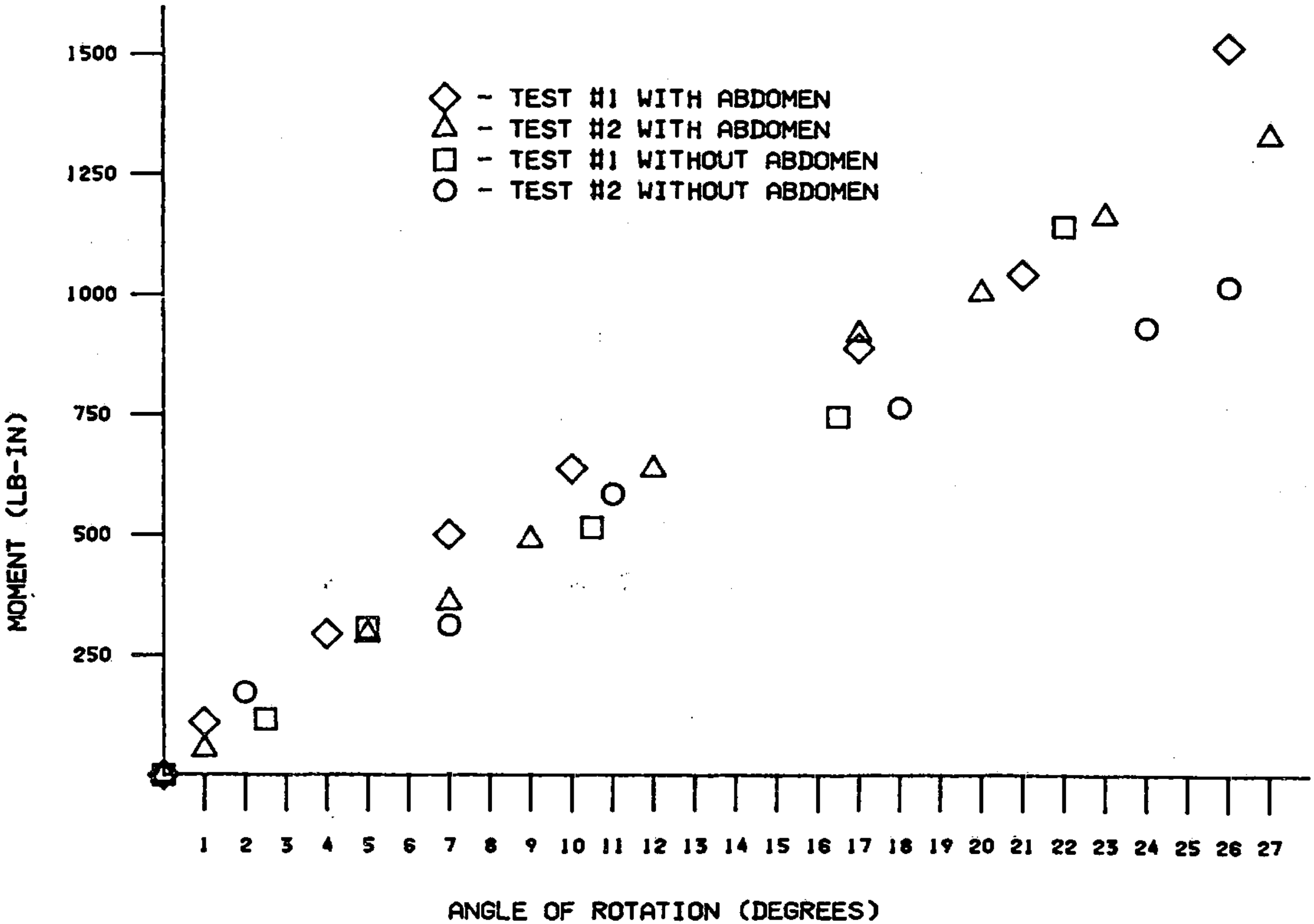

Figure 62. Curved Lumbar Spine Flexion Test With and Without Abdomen

2.1.4.4 Determination of the Characteristics of the Hybrid III Neck

The Hybrid III neck allows torsional, flexion, extension, and lateral motion of the head with respect to the thorax. The neck is constructed of aluminum plates, representing vertebral elements, bonded together with alternate sections of butyl elastomer. The axial strength of the neck is enhanced by a steel cable which is bolted through the center of the neck. Saw cuts through the anterior side of the neck provide reduced extension bending resistance without affecting flexion. Static and dynamic tests were performed on the necks of the standing and seated manikins to determine their stiffness characteristics.

2.1.4.4.1 Static Tests

2.1.4.4.1.1 Test Procedure

In order to conduct tests of the neck to determine the bending stiffnesses in the flexion, extension, and lateral directions, the neck was loaded to obtain a moment versus angle of deflection curve in the same manner as the tests of the lumbar spine. With the base of the neck rigidly secured to the holding frame in a horizontal plane, the top of the neck was attached to a cable through which the load was applied. Figure 63 illustrates the test setup for the static neck test. A load cell was attached to the loading cable to measure the applied load and the angular rotation of the element was measured with an inclinometer. The method described in Section 2.1.4.4.1.2 was used to convert the measured force to the applied moment at the base of the neck. Two tests were performed for each configuration of both necks allowing an hour in between tests for a recovery period.

2.1.4.4.1.2 Data Reduction Procedures and Results

The data reduction procedure outlined herein was that used to reduce the test data obtained for the lumbar spines as well as the neck since all tests were conducted using the same test setup and procedure.

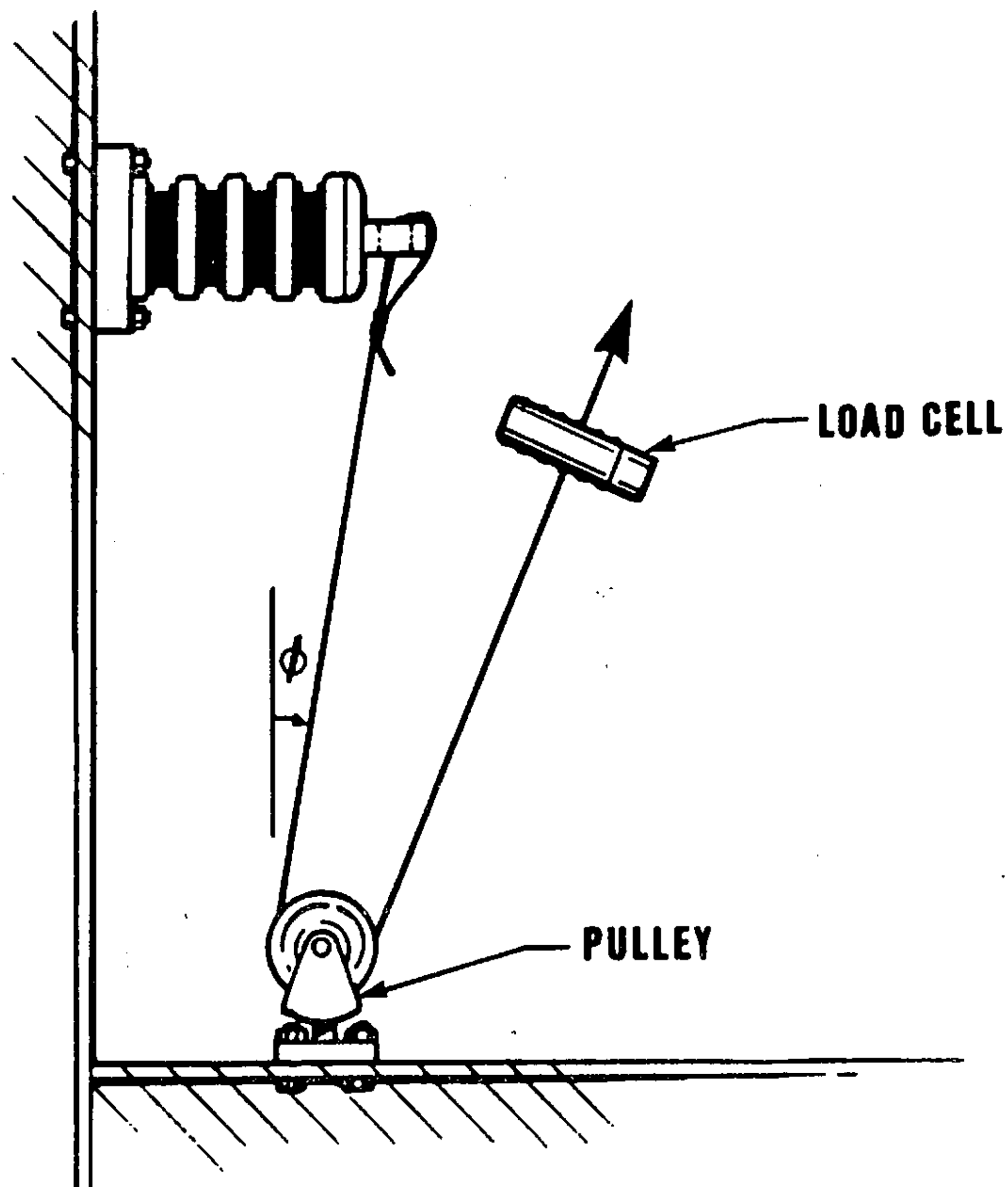

Figure 63. Static Bending Test Setup for the Neck

Assuming that the neck or lumbar deformation acts like that of a continuous beam, the resulting deformation can be approximated as a circular arc. Figure 64 illustrates the force components and deformation geometry. The angle ϕ is the angle of the cable with respect to the vertical or perpendicular to the long axis of the test article. This angle did not change more than one or two degrees and so was assumed a constant. The angle θ is the angle of the deflection of the neck and δ_x and δ_y are the deflected horizontal and vertical locations of the top of the neck respectively. F_o is the applied force read directly from the load cell and F_y and F_x are the resultant forces in the vertical and horizontal directions. Referring to the free body diagram in Figure 65, the arc length, L, is proportional to the circumference of the circle, C, as the angle of deflection, θ, is to the angle 2π. Substituting the equation for the circumference of a circle, the resulting relationship is $R=L/\theta$. Using geometry, $\cos\theta = \delta_y/D$

$$\delta_y = D\cos\theta = R(1-\cos\theta) = \frac{L}{\theta}(1-\cos\theta);\ \delta_x = R\sin\theta = \frac{L}{\theta}\sin\theta$$

Therefore, the moment transferred to the base of the neck, or point 0, is

$$\begin{aligned} M_o &= \delta_x F_y + \delta_y F_x \\ &= \frac{LF_o}{\theta}\sin\theta\cos\phi + \frac{L}{\theta}F_o(1-\cos\theta)\sin\phi \\ &= \frac{LF_o}{\theta}(\sin\theta\cos\phi + (1-\cos\theta)\sin\phi) \end{aligned}$$

The moment deflection curves developed from the test data are presented in Figures 66 through 68 for flexion, extension, and lateral tests of both necks. For the angles of deflection tested (30-50°), the necks displayed linear responses. Deflecting the necks to 70 degrees or more would probably display stiffening at the neck's response. The two tests for a given range of motion on each neck were averaged to provide the stiffnesses presented in Table 8. As expected with the presence of the saw cuts, extension stiffness values are about 1/2 of the stiffness found with flexion or lateral movement for both necks. Resulting stiffness for the seated manikin in the flexion, extension, and lateral

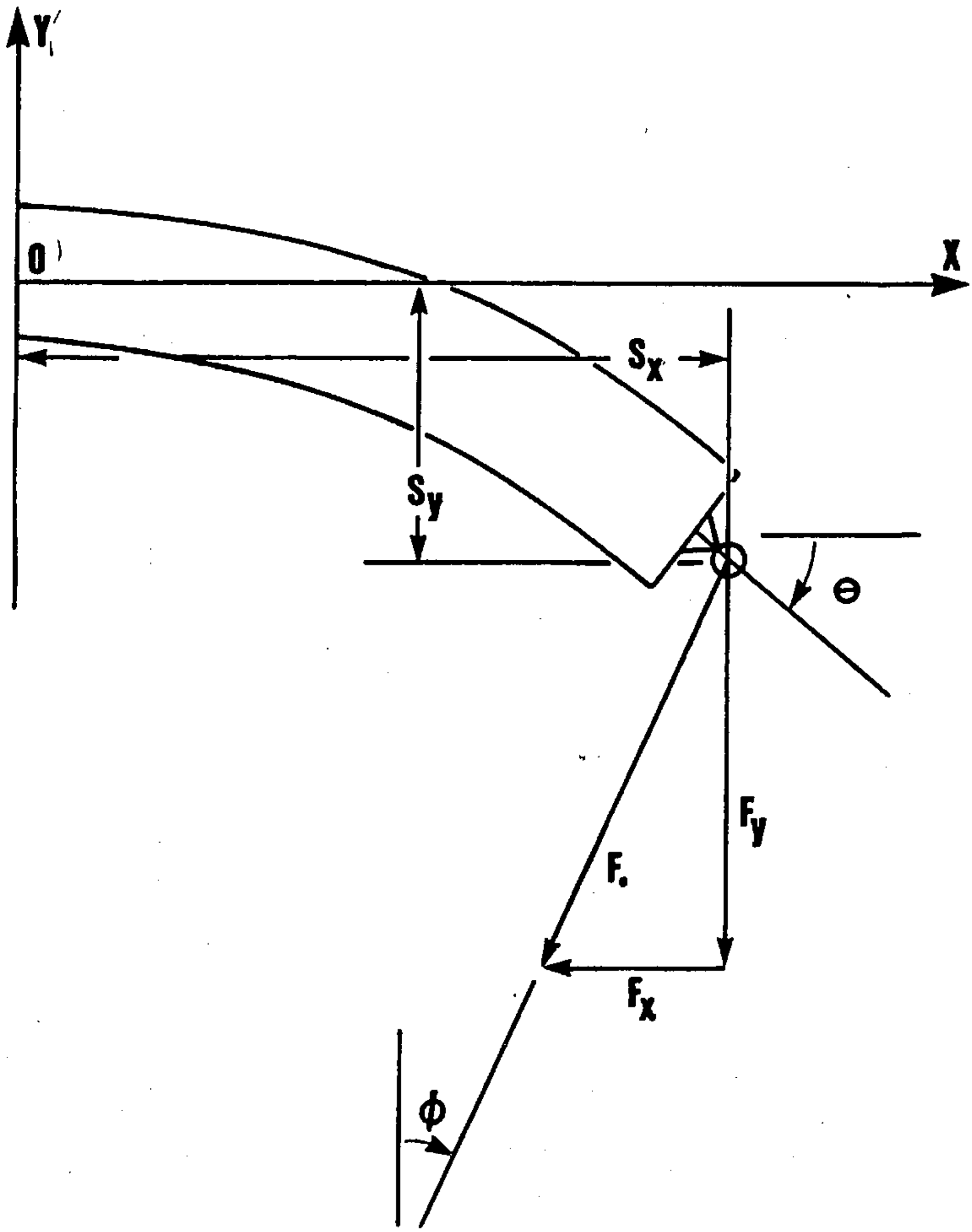

Figure 64. Force Component and Deformation Geometry Diagram

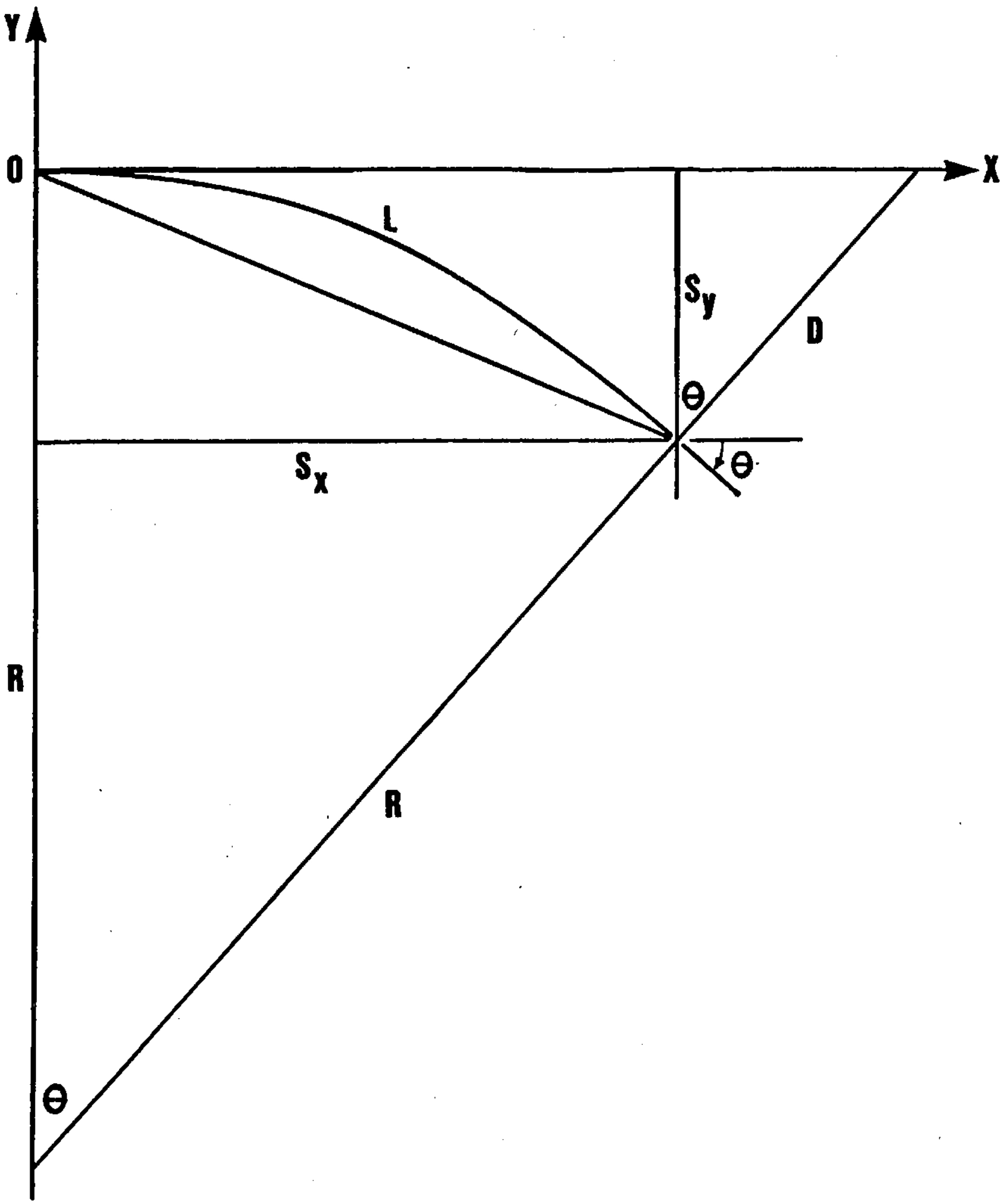

Figure 65. Free Body Diagram of Deformed Segment

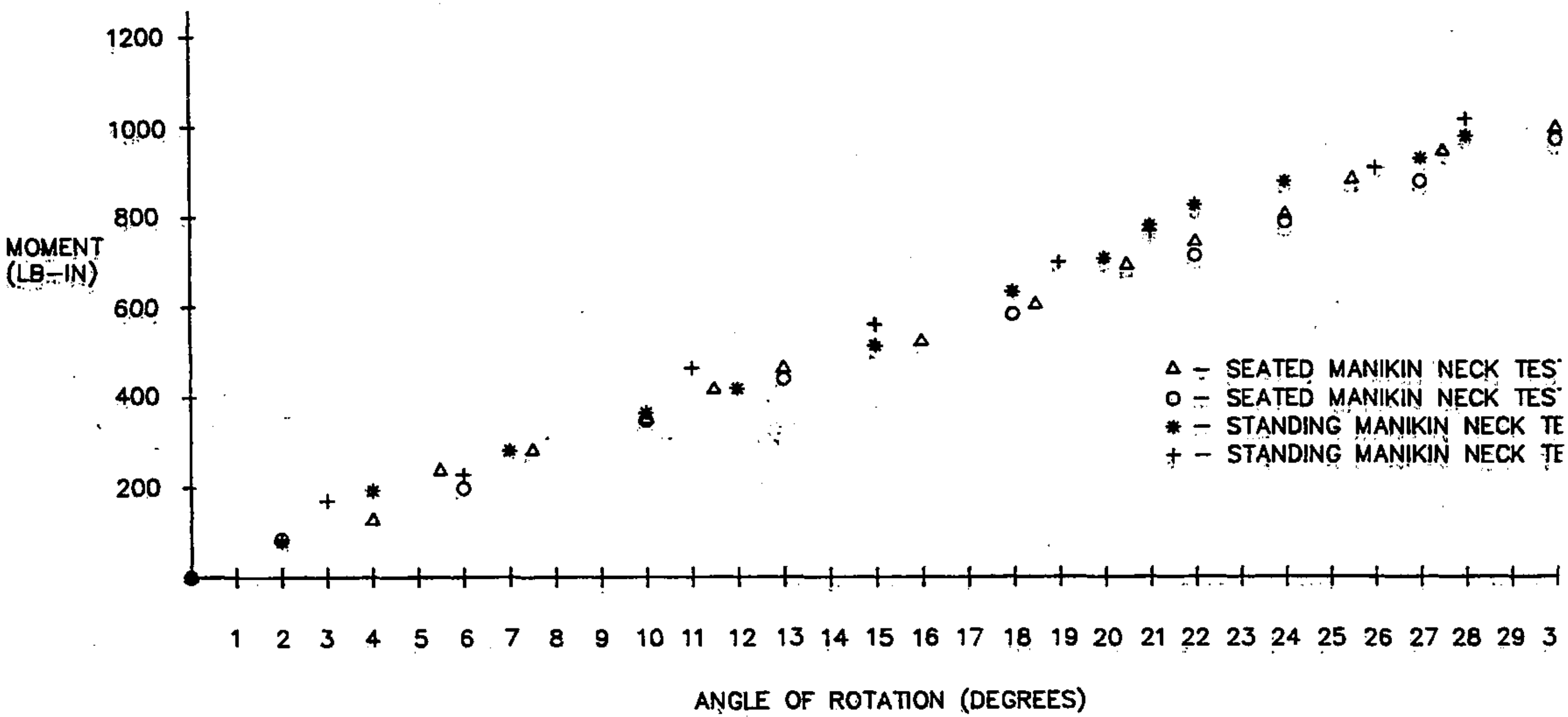

Figure 66. Neck Flexion Tests for Standing and Seated Manikins

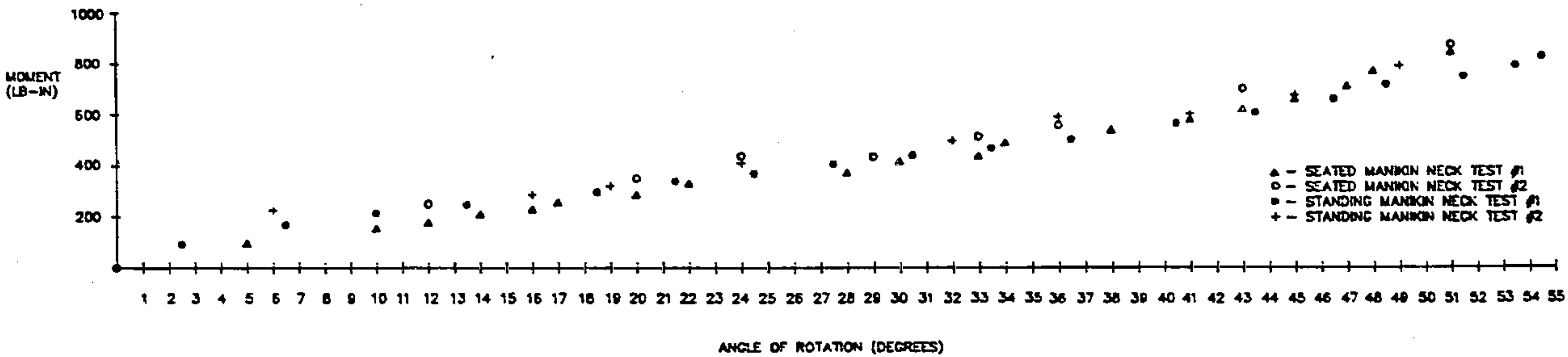

Figure 67. Neck Extension Tests for Standing and Seated Manikins

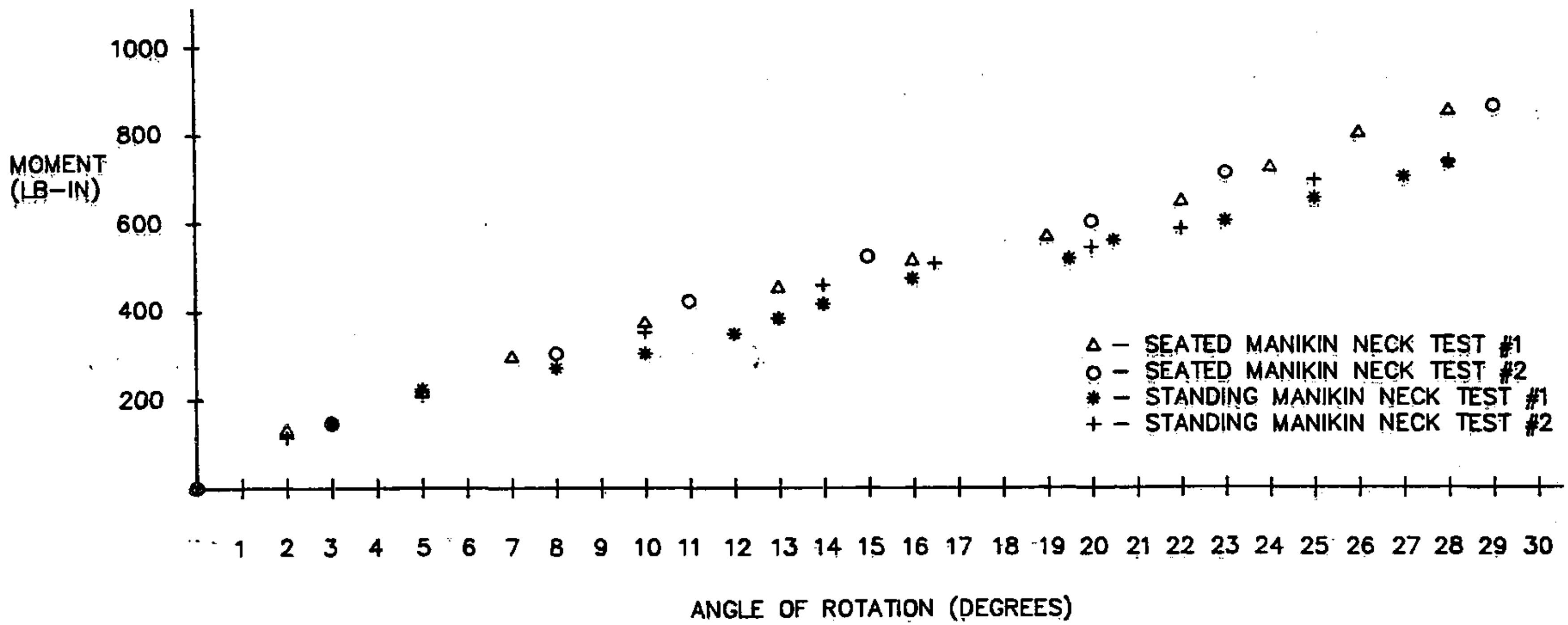

Figure 68. Neck Lateral Bending Tests for Standing and Seated Manikins

stiffnesses for the seated manikin in the flexion, extension, and lateral directions were 32.71 in-lb/deg, 15.55 in-lb/deg, and 28.40 in-lb/deg, respectively. Stiffnesses for the standing manikin neck in the flexion, extension, and lateral directions were 34.84 in-lb/deg, and 13.817 in-lb/deg, and 24.565 in-lb/deg, respectively. Comparing stiffnesses between the two necks, the seated manikin neck is stiffer in the extension and lateral directions, but less stiff in flexion.

2.1.4.4.2 Dynamic Tests

2.1.4.4.2.1 Test Procedure

Dynamic tests were performed on both Hybrid III necks to provide stiffness properties under dynamic loading. These tests were performed in flexion, extension, and lateral directions. Positioning the neck for an extension test, as illustrated in Figure 69, entailed rotating the neck horizontally with the anterior side upward and securely clamping the base of this element to the holding frame. A large disk-shaped weight, weighing several times the weight of the neck, was bolted to the top of the neck, causing an initial extension angle of rotation of about 10 degrees which resulted in the separation of the saw cuts. An Entran accelerometer was placed on the top of the weight and monitored by a storage oscilloscope. Manually disturbing this assembly resulted in decaying oscillations that were recorded with the oscilloscope and analyzed to obtain the natural frequency and damping characteristics. The oscillatory deflections did not close the saw cuts, and therefore, a nonlinear response, such as a combination of flexion and extension motion was not observed. A number of tests were performed for each configuration on both necks. Flexion and lateral tests were performed in the same manner with the anterior side of the neck positioned downward and on the side, respectively. Torsional tests were performed with the neck oriented vertically.

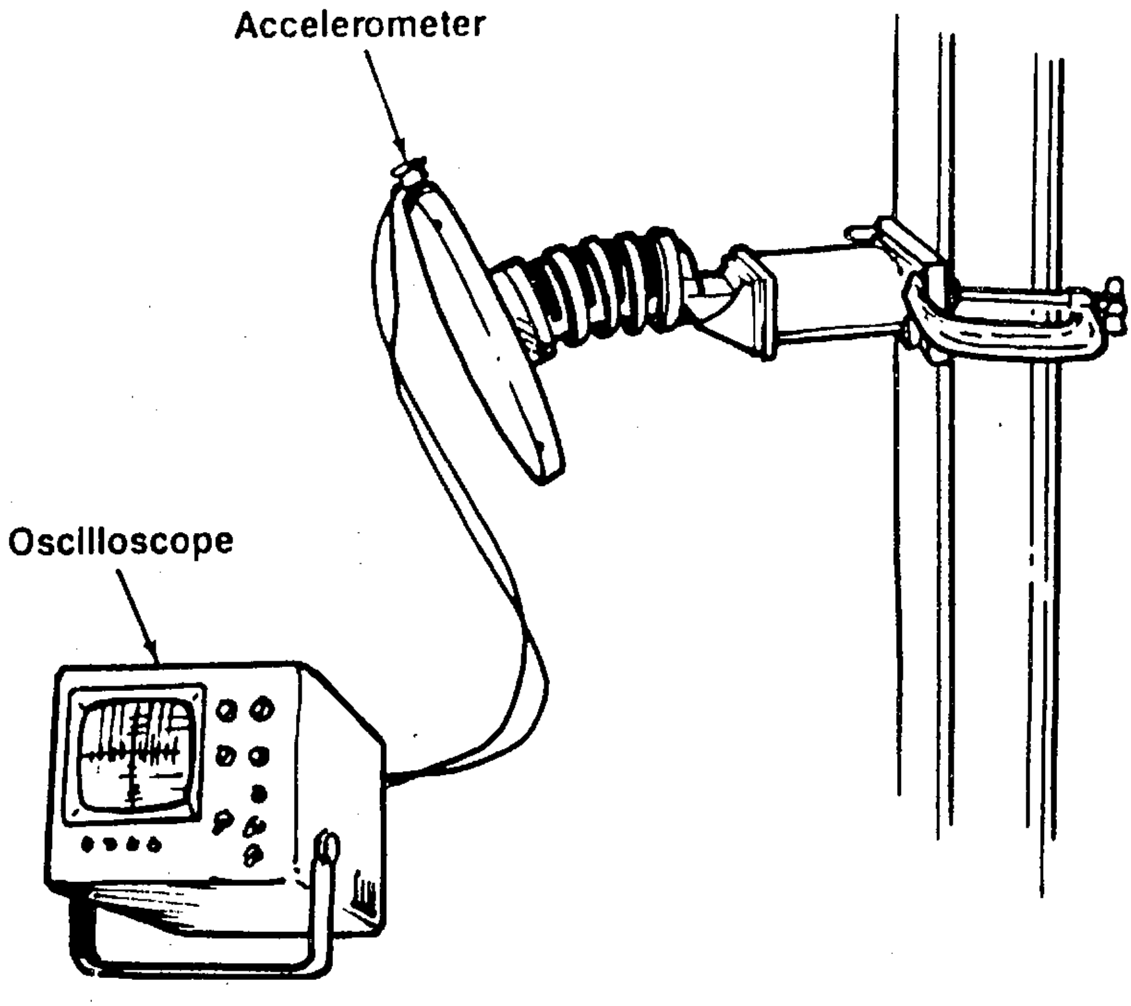

Figure 69. Dynamic Extension Test Setup for the Neck

2.1.4.4.2.2 Data Reduction Procedure and Results

The neck stiffnesses obtained from the dynamic tests were calculated from the natural frequencies assuming the neck to be a cantilever beam with a large mass attached to the end. Given the mass of the weight and neck, the stiffnesses were calculated using the formula

$$w_n = \frac{k}{M+0.23m} \quad \text{or} \quad k = w_n^2\,(M+0.23m)$$

where M = mass of the disk
m = mass of the neck
w_n = natural frequency
k = stiffness

Several tests under the same conditions were performed with natural frequencies differing by no more than 3%. Resulting stiffnesses for the seated manikin neck in the flexion, extension, and lateral directions were 66.68 lb/in, 27.91 lb/in, and 61.49 lb/in, respectively. Stiffnesses for the standing manikin neck in the flexion, extension, and lateral directions were 59.00 lb/in, 34.70 lb/in, and 59.29 lb/in, respectively.

2.1.4.4.3 Comparison of Static and Dynamic Test Results

The comparison of the neck stiffnesses obtained from the static and dynamic tests are presented in Table 8. The dynamic results were changed to in-lb/deg only to directly compare with the static results. As can be seen from the data presented in this table, the stiffnesses determined from the dynamic tests are larger than those determined from the static tests with the largest differences associated with the lateral stiffnesses. A specific reason for the differences between the statically and dynamically derived stiffnesses was not firmly established, but it is believed to be associated with the "creeping" of the rubber when loading is applied slowly. Also presented in the table are the damping factors that were determined from the dynamic tests. As noted the damping is approximately 20% of critical regardless of the direction of motion.

2.1.4.4.4 Measurement of the Nodding Block Stiffness

The two rubber nodding blocks are located anteriorly and posteriorly on top of the head-to-neck adaptor and provide a softening effect during flexion and extension. Although the neck stiffness plays a primary role in the dynamic response of the head-neck system, the stiffness of the block also contributes to this response. To model the net head-neck system it is necessary to include the bending stiffness characteristics of nodding blocks.

The blocks were inserted into the head-to-neck adaptor and the transducer replacement or dummy load cell was attached with the pivot pin. The base was rigidly mounted onto a fixture. An additional bracket was mounted onto the transducer replacement with extended arms on which two symmetrically placed pneumatic pistons acted. To produce bending of the head-neck joint, the pistons provided equal and opposite offset loads from the joint axis during which the angle of rotation was recorded. A curve of the nodding block static bending moment vs. angle data shown in Figure 70. The resulting linear stiffness is about 161 in-lb/deg.

TABLE 8

HYBRID III NECK PROPERTIES

Motion	Static Stiffness	Dynamic Stiffness	% Difference	Damping Factor
Flexion				
- Seated Hybrid III	32.71 in-lb/deg	39.97 in-lb/deg	22.2	0.20
- Standing Hybrid III	34.84 in-lb/deg	35.37 in-lb/deg	1.5	0.20
Extension				
- Seated Hybrid III	15.55 in-lb/deg	16.73 in-lb/deg	7.6	0.22
- Standing Hybrid III	13.82 in-lb/deg	20.80 in-lb/deg	50.5	0.22
Lateral				
- Seated Hybrid III	28.40 in-lb/deg	36.86 in-lb/deg	29.8	0.20
- Standing Hybrid III	24.57 in-lb/deg	35.54 in-lb/deg	44.6	0.20

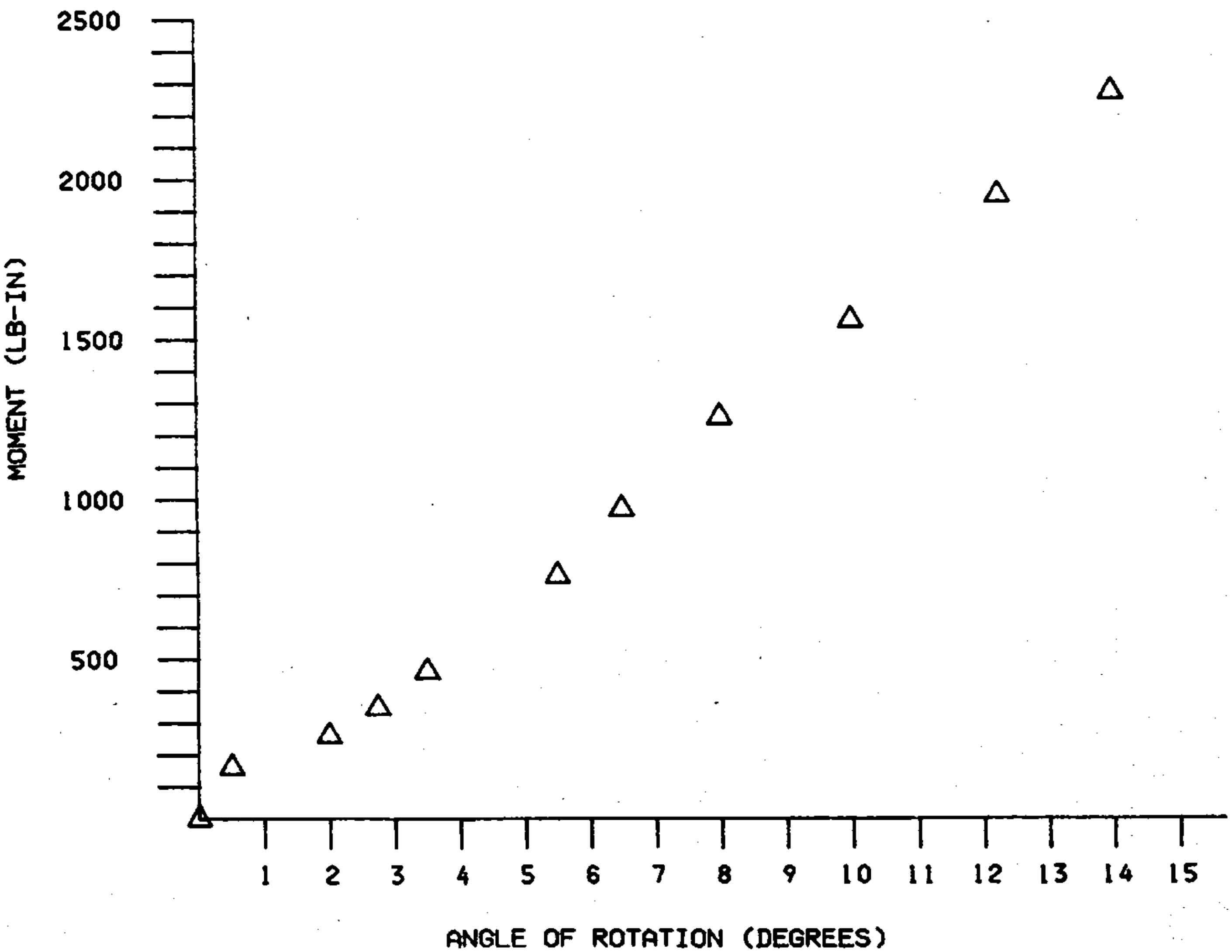

Figure 70. Nodding Block Stiffness Curve

2.1.5 Measurement of the Compliance Characteristics of Segment Skin Coverings

The ATB/CVS model has the capability to account for segment with segment or segment planar surface interactions. In order to perform this prediction, the compliance characteristics of the segment skin coverings are required. The physical features of each segment soft covering can be characterized by a load versus deflection characteristics. The soft covering used for the flesh of the manikins consists of a dense outside layer of polyurethane or vinyl plastisol molded around a pourous foam layer of the same material. As the skin is statically loaded, the vinyl foam deforms such that a hysteresis effect results when the load is removed. The determination of the compliance characteristics of the skin covering over pertinent parts of the manikin was the objective of the tests conducted.

2.1.5.1 Description of Equipment and Techniques Utilized to Establish Compliance of Skin Covering

The density and thickness of the manikin soft covering will vary from segment to segment and also over a given segment. To determine an average compliance for a segment, deflection measurements were made at different locations for that particular segment. If the compliances were drastically different, as with the front and back of the thorax, then two separate skin compliance functions were recorded. Exceptions to this were the hand, foot, and abdomen which were tested at only one location. All test locations for each segment are presented within the segment data tables found in Section 2.1.6.2. These test locations were chosen as segment surface areas most likely to contact with another segment, the steering wheel, seat, or dashboard. Again, because an average compliance was desired, these test points were located to include the effects of varying hardware interference as well as varying soft covering density and thickness.

To test the surface compliance, a pneumatic piston, monitored with a load cell, applied static loads at the designated location on the segment under investigation and the deflection was measured as the distance traveled by the piston. Figure 71, for example, illustrates the test apparatus being used in conjunction with the left forearm. The point of application through which the load was applied was a saucer-shaped probe having either 1" or 2.5" diameter. The small and large probes were used to simulate either a console or steering wheel or a harness or seat contour, respectively. The large probe was used to test the thorax, abdomen, buttocks, and upper leg and the smaller probe was used for the remaining segments. The test consisted of incrementally loading and then unloading the surface while recording the deflection and load cell reading. The amount of penetration depth was determined by either the interference of the hardware or the stroke length of the piston. The tabular data were then plotted to obtain a load versus deflection curve.

2.1.5.2 Discussion of Results

As the objective of the tests was to obtain an average compliance parameter for a given segment, the test locations for different general areas of a segment were only approximately the same for the same segments of the two manikins. It is noted that the degree to which underlying segment hardware resisted the deflection produced different stiffening effects which were apparent in the data. In addition, since the density and thickness of both the external and foam skin layers affect the stiffness characteristics of the skin covering, the force-deflection data reflected those characteristics. These differences are reflected in the skin force-deflection curves, presented in Figure 72, which were obtained at one test location on the forearm of the two different manikins. While these curves are not to be directly compared in detail, their different characteristics demonstrate the differences found with varying skin density and thickness and hardware interference. As all of these factors vary from location to location, an average compliance was used to represent these properties of the soft

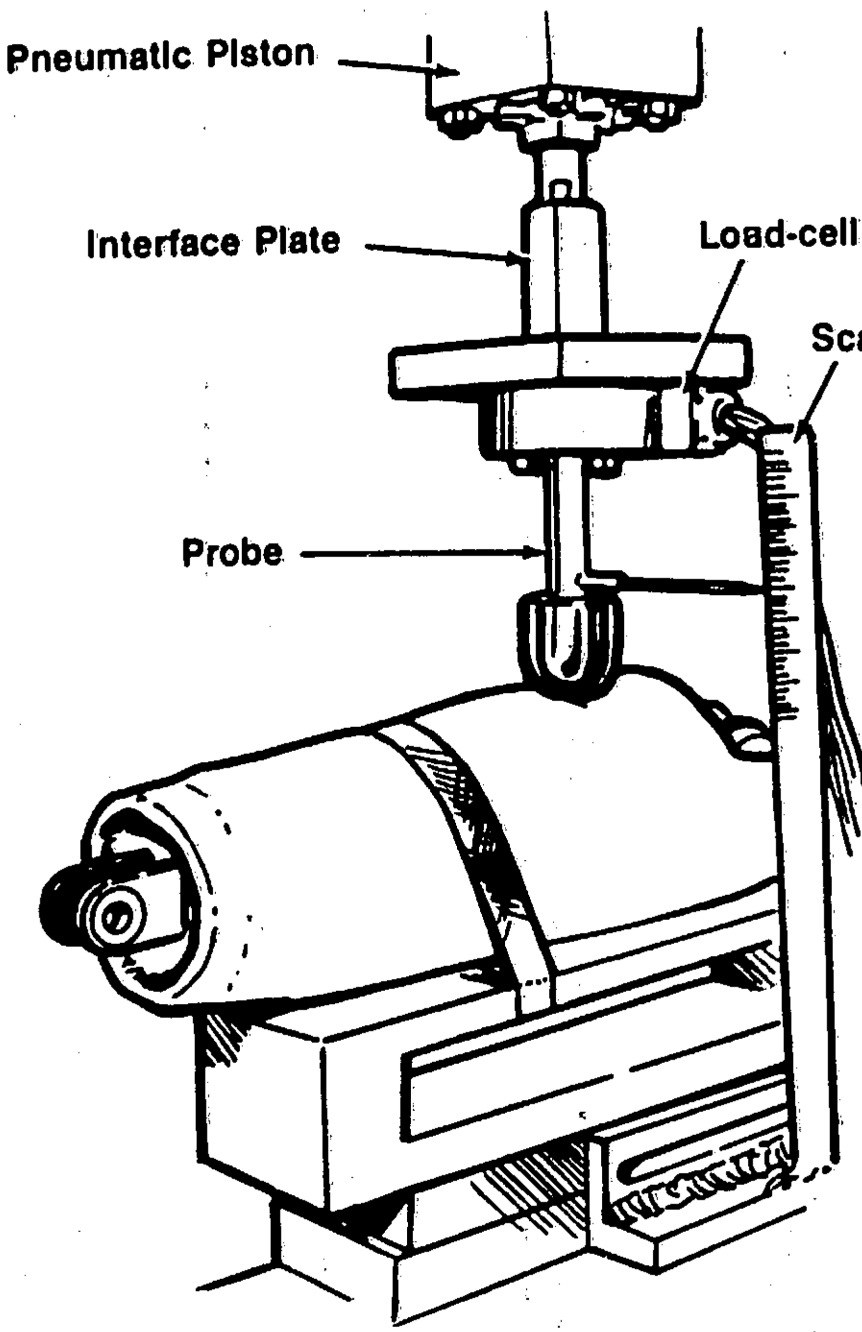

Figure 71. Compliance Test Apparatus With Forearm

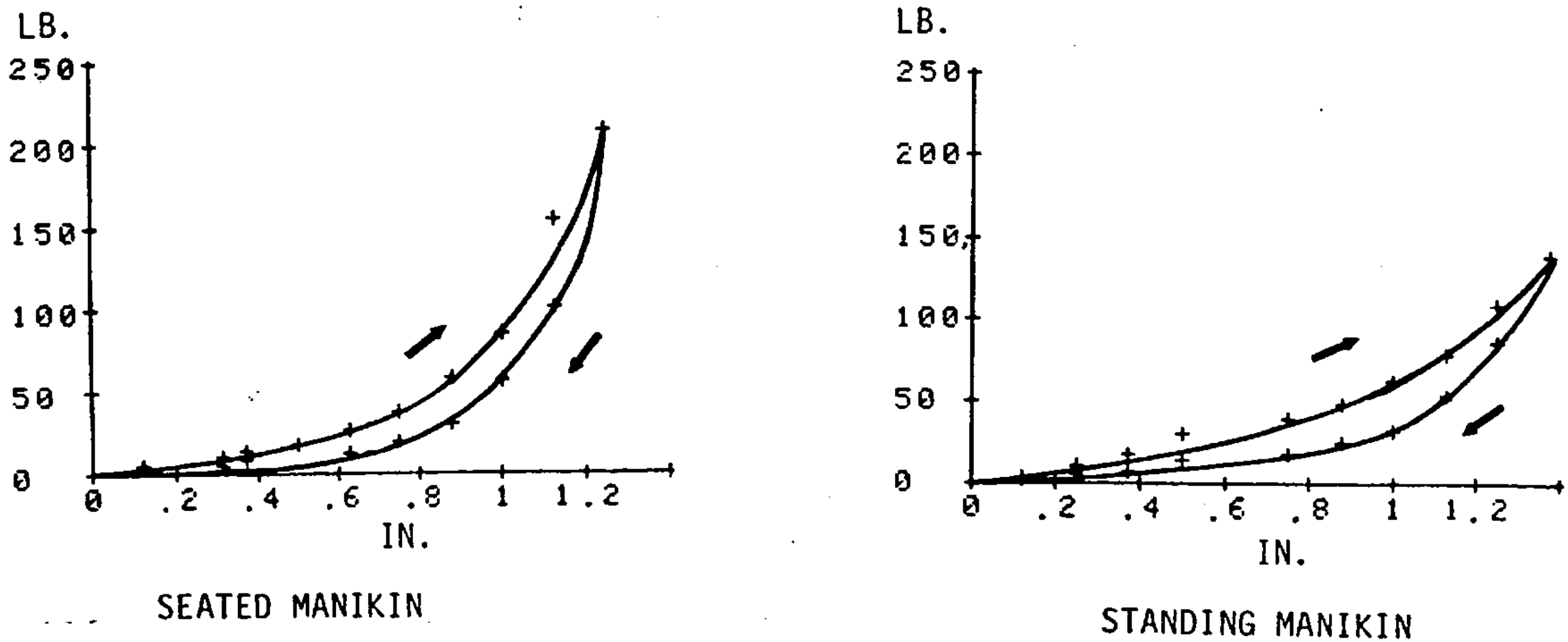

Figure 72. Compliance Test Results for Forearm

covering for a given segment. The measured data obtained from the skin compliance testing are presented in Section 2.1.5.3 for all of the manikin components.

2.1.5.3 Plots of Skin Compliance

Figures 73 through 98 present plots of applied force vs deflection of the skin coverings for the various manikin segments. From the results presented in these figures the skin compliance data required for the ATB prediction program were determined.

2.1.6 Data Tables of Segment Physical Characteristics

The experimental data describing segment properties presented and discussed in the previous sections of this report are summarized in the data Tables 9 through 31 provided in this section. All the data that were developed for a given segment have been collected and tabulated on separate pages for easy reference and use. The description of the geometric, mass distribution and surface characteristic data for each of the Hybrid III segments that are presented in the data Tables are defined in this section. For those segments unique to each manikin (i.e., spine, pelvis, and upper legs), separate tables are presented. Only one set of tables is necessary for each of the remaining segments, which are identical in design for both manikins. For discussions on how the data were obtained in these tables, see the appropriate report chapter.

The following information is provided for each of the segments in the Tables:

1. Local Reference Axes. These have been defined to best represent the symmetry of the segment and are generally based on segment mechanical features. They are illustrated as axes X_L, Y_L, and Z_L.
2. Anatomical Axes. Identical to segment definitions in Young, et al. [5] and are based on equivalent human anatomical landmarks. They are illustrated as X_A, Y_A, and Z_A.

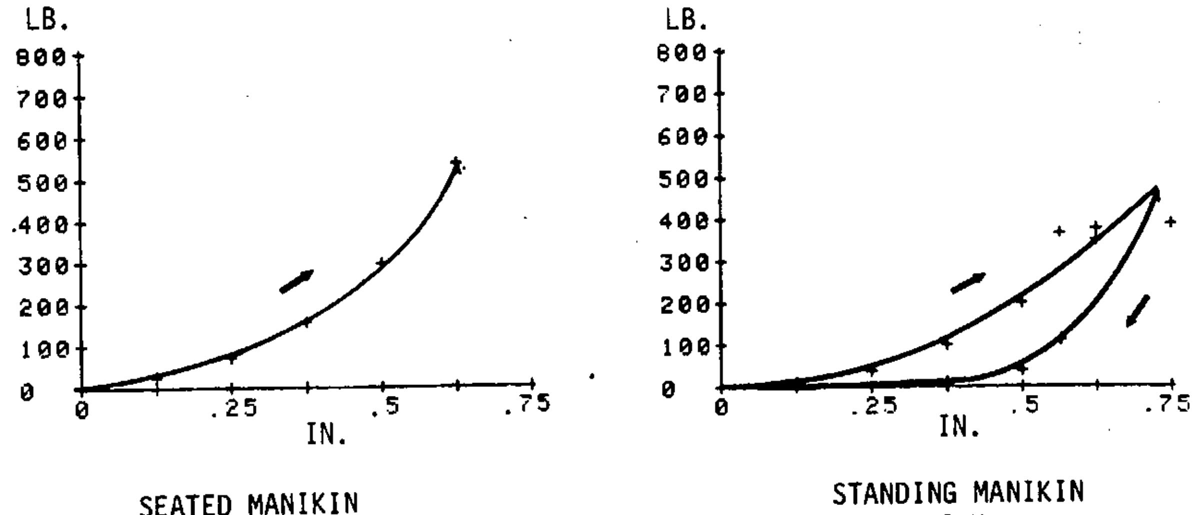

Figure 73. Skin Compliance Curves for Front of Head

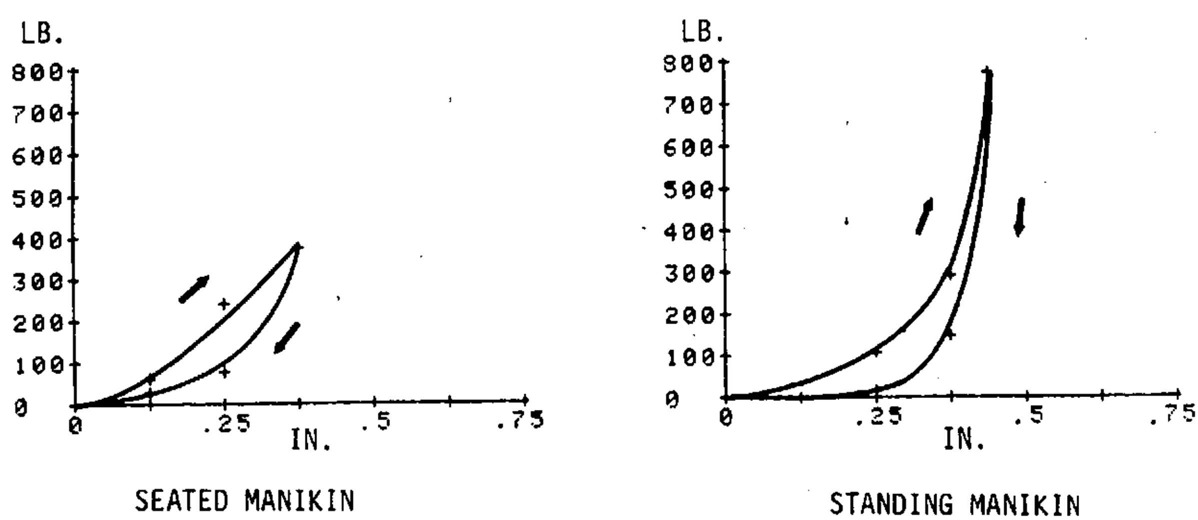

Figure 74. Skin Compliance Curves for Back of Head

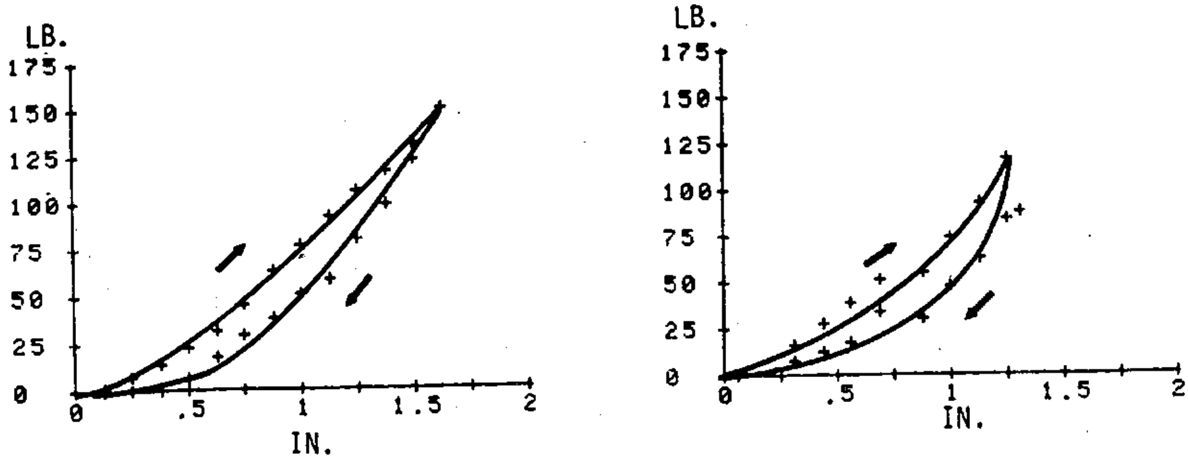

SEATED MANIKIN STANDING MANIKIN

Figure 75. Skin Compliance Curves for Front of Thorax-Position 1

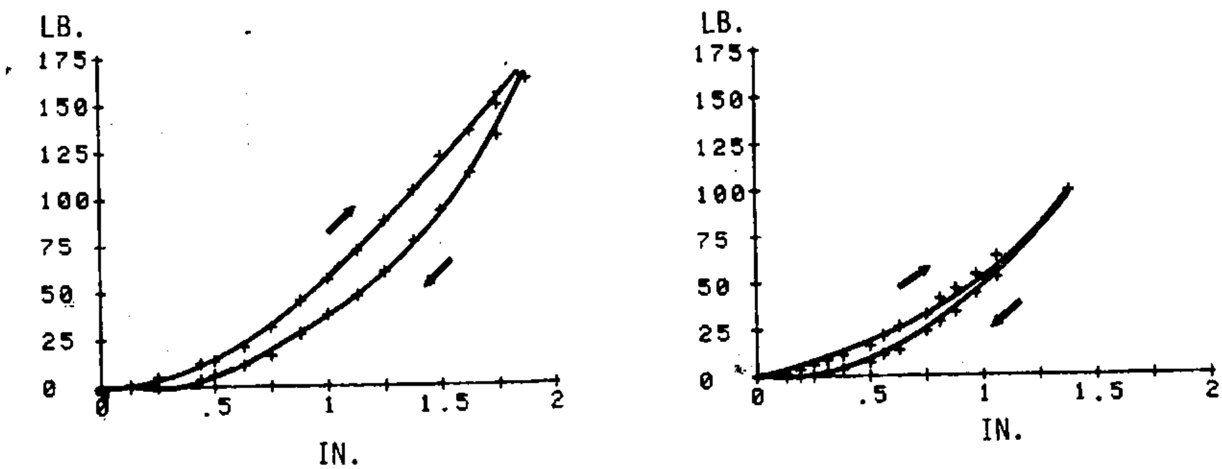

SEATED MANIKIN STANDING MANIKIN

Figure 76. Skin Compliance Curves for Front of Thorax-Position 2

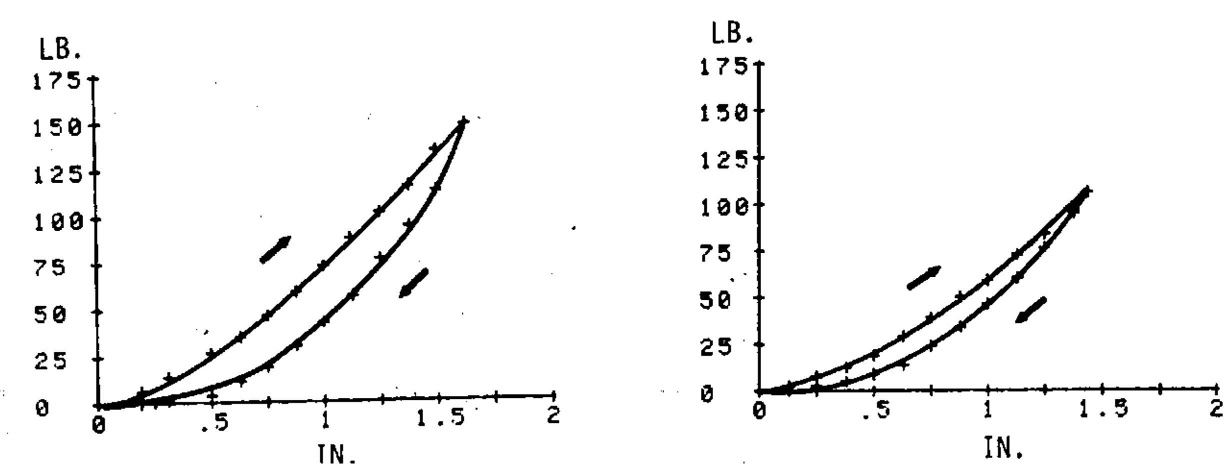

SEATED MANIKIN STANDING MANIKIN

Figure 77. Skin Compliance Curves for Front of Thorax-Position 3

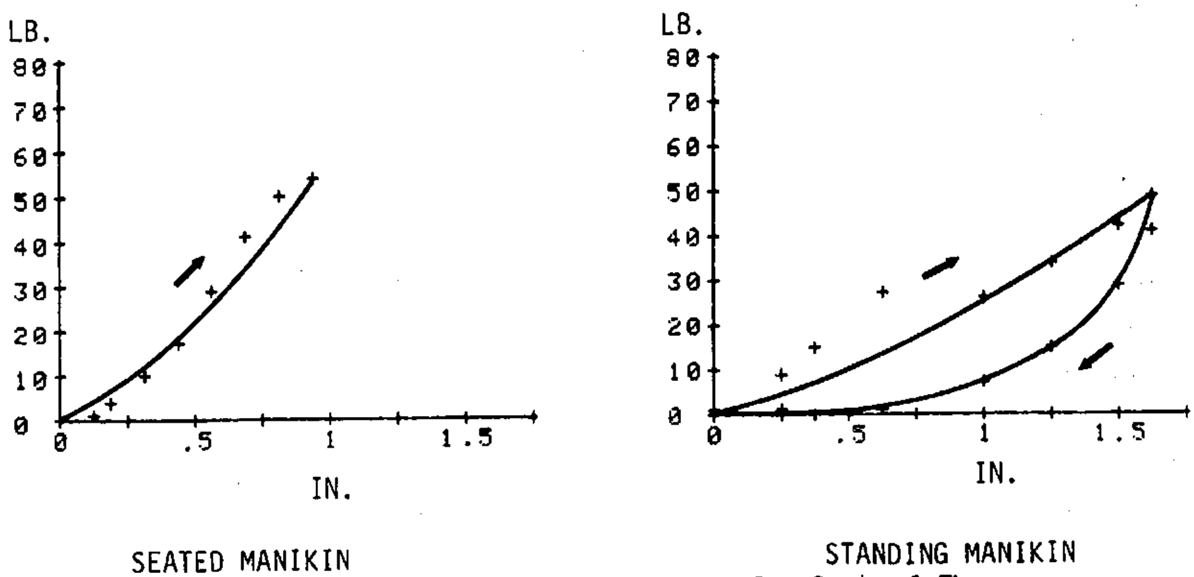

Figure 78. Skin Compliance Curves for Back of Throax

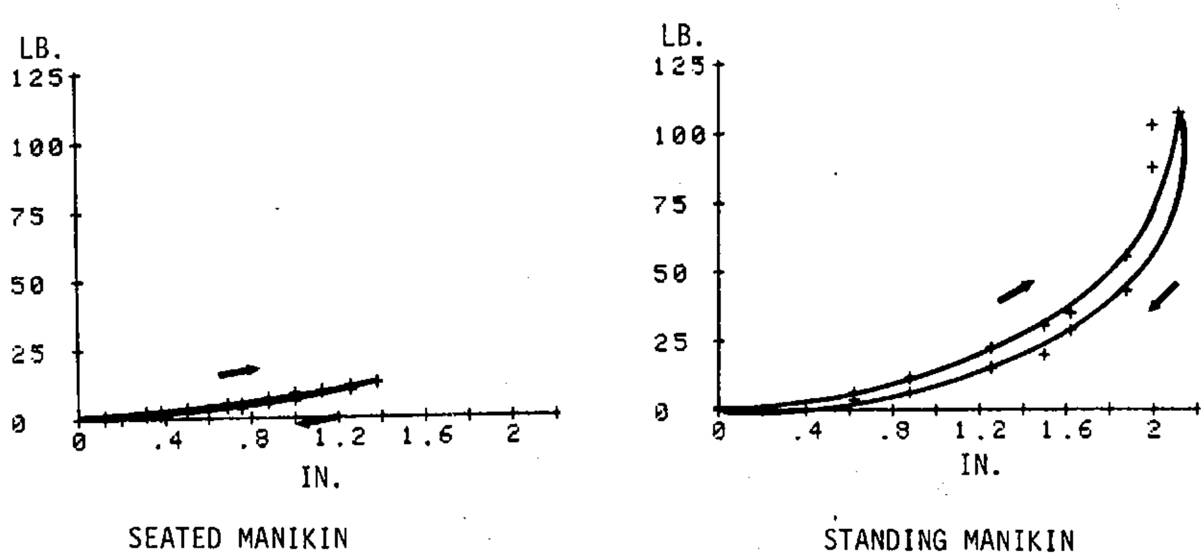

Figure 79. Skin Compliance Curves for Abdominal Insert

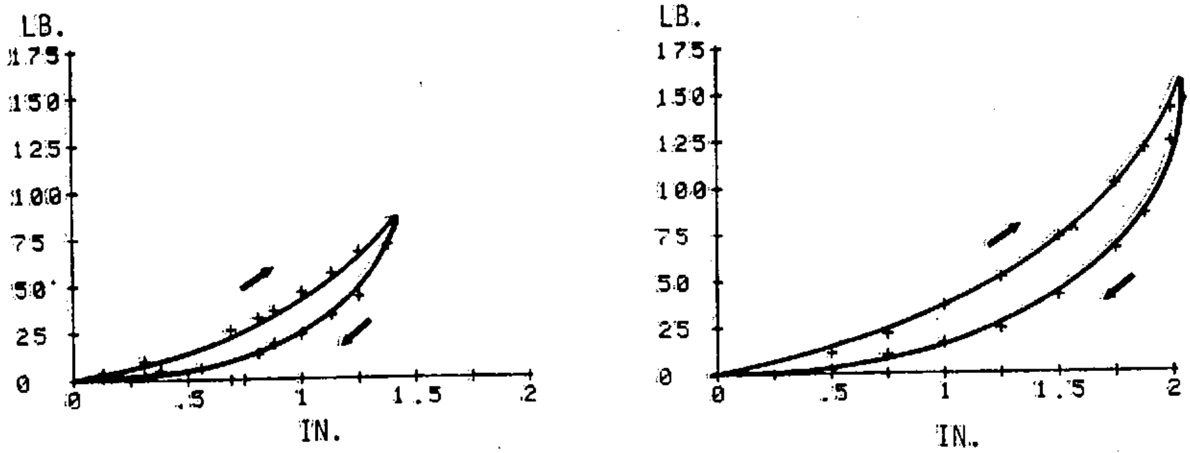

SEATED MANIKIN   STANDING MANIKIN

Figure 80. Skin Compliance Curves for Buttocks-Position 1

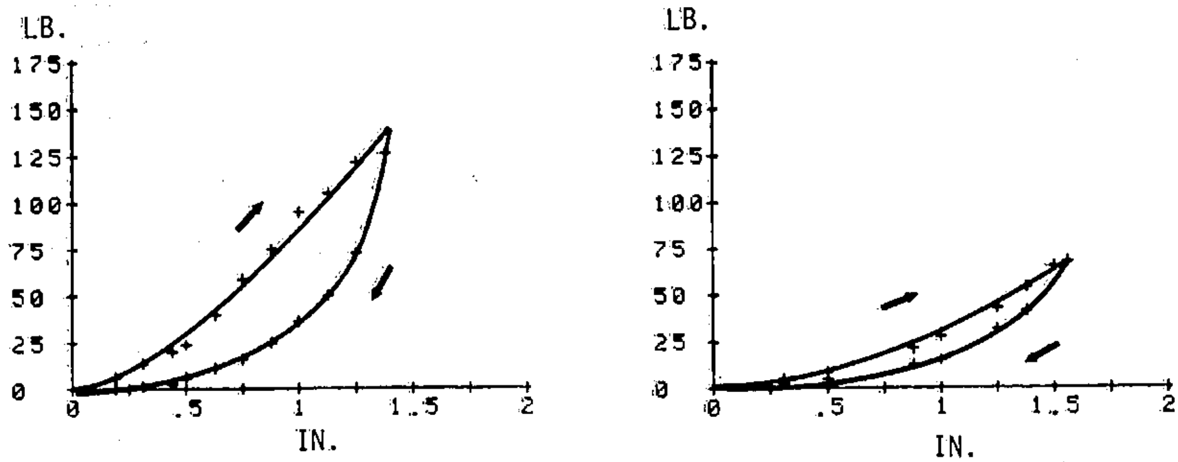

SEATED MANIKIN   STANDING MANIKIN

Figure 81. Skin Compliance Curves for Buttocks-Position 2

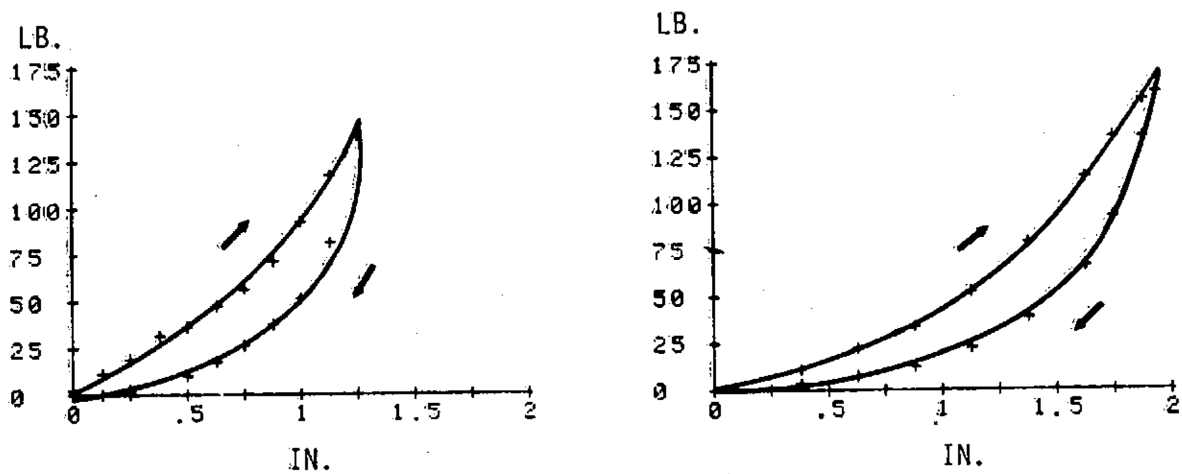

SEATED MANIKIN   STANDING MANIKIN

Figure 82. Skin Compliance Curves for Buttocks-Position 3

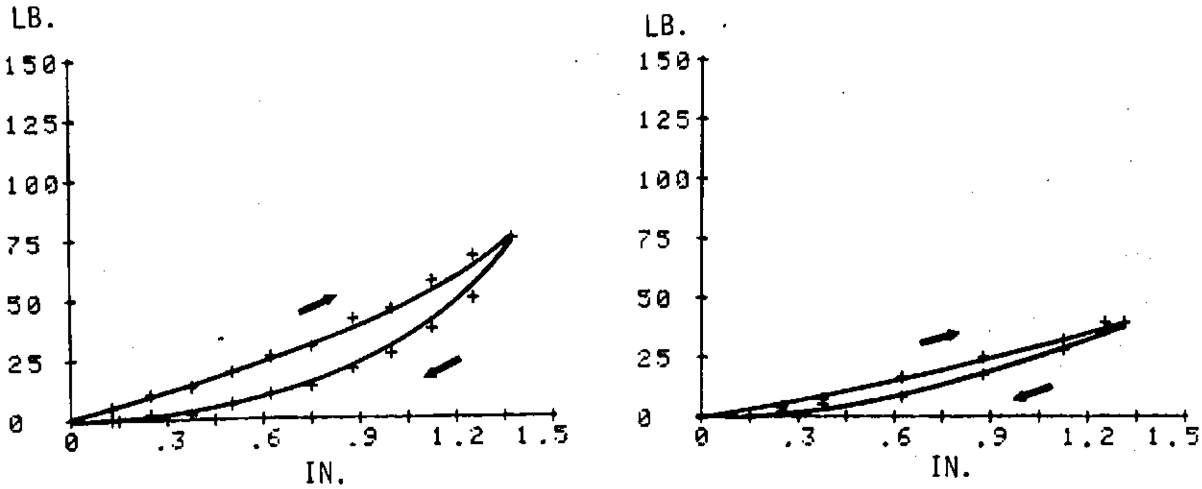

SEATED MANIKIN STANDING MANIKIN

Figure 83. Skin Compliance Curves for Upper Leg-Position 1

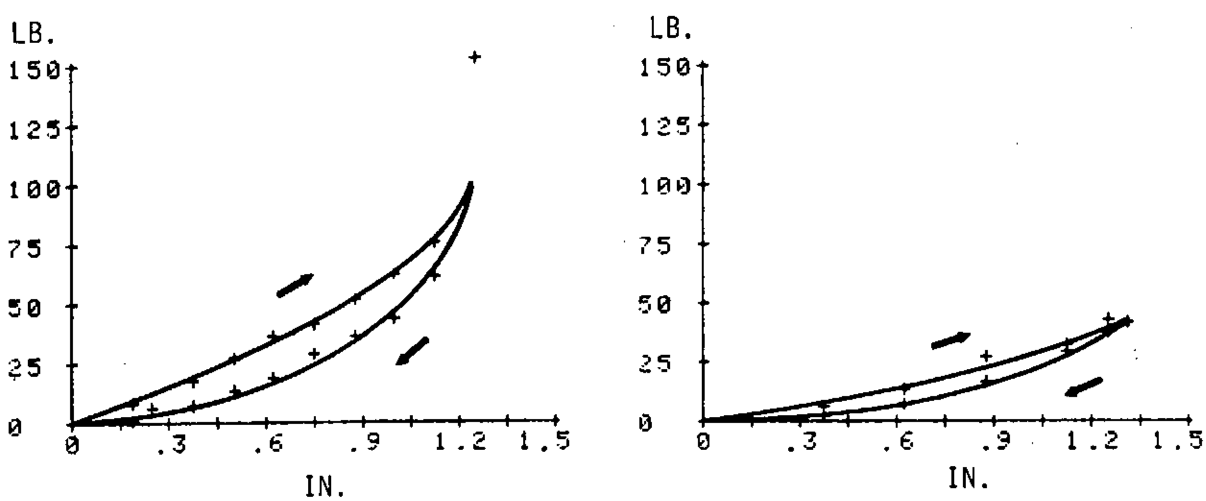

SEATED MANIKIN STANDING MANIKIN

Figure 84. Skin Compliance Curves for Upper Leg-Position 2

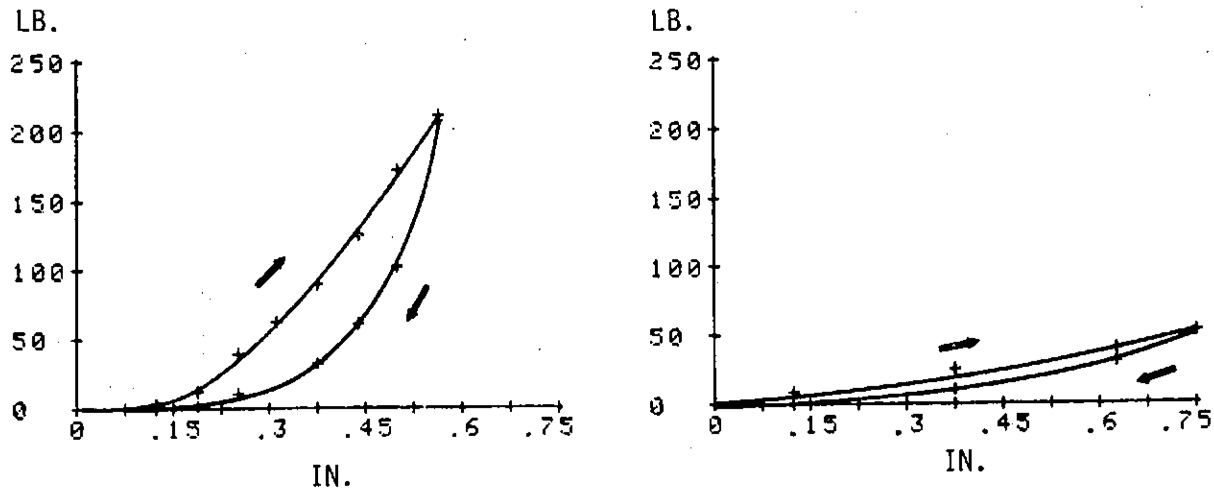

SEATED MANIKIN STANDING MANIKIN

Figure 85. Skin Compliance Curves for Knee-Position 1

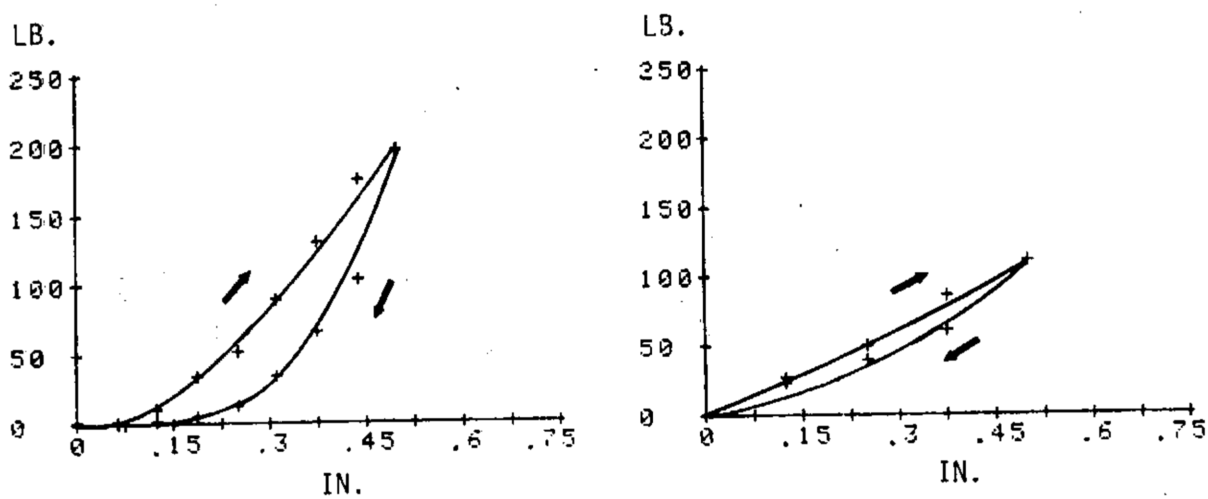

SEATED MANIKIN STANDING MANIKIN

Figure 86. Skin Compliance Curves for Knee-Position 2

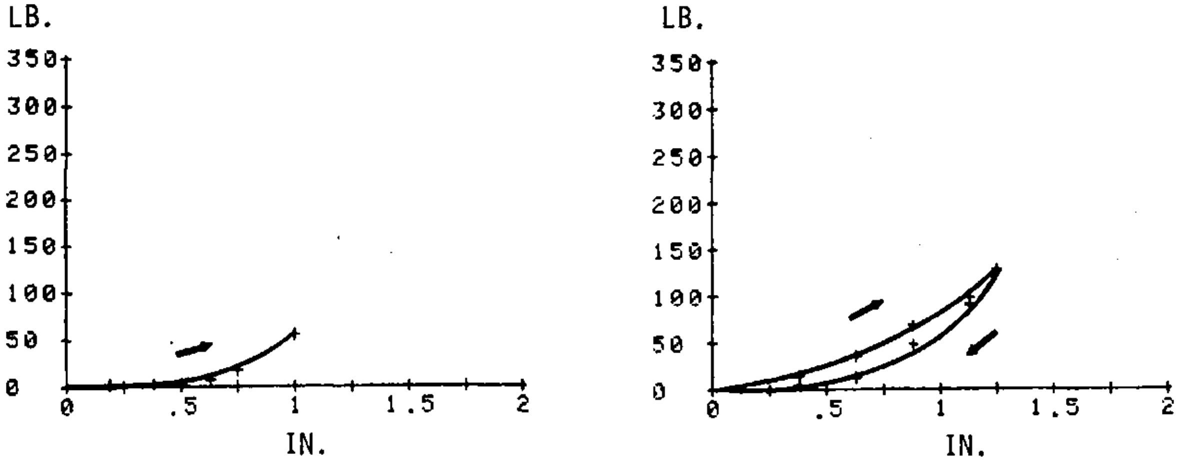

SEATED MANIKIN STANDING MANIKIN

Figure 87. Skin Compliance Curves for Front of Lower Leg-Position 1

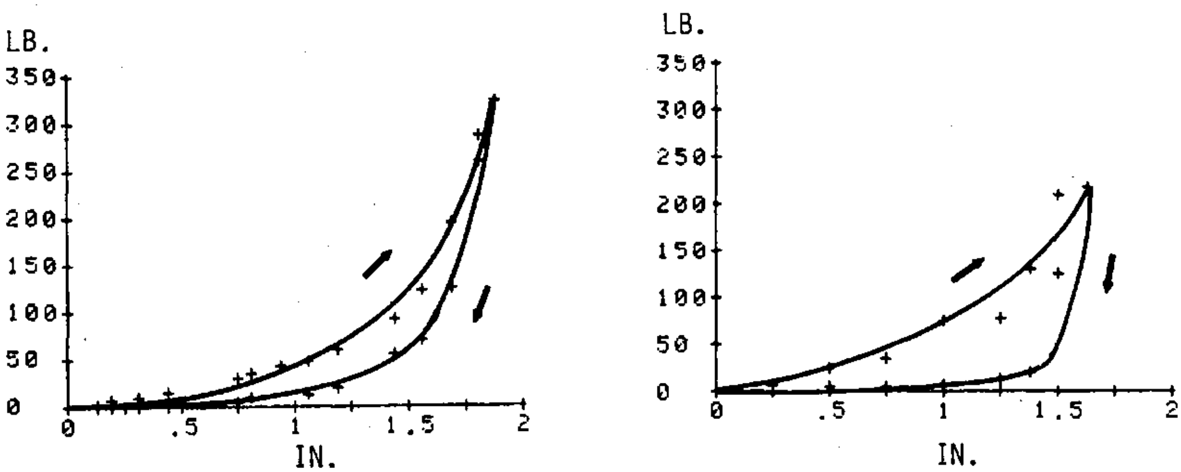

SEATED MANIKIN STANDING MANIKIN

Figure 88. Skin Compliance Curves for Front of Lower Leg-Position 2

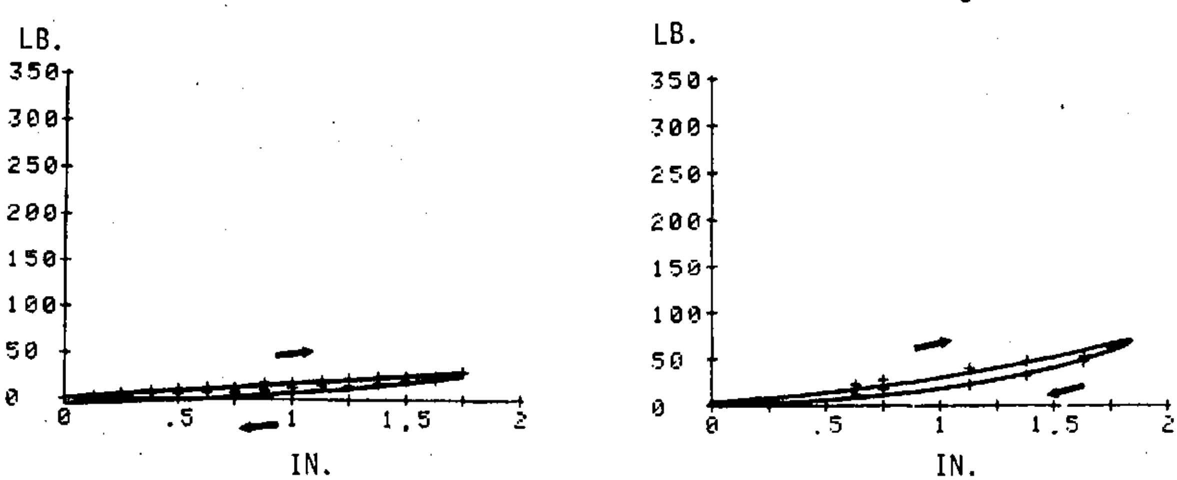

SEATED MANIKIN STANDING MANIKIN

Figure 89. Skin Compliance Curves for Back of Lower Leg-Position 3

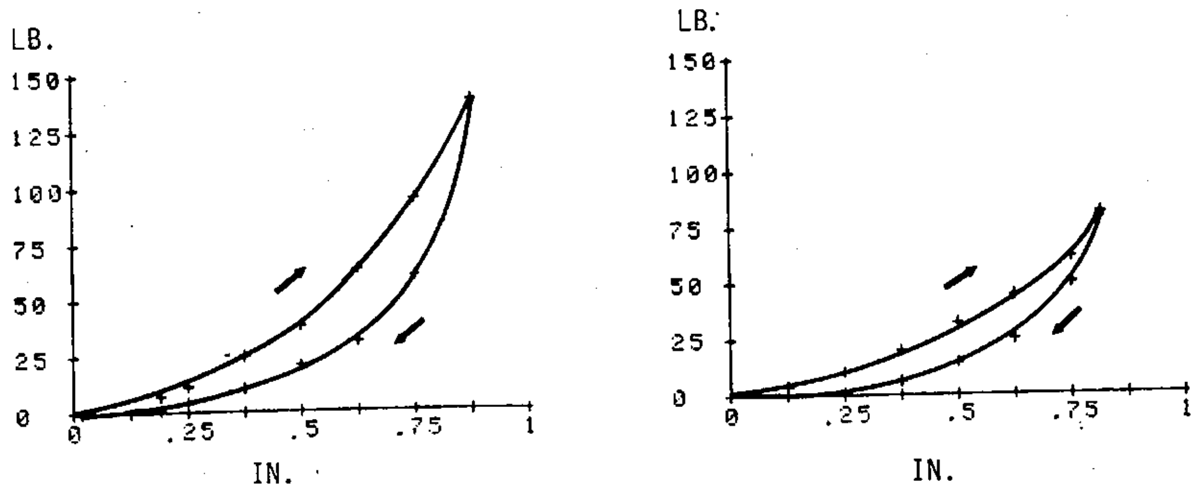

SEATED MANIKIN STANDING MANIKIN

Figure 90. Skin Compliance Curves for Foot

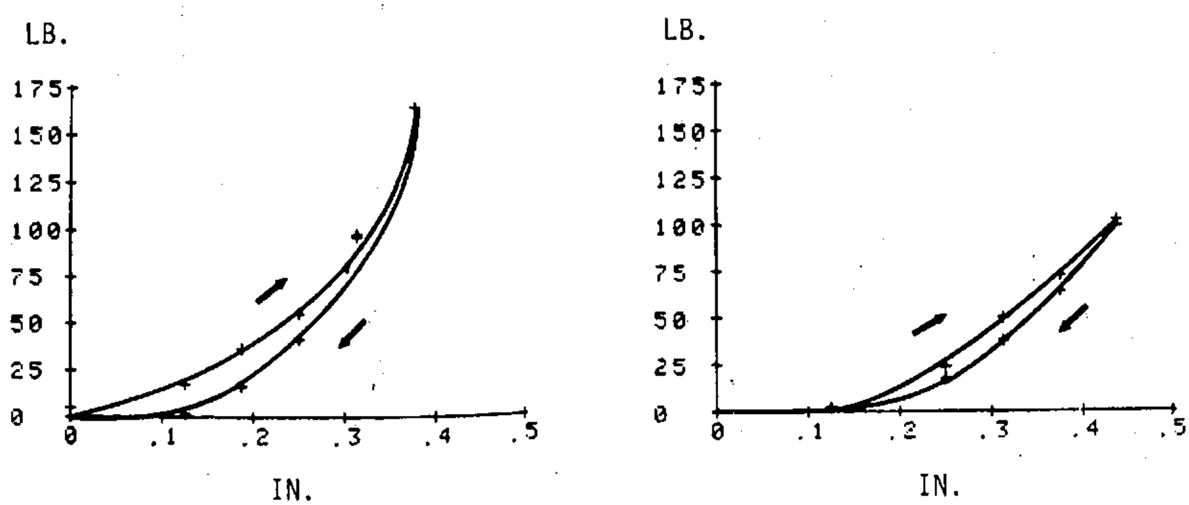

SEATED MANIKIN STANDING MANIKIN

Figure 91. Skin Compliance Curves for Hand

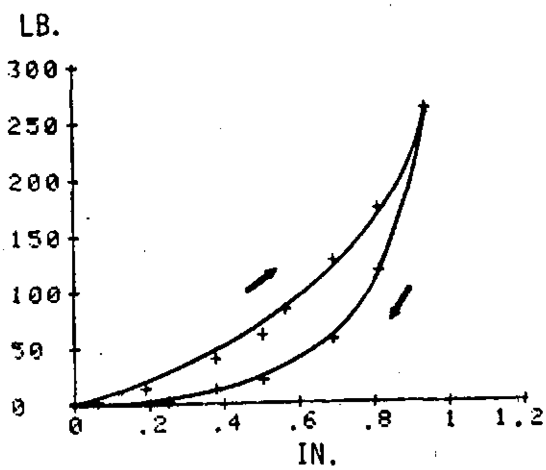

SEATED MANIKIN STANDING MANIKIN

Figure 92. Skin Compliance Curves for Upper Arm-Position 1

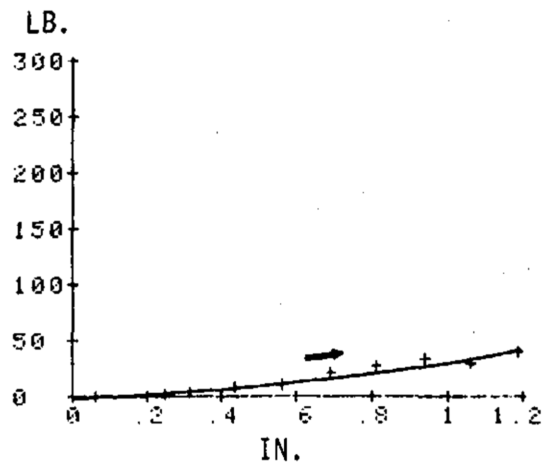

SEATED MANIKIN STANDING MANIKIN

Figure 93. Skin Compliance Curves for Upper Arm-Position 2

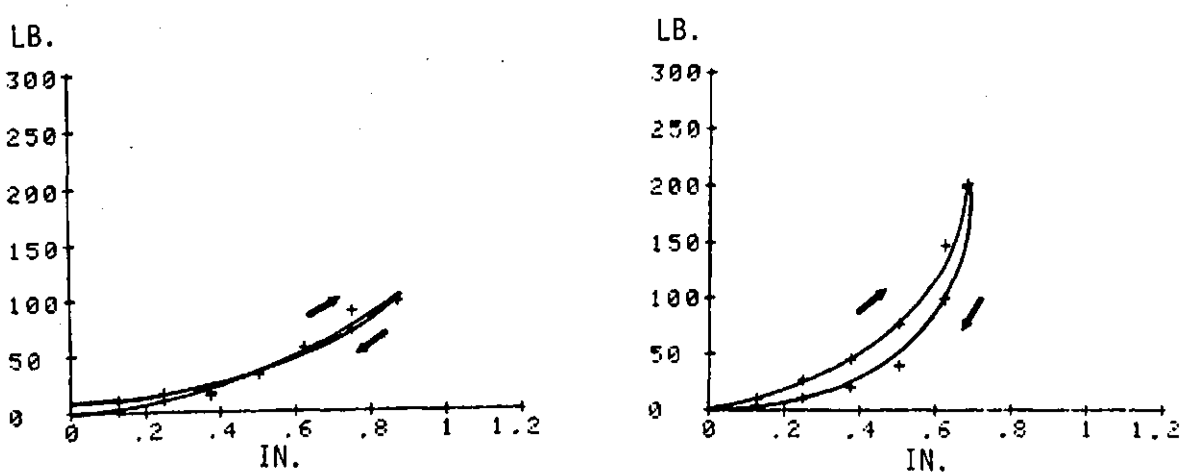

SEATED MANIKIN STANDING MANIKIN

Figure 94. Skin Compliance Curves for Upper Arm-Position 3

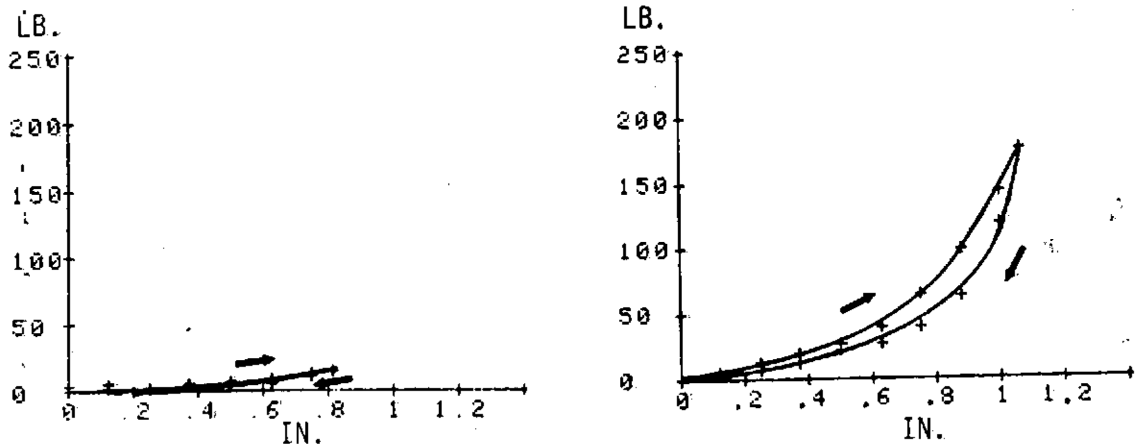

SEATED MANIKIN STANDING MANIKIN

Figure 95. Skin Compliance Curves for Forearm-Position 1

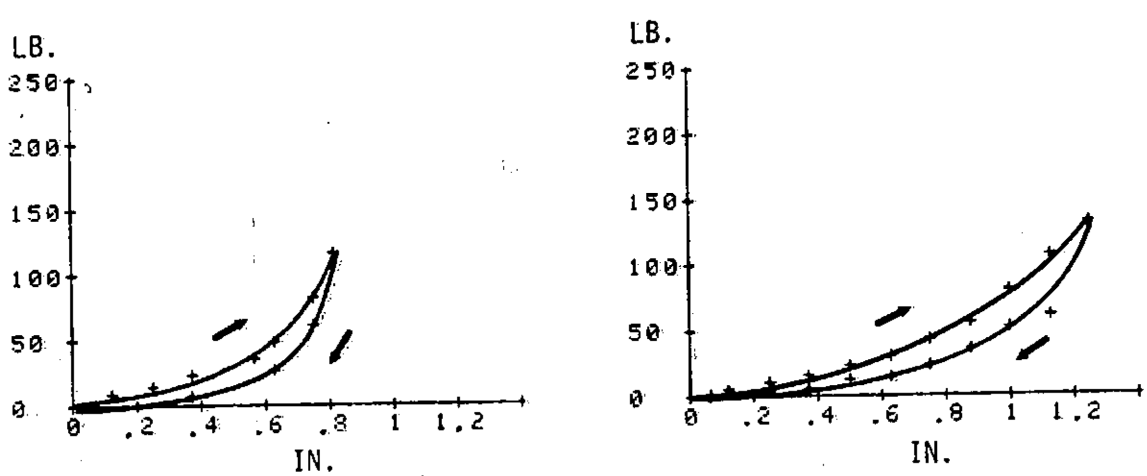

SEATED MANIKIN STANDING MANIKIN

Figure 96. Skin Compliance Curves for Forearm-Position 2

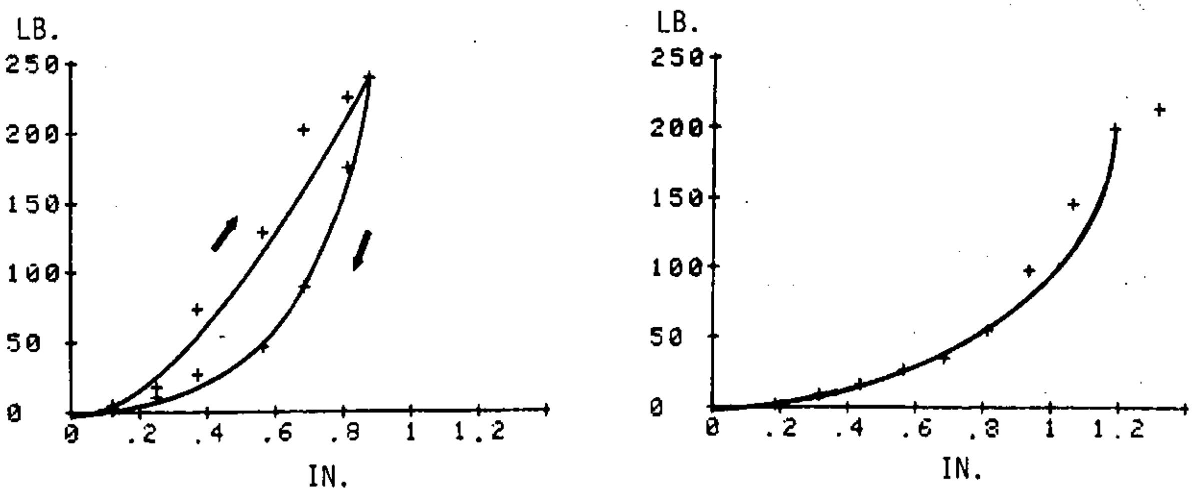

SEATED MANIKIN STANDING MANIKIN

Figure 97. Skin Compliance Curves for Forearm-Position 3

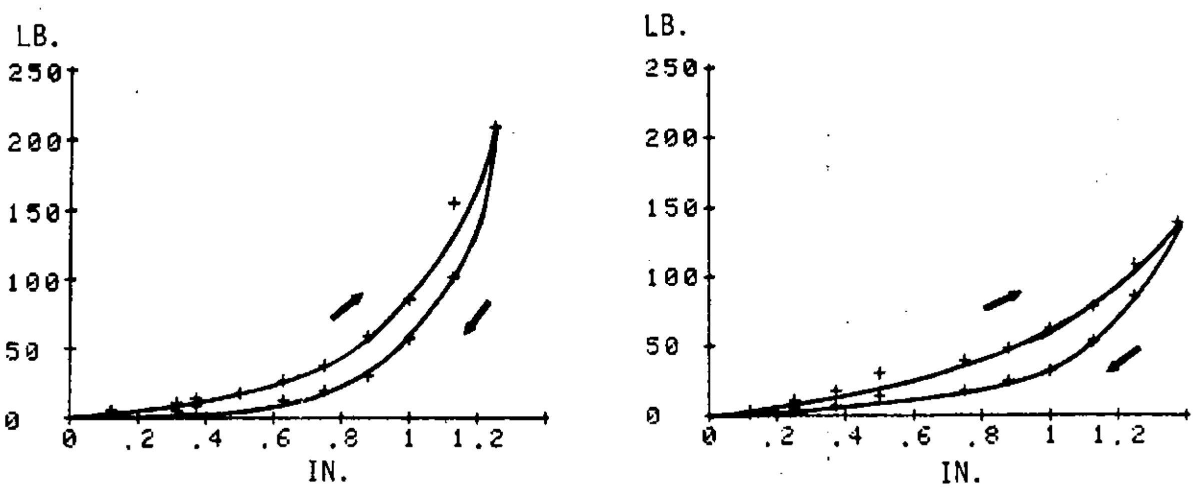

SEATED MANIKIN STANDING MANIKIN

Figure 98. Skin Compliance Curves for Forearm-Position 4

3. Segment Landmarks. These are the points used in the axes definitions. The analogous manikin locations are described and illustrated, and the coordinates (in inches) are presented for both axis systems.

4. Transformation from Local Reference to Anatomical Axes. This is the rotational cosine transformation matrix that transforms vector components from the Local Reference to the Anatomical Axes Coordinate System. Note that these two coordinate systems linear offset can be obtained from the Segment Landmark coordinate points given in each table.

5. Segment Contact Ellipsoid Semiaxes. These are the values (in inches) used in defining ellipsoids for the accompanying ATB body description input file with the axes assumed to be aligned with the local reference axes.

6. Weight in pounds. This is the average weight of segments.

7. Principal Moments of Inertia ($\text{lbs-sec}^2\text{-in}$). These values are the averages of those found from the manikin segment measurements.

8. Transformation from Principal Axes to Local Reference Axes. This is the rotation cosine transformation matrix that transforms vector components from the Principal Axes to the Local Reference Axes coordinate system. Both of the coordinate systems have their origin at the center of mass of the segment therefore there is no linear offset between these two coordinate systems.

9. Surface Force-Deflection Characterization. The surface force-deflection properties are given by a fifth order polynomial,

$$F(D) = A_o + A_1D + A_2D^2 + A_3D^3 + A_4D^4 + A_5D^5,$$

where F(D) is the force in pounds, D is the deflection in inches and the A_i's are the polynomial coefficients. The test points are illustrated by one or more x 's on the segment.

TABLE 9

RIGHT UPPER ARM

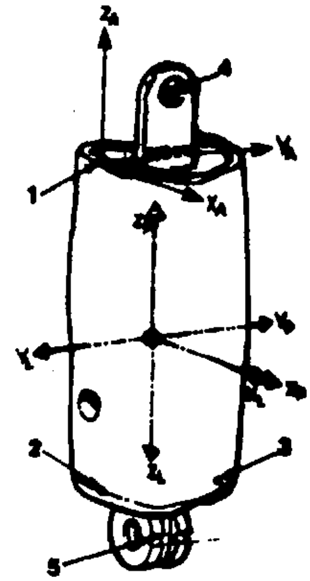

Local Reference Axes

Z axis - vector from right shoulder center to right elbow center.
Y-Z plane - right lateral epicondyle on the arm sleeve.
X axis - Y x Z.
Origin - center of gravity.

Anatomical Axes

Z axis - vector from lateral humeral epicondyle to acromiale.
Y axis - normal from Z axis to medial humeral epicondyle.
X axis - Y x Z.
Origin - at acromiale.

Segment Landmarks

1. Right Acromiale on arm sleeve - lateral superior edge of the arm covering.
2. Right Lateral Humeral Epicondyle on arm sleeve - lateral inferior edge of the arm covering.
3. Right Medial Humeral Epicondyle on arm sleeve - medial inferior edge of the arm covering.
4. Right Shoulder Joint Center.
5. Right Elbow Joint Center.

	Local Reference Axes (in)			Anatomical Axes (in)		
	X	Y	Z	X	Y	Z
1. Right Acromiale on arm sleeve	0.00	1.77	-4.84	0.00	0.00	0.00
2. Right Lateral Humeral Epicondyle on sleeve	0.00	1.62	3.54	0.00	0.00	-8.38
3. Right Medial Humeral Epicondyle on sleeve	0.00	-1.61	3.48	0.00	3.23	-8.38
4. Right Shoulder Joint Center	0.00	0.00	-5.43	0.00	1.78	0.55
5. Right Elbow Joint Center	0.00	0.00	4.94	0.00	1.59	-9.81
6. Right Upper Arm Center of Gravity	0.00	0.00	0.00	0.00	1.69	-4.88

Transformation from Local Reference to Anatomical Axes

$$A_{AL} = \begin{bmatrix} 0.99998 & -0.00300 & -0.00572 \\ -0.00310 & -0.99983 & -0.01818 \\ -0.00567 & 0.01819 & -0.99982 \end{bmatrix}$$

Segment Contact Ellipsoid Semiaxes (in)

X: 1.900 Y: 1.800 Z: 6.000

Weight (lbs)

4.60

Principal Moments of Inertia (lbs - sec^2 - in)

X: 0.1025 Y: 0.0997 Z: 0.0110

Transformation from Principal to Local Reference Axes

$$A_{LP} = \begin{bmatrix} 0.99974 & -0.00004 & 0.02288 \\ -0.00004 & -1.00000 & 0.00000 \\ 0.02288 & 0.00000 & -0.99974 \end{bmatrix}$$

Surface Characteristics Coefficients Relating Load (lbs) to Deflection (in) (from Test of Left Upper Arm)

A_0 = 1.5352 A_1 = -30.6266 A_2 = 627.089 A_3 = -1197.70 A_4 = 917.233 A_5 = 0

TABLE 10

LEFT UPPER ARM

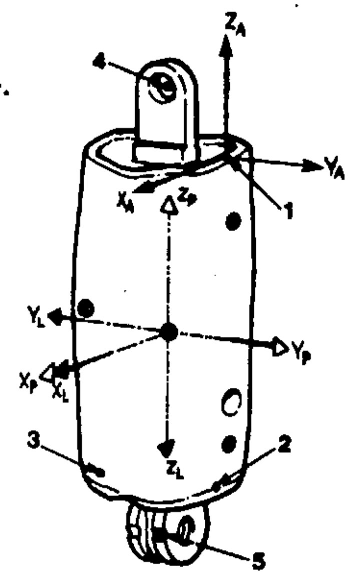

Local Reference Axes

Z axis - vector from the left shoulder center to the left elbow center.
Y-Z plane - left medial epicondyle on the arm sleeve.
X axis - Y x Z.
Origin - center of gravity.

Anatomical Axes

Z axis - vector from lateral humeral epicondyle to acromiale.
Y axis - normal from medial humeral epicondyle to Z axis.
X axis - Y x Z.
Origin - at acromiale.

Segment Landmarks

1. Left Acromiale on arm sleeve - lateral superior edge of the arm covering.
2. Left Lateral Humeral Epicondyle on arm sleeve - lateral inferior edge of the arm covering.
3. Left Medial Humeral Epicondyle on arm sleeve - medial inferior edge of the arm covering.
4. Left Shoulder Joint Center.
5. Left Elbow Joint Center.

	Local Reference Axes (in)			Anatomical Axes (in)		
	X	Y	Z	X	Y	Z
1. Left Acromiale on arm sleeve	0.00	-1.77	-4.84	0.00	0.00	0.00
2. Left Lateral Humeral Epicondyle on sleeve	0.00	-1.62	3.54	0.00	0.00	-8.38
3. Left Medial Humeral Epicondyle on sleeve	0.00	1.61	3.48	0.00	-3.23	-8.38
4. Left Shoulder Joint Center	0.00	0.00	-5.43	0.00	-1.78	0.55
5. Left Elbow Joint Center	0.00	0.00	4.94	0.00	-1.59	-9.81
6. Left Upper Arm Center of Gravity	0.00	0.00	0.00	0.00	-1.69	-4.88

Transformation from Local Reference to Anatomical Axes

$$A_{AL} = \begin{bmatrix} 0.99998 & 0.00300 & -0.00572 \\ 0.00310 & -0.99983 & 0.01818 \\ -0.00567 & -0.01819 & -0.99982 \end{bmatrix}$$

Segment Contact Ellipsoid Semiaxes (in)

X: 1.900 Y: 1.800 Z: 6.000

Weight (lbs)

4.60

Principal Moments of Inertia (lbs - sec^2 - in)

X: 0.1025 Y: 0.0997 Z: 0.0110

Transformation from Principal to Local Reference Axes

$$A_{LP} = \begin{bmatrix} 0.99974 & 0.00004 & 0.02288 \\ 0.00004 & -1.00000 & 0.00000 \\ 0.02288 & 0.00000 & -0.99974 \end{bmatrix}$$

Surface Characteristics Coefficients Relating Load (lbs) to Deflection (in)

A_0 = 1.5352 A_1 = -30.6266 A_2 = 627.089 A_3 = -1197.70 A_4 = 917.233 A_5 = 0

TABLE 11

RIGHT FOREARM

Local Reference Axes

Z axis - vector from right elbow center to the right wrist center.
Y-Z plane - lateral end of the right wrist flexion axis.
X axis - Y x Z.
Origin - center of gravity.

Anatomical Axes

Z axis - vector from ulnar styloid to radiale.
Y axis - vector from radial styloid normal to Z axis.
X axis - Y x Z.
Origin - at radiale.

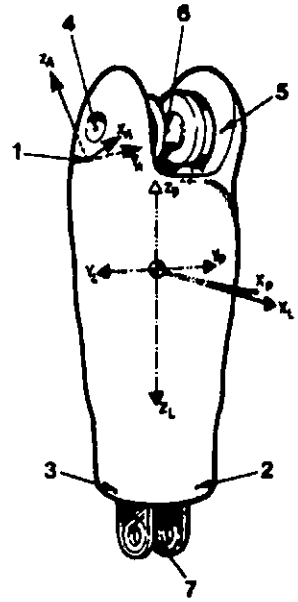

Segment Landmarks

1. Right Radiale - at the level of the distal lateral edge of the elbow hardware, approximately two-thirds of the distance from the anterior to the posterior midlines.
2. Right Ulnar Styloid Process on arm sleeve - distal medial edge of the arm covering.
3. Right Radial Styloid Process on arm sleeve - distal lateral edge of the arm covering.
4. Right Lateral Humeral Epicondyle - projection of the lateral end of the right elbow axis to the surface covering.
5. Right Medial Humeral Epicondyle - projection of the medial end of the right elbow axis to the surface covering.
6. Right Elbow Joint Center.
7. Right Wrist Joint Center.

	Local Reference Axes (in)			Anatomical Axes (in)		
	X	Y	Z	X	Y	Z
1. Right Radiale	-1.20	1.36	-2.91	0.00	0.00	0.00
2. Right Ulnar Styloid Process on sleeve	0.00	-1.11	5.52	0.00	0.00	-8.86
3. Right Radial Styloid Process on sleeve	0.20	1.11	5.47	0.00	-2.13	-8.23
4. Right Lateral Humeral Epicondyle	0.25	0.90	-3.70	1.60	0.44	0.43
5. Right Medial Humeral Epicondyle	-0.28	-0.90	-3.69	1.26	2.24	0.00
6. Right Elbow Joint Center	0.00	0.00	-3.67	1.52	1.32	0.17
7. Right Wrist Joint Center	0.00	0.00	6.07	-0.10	-1.21	-9.09
8. Right Forearm Center of Gravity	0.00	0.00	0.00	0.92	0.37	-3.03

Transformation from Local Reference to Anatomical Axes

$$A_{AL} = \begin{bmatrix} 0.98113 & 0.09808 & -0.16665 \\ -0.13971 & -0.95537 & -0.26029 \\ -0.13369 & 0.27866 & -0.95104 \end{bmatrix}$$

Segment Contact Ellipsoid Semiaxes (in)

X: 1.775 Y: 1.775 Z: 5.800

Weight (lbs)

3.80

Principal Moments of Inertia (lbs - sec^2 - in)

X: 0.1191 Y: 0.1128 Z: 0.0069

Transformation from Principal to Local Reference Axes

$$A_{LP} = \begin{bmatrix} 0.99974 & 0.00000 & 0.02291 \\ 0.00000 & -1.00000 & 0.00000 \\ -0.02291 & 0.00000 & -0.99974 \end{bmatrix}$$

Surface Characteristics Coefficients Relating Load (lbs) to Deflection (in) (from Tests of Left Forearm)

A_0 = -2.39718 A_1 = 107.370 A_2 = -313.365 A_3 = 504.614 A_4 = -196.370 A_5 = 0

TABLE 12

LEFT FOREARM

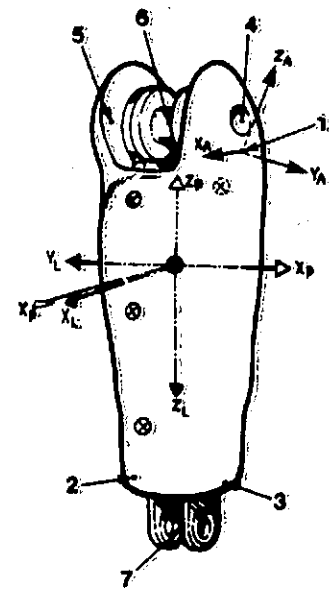

Local Reference Axes

Z axis - vector from left elbow center to the left wrist center.
Y-Z plane - lateral end of the left wrist flexion axis.
X axis - Y x Z.
Origin - center of gravity.

Anatomical Axes

Z axis - vector from ulnar styloid to radiale.
Y axis - normal from Z axis to radial styloid.
X axis - Y x Z.
Origin - at radiale.

Segment Landmarks

1. Left Radiale - at the level of the distal lateral edge of the elbow hardware, approximately two-thirds of the distance from the anterior to the posterior midlines.
2. Left Ulnar Styloid Process on arm sleeve - distal medial edge of the arm covering.
3. Left Radial Styloid Process on arm sleeve - distal lateral edge of the arm covering.
4. Left Lateral Humeral Epicondyle - projection of the lateral end of the left elbow axis to the surface covering.
5. Left Medial Humeral Epicondyle - projection of the medial end of the left elbow axis to the surface covering.
6. Left Elbow Joint Center.
7. Left Wrist Joint Center.

	Local Reference Axes (in)			Anatomical Axes (in)		
	X	Y	Z	X	Y	Z
1. Left Radiale	-1.20	-1.36	-2.91	0.00	0.00	0.00
2. Left Ulnar Styloid Process on sleeve	0.00	1.11	5.52	0.00	0.00	-8.86
3. Left Radial Styloid Process on sleeve	0.20	-1.11	5.47	0.00	2.13	-8.23
4. Left Lateral Humeral Epicondyle	0.25	-0.90	-3.70	1.60	-0.44	0.43
5. Left Medial Humeral Epicondyle	-0.28	0.90	-3.69	1.26	-2.24	0.00
6. Left Elbow Joint Center	0.00	0.00	-3.67	1.52	-1.32	0.17
7. Left Wrist Joint Center	0.00	0.00	6.07	-0.10	1.21	-9.09
8. Left Forearm Center of Gravity	0.00	0.00	0.00	0.92	-0.37	-3.03

Transformation from Local Reference to Anatomical Axes

$$A_{AL} = \begin{bmatrix} 0.98113 & 0.09808 & -0.16665 \\ 0.13971 & -0.95537 & 0.26029 \\ -0.13369 & -0.27866 & -0.95104 \end{bmatrix}$$

Segment Contact Ellipsoid Semiaxes (in)

X: 1.775 Y: 1.775 Z: 5.800

Weight (lbs)

3.80

Principal Moments of Inertia ($lbs - sec^2 - in$)

X: 0.1191 Y: 0.1128 Z: 0.0069

Transformation from Principal to Local Reference Axes

$$A_{LP} = \begin{bmatrix} 0.99974 & 0.00000 & -0.02291 \\ 0.00000 & -1.00000 & 0.00000 \\ -0.02291 & 0.00000 & -0.99974 \end{bmatrix}$$

Surface Characteristics Coefficients Relating Load (lbs) to Deflection (in)

$A_0 = -2.39718$ $A_1 = 107.370$ $A_2 = -313.365$ $A_3 = 504.614$ $A_4 = -196.370$ $A_5 = 0$

TABLE 13

RIGHT HAND

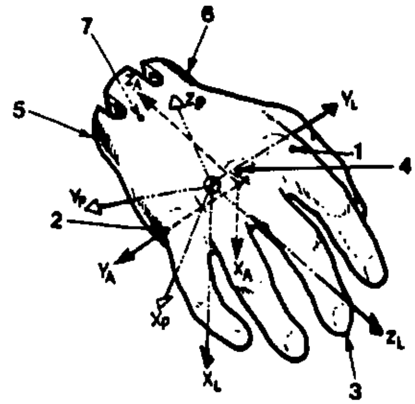

Local Reference Axes

Z axis - vector from the right wrist center to metacarpale III.
Y-Z plane - right radial styloid process.
X axis - Y x Z.
Origin - center of gravity.

Anatomical Axes

Y axis - vector from metacarpale II to metacarpale V.
Z axis - normal from dactylion to Y axis.
X axis - Y x Z.
Origin - at intersection of Y axis and the normal passing through metacarpale III.

Segment Landmarks

1. Right Lateral Aspect of Metacarpal-Phalangeal Joint II - lateral side of the location where digit II attaches to the palm.
2. Right Lateral Aspect of Metacarpal-Phalangeal Joint V - lateral side of the location where digit V attaches to the palm.
3. Right Dactylion - tip of digit III.
4. Right Metacarpale III - top of the bump on the back of the hand representing the knuckle of digit III.
5. Right Ulnar Styloid Process - medial projection of the wrist flexion axis to the surface covering.
6. Right Radial Styloid Process - lateral projection of the wrist flexion axis to the surface covering.
7. Right Wrist Joint Center.

	Local Reference Axes (in)			Anatomical Axes (in)		
	X	Y	Z	X	Y	Z
1. Right Lateral Aspect of M-P II	-0.54	1.39	1.31	-0.00	-1.20	0.00
2. Right Lateral Aspect of M-P V	0.32	-1.54	0.65	0.00	1.92	0.00
3. Right Dactylion	2.83	0.12	3.15	0.00	0.53	-3.66
4. Right Metacarpale III	-0.66	0.00	1.65	-0.79	0.00	0.00
5. Right Ulnar Styloid Process	-0.66	-0.88	-2.22	1.89	1.65	2.45
6. Right Radial Styloid Process	-0.66	0.88	-1.90	2.24	0.00	2.08
7. Right Wrist Joint Center	-0.66	0.00	-2.06	2.06	0.79	2.27
8. Right Hand Center of Gravity	0.00	0.00	0.00	+0.84	+0.53	0.50

Transformation from Local Reference to Anatomical Axes

$$A_{AL} = \begin{bmatrix} 0.54572 & 0.33395 & -0.76855 \\ 0.27523 & -0.93771 & -0.21202 \\ -0.79148 & -0.09582 & -0.60364 \end{bmatrix}$$

Segment Contact Ellipsoid Semiaxes (in)

X: 1.000 Y: 1.870 Z: 3.650

Weight (lbs)

1.29

Principal Moments of Inertia (lbs - sec^2 -in)

X: 0.0115 Y: 0.0093 Z: 0.0036

Transformation from Principal to Local Reference Axes

$$A_{LP} = \begin{bmatrix} 0.85565 & -0.03518 & 0.51636 \\ -0.08014 & -0.99466 & -0.06504 \\ -0.51131 & 0.09703 & -0.85390 \end{bmatrix}$$

Surface Characteristics Coefficients Relating Load (lbs) to Deflection (in) (from Test Data of Left Hand)

A_0 = -4.0703 A_1 = -31.0454 A_2 = 2384.47 A_3 = -10193.9 A_4 = 19172.5 A_5 = 0

TABLE 14

LEFT HAND

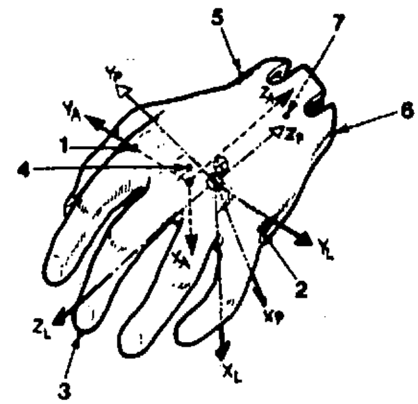

Local Reference Axes

Z axis - vector from the left wrist center to metacarpale III.
Y-Z plane - left ulnar styloid process.
X axis - Y x Z.
Origin - center of gravity.

Anatomical Axes

Y axis - vector from metacarpale V to metacarpale II.
Z axis - normal from dactylion to Y axis.
X axis - Y x Z.
Origin - at intersection of Y axis and the normal passing through metacarpale III.

Segment Landmarks

1. Left Lateral Aspect of Metacarpal-Phalangeal Joint II - lateral side of the location where digit II attaches to the palm.
2. Left Lateral Aspect of Metacarpal-Phalangeal Joint V - lateral side of the location where digit V attaches to the palm.
3. Left Dactylion - tip of digit III.
4. Left Metacarpale III - top of the bump on the back of the hand representing the knuckle of digit III.
5. Left Radial Styloid Process - lateral projection of the wrist flexion axis to the surface covering.
6. Left Ulnar Styloid Process - medial projection of the wrist flexion axis to the surface covering.
7. Left Wrist Center.

	Local Reference Axes (in)			Anatomical Axes (in)		
	X	Y	Z	X	Y	Z
1. Left Lateral Aspect of M-P II	-0.54	-1.39	1.31	0.00	1.20	0.00
2. Left Lateral Aspect of M-P V	0.32	1.54	0.65	0.00	-1.92	0.00
3. Left Dactylion	2.83	-0.12	3.15	0.00	-0.53	-3.66
4. Left Metacarpale III	-0.66	0.00	1.65	0.79	0.00	0.00
5. Left Radial Styloid Process	-0.66	-0.88	-1.90	-2.24	0.00	2.08
6. Left Ulnar Styloid Process	-0.66	0.88	-2.22	-1.89	-1.65	2.45
7. Left Wrist Joint Center	-0.66	0.00	-2.06	-2.06	-0.79	2.27
8. Left Hand Center of Gravity	0.00	0.00	0.00	-0.84	-0.53	0.50

Transformation from Local Reference to Anatomical Axes

$$A_{AL} = \begin{bmatrix} -0.54572 & -0.33395 & 0.76855 \\ -0.27523 & 0.93771 & 0.21202 \\ -0.79148 & -0.09582 & -0.60364 \end{bmatrix}$$

Segment Contact Ellipsoid Semiaxes (in)

X: 1.000 Y: 1.870 Z: 3.650

Weight (lbs)

1.29

Principal Moments of Inertia (lbs - sec^2 - in)

X: 0.0115 Y: 0.0093 Z: 0.0036

Transformation from Principal to Local Reference Axes

$$A_{LP} = \begin{bmatrix} 0.85565 & 0.03518 & 0.51636 \\ 0.08014 & -0.99466 & 0.06504 \\ -0.51131 & -0.09703 & -0.85390 \end{bmatrix}$$

Surface Characteristics Coefficients Relating Load (lbs) to Deflection (in)

A_0 = -4.0703 A_1 = -31.0454 A_2 = 2384.47 A_3 = -10193.9 A_4 = 19172.5 A_5 = 0

TABLE 15

SEATED RIGHT UPPER LEG

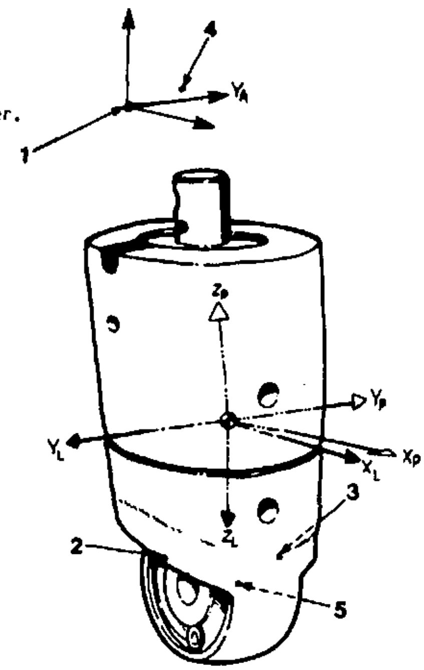

Local Reference Axes

Z axis - vector from right hip joint center to the right knee joint center.
Y-Z plane - right lateral femoral condyle on the thigh.
Origin - center of gravity.

Anatomical Axes

Z axis - vector from lateral femoral epicondyle to trochanterion.
Y axis - normal from Z axis to medial femoral epicondyle.
X axis - Y x Z.
Origin - at trochanterion.

Segment Landmarks

1. Right Trochanterion - on the seated pelvis, a point lateral to the right hip joint center.
2. Right Lateral Femoral Condyle on Thigh - a point on the inferior lateral edge of the thigh covering superior to the knee axis.
3. Right Medial Femoral Condyle on Thigh - a point on the inferior medial edge of the thigh covering superior to the knee axis.
4. Right Hip Joint Center - located in the seated pelvis.
5. Right Knee Joint Center.

	Local Reference Axes (in)			Anatomical Axes (in)		
	X	Y	Z	X	Y	Z
1. Right Trochanterion	-0.17	3.92	-9.36	0.00	0.00	0.00
2. Right Lateral Femoral Condyle on Thigh	0.16	2.09	5.93	0.00	0.00	-15.41
3. Right Medial Femoral Condyle on Thigh	0.23	-2.89	5.40	0.00	5.00	-15.48
4. Right Hip Joint Center	0.00	0.00	-9.96	0.44	3.96	0.12
5. Right Knee Joint Center	0.00	0.00	6.56	-0.29	1.99	-16.28
6. Right Upper Leg Center of Gravity	0.00	0.00	0.00	0.00	2.78	-9.76

Transformation from Local Reference to Anatomical Axes

$$A_{AL} = \begin{bmatrix} 0.99968 & 0.01616 & -0.01963 \\ 0.01370 & -0.99275 & -0.11940 \\ -0.02142 & 0.11909 & -0.99265 \end{bmatrix}$$

Segment Contact Ellipsoid Semiaxes (in)

X: 2.950 Y: 3.050 Z: 7.285

Weight (lbs)

13.71

Principal Moments of Inertia ($lbs - sec^2 - in$)

X: 0.6092 Y: 0.5934 Z: 0.1068

Transformation from Principal to Local Reference Axes

$$A_{LP} = \begin{bmatrix} 0.99740 & 0.00006 & -0.07208 \\ 0.00005 & -1.00000 & -0.00008 \\ -0.07208 & 0.00008 & -0.99740 \end{bmatrix}$$

Surface Characteristics Coefficients Predicting Loads (lbs) from Deflection (in)

Front of Thigh: A_0 = -0.2846 A_1 = 14.1866 A_2 = 81.9368 A_3 = -122.624 A_4 = 98.7298 A_5 = -29.0903

Knee: A_0 = -0.0368 A_1 = 2.2174 A_2 = 867.345 A_3 = -401.606 A_4 = 0 A_5 = 0

TABLE 16

SEATED LEFT UPPER LEG

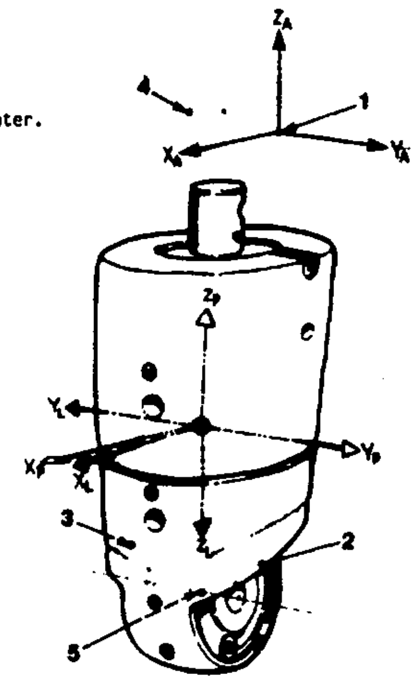

Local Reference Axes

Z axis - vector from left hip joint center to the left knee joint center.
Y-Z plane - left lateral femoral condyle on the thigh.
Origin - center of gravity.

Anatomical Axes

Z axis - vector from lateral femoral epicondyle to trochanterion.
Y axis - vector from medial femoral epicondyle normal to Z axis.
X axis - Y x Z.
Origin - at trochanterion.

Segment Landmarks

1. Left Trochanterion - on the seated pelvis, a point on the surface lateral to the left hip joint center.
2. Left Lateral Femoral Condyle on Thigh - a point on the inferior lateral edge of the thigh covering superior to the knee axis.
3. Left Medial Femoral Condyle on Thigh - a point on the inferior medial edge of the thigh covering superior to the knee axis.
4. Left Hip Joint Center - located in the seated pelvis.
5. Left Knee Joint Center.

	Local Reference Axes (in)			Anatomical Axes (in)		
	X	Y	Z	X	Y	Z
1. Left Trochanterion	-0.17	-3.92	-9.36	0.00	0.00	0.00
2. Left Lateral Femoral Condyle on Thigh	0.16	-2.09	5.93	0.00	0.00	-15.41
3. Left Medial Femoral Condyle on Thigh	0.23	2.89	5.40	0.00	-5.00	-15.48
4. Left Hip Joint Center	0.00	0.00	-9.96	0.44	-3.96	0.12
5. Left Knee Joint Center	0.00	0.00	6.56	-0.29	-1.99	-16.28
6. Left Upper Leg Center of Gravity	0.00	0.00	0.00	0.00	-2.78	-9.76

Transformation from Local Reference to Anatomical Axes

$$A_{AL} = \begin{bmatrix} 0.99968 & -0.01616 & -0.01963 \\ -0.01370 & -0.99275 & 0.11940 \\ -0.02142 & -0.11909 & -0.99265 \end{bmatrix}$$

Segment Contact Ellipsoid Semiaxes (in)

X: 2.950 Y: 3.050 Z: 7.285

Weight (lbs)

13.71

Principal Moments of Inertia (lbs - sec^2 - in)

X: 0.6092 Y: 0.5934 Z: 0.1068

Transformation from Principal to Local Reference Axes

$$A_{LP} = \begin{bmatrix} 0.99740 & +0.00006 & -0.07208 \\ -0.00005 & -1.00000 & +0.00008 \\ 0.07208 & +0.00008 & -0.99740 \end{bmatrix}$$

Surface Characteristics Coefficients Predicting Loads (lbs) from Deflection (in)

Front of Thigh: A_0 = -0.2846 A_1 = 14.1866 A_2 = 81.9368 A_3 = -122.624 A_4 = 98.7298 A_5 = -29.0903

Knee: A_0 = -0.0368 A_1 = 2.2174 A_2 = 867.345 A_3 = -401.606 A_4 = 0 A_5 = 0

TABLE 17

STANDING RIGHT UPPER LEG

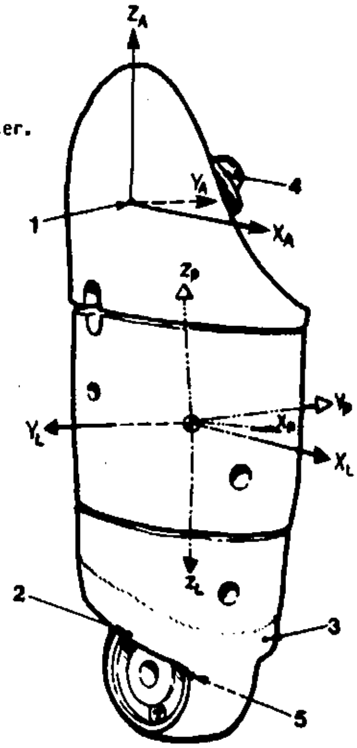

Local Reference Axes

Z axis - vector from right hip joint center to the right knee joint center.
Y-Z plane - right medial femoral condyle on the thigh.
X axis - Y x Z.
Origin - center of gravity.

Anatomical Axes

Z axis - vector from lateral femoral epicondyle to trochanterion.
Y axis - normal from Z axis to medial femoral epicondyle.
X axis - Y x Z.
Origin - at trochanterion.

Segment Landmarks

1. Right Trochanterion - a point on the surface lateral to the right hip joint center.
2. Right Lateral Femoral Condyle on Thigh - a point on the inferior lateral edge of the thigh covering superior to the knee axis.
3. Right Medial Femoral Condyle on Thigh - a point on the inferior medial edge of the thigh covering superior to the knee axis.
4. Right Hip Joint Center.
5. Right Knee Joint Center

	Local Reference Axes (in)			Anatomical Axes (in)		
	X	Y	Z	X	Y	Z
1. Right Trochanterion	-0.68	3.82	-5.68	0.00	0.00	0.00
2. Right Lateral Femoral Condyle on Thigh	-0.10	2.21	8.26	0.00	0.00	-14.04
3. Right Medial Femoral Condyle on Thigh	0.00	-2.90	7.78	0.00	5.13	-14.15
4. Right Hip Joint Center	-0.24	0.00	-7.23	0.44	3.98	1.08
5. Right Knee Joint Center	-0.24	0.00	8.90	-0.20	2.12	-14.92
6. Right Upper Leg Center of Gravity	0.00	0.00	0.00	0.39	3.15	-6.10

Transformation from Local Reference to Anatomical Axes

$$A_{AL} = \begin{bmatrix} 0.99902 & 0.01937 & -0.03970 \\ 0.01467 & -0.99321 & -0.11537 \\ -0.04167 & 0.11467 & -0.99253 \end{bmatrix}$$

Segment Contact Ellipsoid Semiaxes (in)

X: 2.950 Y: 3.050 Z: 7.285

Weight (lbs)

19.98

Principal Moments of Inertia (lbs - sec^2 - in)

X: 1.4494 Y: 1.4968 Z: 0.1989

Transformation from Principal to Local Reference Axes

$$A_{LP} = \begin{bmatrix} 0.97399 & 0.19066 & -0.12246 \\ 0.20374 & -0.97339 & 0.10493 \\ -0.09920 & -0.12715 & -0.98691 \end{bmatrix}$$

Surface Characteristics Coefficients Relating Load (lbs) to Deflection (in) (from Tests of Left Upper Leg)

Front of Thigh: A_0 = -0.2846 A_1 = 14.1866 A_2 = 81.9368 A_3 = -122.624 A_4 = 98.7298 A_5 = -29.0903

Knee: A_0 = -0.0368 A_1 = 2.2174 A_2 = 867.345 A_3 = -401.606 A_4 = 0 A_5 = 0

TABLE 18

STANDING LEFT UPPER LEG

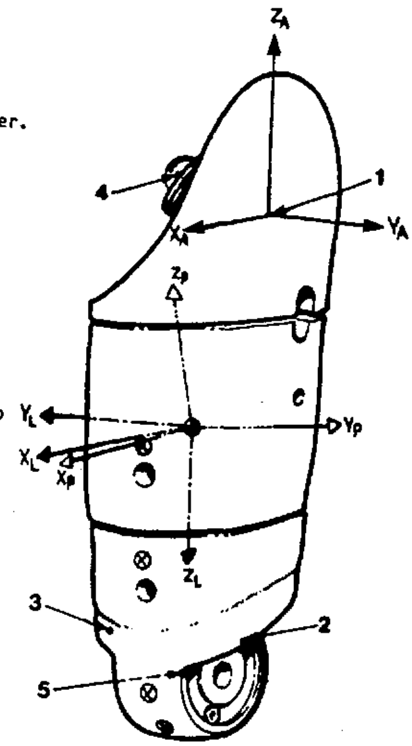

Local Reference Axes

Z axis - vector from left hip joint center to the left knee joint center.
Y-Z plane - left medial femoral condyle on the thigh.
X axis - Y x Z.
Origin - center of gravity.

Anatomical Axes

Z axis - vector from lateral femoral epicondyle to trochanterion.
Y axis - vector from medial femoral epicondyle normal to Z axis.
X axis - Y x Z.
Origin - at trochanterion.

Segment Landmarks

1. Left Trochanterion - a point on the surface lateral to the left hip joint center.
2. Left Lateral Femoral Condyle on Thigh - a point on the inferior lateral edge of the thigh covering superior to the knee axis.
3. Left Medial Femoral Condyle on Thigh - a point on the inferior medial edge of the thigh covering superior to the knee axis.
4. Left Hip Joint Center.
5. Left Knee Joint Center

	Local Reference Axes (in) X	Y	Z	Anatomical Axes (in) X	Y	Z
1. Left Trochanterion	-0.68	-3.82	-5.68	0.00	0.00	0.00
2. Left Lateral Femoral Condyle on Thigh	-0.10	-2.21	8.26	0.00	0.00	-14.04
3. Left Medial Femoral Condyle on Thigh	0.00	2.90	7.78	0.00	-5.13	-14.15
4. Left Hip Joint Center	-0.24	0.00	-7.23	0.44	-3.98	1.08
5. Left Knee Joint Center	-0.24	0.00	8.90	-0.20	-2.12	-14.92
6. Left Upper Leg Center of Gravity	0.00	0.00	0.00	0.39	-3.15	-6.10

Transformation from Local Reference to Anatomical Axes

$$A_{AL} = \begin{bmatrix} 0.99902 & -0.01937 & -0.03970 \\ -0.01467 & -0.99321 & 0.11537 \\ -0.04167 & -0.11467 & -0.99253 \end{bmatrix}$$

Segment Contact Ellipsoid Semiaxes (in)

X: 2.950 Y: 3.050 Z: 7.285

Weight (lbs)

19.98

Principal Moments of Inertia (lbs - sec^2 - in)

X: 1.4494 Y: 1.4968 Z: 0.1989

Transformation from Principal to Local Reference Axes

$$A_{LP} = \begin{bmatrix} 0.97399 & -0.19066 & -0.12246 \\ 0.20374 & -0.97339 & -0.10493 \\ -0.09920 & 0.12715 & -0.98691 \end{bmatrix}$$

Surface Characteristics Coefficients Relating Load (lbs) to Deflection (in)

Front of Thigh: A_0 = -0.2846 A_1 = 14.1866 A_2 = 81.9368 A_3 = -122.624 A_4 = 98.7298 A_5 = -29.0903

Knee: A_0 = -0.0368 A_1 = 2.2174 A_2 = 867.345 A_3 = -401.606 A_4 = 0 A_5 = 0

TABLE 19

RIGHT LOWER LEG

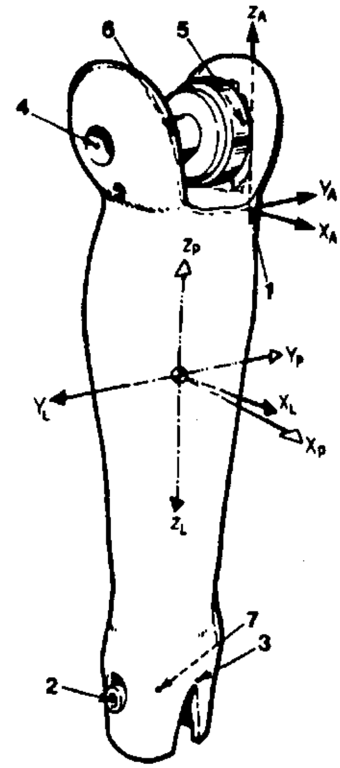

Local Reference Axes

Z axis - vector from right knee joint center to the right ankle joint center.
Y-Z plane - right medial femoral condyle.
X axis - Y x Z.
Origin - *center of gravity*.

Anatomical Axes

Z axis - vector from sphyrion to tibiale.
Y axis - vector from lateral malleolus normal to Z axis.
X axis - Y x Z.
Origin - at tibiale.

Segment Landmarks

1. Right Tibiale - at the level of the inferior edge of the knee hardware, a point on the antero-medial surface of the lower leg.
2. Right Lateral Malleolus - the lateral projection to the covering surface of the ankle flexion axis.
3. Right Sphyrion - the medial projection to the covering surface of the ankle flexion axis.
4. Right Lateral Femoral Condyle - the lateral projection to the covering surface of the right knee axis.
5. Right Medial Femoral Condyle - the medial projection to the covering surface of the right knee axis.
6. Right Knee Joint Center.
7. Right Ankle Joint Center.

	Local Reference Axes (in)			Anatomical Axes (in)		
	X	Y	Z	X	Y	Z
1. Right Tibiale	0.00	-2.27	-5.01	0.00	0.00	0.00
2. Right Lateral Malleolus	-0.15	1.31	9.63	0.00	-2.83	-14.80
3. Right Sphyrion	-0.15	-1.52	9.61	0.00	0.00	-14.64
4. Right Lateral Femoral Condyle	-0.25	2.73	-6.24	-0.31	-5.06	0.97
5. Right Medial Femoral Condyle	-0.15	-2.69	-6.50	-0.21	0.33	1.51
6. Right Knee Joint Center	-0.20	0.00	-6.74	-0.27	-2.36	1.61
7. Right Ankle Joint Center	-0.20	0.00	9.65	0.00	-1.52	-14.76
8. Right Lower Leg Center of Gravity	0.00	0.00	0.00	0.00	-2.01	-5.12

Transformation from Local Reference to Anatomical Axes

$$A_{AL} = \begin{bmatrix} 0.99991 & -0.00009 & 0.01335 \\ -0.00078 & -0.99868 & 0.05141 \\ 0.01332 & -0.05142 & -0.99859 \end{bmatrix}$$

Segment Contact Ellipsoid Semiaxes (in)

X: 2.165 Y: 2.050 Z: 9.750

Weight (lbs)

7.24

Principal Moments of Inertia (lbs - sec^2 - in)

X: 0.6708 Y: 0.6745 Z: 0.0397

Transformation from Principal to Local Reference Axes

$$A_{LP} = \begin{bmatrix} 0.99945 & 0.00002 & 0.03322 \\ 0.00002 & -1.00000 & 0.00000 \\ 0.03322 & 0.00000 & -0.99945 \end{bmatrix}$$

Surface Characteristics Coefficients Relating Load (lbs) to Deflection (in) (from Tests of Left Lower Leg)

Front of Calf: $A_0 = -0.7367$ $A_1 = 26.7948$ $A_2 = 3.9187$ $A_3 = 29.050$ $A_4 = 0$ $A_5 = 0$

Back of Calf: $A_0 = 0.07702$ $A_1 = 29.4156$ $A_2 = -2.0806$ $A_3 = 0$ $A_4 = 0$ $A_5 = 0$

TABLE 20

LEFT LOWER LEG

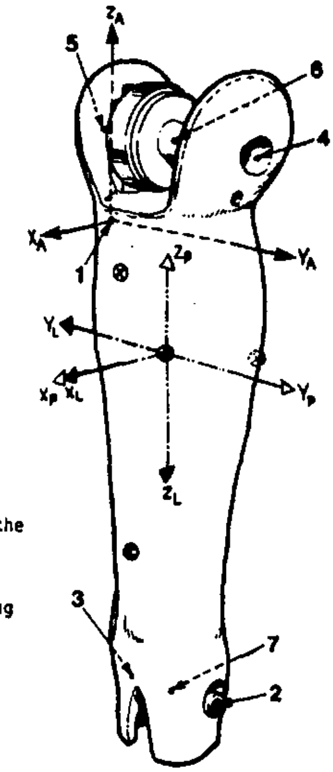

Local Reference Axes

Z axis - vector from left knee joint center to the left ankle joint center.
Y-Z plane - left medial femoral condyle.
X axis - Y x Z.
Origin - center of gravity.

Anatomical Axes

Z axis - vector from sphyrion to tibiale.
Y axis - normal from Z axis to lateral malleolus.
X axis - Y x Z.
Origin - at tibiale.

Segment Landmarks

1. Left Tibiale - at the level of the inferior edge of the knee hardware, a point on the antero-medial surface of the lower leg.
2. Left Lateral Malleolus - the lateral projection to the covering surface of the ankle flexion axis.
3. Left Sphyrion - the medial projection to the covering surface of the ankle flexion axis.
4. Left Lateral Femoral Condyle - the lateral projection to the covering surface of the left knee axis.
5. Left Medial Femoral Condyle - the medial projection to the covering surface of the left knee axis.
6. Left Knee Joint Center.
7. Left Ankle Joint Center.

	Local Reference Axes (in)			Anatomical Axes (in)		
	X	Y	Z	X	Y	Z
1. Left Tibiale	0.00	2.27	-5.01	0.00	0.00	0.00
2. Left Lateral Malleolus	-0.15	-1.31	9.63	0.00	2.83	-14.80
3. Left Sphyrion	-0.15	1.52	9.61	0.00	0.00	-14.64
4. Left Lateral Femoral Condyle	-0.25	-2.73	-6.24	-0.31	5.06	0.97
5. Left Medial Femoral Condyle	-0.15	2.69	-6.50	-0.21	-0.33	1.51
6. Left Knee Joint Center	-0.20	0.00	-6.74	-0.27	2.36	1.61
7. Left Ankle Joint Center	-0.20	0.00	9.65	0.00	1.52	-14.76
8. Left Lower Leg Center of Gravity	0.00	0.00	0.00	0.00	2.01	-5.12

Transformation from Local Reference to Anatomical Axes

$$A_{AL} = \begin{bmatrix} +0.99991 & -0.00009 & -0.01335 \\ +0.00078 & -0.99868 & 0.05141 \\ -0.01332 & +0.05142 & -0.99859 \end{bmatrix}$$

Segment Contact Ellipsoid Semiaxes (in)

X: 2.165 Y: 2.050 Z: 9.750

Weight (lbs)

7.24

Principal Moments of Inertia (lbs - sec^2 - in)

X: 0.6707 Y: 0.6744 Z: 0.0397

Transformation from Principal to Local Reference Axes

$$A_{LP} = \begin{bmatrix} 0.99945 & -0.00002 & 0.03322 \\ -0.00002 & -1.00000 & 0.00000 \\ 0.03322 & 0.00000 & -0.99945 \end{bmatrix}$$

Surface Characteristics Coefficients Relating Load (lbs) to Deflection (in)

Front of Calf: A_0 = -0.7367 A_1 = 26.7948 A_2 = 3.9187 A_3 = 29.050 A_4 = 0 A_5 = 0

Back of Calf: A_0 = 0.07702 A_1 = 29.4156 A_2 = -2.0806 A_3 = 0 A_4 = 0 A_5 = 0

TABLE 21

RIGHT FOOT

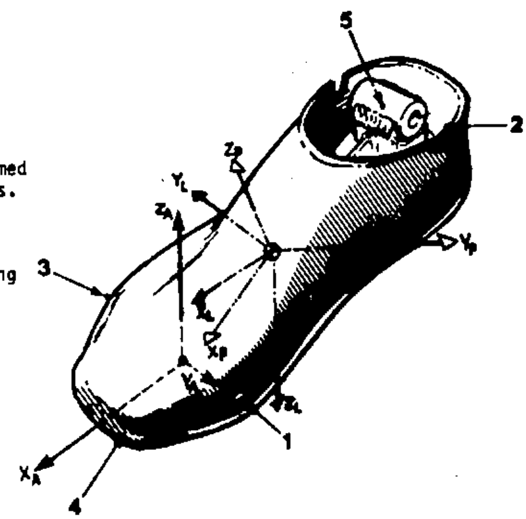

Local Reference Axes

Anatomical axes rotated 180° around the X axis, with the origin at the center of gravity.

Anatomical Axes

Z axis - superiorly directed vector normal to the X-Y plane formed by metatarsal I, metatarsal V, and posterior calcaneous.
X axis - vector from posterior calcaneous to normally projected position of toe II on X-Y plane.
Y axis - Z x X.
Origin - at the intersection of the X axis and the normal passing through metatarsal-phalange I.

Segment Landmarks

1. Right Metatarsal-Phalangeal Joint I - a bulge on the medial side of the foot approximately 2 inches from the front.
2. Right Posterior Calcaneous - the posterior-most point on the foot, approximately 1 inch above the sole.
3. Right Metatarsal-Phalangeal Joint V - a bulge on the lateral side of the foot approximately 2 1/2 inches from the front.
4. Right Toe II - the anterior-most point on the foot.
5. Right Ankle Joint Center.

	Local Reference Axes (in)			Anatomical Axes (in)		
	X	Y	Z	X	Y	Z
1. Right Metatarsal-Phalangeal Joint I	3.99	-1.52	0.49	0.00	1.52	0.00
2. Right Posterior Calcaneous	-4.21	0.00	0.49	-8.19	0.00	0.00
3. Right Metatarsal-Phalangeal Joint V	3.45	2.04	0.49	-0.53	-2.04	0.00
4. Right Toe II	5.99	0.00	0.16	2.01	0.00	0.33
5. Right Ankle Joint Center	-2.12	0.18	-1.54	-6.11	-0.18	2.04
6. Right Foot Center of Gravity	0.00	0.00	0.00	-3.99	0.00	+0.50

Transformation from Local Reference to Anatomical Axes

$$A_{AL} = \begin{bmatrix} 1.0 & 0.0 & 0.0 \\ 0.0 & -1.0 & 0.0 \\ 0.0 & 0.0 & -1.0 \end{bmatrix}$$

Segment Contact Ellipsoid Semiaxes (in)

X: 4.900 Y: 1.675 Z: 1.675

Weight (lbs)

2.76

Principal Moments of Inertia (lbs - sec^2 - in)

X: 0.0067 Y: 0.0524 Z: 0.0491

Transformation from Principal to Local Reference Axes

$$A_{LP} = \begin{bmatrix} 0.98595 & -0.04630 & 0.16048 \\ 0.01649 & -0.92914 & -0.36936 \\ 0.16621 & 0.36682 & -0.91532 \end{bmatrix}$$

Surface Characteristics Coefficients Relating Load (lbs) to Deflection (in) (from Tests of Left Foot)

A_0 = -0.6804 A_1 = 82.7463 A_2 = -704.172 A_3 = 3367.10 A_4 = -5570.69 A_5 = 3188.30

TABLE 22

LEFT FOOT

Local Reference Axes

Anatomical axes rotated 180° around the X axis, with the origin at the center of gravity.

Anatomical Axes

Z axis - superiorly directed vector normal to the X-Y plane formed by metatarsal I, metatarsal V, and posterior calcaneous.
X axis - vector from posterior calcaneous to normally projected position of toe II on X-Y plane.
Y axis - Z x X.
Origin - at the intersection of the X axis and the normal passing through metatarsal-phalange I.

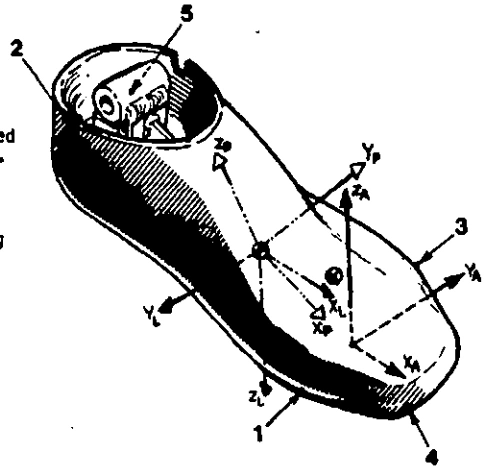

Segment Landmarks

1. Left Metatarsal-Phalangeal Joint I - a bulge on the medial side of the foot approximately 2 inches from the front.
2. Left Posterior Calcaneous - the posterior-most point on the foot, approximately 1 inch above the sole.
3. Left Metatarsal-Phalangeal Joint V - a bulge on the lateral side of the foot approximately 2 1/2 inches from the front.
4. Left Toe II - the anterior-most point on the foot.
5. Left Ankle Joint Center.

	Local Reference Axes (in)			Anatomical Axes (in)		
	X	Y	Z	X	Y	Z
1. Left Metatarsal-Phalangeal Joint I	3.99	1.52	0.49	0.00	-1.52	0.00
2. Left Posterior Calcaneous	-4.21	0.00	0.49	-8.19	0.00	0.00
3. Left Metatarsal-Phalangeal Joint V	3.45	-2.04	0.49	-0.53	2.04	0.00
4. Left Toe II	5.99	0.00	0.16	2.01	0.00	0.33
5. Left Ankle Joint Center	-2.12	-0.18	-1.54	-6.11	0.18	2.04
6. Left Foot Center of Gravity	0.00	0.00	0.00	-3.99	0.00	+0.50

Transformation from Local Reference to Anatomical Axes

$$A_{AL} = \begin{bmatrix} 1.0 & 0.0 & 0.0 \\ 0.0 & -1.0 & 0.0 \\ 0.0 & 0.0 & -1.0 \end{bmatrix}$$

Segment Contact Ellipsoid Semiaxes (in)

X: 4.900 Y: 1.675 Z: 1.675

Weight (lbs)

2.76

Principal Moments of Inertia (lbs - sec^2 - in)

X: 0.0067 Y: 0.0524 Z: 0.0491

Transformation from Principal to Local Reference Axes

$$A_{LP} = \begin{bmatrix} 0.98595 & 0.04630 & 0.16048 \\ -0.01649 & -0.92914 & 0.36936 \\ 0.16621 & -0.36682 & -0.91532 \end{bmatrix}$$

Surface Characteristics Coefficients Relating Load (lbs) to Deflection (in)

A_0 = -0.6804 A_1 = 82.7463 A_2 = -704.172 A_3 = 3367.10 A_4 = -5570.69 A_5 = 3188.30

TABLE 23

SEATED PELVIS WITH SPINE

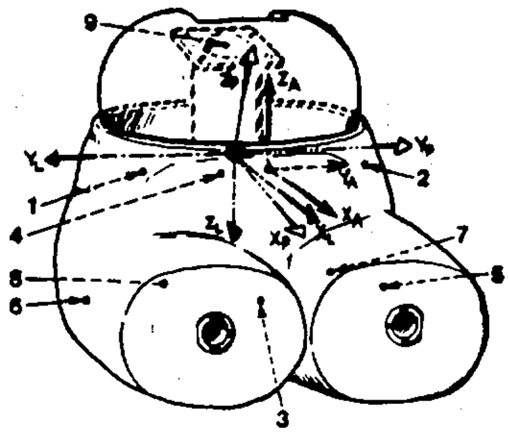

Local Reference Axes

Axes of the inertial test box with the origin at the center of gravity.

Anatomical Axes

Y axis - vector from right anterior superior iliac spine to left anterior superior iliac spine.
Z axis - normal from symphysion to Y axis.
X axis - Y x Z.
Origin - at intersection of Y axis and the normal to it passing through the posterior superior iliac midspine.

Segment Landmarks

1. Right Anterior Superior Iliac Spine (ASIS) - a palpable protrusion at the right anterior superior corner of the internal framework.
2. Left Anterior Superior Iliac Spine (ASIS) - a palpable protrusion at the left anterior superior corner of the internal framework.
3. Symphysion - on the front of the pelvis, a point above the juction of the thighs.
4. Posterior Superior Iliac Midspine - in the posterior midline, a point at the level of the floor of the pelvis.
5. Left Trochanterion - a point on the pelvis surface lateral to the left hip joint.
Right Trochanterion - a point on the pelvis surface lateral to the right hip.
7. Left Hip Joint Center.
8. Right Hip Joint Center.
9. Pelvis Attachment Center - center of the plate which attaches the lumbar spine.

	Local Reference Axes (in)			Anatomical Axes (in)		
	X	Y	Z	X	Y	Z
1. Right ASIS	2.88	4.87	-1.82	0.00	-4.88	0.00
2. Left ASIS	2.88	-4.87	-1.82	0.00	4.88	0.00
3. Symphysion	4.83	0.00	0.13	0.00	0.00	-2.77
4. Posterior Superior Iliac Midspine	-4.43	0.00	-0.15	-6.34	0.00	4.02
5. Left Trochanterion	0.31	-7.23	1.33	-4.04	7.24	-0.40
6. Right Trochanterion	0.31	7.23	1.33	-4.04	-7.24	-0.40
7. Right Hip Joint Center	0.32	-3.15	1.33	-4.02	3.15	-0.41
8. Left Hip Joint Center	0.32	3.15	1.33	-4.02	-3.15	-0.41
9. Pelvis Attachment Center	3.42	0.00	-6.12	0.10	0.00	6.89
10. Pelvis Center of Gravity	0.00	0.00	0.00	-3.32	0.00	0.77

Transformation from Local Reference to Anatomical Axes

$$A_{AL} = \begin{bmatrix} 0.70620 & 0.00000 & -0.70801 \\ 0.00000 & -1.00000 & 0.00000 \\ -0.70801 & 0.00000 & -0.70620 \end{bmatrix}$$

Segment Contact Ellipsoid Semiaxes (in)

X: 5.000 Y: 7.185 Z: 4.800

Weight (lbs)

49.35

Principal Moments of Inertia (lbs - sec^2 - in)

X: 2.5109 Y: 1.6110 Z: 1.4925

Transformation from Principal to Local Reference Axes

$$A_{LP} = \begin{bmatrix} 0.82048 & -0.00004 & 0.57165 \\ 0.00000 & -1.00004 & -0.00001 \\ 0.57164 & -0.00004 & -0.82045 \end{bmatrix}$$

Surface Deflection Characteristics Predicting Load (lbs) from Deflection (in)

1. Front of Abdominal Insert: $A_0 = -0.13539$ $A_1 = 1.57829$ $A_2 = 24.3875$ $A_3 = -29.3317$ $A_4 = 13.7609$ $A_5 = 0$
2. Posterior Pelvis: $A_0 = -0.75858$ $A_1 = 35.1055$ $A_2 = 40.0356$ $A_3 = -12.4884$ $A_4 = 0$ $A_5 = 0$

TABLE 24

STANDING PELVIS WITH SPINE

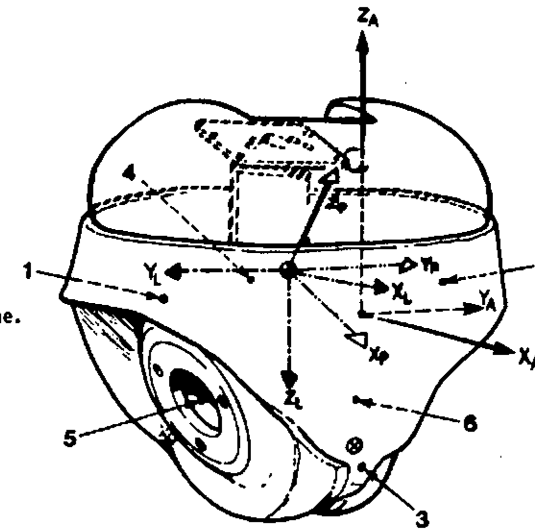

Local Reference Axes

Axes of the inertial test box with the origin at the center of gravity.

Anatomical Axes

Y axis - vector from right anterior superior iliac spine to left anterior superior iliac spine.
Z axis - vector from symphysion normal to Y axis.
X axis - Y x Z.
Origin - at intersection of Y axis and the normal to it passing through the posterior superior iliac midspine.

Segment Landmarks

1. Right Anterior Superior Iliac Spine (ASIS) - a palpable protrusion at the right anterior superior corner of the internal framework.
2. Left Anterior Superior Iliac Spine (ASIS) - a palpable protrusion at the left anterior superior corner of the internal framework.
3. Symphysion - the center of a soft cover protrusion at antero-inferior surface.
4. Posterior Superior Iliac Midspine - in the posterior midline, a point at the level of the floor of the pelvis.
5. Right Hip Joint Center - the center of a plane covering the surface of the right hip socket.
6. Left Hip Joint Center - the center of a plane covering the surface of the left hip socket.
7. Pelvis/Thorax Attachment Center - the center of the plate on the lumbar spine which attaches the pelvis and thorax segments.

	Local Reference Axes (in)			Anatomical Axes (in)		
	X	Y	Z	X	Y	Z
1. Right ASIS	3.36	4.82	-2.25	0.00	-4.86	0.00
2. Left ASIS	3.36	-4.82	-2.25	0.00	4.86	0.00
3. Symphysion	5.83	0.00	0.69	0.00	0.00	-3.83
4. Posterior Superior Iliac Midspine	-3.41	0.00	0.26	-6.80	0.00	2.45
5. Right Hip Joint Center	1.35	3.30	2.01	-4.29	-3.28	-1.94
6. Left Hip Joint Center	1.35	-3.30	2.01	-4.29	3.28	-1.94
7. Pelvis/Thorax Attachment Center	-0.67	0.00	-6.24	-0.52	0.00	5.65
8. Pelvis Center of Gravity	0.00	0.00	0.00	-4.02	0.00	0.45

Transformation from Local Reference to Anatomical Axes

$$A_{AL} = \begin{bmatrix} 0.76576 & 0.00000 & 0.64313 \\ 0.00000 & -1.00000 & 0.00000 \\ -0.64313 & 0.00000 & -0.76576 \end{bmatrix}$$

Segment Contact Ellipsoid Semiaxes (in)

X: 4.725 Y: 7.185 Z: 5.800

Weight (lbs)

24.57

Principal Moments of Inertia (lbs - sec^2 - in)

X: 0.8879 Y: 0.7293 Z: 0.5659

Transformation from Principal to Local Reference Axes

$$A_{LP} = \begin{bmatrix} -0.79521 & -0.00001 & 0.60634 \\ 0.00000 & -0.99999 & 0.00000 \\ 0.60637 & 0.00002 & -0.79521 \end{bmatrix}$$

Surface Characteristics Curve Predicting Load (lbs) from Deflection (in)

1. Anterior Abdominal Insert: A_0 = -0.13539 A_1 = 1.57829 A_2 = 24.3875 A_3 = -29.3317 A_4 = 13.7609 A_5 = 0
2. Posterior Pelvis: A_0 = -0.75858 A_1 = 35.1055 A_2 = 40.0356 A_3 = -12.4884 A_4 = 0 A_5 = 0

TABLE 25

SEATED PELVIS WITHOUT SPINE

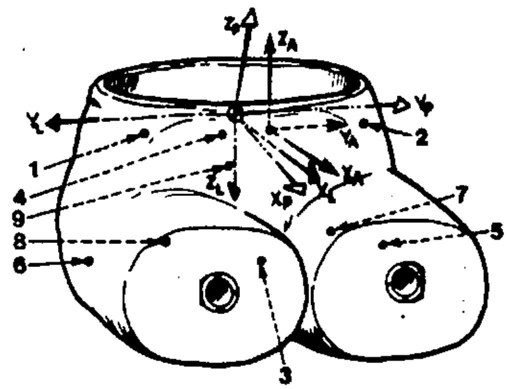

Local Reference Axes

Axes of the inertial test box with the origin at the center of gravity.

Anatomical Axes

Y axis - vector from right anterior superior iliac spine to left anterior superior iliac spine.
Z axis - vector from symphysion normal to Y axis.
X axis - Y x Z.
Origin - at intersection of Y axis and the normal to it passing through the posterior superior iliac midspine.

Segment Landmarks

1. Right Anterior Superior Iliac Spine (ASIS) - a palpable protrusion at the right anterior superior corner of the internal framework.
2. Left Anterior Superior Iliac Spine (ASIS) - a palpable protrusion at the left anterior superior corner of the internal framework.
3. Symphysion - on the front of the pelvis, a point just above the juction of the thighs.
4. Posterior Superior Iliac Midspine - in the posterior midline, a point at the level of the floor of the pelvis.
5. Left Trochanterion - a point on the pelvis surface lateral to the left hip joint.
6. Right Trochanterion - a point on the pelvis surface lateral to the right hip.
7. Left Hip Joint Center.
8. Right Hip Joint Center.
9. Pelvis/Spine Attachment Center - center of the plate which attaches the lumbar spine to the pelvis.

	Local Reference Axes (in)			Anatomical Axes (in)		
	X	Y	Z	X	Y	Z
1. Right ASIS	2.66	4.87	-1.91	0.00	-4.88	0.00
2. Left ASIS	2.66	-4.87	-1.91	0.00	4.88	0.00
3. Symphysion	4.62	0.00	0.00	0.00	0.00	-2.84
4. Posterior Superior Iliac Midspine	-4.65	0.00	-0.23	-6.20	0.00	3.75
5. Left Trochanterion	0.00	-7.23	1.24	-4.11	7.15	-0.72
6. Right Trochanterion	0.00	7.23	1.24	-4.11	-7.15	-0.72
7. Right Hip Joint Center	-0.11	-3.15	1.24	-4.12	3.97	-0.72
8. Left Hip Joint Center	-0.11	3.15	1.24	-4.12	-3.97	-0.72
9. Pelvis/Spine Attachment Center	-2.15	0.00	-1.66	-4.55	0.00	2.64
10. Pelvis Center of Gravity	0.00	0.00	0.00	-3.34	0.00	0.30

Transformation from Local Reference to Anatomical Axes

$$A_{AL} = \begin{bmatrix} 0.70620 & 0.00000 & 0.70801 \\ 0.00000 & -1.00000 & 0.00000 \\ -0.70801 & 0.00000 & -0.70620 \end{bmatrix}$$

Segment Contact Ellipsoid Semiaxes (in)

X: 5.000 Y: 7.185 Z: 4.800

Weight (lbs)

44.46

Principal Moments of Inertia (lbs - sec^2 - in)

X: 2.4575 Y: 1.2969 Z: 1.2080

Transformation from Principal to Local Reference Axes

$$A_{LP} = \begin{bmatrix} 0.79525 & -0.01107 & 0.60618 \\ -0.00390 & -0.99991 & -0.01315 \\ +0.60627 & 0.00810 & -0.79522 \end{bmatrix}$$

Surface Deflection Characteristics Predicting Load (lbs) from Deflection (in)

1. Front of the Abdominal Insert: A_0 = -0.13539 A_1 = 1.57829 A_2 = 24.3875 A_3 = -29.3317 A_4 = 13.7609 A_5 = 0
2. Posterior Pelvis: A_0 = -0.75858 A_1 = 35.1055 A_2 = 40.0356 A_3 = -12.4884 A_4 = 0 A_5 = 0

TABLE 26

STANDING PELVIS WITHOUT SPINE

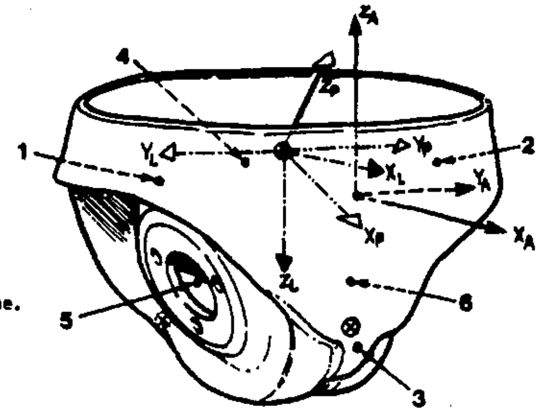

Local Reference Axes

Axes of the inertial test box with the origin at the center of gravity.

Anatomical Axes

Y axis - vector from right anterior superior iliac spine to left anterior superior iliac spine.
Z axis - vector from symphysion normal to Y axis.
X axis - Y x Z.
Origin - at intersection of Y axis and the normal to it passing through the posterior superior iliac midspine.

Segment Landmarks

1. Right Anterior Superior Iliac Spine (ASIS) - a palpable protrusion at the right anterior superior corner of the internal framework.
2. Left Anterior Superior Iliac Spine (ASIS) - a palpable protrusion at the left anterior superior corner of the internal framework.
3. Symphysion - the center of a soft cover protrusion at antero-inferior surface.
4. Posterior Superior Iliac Midspine - in the posterior midline, a point at the level of the floor of the pelvis.
5. Right Hip Joint Center - the center of a plane covering the surface of the right hip socket.
6. Left Hip Joint Center - the center of a plane covering the surface of the left hip socket.
7. Pelvis/Spinex Attachment Center - the center of the plate on the lumbar spine which attaches the pelvis and spine segments.

	Local Reference Axes (in)			Anatomical Axes (in)		
	X	Y	Z	X	Y	Z
1. Right ASIS	3.29	4.82	-2.64	0.00	-4.86	0.00
2. Left ASIS	3.29	-4.82	-2.64	0.00	4.86	0.00
3. Symphysion	5.75	0.00	0.29	0.00	0.00	-3.83
4. Posterior Superior Iliac Midspine	-3.49	0.00	-0.13	-6.80	0.00	2.45
5. Right Hip Joint Center	0.00	3.28	2.04	-4.29	-3.28	-1.94
6. Left Hip Joint Center	0.00	-3.28	2.04	-4.29	3.28	-1.94
7. Pelvis/Spine Attachment Center	-2.50	0.00	-1.08	-3.81	0.00	1.74
8. Pelvis Center of Gravity	0.00	0.00	0.00	-4.22	0.00	0.09

Transformation from Local Reference to Anatomical Axes

$$A_{AL} = \begin{bmatrix} 0.76586 & 0.00000 & -0.64301 \\ 0.00000 & -1.00000 & 0.00000 \\ -0.64301 & 0.00000 & -0.76586 \end{bmatrix}$$

Segment Contact Ellipsoid Semiaxes (in)

X: 4.725 Y: 7.185 Z: 4.800

Weight (lbs)

21.91

Principal Moments of Inertia (lbs - sec^2 - in)

X: 0.8019 Y: 0.6812 Z: 0.4678

Transformation from Principal to Local Reference Axes

$$A_{LP} = \begin{bmatrix} 0.73135 & 0.00000 & 0.68200 \\ 0.00000 & -1.00000 & 0.00000 \\ 0.68200 & 0.00000 & -0.73135 \end{bmatrix}$$

Surface Characteristics Curve Predicting Load (lbs) from Deflection (in)

1. Anterior Abdominal Insert: A_0 = -0.13539 A_1 = 1.57829 A_2 = 24.3875 A_3 = -29.3317 A_4 = 13.7609 A_5 = 0
2. Posterior Pelvis: A_0 = -0.75858 A_1 = 35.1055 A_2 = 40.0356 A_3 = -12.4884 A_4 = 0 A_5 = 0

TABLE 27

SEATED LUMBAR SPINE

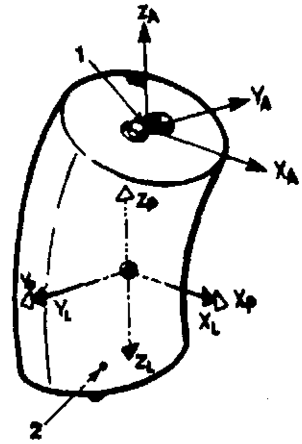

Local Reference Axes

Anatomical axes rotated 180° around X, with the origin at the center of gravity.

Anatomical Axes

Z axis - vector from the spine/pelvis joint center, to the spine/thorax attachment center.
Y axis - normal from the right lateral edge of the spine thorax attachment plate to the Z axis.
X axis - Y x Z.
Origin - spine/thorax attachment center.

Segment Landmarks

1. Spine/Thorax Attachment Center.
2. Spine/Pelvis Joint Center - center of the base of the rubber spine.

	Local Reference Axes (in)			Anatomical Axes (in)		
	X	Y	Z	X	Y	Z
1. Spine/Thorax Attachment Center	-0.35	0.00	-2.56	0.00	0.00	0.00
2. Spine/Pelvis Joint Center	-0.35	0.00	2.56	0.00	0.00	-5.12
3. Lumbar Spine Center of Gravity	0.00	0.00	0.00	0.35	0.00	-2.56

Transformation from Local Reference to Anatomical Axes

$$A_{AL} = \begin{bmatrix} 1.00000 & 0.00000 & 0.00000 \\ 0.00000 & -1.00000 & 0.00000 \\ 0.00000 & 0.00000 & -1.00000 \end{bmatrix}$$

Segment Contact Ellipsoid Semiaxes (in)

X: 4.775 Y: 6.500 Z: 4.000

Weight (lbs)

4.89

Principal Moments of Inertia (lbs - sec^2 - in)

X: 0.0612 Y: 0.0593 Z: 0.0205

Transformation from Principal to Local Reference Axes

$$A_{LP} = \begin{bmatrix} 0.97875 & -0.19158 & -0.07351 \\ -0.19177 & -0.98142 & +0.00522 \\ -0.07315 & +0.00896 & -0.99729 \end{bmatrix}$$

Segment Stiffness (in lb/deg)

Flexion - 230
Extension - 250
Lateral - 340

TABLE 28

STANDING LUMBAR SPINE

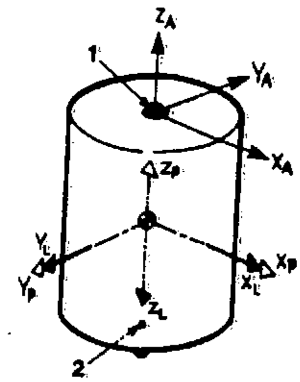

Local Reference Axes

Anatomical axes, rotated 180° around X, with the origin at the center of gravity.

Anatomical Axes

Z axis - vector from the spine/pelvis attachment center to the spine/thorax attachment center.
Y axis - normal from Z axis to the left edge of the spine.
X axis - Y x Z.
Origin - at the thorax attachment center.

Segment Landmarks

1. Spine/Thorax Attachment Center - center of the top of the rubber spine cylinder.
2. Spine/Pelvis Attachment Center - center of the bottom of the rubber spine cylinder.

	Local Reference Axes (in)			Anatomical Axes (in)		
	X	Y	Z	X	Y	Z
1. Spine/Thorax Attachment Center	0.00	0.00	-2.56	0.00	0.00	0.00
2. Spine/Pelvis Attachment Center	0.00	0.00	2.56	0.00	0.00	5.12
3. Spine Center of Gravity	0.00	0.00	0.00	0.00	0.00	-2.56

Transformation from Local Reference to Anatomical Axes

$$A_{AL} = \begin{bmatrix} 1.00000 & 0.00000 & 0.00000 \\ 0.00000 & -1.00000 & 0.00000 \\ 0.00000 & 0.00000 & -1.00000 \end{bmatrix}$$

Segment Contact Ellipsoid Semiaxes (in)

X: 4.775 Y: 6.500 Z: 4.000

Weight (lbs)

2.66

Principal Moments of Inertia (lbs - sec^2 - in)

X: 0.0196 Y: 0.0196 Z: 0.0083

Transformation from Principal to Local Reference Axes

$$A_{LP} = \begin{bmatrix} 0.00000 & 0.00000 & 0.00000 \\ 0.00000 & -1.00000 & 0.00000 \\ 0.00000 & 0.00000 & -1.00000 \end{bmatrix}$$

Segment Stiffness (in lb/deg)

Flexion - 60
Extension - 48
Lateral - 60

TABLE 29

THORAX

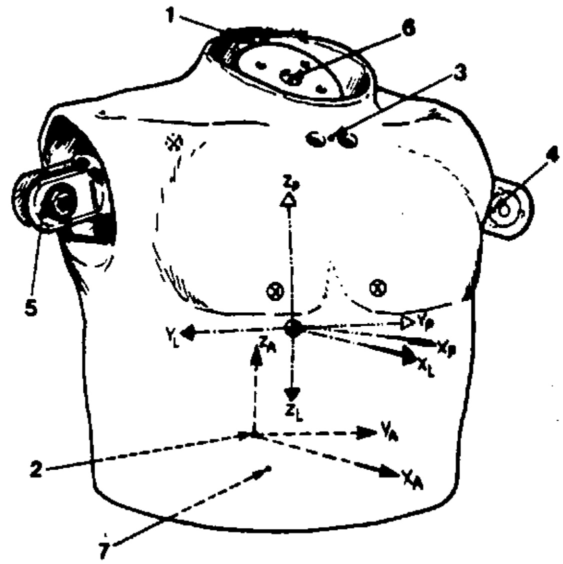

Local Reference Axes

Z axis - vector from a point midway between the two shoulder joint centers to the Thorax/ Lumbar Spine attachment center.
Y-Z plane - right shoulder joint center.
X axis - Y x Z.
Origin - center of gravity.

Anatomical Axes

Z axis - vector from the tenth rib midspine to cervicale.
X axis - normal from Z axis to suprasternale.
Y axis - Z x X.
Origin - at tenth rib midspine.

Segment Landmarks

1. Cervicale - a point on the thorax jacket posterior to the posterior midline of the lowest neck ring.
2. Tenth Rib Midspine - at the level of the lowest rib's inferior edge, a point on the posterior midline of the thorax jacket.
3. Suprasternale - a point in between the two clavicale torque bolt holes.
4. Left Shoulder Joint Center - the midpoint on the abduction - adduction axis of the left shoulder.
5. Right Shoulder Joint Center - the midpoint on the abduction - adduction axis of the right shoulder.
6. Thorax/Neck Attachment Center - the center of the surface of the lowest plate of the neck cylinder.
7. Thorax/Lumbar Spine Attachment Center - the center of the surface of the plate which attaches the thorax to the lumbar spine.

	Local Reference Axes (in)			Anatomical Axes (in)		
	X	Y	Z	X	Y	Z
1. Cervicale	-4.07	0.00	-6.42	0.00	0.00	12.51
2. Tenth Rib Midspine	-3.32	0.00	6.05	0.00	0.00	0.00
3. Suprasternale	3.24	0.00	-4.93	7.19	0.00	10.52
4. Left Shoulder Joint Center	-0.88	-7.38	-2.66	2.92	7.38	8.54
5. Right Shoulder Joint Center	-0.88	7.38	-2.66	2.92	-7.38	8.54
6. Thorax/Neck Attachment Center	0.00	0.00	-5.96	3.94	0.00	11.77
7. Thorax/Pelvis Attachment Center	-0.89	0.00	5.85	2.34	0.00	0.00
8. Thorax Center of Gravity	0.00	0.00	0.00	3.63	0.00	5.83

Transformation from Local Reference to Anatomical Axes

$$A_{AL} = \begin{bmatrix} 0.99769 & 0.00000 & -0.06795 \\ 0.00000 & -1.00000 & 0.00007 \\ -0.06795 & 0.00000 & -0.99769 \end{bmatrix}$$

Segment Contact Ellipsoid Semiaxes (in)

X: 4.825 Y: 6.500 Z: 7.785

Weight (lbs)

39.22

Principal Moments of Inertia (lbs - sec^2 - in)

X: 2.6203 Y: 2.0517 Z: 1.7336

Transformation from Principal to Local Reference Axes

$$A_{LP} = \begin{bmatrix} 0.99621 & -0.00004 & -0.08701 \\ -0.00004 & -1.00000 & 0.00002 \\ -0.08701 & -0.00002 & -0.99621 \end{bmatrix}$$

Surface Characteristics Coefficients Relating Load (lbs) to Deflection (in)

Back of Shoulder: A_0 = 0.01445 A_1 = -26.5900 A_2 = 380.913 A_3 = -678.223 A_4 = 456.528 A_5 = -104.791

Chest: A_0 = 0 A_1 = 5.46357 A_2 = 73.4896 A_3 = 0 A_4 = 0 A_5 = 0

TABLE 30

NECK

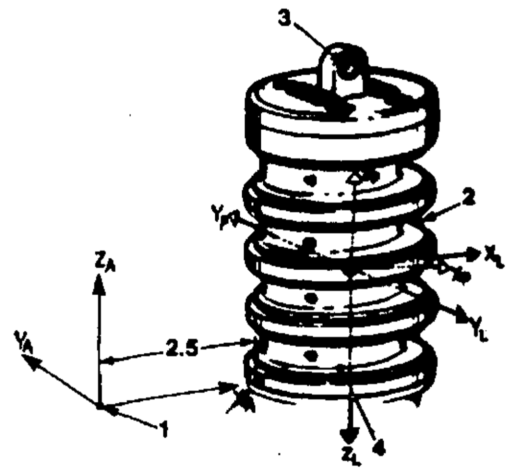

Local Reference Axes

Z axis - vector from the neck/head joint center to the inferior end of the neck cylinder axis.
Y-Z plane - right end of the neck/head joint axis.
Z axis - Y x Z.
Origin - center of gravity.

Anatomical Axes

Y axis - normal vector to the subject's left from the plane formed by cricoid cartilage, cervicale, and suprasternale.
X axis - normal from Y axis through the midpoint of a line between left and right clavicales.
Z axis - X x Y.
Origin - at cervicale.

Segment Landmarks

1. Cervicale - a point on the thorax jacket posterior to the posterior midpoint of the lowest neck ring.
2. "Adam's Apple" - anterior midpoint on the third neck ring.
3. Neck/Head Joint Center.
4. Neck/Thorax Attachment Center - the center of the surface of the lowest plate of the neck cylinder.

	Local Reference Axes (in)			Anatomical Axes (in)		
	X	Y	Z	X	Y	Z
1.Cervicale	-3.85	0.00	2.91	0.00	0.00	0.00
2."Adam's Apple"	1.77	0.00	0.35	5.52	0.00	2.77
3.Neck/Head Joint Center	0.00	0.00	-2.84	3.69	0.00	5.89
4.Neck/Thorax Attachment Center	0.00	0.00	2.76	3.90	0.00	0.30
5.Neck Center of Gravity	0.00	0.00	0.00	3.74	0.00	3.05

Transformation from Local Reference to Anatomical Axes

$$A_{AL} = \begin{bmatrix} 0.99930 & 0.00000 & 0.03747 \\ 0.00000 & -1.00000 & 0.00000 \\ 0.03747 & 0.00000 & -0.99930 \end{bmatrix}$$

Segment Contact Ellipsoid Semiaxes (in)

X: 1.675 Y: 1.675 Z: 3.000

Weight (lbs)

2.67

Principal Moments of Inertia (lbs - sec^2 - in)

X: 0.0254 Y: 0.0257 Z: 0.0084

Transformation from Principal to Local Reference Axes

$$A_{LP} = \begin{bmatrix} 1.00000 & 0.00004 & 0.00100 \\ 0.00004 & -1.00000 & 0.00000 \\ 0.00100 & 0.00000 & -1.00000 \end{bmatrix}$$

Segment Stiffness (in lb/deg)

Flexion - 35
Extension - 15
Lateral - 30

TABLE 31

HEAD

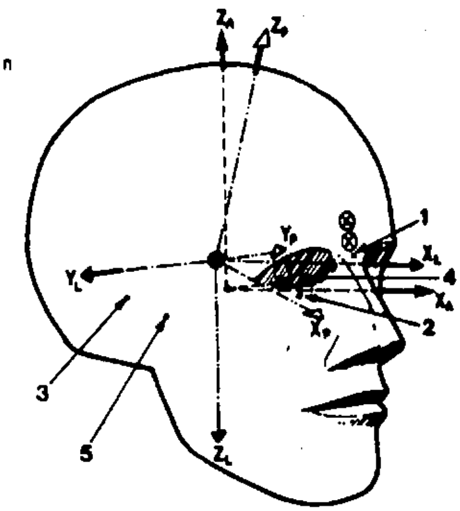

Local Reference Axes

Anatomical axes rotated 180° around the X axis, with the origin at the center of gravity.

Anatomical Axes

Y axis - vector from right tragion to left tragion.
X axis - normal from Y axis to right infraorbitale.
Z axis - X x Y.
Origin - intersection of Y axis and a normal passing through sellion.

Segment Landmarks

1. Sellion - on the bridge of the nose between the eyes.
2. Right Infraorbitale - center of the lower edge of the right eye.
3. Right Tragion - on the right side of the head, a point on a line extending vertically 1 inch above the posterior edge of the lower jaw.
4. Left Tragion - on the left side of the head, a point on a line extending vertically 1 inch above the posterior edge of the lower jaw.
5. Head/Neck Joint Center.

	Local Reference Axes (in)			Anatomical Axes (in)		
	X	Y	Z	X	Y	Z
1. Sellion	3.57	0.00	-0.25	3.45	0.00	0.92
2. Right Infraorbitale	3.26	1.04	0.67	3.14	-1.10	0.00
3. Right Tragion	0.12	2.84	0.67	0.00	-2.77	0.00
4. Left Tragion	0.12	-2.84	0.67	0.00	2.90	0.00
5. Head/Neck Joint Center	-0.55	0.00	2.00	-0.67	-0.00	-1.33
6. Head Center of Gravity	0.00	0.00	0.00	-0.12	0.00	0.67

Transformation from Local Reference to Anatomical Axes

$$A_{AL} = \begin{bmatrix} 1.0 & 0.0 & 0.0 \\ 0.0 & -1.0 & 0.0 \\ 0.0 & 0.0 & -1.0 \end{bmatrix}$$

Segment Contact Ellipsoid Semiaxes (in)

X: 4.250 Y: 2.875 Z: 4.000

Weight (lbs)

9.92

Principal Moments of Inertia (lbs - sec^2 - in)

X: 0.1408 Y: 0.2128 Z: 0.1956

Transformation from Principal to Local Reference Axes

$$A_{LP} = \begin{bmatrix} 0.89426 & 0.00018 & 0.44750 \\ -0.00010 & -1.00000 & 0.00065 \\ 0.44745 & -0.00061 & -0.89426 \end{bmatrix}$$

Surface Characteristics Coefficients Relating Load (lbs) to Deflection (in)

A_0 = 2.5742 A_1 = -175.975 A_2 = 4495.67 A_3 = -8953.11 A_4 = 6029.59 A_5 = 0

2.2 CVS/ATB Model Simulations

2.2.1 Conversion of Basic Data to CVS/ATB Model Format

The ATB model characterizes the body as a set of rigid segments linked together by joints. The seventeen segments and sixteen joints chosen to describe the Hybrid III body are listed in Table 32. Also in the Table is the chaining scheme in which joint J connects segments, j + 1 and JNT(j), where JNT is an input parameter.

Two ATB data sets have been developed; one using the seated manikin and the second using the standing manikin. The data sets are identical except for the lower torso, middle torso and upper leg segments and pelvis, waist, hip and knee joints. The tables in the following sections contain the seated manikin's data, and the standing manikin's data for these segments or joints are included at the bottom of each table. Where data were not available from this study, the data from the Part 572 dummy data set developed by Calspan [8] were used. The complete, formatted input files for both manikins are listed in the Appendix.

2.2.1.1 Segment Characteristics

The ATB model requires the weight and the three principal moments of inertia for each segment. The orientation of the principal axes is also required and is specified in terms of yaw, pitch, and roll rotations from the segment local coordinate system. These rotation angles are obtained from the direction cosine matrix for the transformation from the principal to local reference axes. Table 33 contains the mass properties for each segment and the principal axes yaw, pitch and roll angles.

TABLE 32

Hybrid III Segments and Joints

SEGMENT			JOINT				
No. (I)	Name	Symbol	No. (J)	Name	Symbol	Segments Joined JNT	J+1
1	lower torso	LT					
2	middle torso	MT	1	pelvis	P	1	2
3	upper torso	UT	2	waist	W	2	3
4	neck	N	3	neck pivot	NP	3	4
5	head	H	4	head pivot	HP	4	5
6	right upper leg	RUL	5	right hip	RH	1	6
7	right lower leg	RLL	6	right knee	RK	6	7
8	right foot	RF	7	right ankle	RA	7	8
9	left upper leg	RUL	8	left hip	LH	1	9
10	left lower leg	LLL	9	left knee	LK	9	10
11	left foot	LF	10	left ankle	LA	10	11
12	right upper arm	RUA	11	right shoulder	RS	3	12
13	right lower arm	RLA	12	right elbow	RE	12	13
14	left upper arm	LUA	13	left shoulder	LS	4	14
15	left lower arm	LLA	14	left elbow	LE	14	15
16	right hand	RHD	15	right wrist	RW	13	16
17	left hand	LHD	16	left wrist	LW	15	17

TABLE 33

SEGMENT MASS PROPERTIES

SEGMENT			WEIGHT	PRINCIPAL MOMENTS OF INERTIA (LBS - SEC^2 - IN)			PRINCIPAL AXES (DEG)		
I	SYM	PLOT	(LBS)	X	Y	Z	YAW	PITCH	ROLL
1	LT	5	44.460	2.4575	1.2969	1.2080	-1.05	52.68	180.00
2	MT	4	4.890	0.0612	0.0593	0.0205	-11.08	4.22	180.00
3	UT	3	38.630	2.6203	2.0517	1.7336	0.00	4.99	180.00
4	N	2	2.680	0.0254	0.0257	0.0084	0.00	0.00	180.00
5	H	1	9.921	0.1408	0.2128	0.1956	0.00	-26.58	180.00
6	RUL	6	13.713	0.6086	0.5934	0.1068	0.00	4.13	-180.00
7	RLL	7	7.237	0.6708	0.6745	0.0397	0.00	-1.90	180.00
8	RF	8	2.756	0.0067	0.0524	0.0491	-2.69	-9.23	-158.00
9	LUL	9	13.713	0.6086	0.5934	0.1068	0.00	4.13	180.00
10	LLL	0	7.237	0.6708	0.6745	0.0397	0.00	-1.90	-180.00
11	LF	1	2.756	0.0067	0.0524	0.0491	2.69	-9.23	158.00
12	RUA	2	4.597	0.1025	0.0997	0.0110	0.00	-1.31	180.00
13	RLA	3	3.800	0.1191	0.1128	0.0069	0.00	1.31	180.00
14	LUA	4	4.597	0.1025	0.0997	0.0110	0.00	-1.31	180.00
15	LLA	5	3.800	0.1191	0.1128	0.0069	0.00	1.31	180.00
16	RHD	6	1.290	0.0115	0.0093	0.0036	-2.35	-31.09	-175.60
17	LHD	7	1.290	0.0115	0.0093	0.0036	2.35	-31.09	175.60
				STANDING MANIKIN					
1	LT	5	21.912	0.8019	0.6182	0.4678	0.00	-43.00	180.00
2	MT	4	2.661	0.0196	0.0196	0.0083	0.00	0.00	180.00
6	RUL	6	19.984	1.4494	1.4968	0.1989	11.08	7.03	173.90
9	LUL	9	19.984	1.4494	1.4968	0.1989	-11.08	7.03	-173.90

TABLE 34 SEGMENT CONTACT ELLIPSOIDS

SEGMENT			SEGMENT CONTACT ELLIPSOID SEMIAXES (IN)			CENTER (IN)		
I	SYM	PLOT	X	Y	Z	X	Y	Z
1	LT	5	5.000	7.185	4.800	-1.000	0.000	0.000
2	MT	4	4.775	6.500	4.000	1.000	0.000	-1.000
3	UT	3	4.825	6.500	7.785	0.000	0.000	0.000
4	N	2	1.675	1.675	3.000	0.000	0.000	0.000
5	H	1	4.250	2.875	4.000	0.000	0.000	0.000
6	RUL	6	2.950	3.050	7.285	0.000	0.000	0.000
7	RLL	7	2.165	2.050	9.750	0.000	0.000	2.000
8	RF	8	4.900	1.675	1.675	0.000	0.000	0.000
9	LUL	9	2.950	3.050	7.285	0.000	0.000	0.000
10	LLL	0	2.165	2.050	9.750	0.000	0.000	2.000
11	LF	1	4.900	1.675	1.675	0.000	0.000	0.000
12	RUA	2	1.900	1.800	6.000	0.000	0.000	-1.000
13	RLA	3	1.775	1.775	5.800	0.000	0.000	0.000
14	LUA	4	1.900	1.800	6.000	0.000	0.000	-1.000
15	LLA	5	1.775	1.775	5.800	0.000	0.000	0.000
16	RHD	6	1.000	1.870	3.650	0.000	0.000	0.000
17	LHD	7	1.000	1.870	3.650	0.000	0.000	0.000
				STANDING MANIKIN				
1	LT	5	4.725	7.185	4.800	0.000	0.000	0.000
2	MT	4	4.775	6.500	4.000	1.000	0.000	-1.000
6	RUL	6	2.950	3.050	7.285	0.000	0.000	2.300
9	LUL	9	2.950	3.050	7.285	0.000	0.000	2.300

Ellipsoids are used by the ATB model to represent the surface of each segment for contact calculations and for the graphics program. Using the manikin's exterior measurements, contact ellipsoids for each segment were chosen to approximate the segment's surface. Table 34 lists each segment's contact ellipsoid dimensions and the vector in the local reference system from the segment center of mass to the contact ellipsoid center.

2.2.1.2 Joint Configurations

The joint centers are among the landmarks described in Section 2.1.6. The location of each joint center is required by the ATB model in each of the adjoining segment's local reference systems. Table 35 contains these locations while Table 36 contains the rotations from the segment local reference system to the segment joint coordination system.

Each joint has two coordinate systems associated with it. One fixed within each of the joint's adjoining segments. The relative orientation of the two joint coordinate systems is used to determine the resistive torques applied at the joint based on the joint type.

Three joint types were used to model the Hybrid III joints: pin joint (IPIN = 1) for the knees; Euler joint, with the spin axis locked (IPIN = -8), for the ankles, elbows and wrists; and three degree-of-freedom characteristic joint (IPIN = 0) for the pelvis, waist, neck pivot, head pivot, hips, and shoulders.

The pin joint constrains the y-axes of the two joint coordinate systems to be aligned and measures flexure as the angle between the z-axes as shown in Figure 99. The range of motion and resistive properties of a pin joint are symmetric about 0°. Therefore, the joint coordinate systems selected are aligned when the knees are in the center of their range of motion.

TABLE 35 JOINT LOCATIONS

JOINT				LOCATION(IN) - SEG(JNT)			LOCATION(IN) - SEG(J+1)		
J	SYM	PLOT	JNT	X	Y	Z	X	Y	Z
1	P	M	1	-2.150	0.000	-1.660	-0.350	0.000	2.560
2	W	N	2	-0.350	0.000	-2.560	-0.890	0.000	5.850
3	NP	O	3	0.000	0.000	-5.960	0.000	0.000	2.760
4	HP	P	4	0.000	0.000	-2.840	-0.550	0.000	2.000
5	RH	Q	1	-0.110	3.150	1.240	0.000	0.000	-9.960
6	RK	R	6	0.000	0.000	6.560	-0.200	0.000	-6.740
7	RA	S	7	-0.200	0.000	9.650	-2.120	0.000	-1.540
8	LH	T	1	-0.110	-3.150	1.240	0.000	0.000	-9.960
9	LK	U	9	0.000	0.000	6.560	-0.200	0.000	-6.740
10	LA	V	10	-0.200	0.000	9.650	-2.120	0.000	-1.540
11	RS	W	3	-0.880	7.380	-2.660	0.000	0.000	-5.430
12	RE	X	12	0.000	0.000	4.940	0.000	0.000	-3.670
13	LS	Y	3	-0.880	-7.380	-2.660	0.000	0.000	-5.430
14	LE	Z	14	0.000	0.000	4.940	0.000	0.000	-3.670
15	RW		13	0.000	0.000	6.070	-0.300	0.000	-2.130
16	LW		15	0.000	0.000	6.070	-0.300	0.000	-2.130
					STANDING MANIKIN				
1	P	M	1	-2.500	0.000	-1.080	-0.890	0.000	2.560
2	W	N	2	0.000	0.000	-2.560	-0.890	0.000	5.850
5	RH	Q	1	0.000	3.280	2.040	-0.240	0.000	-7.230
6	RK	R	6	-0.240	0.000	8.900	-0.200	0.000	-6.740
8	LH	T	1	0.000	-3.280	2.040	-0.240	0.000	-7.230
9	LK	U	9	-0.240	0.000	8.900	-0.200	0.000	-6.740

TABLE 36 JOINT COORDINATE SYSTEMS

J	JOINT SYM	PLOT	JNT	IPIN	JOINT AXIS (DEG) SEG(JNT) YAW	PITCH	ROLL	JOINT AXIS (DEG) SEG(J+1) YAW	PITCH	ROLL	CENTER OF SYMMETRY PREC	NUT	SPIN
1	P	M	1	0	0.00	0.00	0.00	0.00	0.00	0.00	-	-	-
2	W	N	2	0	0.00	0.00	0.00	0.00	0.00	0.00	-	-	-
3	NP	O	3	0	0.00	0.00	0.00	0.00	0.00	0.00	-	-	-
4	HP	P	4	0	0.00	0.00	0.00	0.00	0.00	0.00	-	-	-
5	RH	Q	1	0	0.00	90.00	0.00	0.00	0.00	0.00	-	-	-
6	RK	R	6	1	0.00	0.00	0.00	0.00	55.00	0.00	-	-	-
7	RA	S	7	-8	90.00	0.00	0.00	90.00	0.00	0.00	0.00	-10.00	0.00
8	LH	T	1	0	0.00	90.00	0.00	0.00	0.00	0.00	-	-	-
9	LK	U	9	1	0.00	0.00	0.00	0.00	55.00	0.00	-	-	-
10	LA	V	10	-8	90.00	0.00	0.00	90.00	0.00	0.00	0.00	-10.00	0.00
11	RS	W	3	0	0.00	90.00	0.00	0.00	0.00	0.00	-	-	-
12	RE	X	12	-8	90.00	0.00	0.00	90.00	0.00	0.00	0.00	62.50	0.00
13	LS	Y	3	0	0.00	90.00	0.00	0.00	0.00	0.00	-	-	-
14	LE	Z	14	-8	90.00	0.00	0.00	90.00	0.00	0.00	0.00	62.50	0.00
15	RW		13	-8	90.00	0.00	0.00	90.00	0.00	0.00	0.00	15.00	0.00
16	LW		15	-8	90.00	0.00	0.00	90.00	0.00	0.00	0.00	15.00	0.00
							STANDING MANIKIN						
1	P	M	1	0	0.00	0.00	0.00	0.00	0.00	0.00	-	-	-
2	W	N	2	0	0.00	0.00	0.00	0.00	0.00	0.00	-	-	-
5	RH	Q	1	0	0.00	0.00	0.00	0.00	0.00	0.00	-	-	-
6	RK	R	6	1	0.00	0.00	0.00	0.00	55.00	0.00	-	-	-
8	LH	T	1	0	0.00	0.00	0.00	0.00	0.00	0.00	-	-	-
9	LK	U	9	1	0.00	0.00	0.00	0.00	55.00	0.00	-	-	-

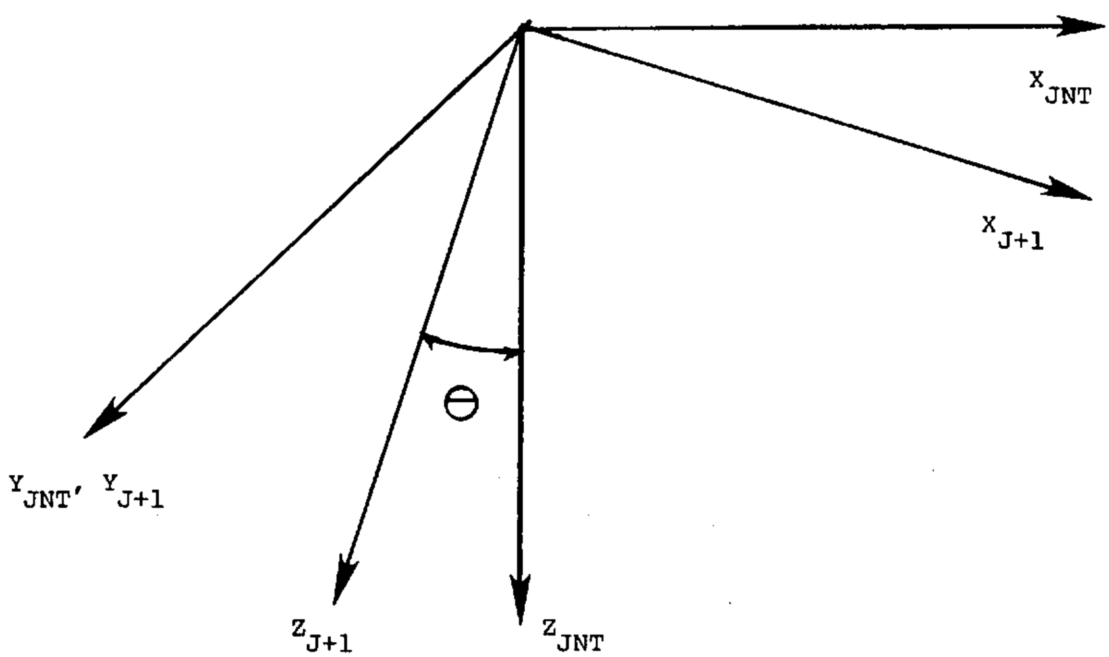

Figure 99. Pin Joint Coordinates

The Euler joint, with the spin axis locked, constrains the rotation between the JNT joint coordinate system to the J+1 joint coordinate system to be a combination of two body fixed rotations: first is a precession rotation through angle ϕ about the z-axis; second is a nutation rotation through angle θ about the new x-axis as shown in Figure 100. Separate ranges of motion and resistive properties are defined for each of these rotations. As with the pin joint, these characteristics are symmetric, but the center of symmetry can be defined as input. The centers of symmetry used for the ankles, elbows, and wrists are included in Table 37.

The three degree-of-freedom characteristic joint requires the joint coordinate systems to be aligned in an equilibrium position, with the z-axis of the JNT joint coordinate system as the torsion axis.

2.2.1.3 Joint Rotation Resistive Torques

The joint resistive properties are prescribed in a number of different ways depending on the joint type. For the pin joints used to model the knees, four parameters (linear, quadratic and cubic spring coefficients and joint stop) are required to define the relationship between torque and flexure, θ. The angle θ is measured from the equilibrium position in which the two joint coordinate systems are aligned. Figure 101 shows how these parameters are used to define the torque. The curve is symmetric about $\theta = 0$, therefore flexion and extension must have the same stop characteristics. A typical curve from the joint testing is shown in Figure 102. The center of the range of motion was chosen as the equilibrium position and the free range of motion determined the joint stop angle, θ_S as that angle at which the resistive torque increases in a nonlinear manner with increasing angle of rotation. The linear spring coefficient, C, was set to zero to model the free range of motion. The remaining two coefficients prescribed the soft stop.

Initially, this resistive range of the soft stop was digitized and a least squares method was used to solve for the quadratic and cubic coefficients. Although this method fit the data well, some

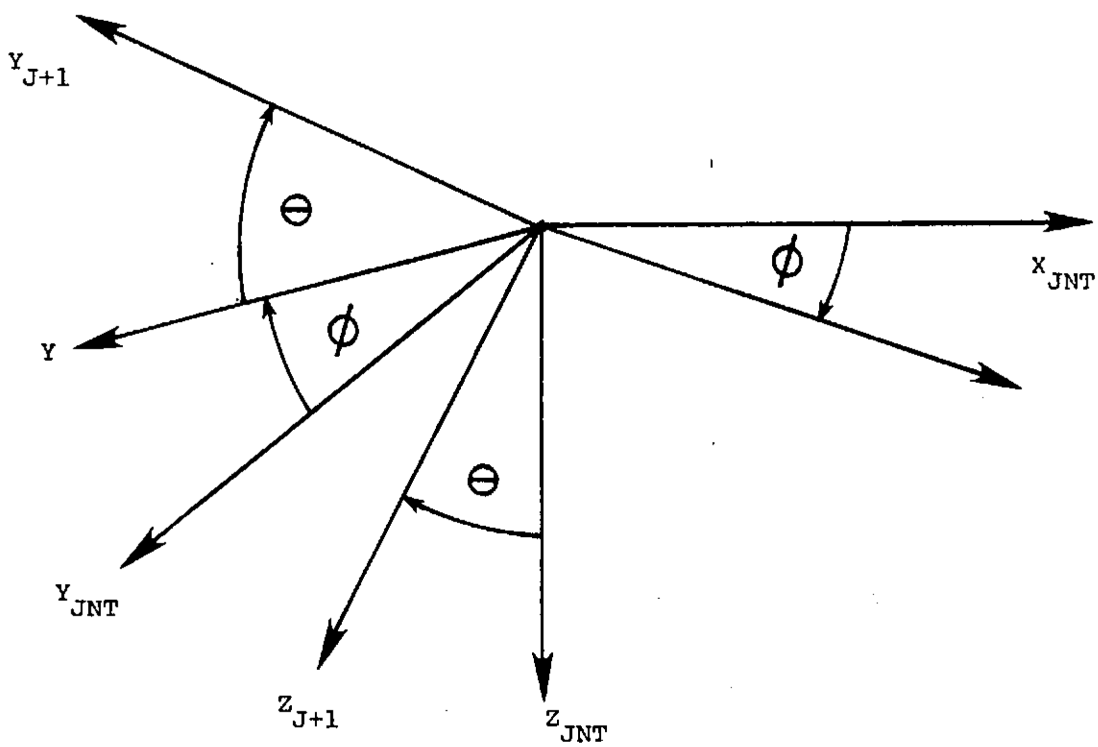

Figure 100. Euler Joint with Spin Axis Locked

Table 37

θm in Degrees

(Average of Standing and Seated Manikins - Except Hip)

Ankle	15.0
Wrist	20.4
Knee	25.5
Elbow	18.0
Shoulder	
Flex 90 ABD	29.4
Ext 90 ABD	33.9
Flex 0 ABD	8.1
Ext 0 ABD	7.5
Flex 45 ABD	4.5
Ext 45 ABD	19.5
Abduction	27.9
Adduction	8.1
HIP - 158 SEATED MANIKIN	
Flexion	27.6
Extension	23.4
ABD 90 Flex	35.4
ADD 90 Flex	10.5
HIP - 061 STANDING MANIKIN	
Flexion	138.0
Extension	36.0
Abduction	86.4
Adduction	37.5

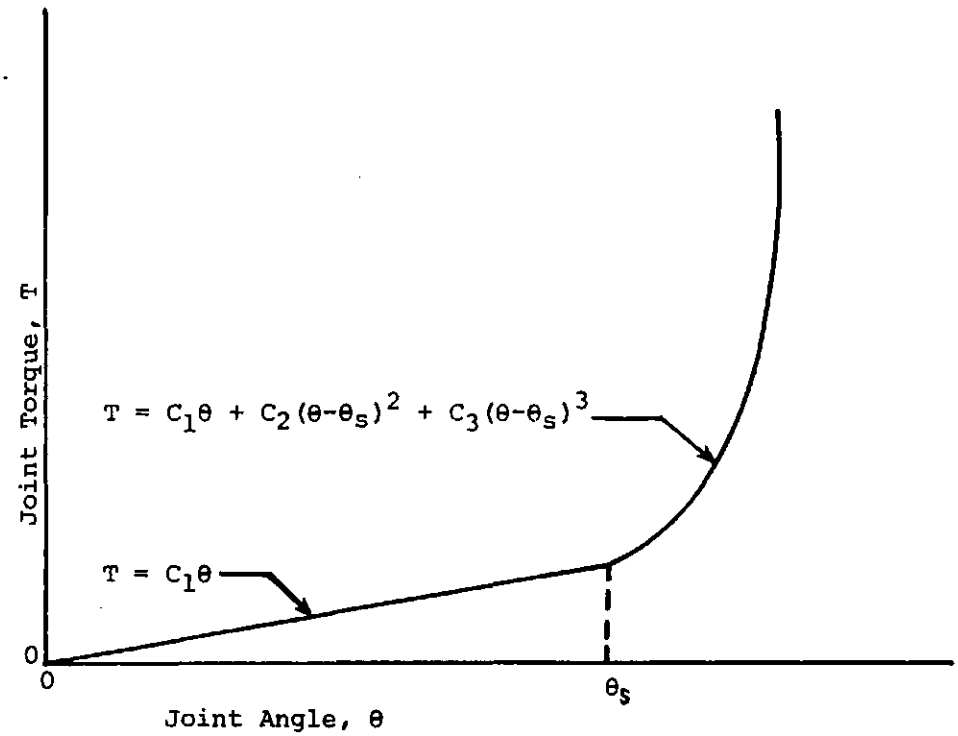

T -joint torque
θ -joint angle
θ_s-joint stop
C_1-linear spring coefficient
C_2-quadratic spring coefficient
C_3-cubic spring coefficient

Figure 101. Joint Torque Dependent on a Single Angle

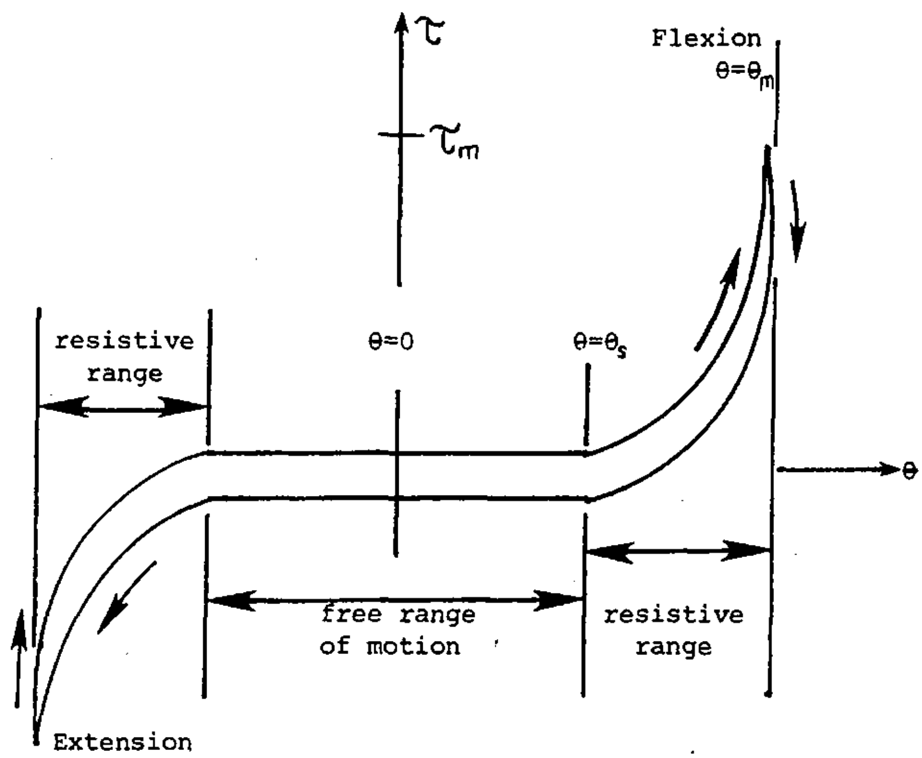

Figure 102. Example Joint Test Curve

characteristics of the resulting curve were not acceptable. These characteristics were negative torques and decreased in the torque beyond the measured data (i.e. the curve did not portray a hard physical stop at the maximum joint angle). Several techniques were used without success in an attempt to avoid these problems and still fit the data. Therefore, it was decided to only match the significant characteristics of the data. Those were:

$T(\theta_s) = 0$, no torque at joint stop;

$\frac{d}{d\theta} T(\theta_s) = 0$, zero slope at joint stop;

$T(0) \simeq 0$, no negative torques for $\theta = 0$; and

$T(\theta = \theta_m) = T_M$, hard stop at maximum angle tested.

With C = 0 the first two conditions were met. The remaining conditions were met using the least squares method on six data points; $(\theta_s, 0)$; (θ_m, T_m), $(\theta_m, 20*T_m)$, $(\theta_m, 40*T_m)$, $(\theta_m, 60*T_m)$, and $(\theta_m, 80*T_m)$.

Data from both manikins, left and right knees and flexion and extension, were all averaged to obtain the test value, θ_m, needed for this method. The value for θ_m for the knee is included in Table 37. The resulting parameters for the knee are included in Table 38.

The same function form is used to prescribe the ankle, wrist and elbow Euler joints, but each rotation axis has a separate function. These joints were not tested in precession, therefore the values from the Part 572 data set were used for this axis. The parameters for the nutation axis were calculated using the same method described for knee flexure. The θ_m values for ankle, wrist and elbow nutation are included in Table 37 and the resulting precession and nutation parameters for these joints are in Table 38.

The pelvis, waist, neck pivot, head pivot, hip and shoulder three degree-of-freedom characteristic joint resistive properties are prescribed using two functions. The first function is of the same form as described above for the knee pin joint and is dependent on torsion, γ , rotation about the JNT z-axis. This rotation was not

TABLE 38 JOINT TORQUE CHARACTERISTICS

JOINT		ROTATION	SPRING COEF. (IN LBS/DEG**J) LINEAR (J=1)	QUADRATIC (J=2)	CUBIC (J=3)	ENERGY DISSIPATION COEF.	JOINT STOP (DEG)
1	P	TORSION	34.380	0.000	0.000	1.000	0.000
2	W	TORSION	34.380	0.000	0.000	1.000	0.000
3	NP	TORSION	15.000	0.000	0.000	1.000	0.000
4	HP	TORSION	15.000	0.000	0.000	1.000	0.000
5	RH	TORSION	7.500	75.000	75.000	1.000	55.000
6	RK	FLEXURE	0.000	2.320	0.000	1.000	48.900
7	RA	PRECESSION	1.000	10.000	10.000	1.000	27.000
		NUTATION	0.000	6.690	0.000	1.000	30.000
8	LH	TORSION	7.500	75.000	75.000	1.000	55.000
9	LK	FLEXURE	0.000	2.320	0.000	1.000	48.900
10	LA	PRECESSION	1.000	10.000	10.000	1.000	27.000
		NUTATION	0.000	6.690	0.000	1.000	30.000
11	RS	TORSION	0.000	100.000	100.000	1.000	125.000
12	RE	PRECESSION	0.000	20.000	20.000	1.000	52.000
		NUTATION	0.000	4.650	0.000	1.000	65.300
13	LS	TORSION	0.000	100.000	100.000	1.000	125.000
14	LE	PRECESSION	0.000	20.000	20.000	1.000	52.000
		NUTATION	0.000	4.650	0.000	1.000	65.300
15	RW	PRECESSION	0.000	0.000	0.000	1.000	0.000
		NUTATION	0.000	4.320	0.143	1.000	55.500
16	LW	PRECESSION	0.000	0.000	0.000	1.000	0.000
		NUTATION	0.000	4.320	0.143	1.000	55.500

tested, therefore the values from the Part 572 data set were used and Table 38 includes the four parameters for the pelvis, waist, neck pivot, head pivot, hip and shoulder torsion.

The second function for these joints is dependent on both flexure, θ and aximuth, Ø, as defined in Figure 103. This function actually can consist of several polynomial functions of θ for constant Øs or of a table of data. The polynomial option allows input of a joint stop angle, θ_s and the coefficients for a polynomial of the form

$$T = C_1\ (\theta-\theta_s) + C_2\ (\theta-\theta_s)^2 + \ldots + C_n\ (\theta-\theta_s)^n$$

for equally spaced values of Ø. Because the shoulders were tested at various θs and since the results were similar to those in Figure 101 this polynomial option is used to model the shoulders. The parameters were determined by averaging data from both manikins and left and right sides and using the same method described earlier. The equilibrium position defined by the orientation of the shoulder joint axes is the position with the arm extending straight out in front of the upper torso. Table 39 presents the parameters for the right shoulder.

For equally spaced azimuth angles, Ø, the tabular option requires a flexure joint stop angle and torque values at equally spaced flexure angles, θ. The ATB model applies no torque until the joint stops are reached and linearly interpolates between data points for the torques. This option was used for the neck, torso and hip joints since they were tested in different orientations and their large ranges of motion would be adequately described using ten degree increments.

The neck and lumbar spines were modeled by using the measured stiffness coefficients up until 120° flexure for the neck and 90° flexure for the spines and then doubling the stiffness for each subsequent ten degree increment. This provides a stop for these joints. For the head pivot the stiffness due to the nodding blocks were combined with the neck flexion and extension stiffness for the 20° of their movement. The neck and the two lumbar spine joint resistances are in Tables 40, 41, 42, and 43. The values in these tables are double those from the test because the neck and lumbar spines were each tested as one unit while they are

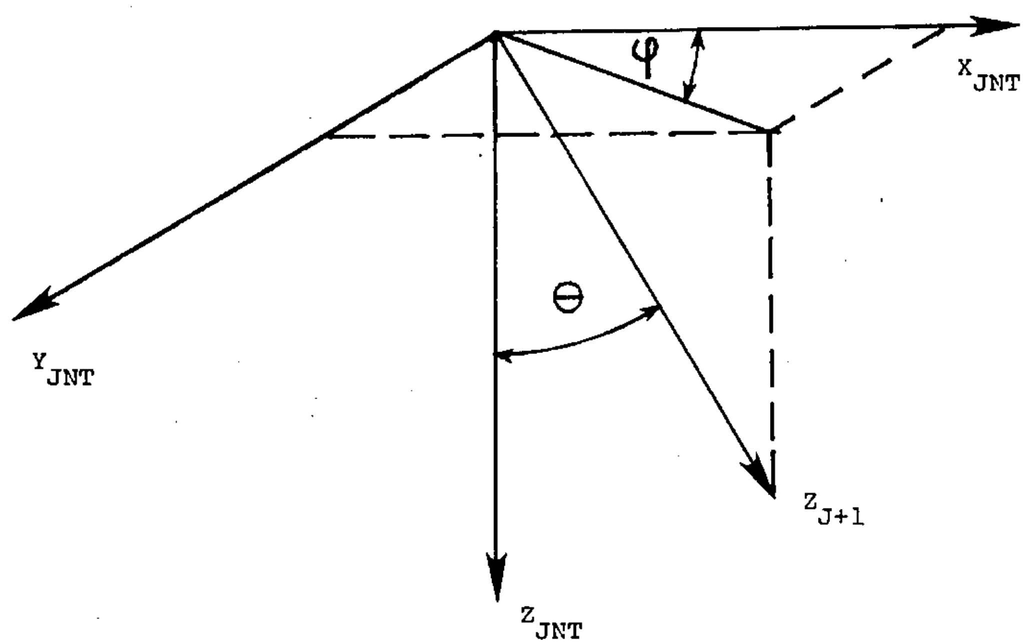

Figure 103. Three Degree-of-Freedom Characteristic Joint's Flexure and Azimuth Angles

TABLE 39 RIGHT SHOULDER JOINT TORQUE FUNCTION

FUNCTION IS COEFFICIENTS OF 3 ORDER POLYNOMIALS IN (THETA-THETAO) FOR 8 VALUES OF PHI.

	PHI	THETA STOP	COEFFICIENTS OF (THETA-THETAO)**N N = 1	N = 2	N = 3
EXTENSION	-180.00	151.000	0.0	87900.0	0.0
FLEXION @ 135° ABDUCTION*	-135.00	75.000	0.0	13700.0	0.0
FLEXION @ 90° ABDUCTION	-90.00	0.000	0.0	-312.0	11800.0
FLEXION @ 45° ABDUCTION	-45.00	66.000	0.0	7780.0	3010000.0
FLEXION	0.00	68.000	0.0	22200.0	376000.0
EXTENSION @ 135° ABDUCTION*	45.00	89.000	0.0	22000.0	0.0
EXTENSION @ 90° ABDUCTION	90.00	111.000	0.0	2470.0	17600.0
EXTENSION @ 45° ABDUCTION	135.00	153.000	0.0	13000.0	0.0

* A test was not done for these orientations therefore the joint stops and resistive curves of the adjacent orientations were averaged to obtain the parameters for flexion and extension at 135° abduction.

TABLE 40 HEAD PIVOT TORQUE FUNCTION

FUNCTION IS TABULAR FOR 19 X 4 VALUES OF THETA AND PHI

	PHI	THETA STOP	THETA 10.000	20.000	30.000	40.000	50.000
FLEXION	-180.00	0.000	490.0	980.0	1680.0	2380.0	3080.0
LATERAL	-90.00	0.000	600.0	1200.0	1800.0	2400.0	3000.0
EXTENSION	0.00	0.000	250.0	500.0	800.0	1100.0	1400.0
LATERAL	90.00	0.000	600.0	1200.0	1800.0	2400.0	3000.0

	PHI	60.000	70.000	80.000	90.000	100.000
FLEXION	-180.00	3780.0	4480.0	5180.0	5880.0	6580.0
LATERAL	-90.00	3600.0	4200.0	4800.0	5400.0	6000.0
EXTENSION	0.00	1700.0	2000.0	2300.0	2600.0	2900.0
LATERAL	90.00	3600.0	4200.0	4800.0	5400.0	6000.0

	PHI	110.000	120.000	130.000	140.000	150.000
FLEXION	-180.00	7280.0	7980.0	9380.0	12180.0	17780.0
LATERAL	-90.00	6600.0	7200.0	8400.0	10800.0	15600.0
EXTENSION	0.00	3200.0	3500.0	4100.0	5300.0	7700.0
LATERAL	90.00	6600.0	7200.0	8400.0	10800.0	15600.0

	PHI	160.000	170.000	180.000
FLEXION	-180.00	28980.0	51380.0	96180.0
LATERAL	-90.00	25200.0	44400.0	82800.0
EXTENSION	0.00	12500.0	22100.0	41300.0
LATERAL	90.00	25200.0	44400.0	82800.0

TABLE 41 NECK PIVOT TORQUE FUNCTION

FUNCTION IS TABULAR FOR 19 X 4 VALUES OF THETA AND PHI

	PHI	THETA STOP	THETA 10.000	20.000	30.000	40.000	50.000
FLEXION	-180.00	0.000	700.0	1400.0	2100.0	2800.0	3500.0
LATERAL	-90.00	0.000	600.0	1200.0	1800.0	2400.0	3000.0
EXTENSION	0.00	0.000	300.0	600.0	900.0	1200.0	1500.0
LATERAL	90.00	0.000	600.0	1200.0	1800.0	2400.0	3000.0
			60.000	70.000	80.000	90.000	100.000
FLEXION	-180.00		4200.0	4900.0	5600.0	6300.0	7000.0
LATERAL	-90.00		3600.0	4200.0	4800.0	5400.0	6000.0
EXTENSION	0.00		1800.0	2100.0	2400.0	2700.0	3000.0
LATERAL	90.00		3600.0	4200.0	4800.0	5400.0	6000.0
			110.000	120.000	130.000	140.000	150.000
FLEXION	-180.00		7700.0	8400.0	9800.0	12600.0	18200.0
LATERAL	-90.00		6600.0	7200.0	8400.0	10800.0	15600.0
EXTENSION	0.00		3300.0	3600.0	4200.0	5400.0	7800.0
LATERAL	90.00		6600.0	7200.0	8400.0	10800.0	15600.0
			160.000	170.000	180.000		
FLEXION	-180.00		29400.0	51800.0	96600.0		
LATERAL	-90.00		25200.0	44400.0	82800.0		
EXTENSION	0.00		12600.0	22200.0	41400.0		
LATERAL	90.00		25200.0	44400.0	82800.0		

TABLE 42 STANDING LUMBAR SPINE TORQUE FUNCTION

FUNCTION IS TABULAR FOR 19 X 4 VALUES OF THETA AND PHI

	PHI	THETA STOP	THETA 10.000	20.000	30.000	40.000	50.000
FLEXION	-180.00	0.000	1200.0	2400.0	3600.0	4800.0	6000.0
LATERAL	-90.00	0.000	1200.0	2400.0	3600.0	4800.0	6000.0
EXTENSION	0.00	0.000	960.0	1920.0	2880.0	3840.0	4800.0
LATERAL	90.00	0.000	1200.0	2400.0	3600.0	4800.0	6000.0

	PHI	60.000	70.000	80.000	90.000	100.000
FLEXION	-180.00	7200.0	8400.0	9600.0	10800.0	13200.0
LATERAL	-90.00	7200.0	8400.0	9600.0	10800.0	13200.0
EXTENSION	0.00	5760.0	6720.0	7680.0	8640.0	10560.0
LATERAL	90.00	7200.0	8400.0	9600.0	10800.0	13200.0

	PHI	110.000	120.000	130.000	140.000	150.000
FLEXION	-180.00	18000.0	27600.0	46800.0	85200.0	162000.0
LATERAL	-90.00	18000.0	27600.0	46800.0	85200.0	162000.0
EXTENSION	0.00	14400.0	22080.0	37440.0	68160.0	129600.0
LATERAL	90.00	18000.0	27600.0	46800.0	85200.0	162000.0

	PHI	160.000	170.000	180.000
FLEXION	-180.00	315600.0	622800.0	1237200.0
LATERAL	-90.00	315600.0	622800.0	1237200.0
EXTENSION	0.00	252480.0	498240.0	989760.0
LATERAL	90.00	315600.0	622800.0	1237200.0

TABLE 43 SEATED LUMBAR SPINE TORQUE FUNCTION

FUNCTION IS TABULAR FOR 19 X 4 VALUES OF THETA AND PHI

	PHI	THETA STOP	THETA 10.000	20.000	30.000	40.000	50.000
FLEXION	-180.00	0.000	4600.0	9200.0	13800.0	18400.0	23000.0
LATERAL	-90.00	0.000	6800.0	13600.0	20400.0	27200.0	34000.0
EXTENSION	0.00	0.000	3000.0	6000.0	9000.0	12000.0	15000.0
LATERAL	90.00	0.000	6800.0	13600.0	20400.0	27200.0	34000.0

			60.000	70.000	80.000	90.000	100.000
FLEXION	-180.00		27600.0	32200.0	36800.0	41400.0	50600.0
LATERAL	-90.00		40800.0	47600.0	54400.0	61200.0	74800.0
EXTENSION	0.00		18000.0	21000.0	24000.0	27000.0	33000.0
LATERAL	90.00		40800.0	47600.0	54400.0	61200.0	74800.0

			110.000	120.000	130.000	140.000	150.000
FLEXION	-180.00		69000.0	105800.0	179400.0	326600.0	621000.0
LATERAL	-90.00		102000.0	156400.0	265200.0	482800.0	918000.0
EXTENSION	0.00		45000.0	69000.0	117000.0	213000.0	405000.0
LATERAL	90.00		102000.0	156400.0	265200.0	482800.0	918000.0

			160.000	170.000	180.000
FLEXION	-180.00		1209800.0	2387400.0	4742600.0
LATERAL	-90.00		1788400.0	3529200.0	7010800.0
EXTENSION	0.00		789000.0	155700.0	3093000.0
LATERAL	90.00		1788400.0	3529200.0	7010800.0

modeled as two three degree-of-freedom characteristic joints on either end of a rigid element. By doubling the stiffnesses obtained from the static test, similar results can be obtained for the joint torque with the model.

A similar method was used for the hip joints. The test curves were digitized at ten degree increments of flexure, θ, and these values used in the table. The slope between the last two measured points was doubled for each subsequent ten degree increment providing a stop. The left and right sides were averaged to obtain the data in Tables 44 and 45. The equilibrium position defined for the seated dummy's hip is the orientation with the upper leg extending straight out in front of the lower torso and for the standing dummy's hip with the upper leg extending down from the lower torso. These orientations are defined by the hip joint axes.

2.2.1.4 Skin Compliance Characteristics

The ATB model's force deflection characteristics are very flexible, allowing the function to be constant, tabular, polynomial or any combination of two of these forms. For the range in which the deflection was tested, it was decided to use the polynomial input, since a method was available in which several test curves for each segment test could be averaged to obtain a single polynomial. Beyond the tested deflection, tabular data were added to provide the model with a hard stop. For each surface tested, the tabular data points of force vs. deflection were initially plotted. There were often 4 to 5 of these plots for each surface. They were compared for general shape and ranges of force and deflection. If there was one set that did not fit the trend, it was not used to find the averaged curve. The data points on the loading portion of the curve were fitted to a univariate curvilinear regression model using orthogonal polynomials. The curves pertaining to the same surface were averaged to obtain a single polynomial for the surface with a characteristic as shown in Figure 104.

TABLE 44 STANDING RIGHT HIP TORQUE FUNCTION

FUNCTION IS TABULAR FOR 19 X 4 VALUES OF THETA AND PHI

	PHI	THETA STOP	THETA 10.000	20.000	30.000	40.000	50.000
EXTENSION	-180.00	0.000	2.0	7.0	21.0	49.0	105.0
ADDUCTION	-90.00	0.000	5.0	11.0	22.0	39.0	73.0
FLEXION	0.00	0.000	1.0	2.0	3.0	5.0	7.0
ABDUCTION	90.00	0.000	1.0	3.0	4.0	6.0	8.0

		60.000	70.000	80.000	90.000	100.000
EXTENSION	-180.00	217.0	441.0	889.0	1790.0	3580.0
ADDUCTION	-90.00	141.0	277.0	549.0	1090.0	2180.0
FLEXION	0.00	10.0	13.0	17.0	22.0	27.0
ABDUCTION	90.00	9.0	10.0	18.0	34.0	66.0

		110.000	120.000	130.000	140.000	150.000
EXTENSION	-180.00	7160.0	14300.0	28700.0	57300.0	115000.0
ADDUCTION	-90.00	4360.0	8710.0	17400.0	34800.0	69600.0
FLEXION	0.00	32.0	38.0	46.0	62.0	94.0
ABDUCTION	90.00	130.0	258.0	514.0	1030.0	2050.0

		160.000	170.000	180.000
EXTENSION	-180.00	229000.0	459000.0	917000.0
ADDUCTION	-90.00	139000.0	279000.0	557000.0
FLEXION	0.00	158.0	286.0	542.0
ABDUCTION	90.00	4100.0	8190.0	16400.0

TABLE 45 SEATED RIGHT HIP TORQUE FUNCTION

FUNCTION IS TABULAR FOR 19 X 4 VALUES OF THETA AND PHI

	PHI	THETA STOP	THETA 10.000	20.000	30.000	40.000	50.000
EXTENSION	-180.00	0.000	7.0	22.0	52.0	112.0	232.0
ADDUCTION @ 90° FLEXION	-90.00	0.000	17.0	51.0	119.0	255.0	527.0
FLEXION	0.00	0.000	8.0	17.0	28.0	50.0	94.0
ABDUCTION @ 90° FLEXION	90.00	0.000	7.0	13.0	18.0	23.0	33.0

	PHI	60.000	70.000	80.000	90.000	100.000
EXTENSION	-180.00	472.0	952.0	1910.0	3830.0	7670.0
ADDUCTION @ 90° FLEXION	-90.00	1070.0	2160.0	4340.0	8690.0	17400.0
FLEXION	0.00	182.0	358.0	710.0	1410.0	2820.0
ABDUCTION @ 90° FLEXION	90.00	53.0	93.0	173.0	333.0	653.0

	PHI	110.000	120.000	130.000	140.000	150.000
EXTENSION	-180.00	15400.0	30700.0	61400.0	123000.0	246000.0
ADDUCTION @ 90° FLEXION	-90.00	34900.0	69700.0	139000.0	279000.0	557000.0
FLEXION	0.00	5640.0	11300.0	22500.0	45100.0	90100.0
ABDUCTION @ 90° FLEXION	90.00	1290.0	2570.0	5130.0	10300.0	20500.0

	PHI	160.000	170.000	180.000
EXTENSION	-180.00	492000.0	983000.0	1970000.0
ADDUCTION @ 90° FLEXION	-90.00	1110000.0	2230000.0	4460000.0
FLEXION	0.00	180000.0	360000.0	721000.0
ABDUCTION @ 90° FLEXION	90.00	41000.0	81900.0	164000.0

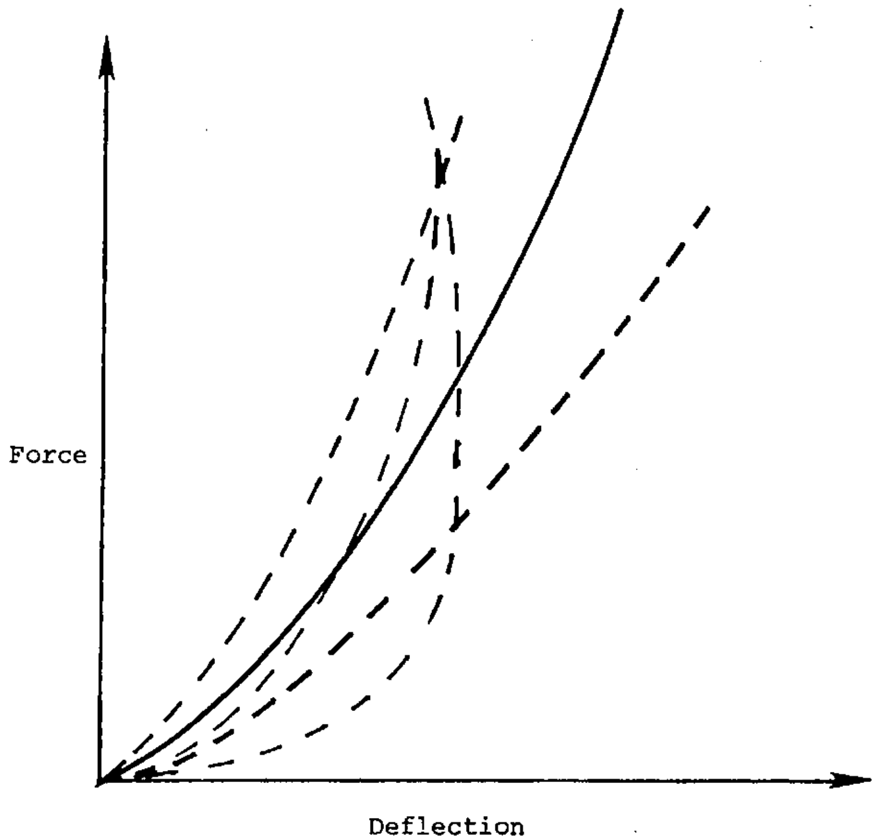

Figure 104. Component Curves for a Body Segment
and the Averaged Curve

Tabular data were used to model the second part of the functions beyond the test deflections. The force at the last deflection input is used by the model for all larger deflections. The tabular forces beyond the tested deflections were chosen so as to avoid problems due to this by providing a more definite hard stop.

Table 46 contains the input parameters for the thirteen displacement functions. These parameters are defined in Figure 105 which is an example ATB force-deflection curve.

It should be noted that these curves are based on the data from the tests done with 1.0 and 2.5 in diameter saucer shaped probes impacting the surface. If the user wishes to use these functions to describe the contact of one of the dummy surfaces with a surface significantly different from the saucer shaped probes that surface's force-deflection characteristics should be combined with this data to provide a mutual force-deflection function.

TABLE 46

				FIRST PART OF FUNCTION 5th DEGREE POLYNOMIAL COEFFICIENTS						SECOND PART OF FUNCTION TABULAR POINTS	
FUNCTION	D0	D1	D2	A0	A1	A2	A3	A4	A5	D	F(D)
1. Head Surface	0.000	0.710	-0.800	2.57	-175.98	4495.67	-8953.11	6029.59	0.000	0.71 0.75 0.80	358.00 3580.00 35800.00
2. Back of Shoulder	0.000	1.620	-1.70	0.01	- 26.59	380.91	- 678.22	456.53	0.000	1.62 1.65 1.70	48.30 483.00 4830.00
3. Chest	0.000	1.31	-1.40	0.55	5.46	73.49	- 15.01	0.00	0.000	1.31 1.35 1.40	158.60 1586.00 15860.00
4. Anterior Pelvis	0.000	2.02	-2.10	-0.14	1.58	24.39	- 29.33	13.76	0.000	2.02 2.05 2.10	89.70 897.00 8970.00
5. Posterior Pelvis	0.000	1.96	-2.10	-0.76	35.10	40.04	- 12.49	0.00	0.000	1.96 2.03 2.10	127.80 1278.00 12780.00
6. Upper Arm	0.000	0.89	-1.00	1.54	- 30.36	627.09	-1197.70	917.23	0.000	0.89 0.95 1.00	203.10 2031.00 20310.00
7. Forearm	0.000	1.31	-1.40	-2.40	107.37	-313.36	504.61	-196.37	0.000	1.31 1.35 1.40	156.20 1562.00 15620.00
8. Hand	0.000	0.38	-0.45	-0.04	- 31.04	2384.47	-10193.90	19172.50	0.000	0.38 0.41 0.45	139.40 1394.00 13940.00

TABLE 46 (continued)

FUNCTION	D0	D1	D2	FIRST PART OF FUNCTION 5th DEGREE POLYNOMIAL COEFFICIENTS						SECOND PART OF FUNCTION TABULAR POINTS	
				A0	A1	A2	A3	A4	A5	D	F(D)
9. Upper Leg	0.000	1.31	-1.40	-0.28	14.19	81.94	- 122.64	98.73	-23.09	1.31 1.35 1.40	61.60 616.00 6160.00
10. Knee	0.000	0.54	-0.58	-0.04	2.22	867.34	- 401.61	0.000	0.000	0.54 0.56 0.58	187.80 1878.00 18780.00
11. Front of Lower Leg	0.000	1.78	-1.9	-0.74	26.79	3.92	29.05	0.00	0.00	1.78 1.84 1.90	223.60 2236.00 22360.00
12. Back of Lower Leg	0.000	1.66	-1.75	-0.08	29.42	- 2.08	0.00	0.00	0.00	1.66 1.70 1.75	43.20 432.00 4320.00
13. Foot	0.000	0.83	-0.95	-0.68	82.75	-704.17	3367.10	-5570.69	3188.30	0.83 0.89 0.95	121.20 1212.00 12120.00

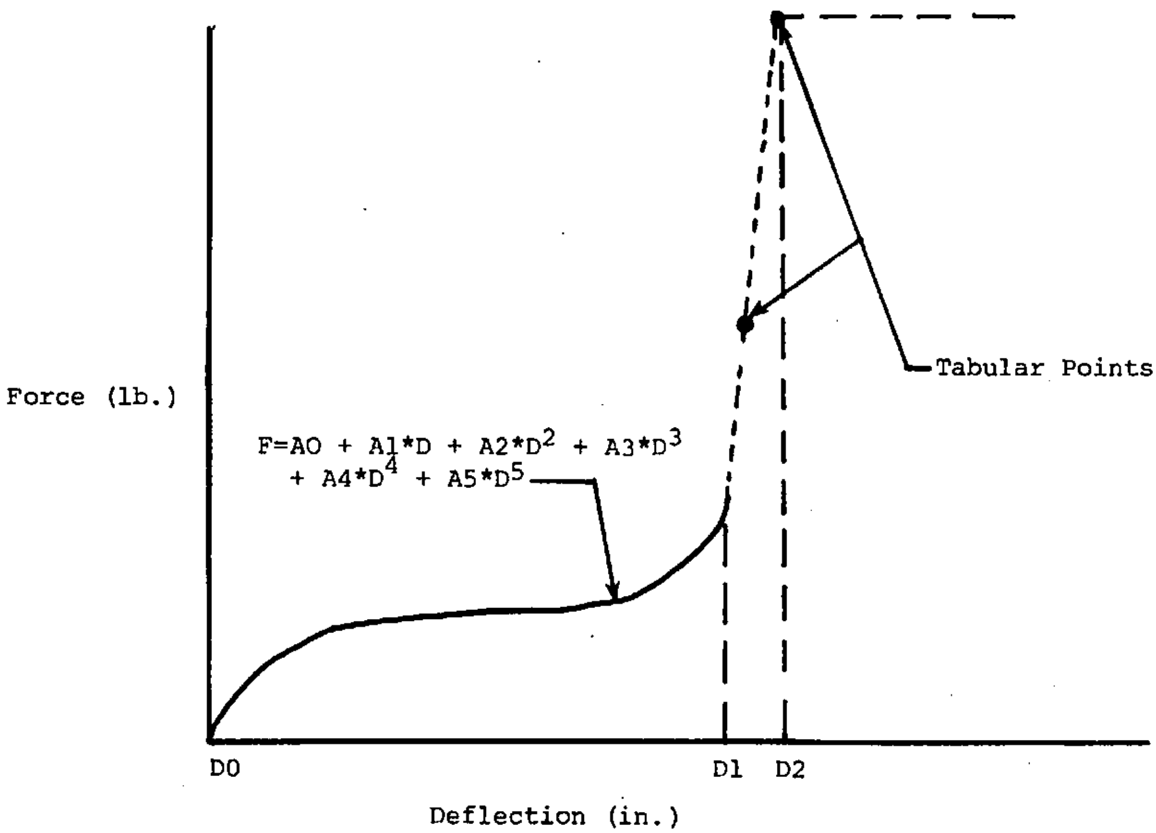

Figure 105. Example ATB Force-Deflection Curve

2.2.2 Demonstration Simulations

Demonstration simulations using the CVS/ATB model were performed to insure that the input data had been properly formatted, the model program would run with these data and the data resulted in physically realistic simulations. Such demonstrations would at least guarantee to subsequent users of the data base that the simulation should execute and that physically reasonable results should occur. These simulations were not made for the purposes of the Hybrid III data base validation.

A simulation was chosen that had previously been performed with the standard Part 572 data base. This simulation was based on a Celebrity frontal impact crash test in which a purely -x axis acceleration was applied with a 22G peak amplitude, 120 millisecond duration, and a pulse shape that resulted in a 31.3 mph velocity change. No harness restraint was applied to the body. The interactive surfaces used in the simulation were for the seat back, seat pan, floorboard, footboard, steering wheel, windshield, dash and roof.

Three simulations were performed using the Part 572, Hybrid III seated and Hybrid III standing data sets. The vehicle geometry and motion time history were identical for all three simulations. The initial positions for the Hybrid III data sets were adjusted to be as close as possible to the Part 572 position while maintaining initial body equilibrium with the external interactive forces.

Both time histories of the responses and graphical kinematics were obtained in the simulations and compared. From an examination of the time histories no numerical instabilities or calculation problems could be identified and all predicted response values were within physically reasonable ranges. A comparison with the Part 572 time histories showed that Hybrid III responses were in general quite similar with primary differences being phase shifts, slightly smoother response curves for the Hybrid III and also somewhat faster responses for the Hybrid III.

These effects were interpreted to be respectively due to slightly different initial positions, a numerically more stable data set for the Hybrid III and a generally stiffer structure for the Hybrid III.

Graphical comparisons of the three simulations are shown in Figures 106 through 108. A comparison of the Hybrid III seated dummy to the Part 572 dummy is shown in Figure 105. The responses through the first 90 milliseconds are very similar. A seemingly much softer extension neck response in the Part 572 appears at about 120 milliseconds when the head impacts the windshield. The Hybrid III neck does not undergo nearly as large a neck extension and rebounds from the steering wheel, windshield and dash impact much sooner than the Part 572.

The responses for the seated and standing Hybrid III are compared in Figure 107. There is very little difference in these two responses. The only readily observable difference is that the seated dummy penetrates deeper into the seat pan than the standing dummy and this penetration increases during the course of the simulation. A comparison of the Part 572 and Hybrid III standing dummy is shown in Figure 108. Since the standing and seated dummy responses were so similar, the comparison comments for the Part 572 and seated dummy apply here as well. The only difference is that the seat penetration for the Part 572 and standing dummy is about the same as opposed to the seated dummy which exhibited much greater penetration.

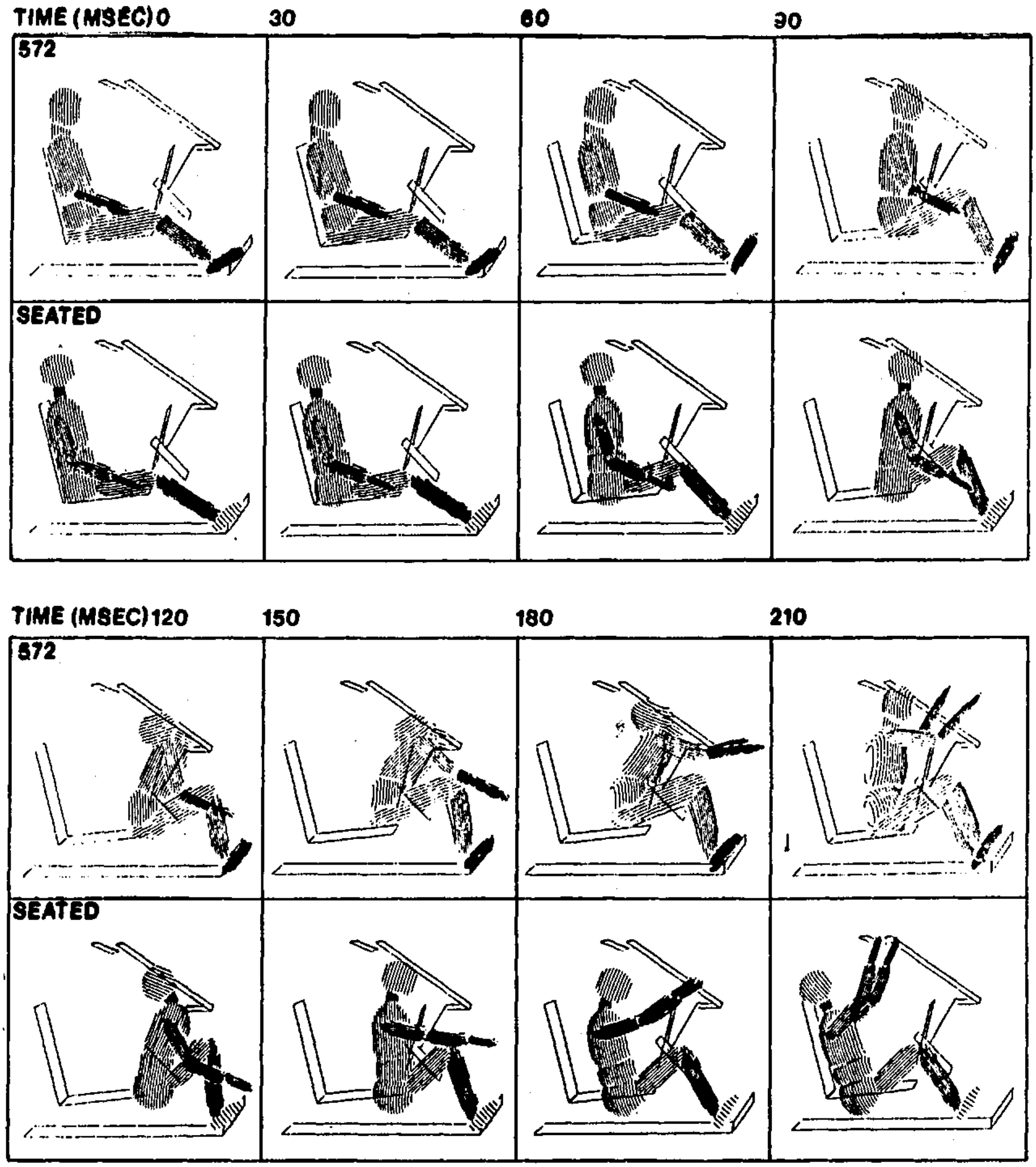

Figure 106. Comparison of Part 572 and Seated Hybrid III Simulations

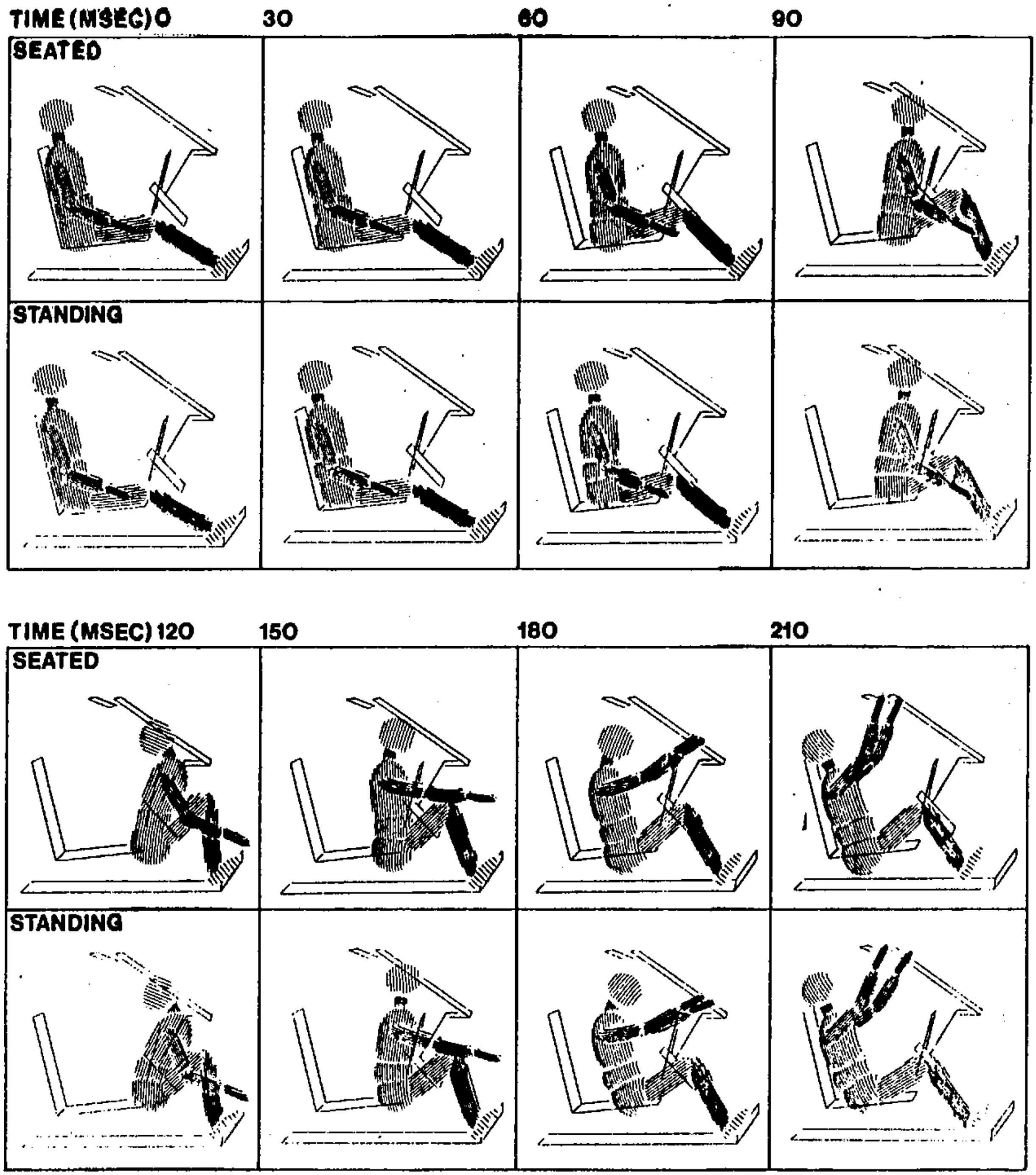

Figure 107. Comparison of Seated and Standing Hybrid III Simulations

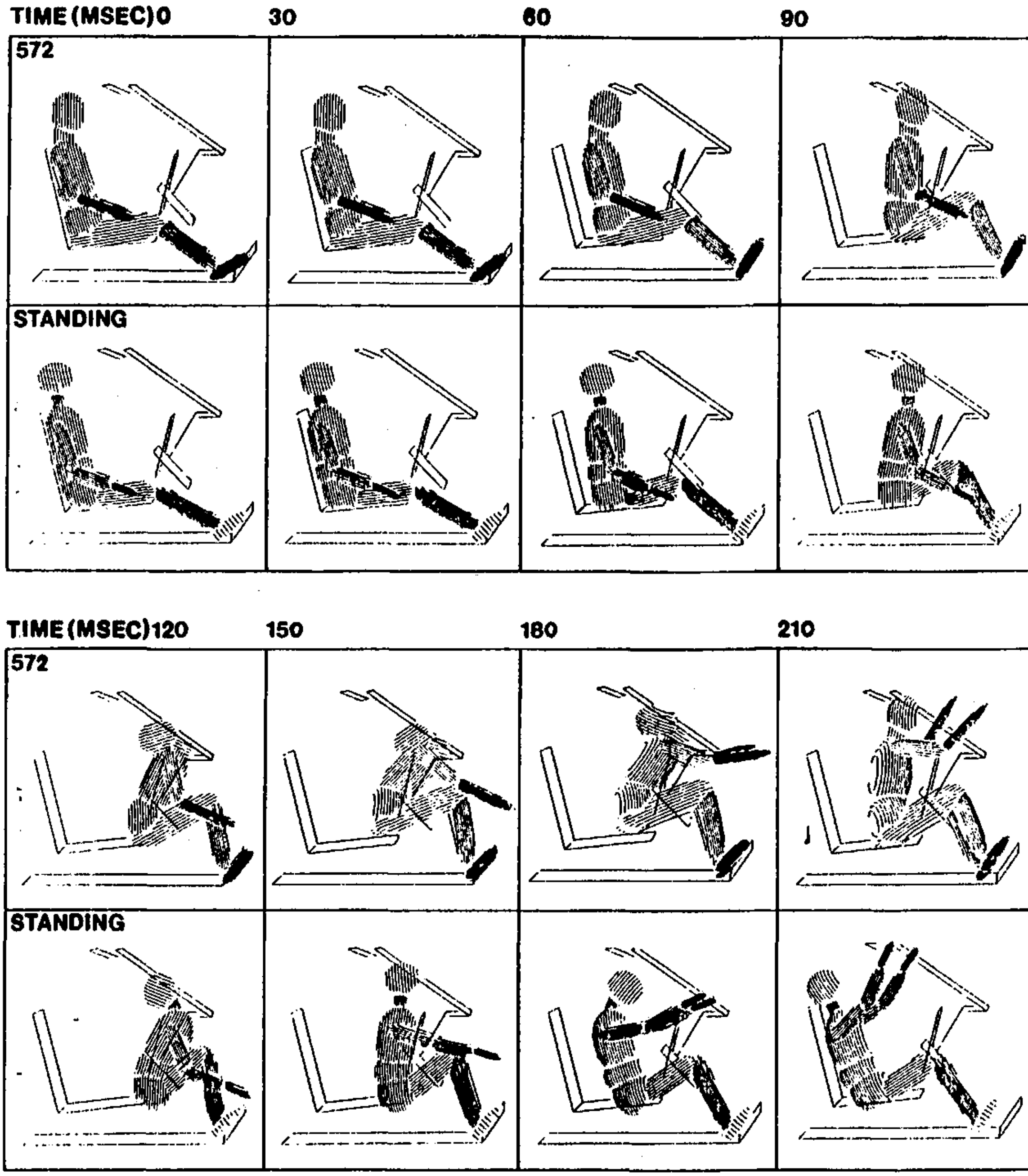

Figure 108. Comparison of Part 572 and Standing Hybrid III Simulations

2.2.3 Discussion of Results

The general objectives and approaches used to develop the Hybrid III data base in this program were similar to those in the Fleck, et al [1] study for the Part 572 simulation data base. One additional aspect that was addressed in this study, and which influenced the data measurement and model data base formatting methodology, was the development of transformations for relating the dummy data to human data. This was achieved by defining equivalent human anatomical landmarks on the Hybrid III dummy and deriving transformations between segment anatomical coordinate systems, defined by these landmarks, and the mechanical coordinate systems defined with respect to dummy structural features, e.g. joint centers, joint pin axes, etc. As dummies attain greater human-like fidelity, the comparison of human and dummy responses during dynamic force exposures becomes more meaningful and the availability of such transformations would make such comparisons possible.

The dummies for this study were selected to provide a data base for automotive and aerospace researchers. For this reason, one of the dummies was a standard seated dummy, with a pelvis molded in a seated position, designed for car crash testing, and the other was a pedestrian or standing dummy which is more appropriate for use in aerospace systems testing. Aside from the spine, pelvic section and upper legs, both dummies should have been identical. This was not found to be the case as was clearly evident from the measurements made on these dummies. While the final data for the parts that were identical were averaged for the two dummies and for left and right sides, the variability in these properties indicates that all Hybrid III dummies are not alike. It would be well if some future studies could be conducted to investigate this variability over a larger dummy population with different production dates and use frequencies.

The formatted simulation data was run on the CVS/ATB model and gave physically reasonable results. In a comparison to equivalent Part 572 responses under the same conditions, the Hybrid III simulation had slightly higher peak accelerations and quicker rebound, but smoother time histories. These characteristics seem to imply that the Hybrid III is overall slightly stiffer and that its data set leads to a more numerically stable solution.

While this is the first comprehensive simulation data set for the Hybrid III and should be quite useful for simulating Hybrid III impacts, several issues should be resolved before such a data base can be accepted as a standard. The first amoung these is whether the dummies tested were reasonably representative of the Hybrid IIIs in general use. The question of property variability, especially for joint ranges of motion and bending resistances of necks and spines, should be resolved. Also the current study almost total ignored, except for the neck and spine elements, rate dependent or damping effects. These obviously have some effect on manikin response, should be further explored and should be added to the Hybrid III data base.

Finally, the most important consideration in the Hybrid III data base acceptance is whether it represents the real world. To demonstrate that it does, carefully conducted validation simulations against well controlled experiments should be performed.

REFERENCES

1. Fleck, J.T., Butler, F.E., and DeLeys, N.J., "Validation of the Crash Victim Simulator," Report Nos DOT-HS-806-279 through 282, 1982, Vols 1-4 (NTIS No. PC E99, PB86-212420).

2. Personal Communications with Stanley Backaitis, National Highway Traffic Safety Administration.

3. General Motors Corporation, Hybrid III Quality and Performance Qualification Manual, Safety Research and Development Laboratory, General Motors Proving Ground, Milford, Michigan.

4. McConville, J., Churchill, T., Kaleps, I., Clauser, C., and Cazzi, J., "Anthropometric Relationships of Body and Body Segment Moments of Inertia," AFAMRL, Wright-Patterson AFB, Ohio, TR-80-119, 1980.

5. Young, J., Chandler, R., Snow, C., Robinette, K., Zehner, G., and Lotberg, M., "Anthropometric and Mass Distribution Characteristics of the Adult Female," FAA Civil Aeromedical Institute, Oklahoma City, Oklahoma, FAA-AM-83-16, 1983.

6. Lephart, S.A., "Measuring the Inertial Properties of Cadaver Segments," Technical note in Journal of Biomechanics, Vol 17, No 7, 1984.

7. Chandler, R.F., Clausen, C.E., McConville, J.T., Reynolds, H.M., and Young, J.W., "Investigation of Inertial Properties of Human Body Segments", DOT HS No-801-430, National Technical Information Service (USA), Springfield, Virginia, 1975.

8. Bartz, J.A. and Butler, F.E., "A Three-Dimensional Computer Simulation of a Motor Vehicle Crash Victim," Calspan Technical Report No. VH-2978-V-2, 1972.

```
FEB. 2. 1988   0   0     0.0                                                      CARD A1A
ATB SEATED - COMBINED DATA
GM HYBRID III 50TH PERCENTILE  #158
 IN. LB.SEC.                              386.088                                 CARD A3
   5   0   0.001   0.001   0.001 0.00025                                          CARD A4
0100010200 0 0 0 0 0 0 0 0 0 0 0 0 0 0 0 0 0 0 0 0 0 0 0 1                      1CARD A5
    17    16        SITTING HYBRID III                                             CARD B.
 LT  544.4602.11730.72801.4671 5.000 7.185 4.800 -1.00   0.00   0.00    1  CARD B.2
              0.00 35.00 180.0
 MT  4 4.8900.03890.03890.0194 4.775 6.500 4.000  1.00   0.00  -1.00    1  CARD B.2
              0.00  0.00 180.0
 UT  339.2162.62002.05201.7340 4.825 6.500 7.785  0.00   0.00   0.00    1  CARD B.2
              0.00  4.99 180.0
 N   2 2.6680.02540.02570.0084 1.675 1.675 3.000  0.00   0.00   0.00    1  CARD B.2
              0.00  0.00 180.0
 H   1 9.9210.14080.21280.1956 4.250 2.875 4.000  0.00   0.00   0.00    1  CARD B.2
              0.00-26.58 180.0
 RUL 613.7130.60860.59610.1068 2.950 3.050 7.285  0.00   0.00   0.00    1  CARD B.2
              0.00  4.13 180.0
 RLL 7 7.2370.67080.67450.0397 2.165 2.050 9.750  0.00   0.00   2.00    1  CARD B.2
              0.00 -1.90 180.0
 RF  8 2.7560.00670.05240.0491 4.900 1.675 1.675  0.00   0.00   0.00    1  CARD B.2
             -2.69 -9.23-158.0
 LUL 913.7130.60860.59610.1068 2.950 3.050 7.285  0.00   0.00   0.00    1  CARD B.2
              0.00  4.13 180.0
 LLL 0 7.2370.67080.67450.0397 2.165 2.050 9.750  0.00   0.00   2.00    1  CARD B.2
              0.0  -1.90 180.0
 LF  1 2.7560.00670.05240.0491 4.900 1.675 1.675  0.00   0.00   0.00    1  CARD B.2
              2.69 -9.23 158.0
 RUA 2 4.5970.10240.09970.0109 1.900 1.800 6.000  0.00   0.00  -1.00    1  CARD B.2
              0.00 -1.31 180.0
 RLA 3 3.8200.12000.12030.0071 1.775 1.775 5.800  0.00   0.00   0.00    1  CARD B.2
              0.0   1.31 180.0
 LUA 4 4.5970.10240.09970.0109 1.900 1.800 6.000  0.00   0.00  -1.00    1  CARD B.2
              0.00 -1.31 180.0
 LLA 5 3.8200.12000.12030.0071 1.775 1.775 5.800  0.00   0.00   0.00    1  CARD B.2
              0.0   1.31 180.0
RHD  6 1.2900.01140.00930.0036 1.000 1.870 3.650  0.00   0.00   0.00    1  CARD B.2
```

```
                  -2.35 31.09-175.6
LHD   7 1.2900.01140.00930.0036 1.000 1.870 3.650  0.00   0.00   0.00    1  CARD B.2
                   2.35 31.09 175.6
   P  M    1    0 -2.15   0.00 -1.66 -0.35  0.00  2.56                      CARD B.3
                   0.00   0.00  0.00  0.00  0.00  0.00
   W  N    2    0 -0.35   0.00 -2.56 -0.89  0.00  5.85                      CARD B.3
                   0.00   0.00  0.00  0.00  0.00  0.00
   NP O    3    0  0.00   0.00 -5.96  0.00  0.00  2.76                      CARD B.3
                   0.00   0.00  0.00  0.00  0.00  0.00
   HP P    4    0  0.00   0.00 -2.84 -0.55  0.00  2.00                      CARD B.3
                   0.00  00.00  0.00  0.00  0.00  0.00
   RH Q    1    0 -0.11   3.15  1.24  0.00  0.00 -9.96                      CARD B.3
                   0.00  90.00  0.00  0.00  0.00  0.00
   RK R    6    1  0.00   0.00  6.56 -0.20  0.00 -6.74                      CARD B.3
                   0.00   0.00  0.00  0.00 55.00  0.00
   RA S    7   -8 -0.20   0.00  9.65 -2.12  0.00 -1.54                      CARD B.3
                  90.00   0.00  0.00 90.00  0.00  0.00  0.00-10.00  0.00
   LH T    1    0 -0.11  -3.15  1.24  0.00  0.00 -9.96                      CARD B.3
                   0.00  90.00  0.00  0.00  0.00  0.00
   LK U    9    1  0.00   0.00  6.56 -0.20  0.00 -6.74                      CARD B.3
                   0.00   0.00  0.00  0.00 55.00  0.00
   LA V   10   -8 -0.20   0.00  9.65 -2.12  0.00 -1.54                      CARD B.3
                  90.00   0.00  0.00 90.00  0.00  0.00  0.00-10.00  0.00
   RS W    3    0 -0.88   7.38 -2.66  0.00  0.00 -5.43                      CARD B.3
                   0.00  90.00  0.00  0.00  0.00  0.00
   RE X   12   -8  0.00   0.00  4.94  0.00  0.00 -3.67                      CARD B.3
                  90.00   0.00  0.00 90.00  0.00  0.00  0.00 62.50  0.00
   LS Y    3    0 -0.88  -7.38 -2.66  0.00  0.00 -5.43                      CARD B.3
                   0.00  90.00  0.00  0.00  0.00  0.00
   LE Z   14   -8  0.00   0.00  4.94  0.00  0.00 -3.67                      CARD B.3
                  90.00   0.00  0.00 90.00  0.00  0.00  0.00 62.50  0.00
   RW     13   -8  0.00   0.00  6.07 -0.30  0.00 -2.13                      CARD B.3
                  90.00   0.00  0.00 90.00  0.00  0.00  0.00 15.00  0.00
   LW     15   -8  0.00   0.00  6.07 -0.30  0.00 -2.13                      CARD B.3
                  90.00   0.00  0.00 90.00  0.00  0.00  0.00 15.00  0.00
    0.0   0.0   0.0   1.0         0.0 34.38   0.0   0.0   1.0          0.0CARD B4A
    0.0   0.0   0.0   1.0         0.0 34.38   0.0   0.0   1.0          0.0CARD B4B
    0.0   0.0   0.0   1.0         0.0  15.0   0.0   0.0   1.0          0.0CARD B4C
```

0.0	0.0	0.0	1.0	0.0	15.0	0.0	0.0	1.0	0.0	CARD B4D
0.0	0.0	0.0	1.0	0.0	7.5	75.0	75.0	1.0	55.0	CARD B4E
0.0	2.32	0.0	1.0	48.9	0.0	0.0	0.0	1.0	0.0	CARD B4F
1.0	10.0	10.0	1.0	27.0	0.0	6.69	0.0	1.0	30.0	CARD B4G
0.0	0.0	0.0	1.0	0.0	0.0	0.0	0.0			
0.0	0.0	0.0	1.0	0.0	7.5	75.0	75.0	1.0	55.0	CARD B4H
0.0	2.32	0.0	1.0	48.9	0.0	0.0	0.0	1.0	0.0	CARD B4I
1.0	10.0	10.0	1.0	27.0	0.0	6.69	0.0	1.0	30.0	CARD B4J
0.0	0.0	0.0	1.0	0.0	0.0	0.0	0.0			
0.0	0.0	0.0	1.0	0.0	0.0	100.0	100.0	1.0	125.0	CARD B4K
0.0	20.0	20.0	1.0	52.0	0.0	4.65	0.0	1.0	65.30	CARD B4L
0.0	0.0	0.0	1.0	0.0	0.0	90.0	0.0			
0.0	0.0	0.0	1.0	0.0	0.0	100.0	100.0	1.0	125.0	CARD B4M
0.0	20.0	20.0	1.0	52.0	0.0	4.65	0.0	1.0	65.30	CARD B4N
0.0	0.0	0.0	1.0	0.0	0.0	90.0	0.0			
0.0	0.0	0.0	1.0	0.0	0.0	4.32	0.143	1.0	55.5	CARD B4O
0.0	0.0	0.0	1.0	0.0	0.0	0.0	0.0			
0.0	0.0	0.0	1.0	0.0	0.0	4.32	0.143	1.0	55.5	CARD B4P
0.0	0.0	0.0	1.0	0.0	0.0	0.0	0.0			
1.200		30.								CARD B5A
1.200		30.								CARD B5B
0.350		30.								CARD B5C
0.192		30.								CARD B5D
1.000		30.								CARD B5E
1.000		30.								CARD B5F
0.500		30.								CARD B5G
0.500		30.								CARD B5G
0.000		30.								CARD B5G
1.000		30.								CARD B5H
1.500		30.								CARD B5I
0.500		30.								CARD B5J
0.500		30.								CARD B5J
0.000		30.								CARD B5J
0.100		30.								CARD B5K
0.100		30.								CARD B5L
0.100		30.								CARD B5L
0.000		30.								CARD B5L
0.100		30.								CARD B5M

```
 0.100          30.                                                                              CARD B5N
 0.100          30.                                                                              CARD B5N
 0.000          30.                                                                              CARD B5N
 0.500          30.                                                                              CARD B5O
 0.500          30.                                                                              CARD B5O
 0.000          30.                                                                              CARD B5O
 0.500          30.                                                                              CARD B5P
 0.500          30.                                                                              CARD B5P
 0.000          30.                                                                              CARD B5P
   .00    .00    .00    .00    .00    .00    0.5    0.5    0.5    .10    .10                 .01CARD B6A
   .00    .00    .00    .00    .00    .00    0.5    0.5    0.5    .00    .00                 .00CARD B6B
   .00    .00    .00    .00    .00    .00    0.5    0.5    0.5    .00    .00                 .00CARD B6C
   .00    .00    .00    .00    .00    .00    0.5    0.5    0.5    .00    .00                 .00CARD B6D
   .00    .00    .00    .00    .00    .00    0.5    0.5    0.5    .00    .00                 .00CARD B6E
   .00    .00    .00    .00    .00    .00    0.5    0.5    0.5    .00    .00                 .00CARD B6F
   .00    .00    .00    .00    .00    .00    0.5    0.5    0.5    .00    .00                 .00CARD B6G
   .00    .00    .00    .00    .00    .00    0.5    0.5    0.5    .00    .00                 .00CARD B6H
   .00    .00    .00    .00    .00    .00    0.5    0.5    0.5    .00    .00                 .00CARD B6I
   .00    .00    .00    .00    .00    .00    0.5    0.5    0.5    .00    .00                 .00CARD B6J
   .00    .00    .00    .00    .00    .00    0.5    0.5    0.5    .00    .00                 .00CARD B6K
   .00    .00    .00    .00    .00    .00    0.5    0.5    0.5    .00    .00                 .00CARD B6L
   .00    .00    .00    .00    .00    .00    0.5    0.5    0.5    .00    .00                 .00CARD B6M
   .00    .00    .00    .00    .00    .00    0.5    0.5    0.5    .00    .00                 .00CARD B6N
   .00    .00    .00    .00    .00    .00    0.5    0.5    0.5    .00    .00                 .00CARD B6O
   .00    .00    .00    .00    .00    .00    0.5    0.5    0.5    .00    .00                 .00CARD B6P
   .00    .00    .00    .00    .00    .00    0.5    0.5    0.5    .00    .00                 .00CARD B6Q
NO ACCELERATION
  00.0    0.0    0.0    0.0    0.0    0.0   0.0     0.0      1   0.00   0.01                   CARD C2A
 0.0  0.0                                                                                       CARD C3A
     1      0      0      0      0      0      0      0      7                                  CARD D1
   1  GROUND                                                                                    CARD D2A
     30.0       30.0      30.0                                                                  CARD D2B
     30.0      -30.0      30.0                                                                  CARD D2C
    -30.0       30.0      30.0                                                                  CARD D2D
                                                                                                CARD D7A
   1   HEAD SURFACE                                                                             CARD E1
        0.          0.71        -0.80           0.             0.                               CARD E2
       2.57      -175.98       4495.67     -8953.11      6029.59                                CARD E3
```

3							CARD E4A
	0.71	358.	0.75	3580.	0.80	35800.	CARD E4B
2	BACK OF SHOULDER						CARD E1
	0.	1.62	-1.70	0.	0.		CARD E2
	0.01	-26.59	380.91	-678.22	456.53		CARD E3
3							CARD E4A
	1.62	48.3	1.65	483.	1.70	4830.	CARD E4B
3	CHEST						CARD E1
	0.	1.31	-1.40	0.	0.		CARD E2
	0.55	5.46	73.49	-15.01			CARD E3
3							CARD E4A
	1.31	158.6	1.35	1586.	1.40	15860.	CARD E4B
4	ANTERIOR PELVIS						CARD E1
	0.	2.02	-2.10	0.	0.		CARD E2
	-0.14	1.58	24.39	-29.33	13.76		CARD E3
3							CARD E4A
	2.02	89.7	2.05	897.	2.10	8970.	CARD E4B
5	POSTERIOR PELVIS						CARD E1
	0.	1.96	-2.10	0.	0.		CARD E2
	-0.76	35.10	40.04	-12.49			CARD E3
3							CARD E4A
	1.96	127.8	2.03	1278.	2.10	12780.	CARD E4B
6	UPPER ARM						CARD E1
	0.	0.89	-1.00	0.	0.		CARD E2
	1.54	-30.63	627.09	-1197.70	917.23		CARD E3
3							CARD E4A
	0.89	203.1	0.95	2031.	1.00	20310.	CARD E4B
7	FOREARM						CARD E1
	0.	1.31	-1.40	0.	0.		CARD E2
	-2.40	107.37	-313.36	504.61	-196.37		CARD E3
3							CARD E4A
	1.31	156.2	1.35	1562.	1.40	15620.	CARD E4B
8	HAND						CARD E1
	0.	0.38	-0.45	0.	0.		CARD E2
	-0.04	-31.04	2384.47	-10193.90	19172.50		CARD E3
3							CARD E4A
	0.38	139.4	0.41	1394.	0.45	13940.	CARD E4B
9	UPPER LEG						CARD E1

```
         0.          1.31       -1.40          0.          0.            CARD E2
      -0.28         14.19       81.94     -122.62       98.73      -29.09CARD E3
    3                                                                    CARD E4A
       1.31          61.6        1.35        616.        1.40       6160.CARD E4B
   10  KNEE                                                              CARD E1
         0.          0.54       -0.58          0.          0.            CARD E2
      -0.04          2.22      867.34     -401.61                        CARD E3
    3                                                                    CARD E4A
       0.54         187.8        0.56       1878.        0.58      18780.CARD E4B
   11  FRONT OF LOWER LEG                                                CARD E1
         0.          1.78       -1.90          0.          0.            CARD E2
      -0.74         26.79        3.92       29.05                        CARD E3
    3                                                                    CARD E4A
       1.78         223.6        1.84       2236.        1.90      22360.CARD E4B
   12  BACK OF LOWER LEG                                                 CARD E1
         0.          1.66       -1.75          0.          0.            CARD E2
      -0.08         29.42       -2.08                                    CARD E3
    3                                                                    CARD E4A
       1.66          43.2        1.70        432.        1.75       4320.CARD E4B
   13  FOOT                                                              CARD E1
         0.          0.83       -0.95          0.          0.            CARD E2
      -0.68         82.75     -704.17     3367.10    -5570.69     3188.30CARD E3
    3                                                                    CARD E4A
       0.83         121.2        0.89       1212.        0.95      12120.CARD E4B
 9999                                                                    CARD E1
   41  RIGHT SHOULDER JOINT                                              CARD E7A
                                                                         CARD E7B
     -4    8                                                             CARD E7C
      151.0           0.0     87900.0         0.0                        CARD E7D
       75.0           0.0     13700.0         0.0                        CARD E7E
        0.0           0.0      -312.0     11800.0                        CARD E7F
       66.0           0.0      7780.0   3010000.0                        CARD E7G
       68.0           0.0     22200.0    376000.0                        CARD E7H
       89.0           0.0     22000.0         0.0                        CARD E7I
      111.0           0.0      2470.0     17600.0                        CARD E7J
      153.0           0.0     13000.0         0.0                        CARD E7K
   42  LEFT SHOULDER JOINT                                               CARD E7A
                                                                         CARD E7B
```

```
  -4     8                                                                   CARD E7C
      151.0         0.0     87900.0         0.0                              CARD E7D
      153.0         0.0     13000.0         0.0                              CARD E7E
      111.0         0.0      2470.0     17600.0                              CARD E7F
       89.0         0.0     22000.0         0.0                              CARD E7G
       68.0         0.0     22200.0    376000.0                              CARD E7H
       66.0         0.0      7780.0   3010000.0                              CARD E7I
        0.0         0.0      -312.0     11800.0                              CARD E7J
       75.0         0.0     13700.0         0.0                              CARD E7K
43     SEATED RIGHT HIP                                                      CARD E7A
                                                                             CARD E7B
  19     4                                                                   CARD E7C
        0.0         7.0        22.0        52.0       112.0        232.0CARD E7D
      472.0       952.0      1910.0      3830.0      7670.0      15400.0CARD E7E
    30700.0     61400.0    123000.0    246000.0    492000.0     983000.0CARD E7F
  1970000.0                                                              CARD E7G
        0.0        17.0        51.0       119.0       255.0        527.0CARD E7H
     1070.0      2160.0      4340.0      8690.0     17400.0      34900.0CARD E7I
    69700.0    139000.0    279000.0    557000.0   1110000.0    2230000.0CARD E7J
  4460000.0                                                              CARD E7K
        0.0         8.0        17.0        28.0        50.0         94.0CARD E7L
      182.0       358.0       710.0      1410.0      2820.0       5640.0CARD E7M
    11300.0     22500.0     45100.0     90100.0    180000.0     360000.0CARD E7N
   721000.0                                                              CARD E7O
        0.0         7.0        13.0        18.0        23.0         33.0CARD E7P
       53.0        93.0       173.0       333.0       653.0       1290.0CARD E7Q
     2570.0      5130.0     10300.0     20500.0     41000.0      81900.0CARD E7R
   164000.0                                                              CARD E7S
44     SEATED LEFT HIP                                                       CARD E7A
                                                                             CARD E7B
  19     4                                                                   CARD E7C
        0.0         7.0        22.0        52.0       112.0        232.0CARD E7D
      472.0       952.0      1910.0      3830.0      7670.0      15400.0CARD E7E
    30700.0     61400.0    123000.0    246000.0    492000.0     983000.0CARD E7F
  1970000.0                                                              CARD E7G
        0.0         7.0        13.0        18.0        23.0         33.0CARD E7H
       53.0        93.0       173.0       333.0       653.0       1290.0CARD E7I
     2570.0      5130.0     10300.0     20500.0     41000.0      81900.0CARD E7J
```

```
 164000.0                                                                       CARD E7K
      0.0         8.0        17.0        28.0        50.0        94.0CARD E7L
    182.0       358.0       710.0      1410.0      2820.0      5640.0CARD E7M
  11300.0     22500.0     45100.0     90100.0    180000.0    360000.0CARD E7N
 721000.0                                                                       CARD E7O
      0.0        17.0        51.0       119.0       255.0       527.0CARD E7P
   1070.0      2160.0      4340.0      8690.0     17400.0     34900.0CARD E7Q
  69700.0    139000.0    279000.0    557000.0   1110000.0   2230000.0CARD E7R
4460000.0                                                                       CARD E7S
45    SEATED LUMBAR SPINE                                                       CARD E7A
                                                                                CARD E7B
 19     4                                                                       CARD E7C
      0.0      4600.0      9200.0     13800.0     18400.0     23000.0CARD E7D
  27600.0     32200.0     36800.0     41400.0     50600.0     69000.0CARD E7E
 105800.0    179400.0    326600.0    621000.0   1209800.0   2387400.0CARD E7F
4742600.0                                                                       CARD E7G
      0.0      6800.0     13600.0     20400.0     27200.0     34000.0CARD E7H
  40800.0     47600.0     54400.0     61200.0     74800.0    102000.0CARD E7I
 156400.0    265200.0    482800.0    918000.0   1788400.0   3529200.0CARD E7J
7010800.0                                                                       CARD E7K
      0.0      3000.0      6000.0      9000.0     12000.0     15000.0CARD E7L
  18000.0     21000.0     24000.0     27000.0     33000.0     45000.0CARD E7M
  69000.0    117000.0    213000.0    405000.0    789000.0   1557000.0CARD E7N
3093000.0                                                                       CARD E7O
      0.0      6800.0     13600.0     20400.0     27200.0     34000.0CARD E7P
  40800.0     47600.0     54400.0     61200.0     74800.0    102000.0CARD E7Q
 156400.0    265200.0    482800.0    918000.0   1788400.0   3529200.0CARD E7R
7010800.0                                                                       CARD E7S
46    NECK PIVOT                                                                CARD E7A
                                                                                CARD E7B
 19     4                                                                       CARD E7C
      0.0       700.0      1400.0      2100.0      2800.0      3500.0CARD E7D
   4200.0      4900.0      5600.0      6300.0      7000.0      7700.0CARD E7E
   8400.0      9800.0     12600.0     18200.0     29400.0     51800.0CARD E7F
  96600.0                                                                       CARD E7G
      0.0       600.0      1200.0      1800.0      2400.0      3000.0CARD E7H
   3600.0      4200.0      4800.0      5400.0      6000.0      6600.0CARD E7I
   7200.0      8400.0     10800.0     15600.0     25200.0     44400.0CARD E7J
```

```
   82800.0                                                                   CARD E7K
       0.0       300.0       600.0       900.0      1200.0      1500.0CARD E7L
    1800.0      2100.0      2400.0      2700.0      3000.0      3300.0CARD E7M
    3600.0      4200.0      5400.0      7800.0     12600.0     22200.0CARD E7N
   41400.0                                                                   CARD E7O
       0.0       600.0      1200.0      1800.0      2400.0      3000.0CARD E7P
    3600.0      4200.0      4800.0      5400.0      6000.0      6600.0CARD E7Q
    7200.0      8400.0     10800.0     15600.0     25200.0     44400.0CARD E7R
   82800.0                                                                   CARD E7S
47    HEAD PIVOT                                                             CARD E7A
                                                                             CARD E7B
  19    4                                                                    CARD E7C
       0.0       490.0       980.0      1680.0      2380.0      3080.0CARD E7D
    3780.0      4480.0      5180.0      5880.0      6580.0      7280.0CARD E7E
    7980.0      9380.0     12180.0     17780.0     28980.0     51380.0CARD E7F
   96180.0                                                                   CARD E7G
       0.0       600.0      1200.0      1800.0      2400.0      3000.0CARD E7H
    3600.0      4200.0      4800.0      5400.0      6000.0      6600.0CARD E7I
    7200.0      8400.0     10800.0     15600.0     25200.0     44400.0CARD E7J
   82800.0                                                                   CARD E7K
       0.0       250.0       500.0       800.0      1100.0      1400.0CARD E7L
    1700.0      2000.0      2300.0      2600.0      2900.0      3200.0CARD E7M
    3500.0      4100.0      5300.0      7700.0     12500.0     22100.0CARD E7N
   41300.0                                                                   CARD E7O
       0.0       600.0      1200.0      1800.0      2400.0      3000.0CARD E7P
    3600.0      4200.0      4800.0      5400.0      6000.0      6600.0CARD E7Q
    7200.0      8400.0     10800.0     15600.0     25200.0     44400.0CARD E7R
   82800.0                                                                   CARD E7S
                                                                             CARD F1
 0   0   0   0   0   0   0   0   0   0   0   0   0   0   0   0   0           CARD F3A
                                                                             CARD F4A
45  45  46  47  43   0   0  44   0   0  41   0  42   0   0   0               CARD F5A
                                          0   0   0   0   0                  CARD G1
      0.0       0.0       0.0                                                CARD G2A
      0.0       0.0       0.0                                         3  2  1  0CARDG3 1
      0.0       0.0       0.0                                         3  2  1  0CARDG3 2
      0.0       0.0       0.0                                         3  2  1  0CARDG3 2
      0.0       0.0       0.0                                         3  2  1  0CARDG3 3
```

0.0	0.0	0.0	3	2	1	0CARDG3 4
0.0	90.0	0.0	3	2	1	0CARDG3 5
0.0	0.0	0.0	3	2	1	0CARDG3 6
0.0	0.0	0.0	3	2	1	0CARDG3 7
0.0	90.0	0.0	3	2	1	0CARDG3 8
0.0	0.0	0.0	3	2	1	0CARDG3 9
0.0	0.0	0.0	3	2	1	0CARDG310
0.0	0.0	0.0	3	2	1	0CARDG311
0.0	90.0	0.0	3	2	1	0CARDG312
0.0	0.0	0.0	3	2	1	0CARDG313
0.0	90.0	0.0	3	2	1	0CARDG314
0.0	90.0	0.0	3	2	1	0CARDG315
0.0	90.0	0.0	3	2	1	0CARDG315
						CARD H1A
						CARD H1B
						CARD H2A
						CARD H2B
						CARD H3A
						CARD H3B
						CARD H4
						CARD H5
						CARD H6
						CARD H7A
						CARD H8
						CARD H9
						CARD H10

```
FEB. 2, 1988   0    0      0.0                                                                  CARD A1A
PEDESTRIAN HYBRID III - COMBINED DATA
STANDING HYBRID III 50TH PERCENTILE   #061
 IN. LB.SEC.                          386.088                                                   CARD A3
  6   0   0.001    0.001    0.001 0.00025                                                       CARD A4
0100010200 0 0 0 0 0 0 0 0 0 0 0 0 0 0 0 0 0 0 0 0 0 0 0 0 1                                  1CARD A5
    17    16        STANDING HYBRID III                                                         CARD B.1
 LT  521.9120.80190.68120.4678 4.725 7.185 4.800  0.00   0.00   0.00    1  CARD B.2A
              0.00-43.00 180.0
 MT  4 2.6610.01960.01960.0083 4.775 6.500 4.000  1.00   0.00  -1.00    1  CARD B.2B
              0.00   0.00 180.0
 UT  339.2162.62002.05201.7340 4.825 6.500 7.785  0.00   0.00   0.00    1  CARD B.2C
              0.00   4.99 180.0
 N   2 2.6680.02540.02570.0084 1.675 1.675 3.000  0.00   0.00   0.00    1  CARD B.2D
              0.00   0.00 180.0
 H   1 9.9210.14080.21280.1956 4.250 2.875 4.000  0.00   0.00   0.00    1  CARD B.2E
              0.00-26.58 180.0
 RUL 619.9841.44941.49680.1989 2.950 3.050 7.285  0.00   0.00   2.30    1  CARD B.2F
             11.08   7.03 173.9
 RLL 7 7.2370.67080.67450.0397 2.165 2.050 9.750  0.00   0.00   2.00    1  CARD B.2G
              0.00 -1.90 180.0
 RF  8 2.7560.00670.05240.0491 4.900 1.675 1.675  0.00   0.00   0.00    1  CARD B.2H
             -2.69 -9.23-158.0
 LUL 919.9841.44941.49680.1989 2.950 3.050 7.285  0.00   0.00   2.30    1  CARD B.2I
            -11.08   7.03-173.9
 LLL 0 7.2370.67080.67450.0397 2.165 2.050 9.750  0.00   0.00   2.00    1  CARD B.2J
              0.0   -1.90 180.0
 LF  1 2.7560.00670.05240.0491 4.900 1.675 1.675  0.00   0.00   0.00    1  CARD B.2K
              2.69 -9.23 158.0
 RUA 2 4.5970.10240.09970.0109 1.900 1.800 6.000  0.00   0.00  -1.00    1  CARD B.2L
              0.00 -1.31 180.0
 RLA 3 3.8200.12000.12030.0071 1.775 1.775 5.800  0.00   0.00   0.00    1  CARD B.2M
              0.0    1.31 180.0
 LUA 4 4.5970.10240.09970.0109 1.900 1.800 6.000  0.00   0.00  -1.00    1  CARD B.2N
              0.00 -1.31 180.0
 LLA 5 3.8200.12000.12030.0071 1.775 1.775 5.800  0.00   0.00   0.00    1  CARD B.2O
              0.0    1.31 180.0
RHD  6 1.2900.01140.00930.0036 1.000 1.870 3.650  0.00   0.00   0.00    1  CARD B.2P
```

```
                 -2.35 31.09-175.6
LHD   7 1.2900.01140.00930.0036 1.000 1.870 3.650  0.00  0.00  0.00   1  CARD B.2Q
                  2.35 31.09 175.6
   P  M    1    0 -2.50  0.00 -1.08 -0.89  0.00  2.56                  CARD B.3
                    0:00  0.00  0.00  0.00  0.00  0.00
   W  N    2    0  0.00  0.00 -2.56 -0.89  0.00  5.85                  CARD B.3
                   0.00  0.00  0.00  0.00  0.00  0.00
   NP O    3    0  0.00  0.00 -5.96  0.00  0.00  2.76                  CARD B.3
                   0.00  0.00  0.00  0.00  0.00  0.00
   HP P    4    0  0.00  0.00 -2.84 -0.55  0.00  2.00                  CARD B.3
                   0.00 00.00  0.00  0.00  0.00  0.00
   RH Q    1    0  0.00  3.28  2.04 -0.24  0.00 -7.23                  CARD B.3
                   0.00  0.00  0.00  0.00  0.00  0.00
   RK R    6    1 -0.24  0.00  8.90 -0.20  0.00 -6.74                  CARD B.3
                   0.00  0.00  0.00  0.00 55.00  0.00
   RA S    7   -8 -0.20  0.00  9.65 -2.12  0.00 -1.54                  CARD B.3
                  90.00  0.00  0.00 90.00  0.00  0.00  0.00-10.00  0.00
   LH T    1    0  0.00 -3.28  2.04 -0.24  0.00 -7.23                  CARD B.3
                   0.00  0.00  0.00  0.00  0.00  0.00
   LK U    9    1 -0.24  0.00  8.90 -0.20  0.00 -6.74                  CARD B.3
                   0.00  0.00  0.00  0.00 55.00  0.00
   LA V   10   -8 -0.20  0.00  9.65 -2.12  0.00 -1.54                  CARD B.3
                  90.00  0.00  0.00 90.00  0.00  0.00  0.00-10.00  0.00
   RS W    3    0 -0.88  7.38 -2.66  0.00  0.00 -5.43                  CARD B.3
                   0.00 90.00  0.00  0.00  0.00  0.00
   RE X   12   -8  0.00  0.00  4.94  0.00  0.00 -3.67                  CARD B.3
                  90.00  0.00  0.00 90.00  0.00  0.00  0.00 62.50  0.00
   LS Y    3    0 -0.88 -7.38 -2.66  0.00  0.00 -5.43                  CARD B.3
                   0.00 90.00  0.00  0.00  0.00  0.00
   LE Z   14   -8  0.00  0.00  4.94  0.00  0.00 -3.67                  CARD B.3
                  90.00  0.00  0.00 90.00  0.00  0.00  0.00 62.50  0.00
   RW     13   -8  0.00  0.00  6.07 -0.30  0.00 -2.13                  CARD B.3
                  90.00  0.00  0.00 90.00  0.00  0.00  0.00 15.00  0.00
   LW     15   -8  0.00  0.00  6.07 -0.30  0.00 -2.13                  CARD B.3
                  90.00  0.00  0.00 90.00  0.00  0.00  0.00 15.00  0.00
    0.0    0.0    0.0    1.0          0.0 34.38   0.0   0.0   1.0       0.0CARD B4A
    0.0    0.0    0.0    1.0          0.0 34.38   0.0   0.0   1.0       0.0CARD B4B
    0.0    0.0    0.0    1.0          0.0  15.0   0.0   0.0   1.0       0.0CARD B4C
```

```
   0.0   0.0   0.0   1.0         0.0  15.0   0.0   0.0   1.0           0.0CARD B4D
   0.0   0.0   0.0   1.0         0.0   7.5  75.0  75.0   1.0          55.0CARD B4E
   0.0  2.32   0.0   1.0        48.9   0.0   0.0   0.0   1.0           0.0CARD B4F
   1.0  10.0  10.0   1.0        27.0   0.0  6.69   0.0   1.0          30.0CARD B4G
   0.0   0.0   0.0   1.0         0.0   0.0   0.0   0.0
   0.0   0.0   0.0   1.0         0.0   7.5  75.0  75.0   1.0          55.0CARD B4H
   0.0  2.32   0.0   1.0        48.9   0.0   0.0   0.0   1.0           0.0CARD B4I
   1.0  10.0  10.0   1.0        27.0   0.0  6.69   0.0   1.0          30.0CARD B4J
   0.0   0.0   0.0   1.0         0.0   0.0   0.0   0.0
   0.0   0.0   0.0   1.0         0.0   0.0 100.0 100.0   1.0         125.0CARD B4K
   0.0  20.0  20.0   1.0        52.0   0.0  4.65   0.0   1.0         65.30CARD B4L
   0.0   0.0   0.0   1.0         0.0   0.0  90.0   0.0
   0.0   0.0   0.0   1.0         0.0   0.0 100.0 100.0   1.0         125.0CARD B4M
   0.0  20.0  20.0   1.0        52.0   0.0  4.65   0.0   1.0         65.30CARD B4N
   0.0   0.0   0.0   1.0         0.0   0.0  90.0   0.0
   0.0   0.0   0.0   1.0         0.0   0.0  4.32 0.143   1.0          55.5CARD B4O
   0.0   0.0   0.0   1.0         0.0   0.0   0.0   0.0
   0.0   0.0   0.0   1.0         0.0   0.0  4.32 0.143   1.0          55.5CARD B4P
   0.0   0.0   0.0   1.0         0.0   0.0   0.0   0.0
 1.200         30.                                                      CARD B5A
 1.200         30.                                                      CARD B5B
 0.350         30.                                                      CARD B5C
 0.192         30.                                                      CARD B5D
 1.000         30.                                                      CARD B5E
 1.000         30.                                                      CARD B5F
 0.500         30.                                                      CARD B5G
 0.500         30.                                                      CARD B5G
 0.000         30.                                                      CARD B5G
 1.000         30.                                                      CARD B5H
 1.500         30.                                                      CARD B5I
 0.500         30.                                                      CARD B5J
 0.500         30.                                                      CARD B5J
 0.000         30.                                                      CARD B5J
 0.100         30.                                                      CARD B5K
 0.100         30.                                                      CARD B5L
 0.100         30.                                                      CARD B5L
 0.000         30.                                                      CARD B5L
 0.100         30.                                                      CARD B5M
```

```
0.100         30.                                                                             CARD B5N
0.100         30.                                                                             CARD B5N
0.000         30.                                                                             CARD B5N
0.500         30.                                                                             CARD B5O
0.500         30.                                                                             CARD B5O
0.000         30.                                                                             CARD B5O
0.500         30.                                                                             CARD B5P
0.500         30.                                                                             CARD B5P
0.000         30.                                                                             CARD B5P
  .00   .00   .00   .00   .00   .00   0.5   0.5   0.5   .10   .10   .01CARD B6A
  .00   .00   .00   .00   .00   .00   0.5   0.5   0.5   .00   .00   .00CARD B6B
  .00   .00   .00   .00   .00   .00   0.5   0.5   0.5   .00   .00   .00CARD B6C
  .00   .00   .00   .00   .00   .00   0.5   0.5   0.5   .00   .00   .00CARD B6D
  .00   .00   .00   .00   .00   .00   0.5   0.5   0.5   .00   .00   .00CARD B6E
  .00   .00   .00   .00   .00   .00   0.5   0.5   0.5   .00   .00   .00CARD B6F
  .00   .00   .00   .00   .00   .00   0.5   0.5   0.5   .00   .00   .00CARD B6G
  .00   .00   .00   .00   .00   .00   0.5   0.5   0.5   .00   .00   .00CARD B6H
  .00   .00   .00   .00   .00   .00   0.5   0.5   0.5   .00   .00   .00CARD B6I
  .00   .00   .00   .00   .00   .00   0.5   0.5   0.5   .00   .00   .00CARD B6J
  .00   .00   .00   .00   .00   .00   0.5   0.5   0.5   .00   .00   .00CARD B6K
  .00   .00   .00   .00   .00   .00   0.5   0.5   0.5   .00   .00   .00CARD B6L
  .00   .00   .00   .00   .00   .00   0.5   0.5   0.5   .00   .00   .00CARD B6M
  .00   .00   .00   .00   .00   .00   0.5   0.5   0.5   .00   .00   .00CARD B6N
  .00   .00   .00   .00   .00   .00   0.5   0.5   0.5   .00   .00   .00CARD B6O
  .00   .00   .00   .00   .00   .00   0.5   0.5   0.5   .00   .00   .00CARD B6P
  .00   .00   .00   .00   .00   .00   0.5   0.5   0.5   .00   .00   .00CARD B6Q
NO ACCELERATION
 00.0   0.0   0.0   0.0   0.0   0.0  0.0    0.0      1  0.00  0.01      CARD C2A
0.0  0.0                                                                CARD C3A
    1     0     0     0     0     0     0     0     7                   CARD D1
  1   GROUND                                                            CARD D2A
    30.0     30.0     30.0                                              CARD D2B
    30.0    -30.0     30.0                                              CARD D2C
   -30.0     30.0     30.0                                              CARD D2D
                                                                        CARD D7A
  1    HEAD SURFACE                                                     CARD E1
       0.        0.71        -0.80          0.           0.             CARD E2
       2.57   -175.98      4495.67     -8953.11      6029.59            CARD E3
```

```
   3                                                                  CARD E4A
    0.71        358.          0.75        3580.         0.80    35800.CARD E4B
2   BACK OF SHOULDER                                                  CARD E1
     0.         1.62         -1.70          0.            0.          CARD E2
    0.01      -26.59        380.91      -678.22       456.53          CARD E3
   3                                                                  CARD E4A
    1.62        48.3          1.65         483.         1.70     4830.CARD E4B
3   CHEST                                                             CARD E1
     0.         1.31         -1.40          0.            0.          CARD E2
    0.55        5.46         73.49       -15.01                       CARD E3
   3                                                                  CARD E4A
    1.31       158.6          1.35        1586.         1.40    15860.CARD E4B
4   ANTERIOR PELVIS                                                   CARD E1
     0.         2.02         -2.10          0.            0.          CARD E2
   -0.14        1.58         24.39       -29.33        13.76          CARD E3
   3                                                                  CARD E4A
    2.02        89.7          2.05         897.         2.10     8970.CARD E4B
5   POSTERIOR PELVIS                                                  CARD E1
     0.         1.96         -2.10          0.            0.          CARD E2
   -0.76       35.10         40.04       -12.49                       CARD E3
   3                                                                  CARD E4A
    1.96       127.8          2.03        1278.         2.10    12780.CARD E4B
6   UPPER ARM                                                         CARD E1
     0.         0.89         -1.00          0.            0.          CARD E2
    1.54      -30.63        627.09     -1197.70       917.23          CARD E3
   3                                                                  CARD E4A
    0.89       203.1          0.95        2031.         1.00    20310.CARD E4B
7   FOREARM                                                           CARD E1
     0.         1.31         -1.40          0.            0.          CARD E2
   -2.40      107.37       -313.36       504.61      -196.37          CARD E3
   3                                                                  CARD E4A
    1.31       156.2          1.35        1562.         1.40    15620.CARD E4B
8   HAND                                                              CARD E1
     0.         0.38         -0.45          0.            0.          CARD E2
   -0.04      -31.04       2384.47    -10193.90     19172.50          CARD E3
   3                                                                  CARD E4A
    0.38       139.4          0.41        1394.         0.45    13940.CARD E4B
9   UPPER LEG                                                         CARD E1
```

```
          0.          1.31       -1.40          0.          0.              CARD E2
        -0.28        14.19       81.94      -122.62       98.73      -29.09CARD E3
    3                                                                       CARD E4A
         1.31         61.6        1.35         616.        1.40       6160.CARD E4B
   10    KNEE                                                               CARD E1
          0.          0.54       -0.58          0.          0.              CARD E2
        -0.04         2.22      867.34      -401.61                         CARD E3
    3                                                                       CARD E4A
         0.54        187.8        0.56         1878.       0.58      18780.CARD E4B
   11    FRONT OF LOWER LEG                                                 CARD E1
          0.          1.78       -1.90          0.          0.              CARD E2
        -0.74        26.79        3.92        29.05                         CARD E3
    3                                                                       CARD E4A
         1.78        223.6        1.84         2236.       1.90      22360.CARD E4B
   12    BACK OF LOWER LEG                                                  CARD E1
          0.          1.66       -1.75          0.          0.              CARD E2
        -0.08        29.42       -2.08                                      CARD E3
    3                                                                       CARD E4A
         1.66         43.2        1.70         432.        1.75       4320.CARD E4B
   13    FOOT                                                               CARD E1
          0.          0.83       -0.95          0.          0.              CARD E2
        -0.68        82.75     -704.17      3367.10    -5570.69     3188.30CARD E3
    3                                                                       CARD E4A
         0.83        121.2        0.89         1212.       0.95      12120.CARD E4B
 9999                                                                       CARD E1
   41    RIGHT SHOULDER JOINT                                               CARD E7A
                                                                            CARD E7B
   -4       8                                                               CARD E7C
        151.0          0.0     87900.0          0.0                         CARD E7D
         75.0          0.0     13700.0          0.0                         CARD E7E
          0.0          0.0      -312.0      11800.0                         CARD E7F
         66.0          0.0      7780.0    3010000.0                         CARD E7G
         68.0          0.0     22200.0     376000.0                         CARD E7H
         89.0          0.0     22000.0          0.0                         CARD E7I
        111.0          0.0      2470.0      17600.0                         CARD E7J
        153.0          0.0     13000.0          0.0                         CARD E7K
   42    LEFT SHOULDER JOINT                                                CARD E7A
                                                                            CARD E7B
```

```
 -4      8                                                                           CARD E7C
    151.0          0.0     87900.0          0.0                                      CARD E7D
    153.0          0.0     13000.0          0.0                                      CARD E7E
    111.0          0.0      2470.0      17600.0                                      CARD E7F
     89.0          0.0     22000.0          0.0                                      CARD E7G
     68.0          0.0     22200.0     376000.0                                      CARD E7H
     66.0          0.0      7780.0    3010000.0                                      CARD E7I
      0.0          0.0      -312.0      11800.0                                      CARD E7J
     75.0          0.0     13700.0          0.0                                      CARD E7K
43     STANDING RIGHT HIP                                                            CARD E7A
                                                                                     CARD E7B
 19      4                                                                           CARD E7C
      0.0          2.0         7.0         21.0         49.0       105.0CARD E7D
    217.0        441.0       889.0       1790.0       3580.0      7160.0CARD E7E
  14300.0      28700.0     57300.0     115000.0     229000.0    459000.0CARD E7F
 917000.0                                                                            CARD E7G
      0.0          5.0        11.0         22.0         39.0        73.0CARD E7H
    141.0        277.0       549.0       1090.0       2180.0      4360.0CARD E7I
   8710.0      17400.0     34800.0      69600.0     139000.0    279000.0CARD E7J
 557000.0                                                                            CARD E7K
      0.0          1.0         2.0          3.0          5.0         7.0CARD E7L
     10.0         13.0        17.0         22.0         27.0        32.0CARD E7M
     38.0         46.0        62.0         94.0        158.0       286.0CARD E7N
    542.0                                                                            CARD E7O
      0.0          1.0         3.0          4.0          6.0         8.0CARD E7P
      9.0         10.0        18.0         34.0         66.0       130.0CARD E7Q
    258.0        514.0      1030.0       2050.0       4100.0      8190.0CARD E7R
  16400.0                                                                            CARD E7S
44     STANDING LEFT HIP                                                             CARD E7A
                                                                                     CARD E7B
 19      4                                                                           CARD E7C
      0.0          2.0         7.0         21.0         49.0       105.0CARD E7D
    217.0        441.0       889.0       1790.0       3580.0      7160.0CARD E7E
  14300.0      28700.0     57300.0     115000.0     229000.0    459000.0CARD E7F
 917000.0                                                                            CARD E7G
      0.0          1.0         3.0          4.0          6.0         8.0CARD E7H
      9.0         10.0        18.0         34.0         66.0       130.0CARD E7I
    258.0        514.0      1030.0       2050.0       4100.0      8190.0CARD E7J
```

```
  16400.0                                                                   CARD E7K
      0.0          1.0          2.0          3.0          5.0          7.0CARD E7L
     10.0         13.0         17.0         22.0         27.0         32.0CARD E7M
     38.0         46.0         62.0         94.0        158.0        286.0CARD E7N
    542.0                                                                   CARD E7O
      0.0          5.0         11.0         22.0         39.0         73.0CARD E7P
    141.0        277.0        549.0       1090.0       2180.0       4360.0CARD E7Q
   8710.0      17400.0      34800.0      69600.0     139000.0     279000.0CARD E7R
 557000.0                                                                   CARD E7S
45    STANDING LUMBAR SPINE                                                 CARD E7A
                                                                            CARD E7B
  19     4                                                                  CARD E7C
      0.0       1200.0       2400.0       3600.0       4800.0       6000.0CARD E7D
   7200.0       8400.0       9600.0      10800.0      13200.0      18000.0CARD E7E
  27600.0      46800.0      85200.0     162000.0     314600.0     622800.0CARD E7F
1237200.0                                                                   CARD E7G
      0.0       1200.0       2400.0       3600.0       4800.0       6000.0CARD E7H
   7200.0       8400.0       9600.0      10800.0      13200.0      18000.0CARD E7I
  27600.0      46800.0      85200.0     162000.0     314600.0     622800.0CARD E7J
1237200.0                                                                   CARD E7K
      0.0        960.0       1920.0       2880.0       3840.0       4800.0CARD E7L
   5760.0       6720.0       7680.0       8640.0      10560.0      14400.0CARD E7M
  22080.0      37440.0      68160.0     129600.0     252480.0     498240.0CARD E7N
 989760.0                                                                   CARD E7O
      0.0       1200.0       2400.0       3600.0       4800.0       6000.0CARD E7P
   7200.0       8400.0       9600.0      10800.0      13200.0      18000.0CARD E7Q
  27600.0      46800.0      85200.0     162000.0     314600.0     622800.0CARD E7R
7010800.0                                                                   CARD E7S
46    NECK PIVOT                                                            CARD E7A
                                                                            CARD E7B
  19     4                                                                  CARD E7C
      0.0        700.0       1400.0       2100.0       2800.0       3500.0CARD E7D
   4200.0       4900.0       5600.0       6300.0       7000.0       7700.0CARD E7E
   8400.0       9800.0      12600.0      18200.0      29400.0      51800.0CARD E7F
  96600.0                                                                   CARD E7G
      0.0        600.0       1200.0       1800.0       2400.0       3000.0CARD E7H
   3600.0       4200.0       4800.0       5400.0       6000.0       6600.0CARD E7I
   7200.0       8400.0      10800.0      15600.0      25200.0      44400.0CARD E7J
```

```
     82800.0                                                                           CARD E7K
         0.0         300.0         600.0         900.0        1200.0        1500.0CARD E7L
      1800.0        2100.0        2400.0        2700.0        3000.0        3300.0CARD E7M
      3600.0        4200.0        5400.0        7800.0       12600.0       22200.0CARD E7N
     41400.0                                                                           CARD E7O
         0.0         600.0        1200.0        1800.0        2400.0        3000.0CARD E7P
      3600.0        4200.0        4800.0        5400.0        6000.0        6600.0CARD E7Q
      7200.0        8400.0       10800.0       15600.0       25200.0       44400.0CARD E7R
     82800.0                                                                           CARD E7S
  47     HEAD PIVOT                                                                    CARD E7A
                                                                                       CARD E7B
   19      4                                                                           CARD E7C
         0.0         490.0         980.0        1680.0        2380.0        3080.0CARD E7D
      3780.0        4480.0        5180.0        5880.0        6580.0        7280.0CARD E7E
      7980.0        9380.0       12180.0       17780.0       28980.0       51380.0CARD E7F
     96180.0                                                                           CARD E7G
         0.0         600.0        1200.0        1800.0        2400.0        3000.0CARD E7H
      3600.0        4200.0        4800.0        5400.0        6000.0        6600.0CARD E7I
      7200.0        8400.0       10800.0       15600.0       25200.0       44400.0CARD E7J
     82800.0                                                                           CARD E7K
         0.0         250.0         500.0         800.0        1100.0        1400.0CARD E7L
      1700.0        2000.0        2300.0        2600.0        2900.0        3200.0CARD E7M
      3500.0        4100.0        5300.0        7700.0       12500.0       22100.0CARD E7N
     41300.0                                                                           CARD E7O
         0.0         600.0        1200.0        1800.0        2400.0        3000.0CARD E7P
      3600.0        4200.0        4800.0        5400.0        6000.0        6600.0CARD E7Q
      7200.0        8400.0       10800.0       15600.0       25200.0       44400.0CARD E7R
     82800.0                                                                           CARD E7S
                                                                                       CARD F1
   0   0   0   0   0   0   0   0   0   0   0   0   0   0   0   0   0                   CARD F3A
                                                                                       CARD F4A
  45  45  46  46  43   0   0  44   0   0  41   0  42   0   0   0                       CARD F5A
                                   0   0   0   0   0                                   CARD G1
       0.0           0.0           0.0                                                 CARD G2A
       0.0           0.0           0.0                                        3  2  1  0CARDG3 1
       0.0           0.0           0.0                                        3  2  1  0CARDG3 2
       0.0           0.0           0.0                                        3  2  1  0CARDG3 3
       0.0           0.0           0.0                                        3  2  1  0CARDG3 4
```

0.0	0.0	0.0	3	2	1	0CARDG3 5
0.0	90.0	0.0	3	2	1	0CARDG3 6
0.0	0.0	0.0	3	2	1	0CARDG3 7
0.0	0.0	0.0	3	2	1	0CARDG3 8
0.0	90.0	0.0	3	2	1	0CARDG3 9
0.0	0.0	0.0	3	2	1	0CARDG310
0.0	0.0	0.0	3	2	1	0CARDG311
0.0	0.0	0.0	3	2	1	0CARDG312
0.0	0.0	0.0	3	2	1	0CARDG313
0.0	0.0	0.0	3	2	1	0CARDG314
0.0	0.0	0.0	3	2	1	0CARDG315
0.0	0.0	0.0	3	2	1	0CARDG315
0.0	0.0	0.0	3	2	1	0CARDG315
						CARD H1A
						CARD H1B
						CARD H2A
						CARD H2B
						CARD H3A
						CARD H3B
						CARD H4
						CARD H5
						CARD H6
						CARD H7A
						CARD H8
						CARD H9
						CARD H10

U S GOVERNMENT PRINTING OFFICE 1989 - 648-002/80224